AD_____

CONTRACT NO: DAMD17-00-C-0021

TITLE: DESIGN AND PRODUCTION OF AN ORGANOPHOSPHORUS-BIOSCAVENGER VIA PROTEIN ENGINEERING OF THE HUMAN ACETYLCHOLINESTERASE

PRINCIPAL INVESTIGATOR: Avigdor Shafferman Ph.D.

CONTRACTING ORGANIZATION: Israel Institute for Biological Research
P.O.Box 19
74100, Ness-Ziona
ISRAEL

REPORT DATE: September, 2002

TYPE OF REPORT: FINAL

PREPARED FOR: U.S. Army Medical
Research and Materiel Command
Fort Detrick, Frederick, Maryland, 21702-5012.

REPORT DOCUMENTATION PAGE

Form Approved
OMB No. 074-0188

1. Agency Use Only (Leave blank)	2. Report Date	3. Report Type and Period Covered
	September 2002	Final (1 June 00- 31 August 02)

4. Title and Subtitle
Design and Production of an Organophosphorus Bioscavenger Via Protein Engineering of the Human Acetylcholinesterase

5. Award Number
DAMD17-00-C-0021

6. Author(s)
Avigdor Shafferman, Ph.D.

7. Performing Organization Name (Include Name, City, State, Zip Code and Email for Principal Investigator)
Israel Institute for Biological Research
Ness-Ziona, Israel, 74100

E-Mail: avigdor@iibr.gov.il

8. Performing Organization Report Number (Leave Blank)

9. Sponsoring/Monitoring Agency Name and Address
U.S. Army Medical Research and Materiel Command
Fort Detrick, Maryland 21702-5012

10. Sponsoring/Monitoring Agency Report Number (Leave

11. Supplementary Notes (i.e., report contains color photos, report contains appendix in non-print form, etc.)
Original contains color plates: All DTIC reproductions will be in black and white.

12a. Distribution/Availability Statement)
Approved for public release; distribution unlimited

12b. Distribution Code
(Leave Blank)

13. Abstract *(Maximum 200 Words)*

The design of novel biocatalysts with potential pharmacological use against organophosphate (OP) poisoning, within the mold of recombinant human acetylcholinesterase (rHuAChE), was carried out by two complementing research approaches: a. Kinetic studies combined with mass spectrometric analysis of rHuAChE and selected mutants thereof, with a variety of OPs for better understanding of the chemical environment for the OPs in the active center of AChE. Specifically, here we describe the effects of multiple replacements of aromatic residues at the active center on reactivity toward OP agents, as well as report on the resolution of some of the less understood reaction pathways of phosphylation, and "aging" involving phosphoroamidates (P-N agents) such as tabun and butyl-tabun. b. Analyses of post-translation modifications responsible for the limited residence time of rHuAChE: Extensive structural analysis of the N-glycans of recombinant bovine and human AChE and native bovine AChE, identified specific termini that account for the observed differential behavior of the recombinant and native enzymes. Accordingly, we generated a series of recombinant enzyme products differing in sialylation, oligomerization and number of glycans. A unique hierarchical order of post-translation modifications that determine the circulatory residence time was revealed. Based on these studies recombinant products exhibiting a pharmacodynamic profile indistinguishable from that of the native enzyme was generated. Finally, we demonstrated that PEG-conjugation of recombinant HuAChE by resulted in the generation of an enzyme form which is retained in the circulation for periods of time, exceeding that of other recombinant or native acetylcholinesterases.

14. Subject Terms (keywords previously assigned to proposal abstract or terms which apply to this award)
Chemical Defense

15. Number of Pages
194

16. Price Code

17. Security Classification of Report	18. Security Classification of this Page	19. Security Classification of Abstract	20. Limitation of Abstract
Unclassified			Unlimited

FOREWORD

Opinions, interpretations, conclusions and recommendations are those of the author and are not necessarily endorsed by the US Army.

_____ Where copyrighted material is quoted, permission has been obtained to use such material.

_____ Where material from documents designated for limited distribution is quoted, permission has been obtained to use the material.

_____ Citations of commercial organizations and trade names in this report do not constitute an official Department of Army endorsement or approval of the products or services of these organizations.

___X___ In conducting research using animals, the investigator(s) adhered to the "Guide for the Care and Use of Laboratory Animals," prepared by the Committee on Care and Use of Laboratory Animals of the Israel Institute for Biological Research.

_____ For the protection of human subjects, the investigator(s) adhered to policies of applicable Federal Law 45 CFR 46.

___X___ In conducting research utilizing recombinant DNA technology, the investigator(s) adhered to current guidelines promulgated by the National Institutes of Health.

___X___ In the conduct of research utilizing recombinant DNA, the investigator(s) adhered to the NIH Guidelines for Research Involving Recombinant DNA Molecules.

_____ In the conduct of research involving hazardous organisms, the investigator(s) adhered to the CDC-NIH Guide for Biosafety Microbiological and Biomedical Laboratories.

17 Sept. 2002

PI - Signature Date

DESIGN AND PRODUCTION OF AN ORGANOPHOSPHORUS-BIOSCAVENGER VIA PROTEIN ENGINEERING OF THE HUMAN ACETYLCHOLINESTERASE

FINAL REPORT

BARUCH VELAN*
ARIE ORDENTLICH*
DOV BARAK#
NAOMI ARIEL*
YOFFI SEGALL#
DANA KAPLAN*
ARIE LAZAR§
DANA STEIN*
GALIT SOD-MORIA#
CHANOCH KRONMAN*
THEODOR CHITLARU*
OFER COHEN*
TAMAR SERY*
NEHAMA SELIGER*
EYTAN ELHANANY*
SHIRLEY LAZAR*
LEA ZILBERSTEIN§

AVIGDOR SHAFFERMAN*§

* DEPARTMENT OF BIOCHEMISTRY AND MOLECULAR GENETICS
# DEPARTMENT OF ORGANIC CHEMISTRY
§ DEPARTMENT OF BIOTECHNOLOGY

CONTENTS

LIST OF FIGURES

LIST OF TABLES

I. GENERAL INTRODUCTION

The primary role of acetylcholinesterase (acetylcholine acetylhydrolase 3.1.1.7, AChE), is the termination of impulse transmission in cholinergic synapses by rapid hydrolysis of the neurotransmitter acetylcholine (ACh). The enzyme has been the subject of intense research due to its focal position in several fields of interest. Modification in the levels of human brain AChE have been reported in various disorders such as Down's syndrome (Yates *et al.*, 1980) and Alzheimer's disease (Coyle *et al.*, 1983). Several cholinesterase inhibitors have proven to be of value as medicinal agents and are used for the treatment of glaucoma or myasthenia gravis (Taylor, 1990). Some organophosphorus (OP) inhibitors of ChEs such as malathion and diazinon, act as efficient insecticides and have been widely used in combating medfly and other agricultural pests. Other OP compounds, such as the nerve agent sarin and soman, inhibit AChE irreversibly by rapid phosphorylation of the serine residue in the enzyme active site. The acute toxicity of these nerve agents is elicited in motor and respiratory failure following inhibition of AChE in the peripheral and central nervous system.

The current treatment regimes against nerve agent exposure are designed to protect life but are not able to prevent severe incapacitation. The high reactivity of ChEs towards OP-agents led to propose these biomolecules as exogenous scavengers for sequestration of toxic OP-agents before they reach their physiological target (Wolfe *et al* 1987; Raveh *et al* 1989; Broomfield *et al* 1991; Doctor *et al* 1992). The AChEs react irreversibly, and on a molar basis, with the OP agents. Therefore, the amounts of AChE required for treatment are high. This limitation could be overcome provided that the OP-enzyme conjugates could be efficiently reactivated before the excess OP has reached its physiological target. This goal is difficult to attain especially in cases where the OP-AChE conjugates undergo catalytic post-inhibitory processes termed aging. In native AChEs the spontaneous reactivation, through displacement of the phosphyl moiety from the active site, is usually very slow and unable to compete with the aging process, yet efficient enzyme reactivation can be achieved by various oxime nucleophiles. Our goal is therefore to generate enzymes based on the HuAChE template, the OP-adducts of which are more readily reactivated and are resistant to aging, yet still retain their high reactivity towards the OP agents. To meet this challenge, we as well as others initiated studies designed for better understanding of the functional architecture of the AChE active center. These include X-ray crystallography (Sussman *et al* 1991; Harel *et al* 1996; Raves *et al* 1997; Kryger et 1998; Millard *et al* 1999a; Bourne *et al* 1999; Kryger *et al* 2000); site directed mutagenesis and molecular modeling together with kinetic studies of the AChE muteins with substrates and reversible inhibitors (Shafferman *et al* 1992a,b; Ordentlich *et al* 1993a; Barak *et al* 1994; Vellom *et al* 1993; Radic *et al*; 1992; Radic *et al*; 1993; Shafferman *et al* 1995; Ordentlich *et al* 1996; Ariel *et al* 1998; Ordentlich *et al* 1998). The functional role of the various active center subsites, identified this way include: a) the esteratic site containing the catalytic triad Ser203, His447 and Glu334; b) the

"oxyanion hole" consisting of residues Gly121, Gly122 and Ala204; c) the "anionic subsite" or the choline binding subsite -Trp86; d) the hydrophobic site for the alkoxy leaving group of the substrate containing an "aromatic patch" that includes residues Trp86, Tyr337 and Phe338; e) the acyl pocket - Phe295 and Phe297 and f) the peripheral anionic subsite (PAS) including residues Tyr72, Asp74, Tyr124, Trp286 and Tyr341. Recently, we have examined the specific involvement of all these elements of the active center functional architecture, in determining reactivity and specificity of human AChE (HuAChE) towards different OP-inhibitors. We have also demonstrated the ability to generate novel enzymes that are more efficient in OP scavenging through the combined effects of improved activity toward the OP-agents together with higher resistance to the aging process (Ordentlich *et al.*, 1996; Shafferman *et al.*, 1996a). Such studies, by us and others (see review in Taylor and Radic, 1994; Hosea *et al.* 1995, 1996; Millard *et al.*, 1995; Lockridge *et al.*, 1997), reveal the structural and mechanistic determinants of AChE activity that are essential for the design of true OP hydrolytic activity into the AChE mold. Information regarding the potential diversity of aging mechanisms is essential for further elucidation of the role of AChE active center in these processes, as part of the development of effective treatment for human intoxication by organophosphorus agents, like certain insecticides and nerve agents. Efficiency of these mechanisms as well as the catalytic perfection of cholinesterases is determined by the optimized juxtaposition of the catalytic triad. In particular the exact positioning of the catalytic histidine is achieved through an array of interactions with acidic and aromatic residues adjacent to the active center.

Exploitation of the bioscavenging potential of the recombinant bioengineered mutant derivatives of AChE depends on large-scale production systems (Fischer *et al* 1993; Kronman *et al* 1992). However pharmacokinetic studies (Kronman *et al* 1992; Mendelson *et al* 1998) have shown that the recombinant enzymes generated by these systems, relying on either bacterial or mammalian cells, are retained in the circulation of experimental animals for much shorter periods of time than native fetal bovine serum acetylcholinesterase (FBS-AChE) or human serum butyrylcholinesterase (BChE). Therefore, deciphering the mechanisms involved in clearance of cholinesterases from the bloodstream is of importance for the development of enzyme-based bioscavangers for treatment of organophosphorus poisoning.

Our previous studies (Kronman *et al.*, 1995) have shown that the structures of the appended glycans of rHuAChE, and in particular the distal termini of these glycan projections, constitute a major factor in determining the circulatory duration of rHuAChE. This was exemplified by establishing the major role of N-glycan sialylation in determining the circulatory life-time of forms of rHuAChE. As a continuation of these studies, we have demonstrated (Chitlaru *et al.*, 1998) that production of rHuAChE with highly sialylated glycans (achieved by genetic modification of rHuAChE producer cell lines to coexpress a sialyltransferase gene) resulted in the generation of high levels of rHuAChE which exhibited increased circulatory retention, yet was still eliminated from the circulation more rapidly than native serum-derived cholinesterases. HPAEC-PAD analysis as well as determination of sialic acid content of oversialylated

rHuAChE indicated that a fraction of the N-glycan population remained refractive to sialylation. This subset of glycan termini, which are refractive to sialylation, may serve as substrates for clearance pathways, and therefore may be responsible for the relatively rapid clearance of oversialylated rHuAChE.

The persistence of asialylated glycan termini associated with AChE following α2,6ST treatment may reflect the presence of immature glycan projections and/or of glycans which were processed in an unusual manner which precludes sialylation. Incomplete glycans containing exposed mannose (Man) or N-acetylglucosamine (GlcNAc) may be the result of a relative inefficiency in the glycosylation machinery, which could indeed be a limiting factor in systems aimed at the high expression of recombinant proteins (Matsuura *et al.*, 1998). Glycoproteins containing such oligosaccharide projections may be recognized by specific receptors, which facilitate their removal from the circulation. Conversely, the sialylation-refractive glycans may contain processed outer-arm structures other than the common Man--GlcNAc-Gal. For instance, the galactose residue may be substituted by N-acetylgalactosamine (GalNAc). Indeed, preliminary lectin analyses carried out in our laboratory, indicated that the N-glycans of rHuAChE contain GalNAc residues. GalNAc residues may undergo terminal sulfation, which would preclude terminal sialylation. This structure can serve as a ligand, which is recognized and cleared by a specific receptor, expressed in liver endothelial cells (Fiete *et al.*, 1991; Smith *et al.*, 1993). Glycans containing SO_4-GalNAc termini have been indeed reported to occur in recombinant glycoproteins expressed in HEK-293 cells (Smith *et al.*,1992). In addition, glycans terminating in non-sulfated GalNAc may remain asialylated if the penultimate GlcNAc residue carries a fucose (Fuc) substitution (Yan *et al*, 1993). Glycoproteins containing terminal GalNAc are removed from the circulation via the hepatic asialoglycoprotein receptor, which recognizes both galactose and GalNAc as ligands. In addition, the outer-arm fucose residue can mediate protein removal via a specific hepatic clearance receptor (Ashwell and Harford, 1982). Glycans containing nonsialylated GalNAc-GlcNAc (Fuc) have been reported to occur in recombinant glycoproteins expressed in HEK-293 cells (Yan *et al.*, 1993).

One possible approach to limit enzyme removal via specific glycan termini, would be to alter these glycan structures. This would require a detailed structural analysis of the glycans, to fully define and quantitate the carbohydrate elements, which may contribute to clearance. Once such glycan structures have been determined, they can be modified by subjecting the glycoprotein to a series of i*n vitro* glycosidase and glycosyltransferase treatments utilizing commercially-available glycan-modifying enzymes. These would allow the stepwise removal and addition of specific monosaccharide residues, to generate a mature form, which is compatible with circulatory longevity. The end product of such a glycan remodeling procedure, as well as various intermediates, could be subjected to pharmacokinetic profile studies to test the acquisition of extended circulatory residence. Our studies focusing on sialic acid manipulation (Chitlaru *et al.*, 1998), have demonstrated that *in vitro* experiments can serve as informative guidelines for designing the *in vivo* genetic modulations required for generation of

pharmacokinetically-improved rHuAChE. Accordingly, the information gathered from the *in vitro* glycan remodelling experiments, might be implemented to genetically alter the cellular glycosylation machinery of rHuAChE and rBoAChE producer cell lines. This can be achieved by the introduction of the genes for specific underexpressed glycosyltransferases or glycosidases to generate glycoproteins, which carry N-glycans, which are compatible with extended circulatory residence. The generation of rHuAChE or rBoAChE carrying such pharmacokinetically-optimized N-glycans will also allow a re-evaluation of other post-translation-related factors which may play a role in determining circulatory longevity, and which otherwise may pass unnoticed, due to the overriding effect of unfavorably-processed glycans on rapid elimination of glycoproteins from the circulation. All these points of consideration, provided the basis for the current research, which is directed towards the design of an efficient OP-bioscavenger.

This report covers the progress in all these research areas. The following section (section II) provides evidence for a new mechanism involving P-N rather than O-C bond scission in aging of certain AChE adducts with phosphoroamidates. In particular, by utilizing combination of site directed Mutagenesis and mass spectrometric techniques we elucidated the reaction path for aging of AChE adduct with the nerve agent tabun (section III). In section IV, we outline the investigation of involvement of the HuAChE active center aromatic residues in maintaining the integrity of the catalytic machinery, carried out by replacement of up to 6 of these amino acids by the corresponding aliphatic residues of HuBChE.

Section V describes the progress made in elucidating the structures and relative abundance of the entire array of glycan forms associated with rBoAChE and its native counterpart, FBS-AChE. The possible involvement of specific glycan structures in determining circulatory retention is experimentally examined. Likewise, the role of post-translation-related traits, other than glycan processing, are examined in optimally sialylated forms of the rBoAChE to determine their contribution to circulatory longevity. These studies serve as the basis for unraveling the post-translation-related set of rules governing the circulatory retention of the human AChE enzyme, described in Section VI., and allow determination of the contribution of glycan loading to circulatory longevity of the human enzyme (Section VII). Finally, in Section VIII we demonstrate that chemical modification of human AChE results in the generation of an enzyme form, which resides in the circulation for an extended period of time, exhibiting circulatory residence-time values, exceeding those, which characterize native serum-derived cholinesterases. Each of these sections includes a brief background introduction, methods and a result and discussion subsection. A summary of the main findings of the research concludes this report (Section IX)

II. Evidence for P-N Bond Scission in Phosphoroamidate Nerve Agent Adducts of Human Acetylcholinesterase

INTRODUCTION

Phosphylation of acetylcholinesterases (AChE, EC 3.1.1.7) leads to formation of stable covalent conjugates from which the enzyme can be usually reactivated through reaction with nucleophilic agents such as quaternary oximes or fluoride ions (Aldrich and Reiner, 1972; Chambers, 1992). In certain cases, reactivability of these conjugates decreases with time due to a unimolecular process termed "aging" (Benschop and Keijer, 1966; Michel et al.,1967; Segall *et al.*, 1993). While aging of phosphonyl-AChE derivatives of the organophosphorus (OP) nerve agents soman and sarin, involves the loss of an alkyl group from the phosphyl alkoxy substituent (Ordentlich *et al.*, 1993b; Shafferman *et al.*,1996a ;Barak *et al.*, 1997; Millard *et al.*, 1999a), there is no information regarding the nature of the aging process for conjugates with tabun and other phosphoroamidates. Reactivation of these conjugates may be impeded due to conformational change of the protein-inhibitor adducts turning it less accessible to reactivators (Thompson *et al.* 1992). For example, recent study has suggested that the non-reactivability of AChE and BuChE adducts with N,N'-dialkyl phosphorodiamidates like mipafox, which was thought to involve a rapid aging process, is in fact due to combination of a non-reactive phosphoryl moiety and of a local disturbance around the active site (Milatovic and Johnson, 1993). In the case of AChE-tabun conjugate reaction with reactivators was found to regenerate catalytic activity but also accelerate the development of non-reactivability (De Jong and Wolring, 1978). Thus, the mechanism by which AChE conjugates of P-N agents become resistant to reactivation may be different from those proposed for the corresponding phosphate and phosphonate adducts (Segall *et al.*, 1993; Ordentlich *et al.*, 1993b; Shafferman *et al.*, 1996a,b; Barak *et al.*, 1997; Masson *et al.*, 1997; Shafferman *et al.*, 1997; Saxena *et al.*, 1998a; Millard *et al.*, 1999a; Ordentlich *et al.*, 1999; Viragh *et al.*, 2000). Information regarding the potential diversity of aging mechanisms is essential for further elucidation of the role of AChE active center in these processes, as part of the development of effective treatment for human intoxication by organophosphorus agents, like certain insecticides and nerve agents. Any progress in this direction is of considerable importance since aging is probably the major factor limiting the effectiveness of oxime reactivation therapy in cases of OP poisoning (Wilson *et al.*, 1992).

Recent studies of aging of phosphonyl-AChE conjugates assessed the participation of various active center residues in the dealkylation reaction (Ordentlich *et al.*, 1993b; Saxena *et al.*, 1993 Shafferman *et al.*, 1996a,c; Barak *et al.*, 1997; Shafferman *et al.*, 1997; Saxena *et al.*, 1998a). In particular, replacement of either of the residues Glu-202 or Phe338 in HuAChE reduced by about 150-fold the rates of aging of the respective soman conjugates (Shafferman

et al., 1996a,b; Shafferman *et al.*, 1997; Ordentlich *et al.*, 1999*)*. These residues are thought to contribute to the aging process by stabilizing the imidazolium of the catalytic triad His-447, facilitating the formation of an oxonium on the phosphonyl moiety. The proposed mechanism is consistent with the previously proposed scission of the O-C bond and formation of a carbocation *(*Michel *et al.*, 1967; Cadogan *et al.*, 1969*)*, with the structures of the aging products as determined by x-ray crystallography *(*Millard *et al.*, 1999a*)* and electrospray-ionization mass spectrometry (ESI-MS; Barak *et al* .,1997), and with the observed absolute stereoselectivity of the aging process *(*Ordentlich *et al* ., 1999; Keijer and Wolring, 1969*)*. In marked contrast to these results, we now find that conjugates of the E202Q and F338A enzymes with P-N agents like tabun age at rates similar to those of the wild type HuAChE enzyme, suggesting that different products as well as aging mechanism may be involved (scheme 1).

Further investigation of this possibility included monitoring the phosphylation rates of certain HuAChE enzymes by P-N agents like tabun (see scheme 1) and its butyl analog (butyl-tabun) and the aging rates of the corresponding conjugates, as well as mass spectrometric

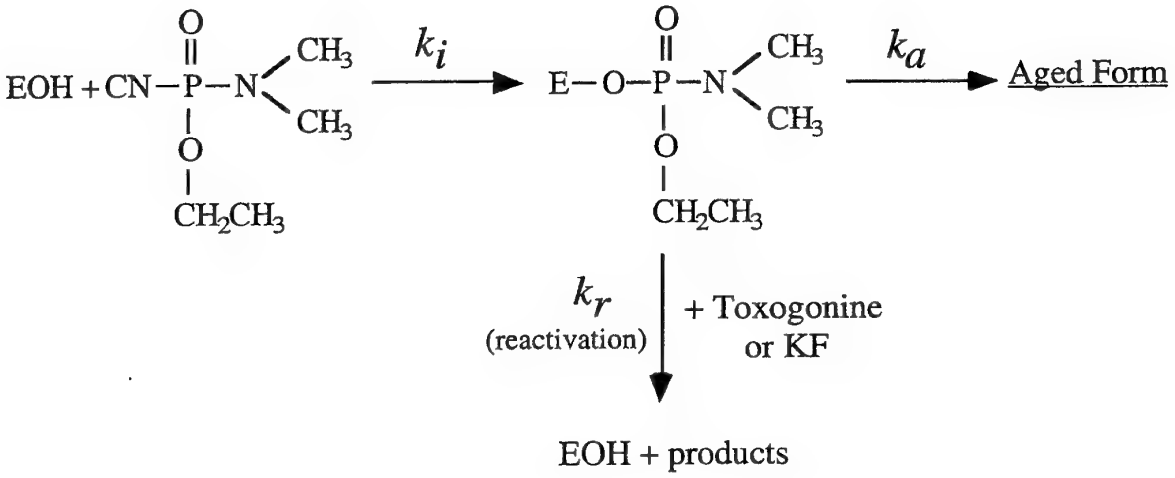

Scheme 1

measurements of the macromolecular aging products. The results indicate that HuAChE adducts with toxic OP agents like P-N derivatives and with phosphonates undergo aging by different mechanisms.

MATERIALS AND METHODS

Enzymes reagents and inhibitors -Expression of recombinant HuAChE and its mutants in a human embryonal kidney derived cell line (HEK-293) (Velan *et al.*, 1991; Shafferman *et al.*,1992a; Kronman *et al*, 1992) and generation of all the mutants was described previously (Shafferman *et al* ., 1992a,b; Ordentlich *et al.*, 1993a,b; Ordentlich *et al.*, 1995). Stable recombinant cell clones expressing high levels of each of the mutants were established according to the procedure described previously (Kronman *et al.;* 1992). Enzymes were purified (over 90% purity) either by ligand affinity chromatography (Kronman *et al.*, 1992) or by fractionation on monoclonal antibody affinity column (Kronman *et al.*, 1992) . The monomeric C580S HuAChE enzyme, expressed in *Escherichia coli* with an N-terminus sequence Met-Glu-Gly-Arg (Fischer *et al.*, 1993) and TcAChE were a gift from Prof. I. Silman. Acetylthiocholine iodide (ATC), toxogonine and 5:5'-dithiobis (2-nitrobenzoic acid) (DTNB) were purchased from Sigma. Generation of the alkyl N,N-dimethyl-phosphoramidocyanidates used in this study were carried out by modification of previously published procedure (Holmstedt, 1951), using dimethylamidophosphoric dichloride and the appropriate alcohol. Phosphoroamidates were purified either by distillation (tabun, 72-74°C/1.5 mmHg) or by column chromatography (butyl analog) to >95% purity according to P^{31} NMR.

Kinetic studies - HuAChE activity was assayed according to Ellman *et al.* (1961) in the presence of 0.1 mg/ml BSA, 0.3mM DTNB, 50mM sodium-phosphate buffer pH-8.0 and various concentrations of ATC), carried out at 27°C and monitored by a Thermomax microplate reader (Molecular Devices).

Measurements of phosphylation rates, with the mammalian recombinant HuAChE, were carried out in at least four different concentrations of tabun and butyl-tabun (I), and enzyme residual activity (E) at various times was monitored. The apparent bimolecular phosphonylation rate constants (ki, see scheme 1) determined under pseudo-first order conditions were computed from the plot of slopes of ln(E) vs time at different inhibitor concentrations. Rate constants under second order conditions were determined from plots of $\ln\{E/[I_o-(E_o-E)]\}$ versus time (Shafferman *et al.*, 1996a).

The rates of aging were monitored by measuring the reactivatable fraction of the conjugate in the presence of oxime reactivator (toxogonin or potassium fluoride) under conditions where the rates of reactivation (the pseudo first order rates) were greater than the corresponding rates of aging (Shafferman *et al.*, 1996a; Ordentlich *et al.*, 1999). Under the experimental conditions used for reactivation (pH=8.0; 37 °C), full regeneration of the enzymatic activity was observed.

Mass spectrometry analysis - Molecular mass measurements were carried out on a VG Platform mass spectrometer, which consists essentially of an electrospray ion source operating at atmospheric pressure followed by a quadrupole mass analyzer. Samples of phosphonoamidoyl-HuAChE conjugates, prepared by mixing the enzyme (30-40pmol/μl) with an excess of appropriate phosphonoamidate in deionized water (pH ~6.5), were assayed as described before (Barak *et al.*, 1997; Ordentlich *et al.*, 1999). The multiply charged electrospray ionization mass spectra were converted to the true molecular weight spectra using the VG MaxEnt algorithm of the MassLynx NT software. The process of dealkylation of phosphonoamidoyl-HuAChE conjugates was monitored over the period of 90hrs by mixing aliquots from an appropriate phosphylation mixture (20 μl) with formic acid (1 μl) followed by immediate mass spectrometric analysis using a mass range of 64000-66000 Da.

Molecular Modeling - Molecular models of P_S- and P_R-diastereomeric HuAChE conjugates with tabun and butyl-tabun were generated as described before for conjugates of soman (Ordentlich *et al.*, 1999), using HuAChE coordinates from the recently determined crystal structure of its complex with fasciculin (Kryger *et al.*, 1998) and SYBYL modeling software (Tripos Inc.). In these experiments it is essential to use HuAChE coordinates since the measured stereoselectivity of eel AChE is low (6.3-fold, see Benschop and De Jong, 1988) and therefore minor changes in the active center may reverse stereoselectivity. The models were optimized by molecular mechanics using the MAXMIN force field (and AMBER charge parameters for the enzyme) and zone refined, including 127 amino acids (15 Å substructure sphere around O^{γ}-Ser203). Optimization of the initial models included restriction of the distances between the phosphonyl oxygen and the amide nitrogen atoms of residues Gly121, Gly122 which were relieved in the subsequent refinement.

RESULTS AND DISCUSSION

Reactivation of AChE conjugates with P-N agents may be impeded by either a chemical process at the phosphonoamidyl moiety (aging) or by another postinhibitory event like conformational changes of the protein. Different elimination mechanisms leading to somewhat different aging products can be also envisaged (Thompson *et al.*, 1992). Indeed, the possibility of an alternative aging mechanism of tabun-AChE conjugates, in which the ethoxy group or even the dimethylamino group is split off from the tabun-enzyme conjugate, has already been suggested (De Jong and Wolring, 1978). Unlike the classical aging mechanism, it may involve P-N or P-O, rather than O-C bond scission. Such bond scission should involve a displacement at the phosphoroamidoyl moiety by water molecule, in analogy to the aging processes of diphenylphosphoryl-AChE (Maglothin *et al.*, 1975) or methylfluorophosphonyl-AChE. To further explore these alternative mechanisms, the kinetics of aging for tabun-HuAChE conjugates were compared to those of the homologous phosphonoamidate, bearing butoxy substituent on the phosphorus atom (butyl-tabun).

Both phosphoroamidates are nearly equally efficient in phosphylating various HuAChE mutant enzymes (see Table 1), suggesting that the two inhibitors are similarly accommodated in the active center (see Fig. 1). In particular, this is implied by the similar reactivity variations of the two P-N agents toward the different mutants of the HuAChE acyl pocket. Relative to the wild type HuAChE, both agents exhibit comparable reactivity toward the F297A mutant, 2-4-fold higher reactivity toward the F295A enzyme, and 4-fold lower reactivity toward the F295L/F297V HuAChE. These findings are consistent with the notion that the acyl pocket subsite is juxtaposed with equivalent substituents of the phosphoroamidyl moiety. Another significant observation in this respect is the relatively minor effect of phosphylation rates by tabun and its analog due to replacement of residue Glu202 (Table 1), as compared to the corresponding effects on the phosphylation rates by phosphates or phosphonates (about 30-fold decrease in E202Q HuAChE) (Shafferman *et al.*, 1996a,c; Ordentlich *et al.*, 1996). This difference may suggest that during phosphylation by these phosphonoamidates the dimethylamino rather than the alkoxy substituent is preferentially introduced in the vicinity of residue Glu202 of the HuAChE active center (see Fig. 1A). We note that in molecular modeling of the diastereomeric tabun- and butyl-tabun-HuAChE conjugates, the P_S-diastereomers were found to be somewhat more stable than the corresponding P_R-isomers (Fig. 1B).

Table 1- Rate constants of phosphoroamidation (k_i) and aging (k_a) of tabun, or butyl-tabun -inhibited HuAChE enzymes

	Phosphoroamidation k_i ($x10^{-6}$ M^{-1} min^{-1})[a]	
	Tabun	**butyl-Tabun**
Wild Type	15 ±4 [1.0][b]	6.0±0.8 [1.0]
E202Q	1.6±0.1 [9.4]	1.3±0.1 [4.6]
F338A	48 ±9 [0.3]	6.0±1.0 [1.0]
F295A	30 ±9 [0.5]	25.0±4.0 [0.2]
F297A	21 ±3 [0.7]	5.8±0.3 [1.0]
F295L/F297V	4.0±0.3 [3.8]	1.4±0.1 [4.3]

	Aging k_a ($x10^4 x min^{-1}$)[c]			
	Tabun		**butyl-Tabun**	
	pH 6	pH 8	pH 6	pH 8
Wild Type	16.0±4.0 [1.0]	1.7±0.5 [1.0]	9.0±3.0 [1.0]	0.6±0.3 [1.0]
E202Q	3.0±1.0 [5.3]	0.4±0.2 [4.3]	1.5±0.5 [6.0]	0.2±0.1 [3.0]
F338A	ND	0.6±0.2 [3.8]	ND	0.2±0.1 [3.0]
F295A	5.5±2.0 [2.9]	ND	4.5±1.5 [2.0]	ND
F297A	7.5±3.0 [2.1]	ND	5.5±2.0 [1.6]	ND
F295L/F297V	ND	ND	ND	ND

[a] Measured at pH 8, 24°C; values are means ± S.D. for at least three independent experiments.
[b] Number in parenthesis represent ratio of rate constants relative to wild type HuAChE
[c] Measured at indicated pH, 37°C; Values are means ± S.D. for at least three independent experiments; ND - not done.

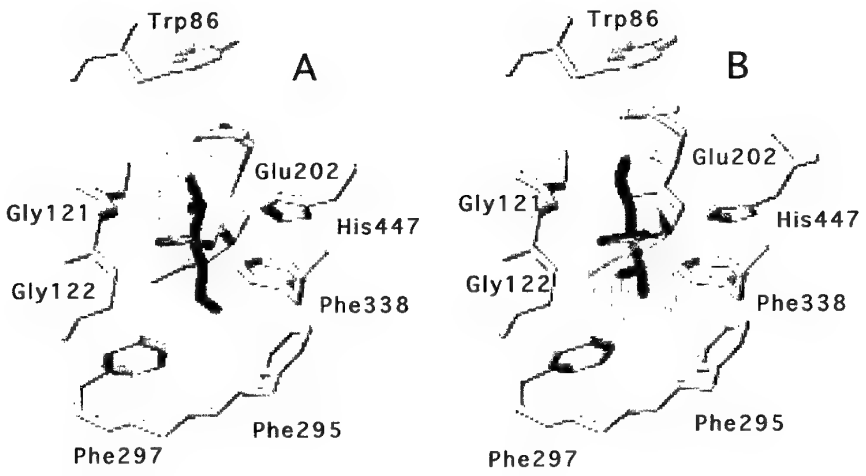

Figure 1: Covalent HuAChE conjugates of the PS- and the PR -tabun diastereomers. Only amino acids adjacent to the inhibitor are shown and hydrogen atoms of the protein are omitted for clarity. The phosphoroamidyl moiety is shown in heavy line and the volume of the dimethylamino group is illustrated by grid. **A**. PS-tabun-HuAChE conjugate. Note that the nitrogen of the phosphyl dimethylamino substituent is proximal to the carboxylate of Glu202 and within hydrogen bond distance (2.72 Å) from Nε1-His447; the ethoxy moiety is accommodated within the acyl pocket (Phe295, Phe297) and the phosphoryl oxygen interacts with the oxyanion hole residues Gly121 and Gly122. **B**. PR-tabun-HuAChE conjugate. The dimethylamino group points toward the acyl pocket; the alkoxy oxygen is within H-bond distance (2.95 Å) from Nε1-His447. The PSdiastereomeric conjugate was calculated to be more stable than the corresponding PR-diastereomer by 1.65 kcal/mole.

The rate constants of aging of tabun adducts with the E202Q and F338A HuAChEs are similar to those of the corresponding butyl-tabun adducts (see Table 1). These results suggest that the nature of the phosphoroamidyl alkoxy substituent studied has a limited effect, if any, on the aging process, and that the aging mechanism may involve displacement of the dimethylamino group by water (see scheme 2, pathway II).

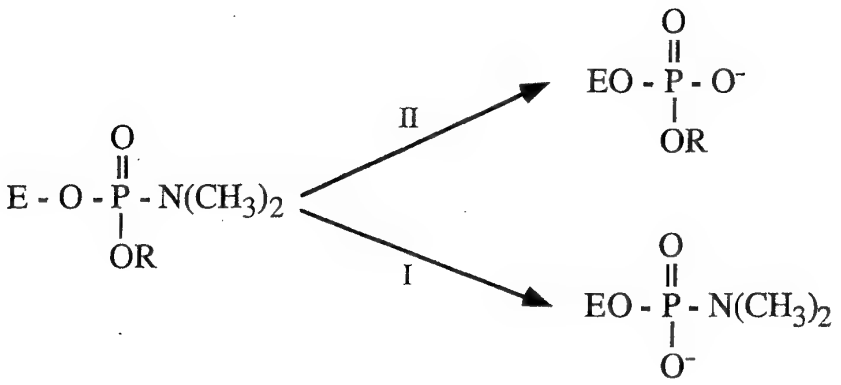

Scheme 2: Alternative pathways of the aging process in AChE adducts of alkyl N,N-dimethyl-phosphoramidates (tabun - R=C_2H_5; butyl -tabun - R=n-C_4H_9)

In accordance with the effect of pH on the rates of aging (Table 1) the loss of the dimethylamino moiety from the P-N adducts, is most probably facilitated through proton transfer from residue His447 to the phosphoroamidoyl-nitrogen, in analogy to the dealkylation processes in methylphosphono-AChEs (Shafferman *et al.*, 1996a,b). However in the case of phosphoroamidates the rate limiting steps are probably the development of a trigonal bipyramidal intermediate, its reorganization (pseudorotation) to position the dimethylammonium group in an apical position (Hall and Inch, 1990) and its elimination. This could explain the surprisingly minimal effects due to replacement of residues Glu202 or Phe338 on the facility of aging the studied P-N agents.

Replacement of either residue Phe295 or Phe297 by alanine had small and equivalent effects on the aging of the respective tabun and butyl-tabun conjugates (see Table 1). Like in case of the corresponding phosphoroamidation reactions, this observation is consistent with the idea that the acyl pocket accommodates equivalent substituents of the phosphoroamidyl moiety.

Although aging of HuAChE conjugates of the two phosphoroamidates seems to proceed by pathway II (scheme 2), contributions of the alternative pathway I cannot be ruled out. Such a contribution is related to the stereoselectivity of HuAChE phosphylation since in both pathways elimination seems to include the phosphoramidyl substituent vicinal to residues Glu202 and His447. These points are exemplified by the recently resolved structures of ethyl methylphosphono-TcAChE and of its aging product (Millard *et al.*, 1999a) where the ethyl group, to be cleaved off during aging, is juxtaposed with residues Glu199 and His440 (corresponding to Glu202 and His447 in HuAChE). Stereoselectivity of both agents toward HuAChE is presently unknown. Yet, it is probably low as suggested by the previously observed very limited (6.3-fold) stereoselectivity of AChE from electric eel toward the (-)-tabun enantiomer (Benschop and De Jong, 1988).

The comparable reactivities of tabun and butyl-tabun toward the different HuAChE enzymes combined with the similar aging rate constants of the corresponding phosphoroamidyl-

HuAChE conjugates and the results from molecular modeling are all consistent with an aging process proceeding according to pathway II in scheme 2. To provide direct evidence for this conclusion, mass spectrometric characterization of both the P-N phosphyl-conjugates and of their respective aging products was carried out. Recently we have shown that the aging products of certain methylphosphono-HuAChEs can be characterized by electrospray-ionization mass spectrometry (ESI-MS), with mass resolution that allows to distinguish between elimination of alkyl groups differing by a single methylene (Barak *et al.* 1997; Ordentlich *et al.*, 1999). While in case of the aged tabun conjugate the mass changes resulting from elimination of the ethyl group or of the dimethyl amino moiety, are nearly equivalent, such limitation does not apply to the corresponding butyl-tabun conjugate (see Table 2). Mass spectrometric monitoring of the progressive changes in the molecular masses of HuAChE adducts with tabun and butyl-tabun was carried out over a time period required to complete the aging process. For these measurements, recombinant HuAChE expressed in bacteria was used since with such an enzyme we could avoid the extensive molecular heterogeneity due to glycosylation (Barak *et al.*, 1997). Examination of Fig. 2 shows that the molecular masses of the phosphoroamidyl-HuAChEs appear immediately after addition of the phosphylating agents, with mass increase in excellent agreement with those expected from the respective phosphoroamidyl fragments following displacement of cyanide [136 Da for $C_2H_5OP(O)N(CH_3)_2$; 164 Da for $C_4H_9OP(O)N(CH_3)_2$]. The molecular species of the adducts are progressively replaced by the aged products which in both cases exhibit mass decrease of 28±4 Da compared with that of the original adduct. For the butyl-tabun conjugate these observations unequivocally demonstrate that the aging process involves replacement of the dimethylamino substituent according to a pathway involving P-N bond scission (pathway II, scheme 2), rather than elimination of either butyl or butoxy moieties (see Table 2).

The molecular masses of aging products of the HuAChE conjugates with P-N agents like tabun and butyl-tabun demonstrate that like for other phosphylated AChEs the aging process involves elimination at the phosphyl moiety. Although in this case elimination seems to occur through scission of the P-N bond, the nature of the aging products should be equivalent to those resulting from phosphoryl-AChEs. Therefore, regardless of the aging mechanism, the non-reactivability of the aged adducts may be attributed mainly to the stabilization imparted by a salt bridge between the negative charge on the phosphoryl oxygen and the His447 imidazolium. Structures of the aged phosphoroamidyl-HuAChEs are probably similar to those recently observed for the corresponding adducts with phosphonates (soman and sarin), phosphates (diisopropylphosphorofluoridate -DFP) (Millard *et al.*, 1999b) and phosphonothiolates (VX) (Millard *et al.*, 1999a).

Due to the relative resistance to reactivation (De Jong *et al.*, 1989) of AChE conjugates with certain P-N nerve agents like tabun, their aging can become a major obstacle to an effective treatment of intoxication by these agents. Recently certain AChE mutants, for which aging of the phosphonate adducts is severely retarded, have been proposed as potential OP scavengers in

combination with appropriate oxime reactivators (Shafferman *et al.*, 1996a,b; Saxena *et al.*, 1997a). In view of the different aging mechanism such enzymes may not be effective in cases of tabun and related phosphonoamidates. On the other hand, elucidation of this mechanism may be of considerable value in guiding further enzyme engineering of ChEs to enhance their tabun scavenging properties.

Table 2: Calculated and ESMS measured molecular masses of the P-N phosphylated AChEs adducts and their aging products

	Formation of Phosphoroamidyl-HuAChEs		"Aging" of Phosphoroamidyl-HuAChEs					
	Molecular Mass (Da)		Molecular Mass (Da)			Δ Mass (Da)[c]		
	Calculated[a]	Measured	Calculated[b]		Measured	Calculated[b]		Measured
			I	II		I	II	
Tabun	64836	64836±4	64807	64808	64808±4	29	28	28±4
Bu-Tabun	64864	64864±4	64807	64836	64836±4	57	28	28±4

[a] Calculated molecular mass based on the measured mass of the free enzyme (64,700 Da) and theoretical mass increase due to the corresponding phosphoroamidyl fragment assuming that cyanide is the leaving group.
[b] Mass calculated according to pathway I (scheme 2) where aging occurs through loss of the alkoxy substituent or pathway II where aging involves loss of dimethylamine.
[c] Difference between mass values of phosphoroamidyl-HuAChE and their corresponding aged forms.

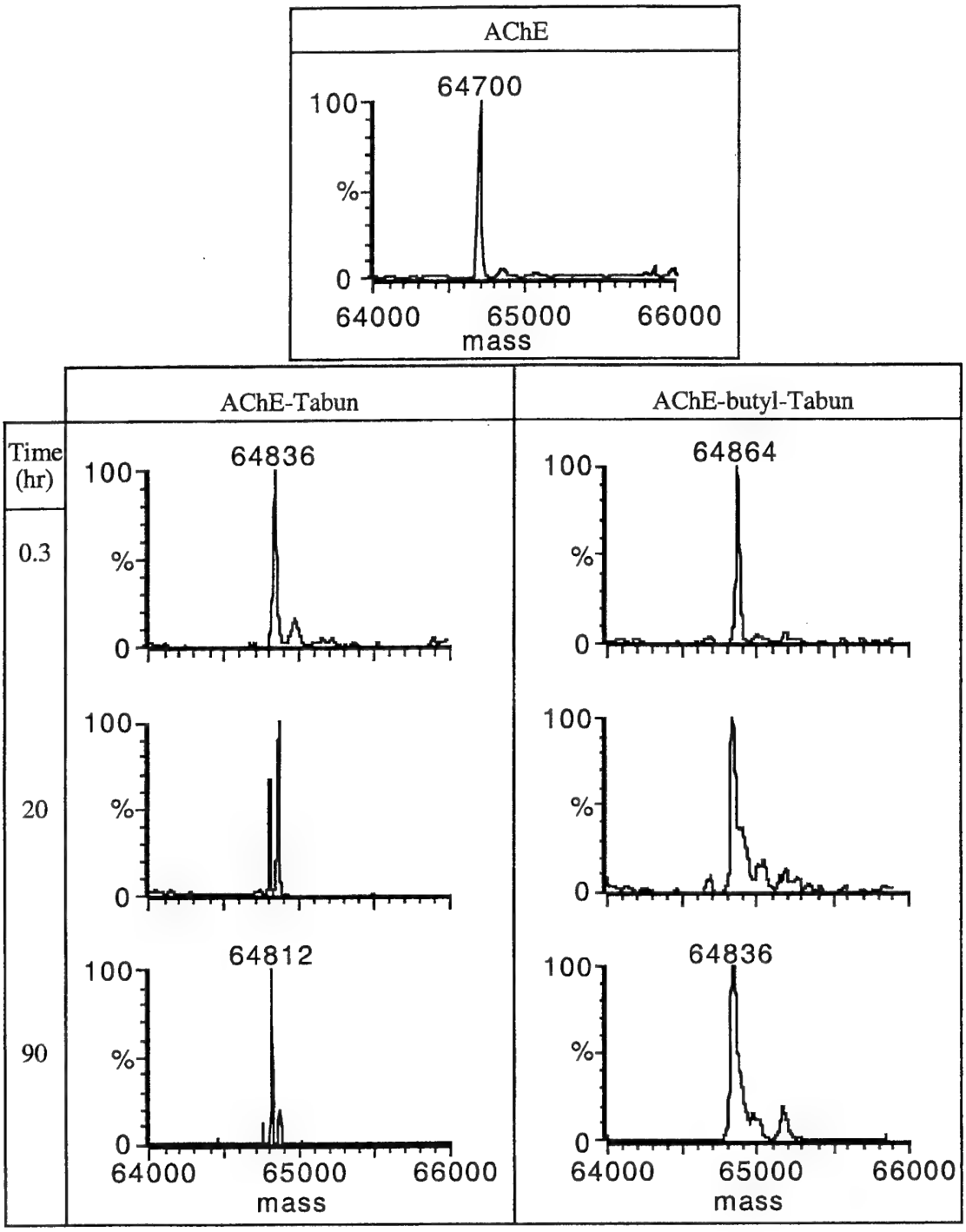

Figure 2: Molecular mass changes during phosphylation of HuAChE by tabun and butyl-tabun and during the aging of the corresponding conjugates monitored by positive-ion ESI-MS mass spectrometry. Masses of the molecular species were obtained for each spectrum after processing by the VG MaxEnt software over a mass range of 64,000-68,000 Da (Barak *et al.*, 1997; Ordentlich *et al.*, 1999). Note that due to this method of data transformation the shapes of the peaks are not related to the mass resolution of the spectrum. **Upper panel**. Analysis of the free C580S HuAChE from a bacterial source yielded experimental molecular mass 64,700 Da. Mass spectra of the reaction mixtures with tabun (**Left panels**) and with butyl-tabun (**Right panels**) determined at the indicated time intervals after reaction onset.

III. Resolving Pathways of Interaction of Covalent Inhibitors with the Active-site of Acetylcholinesterases- MALDI-TOF/MS Analysis of Various Nerve Agent Phosphyl Adducts.

INTRODUCTION

The inhibition of serine hydrolases such as cholinesterases (ChEs) by organophosphorus (OP) compounds involves phosphylation of the active site serine and the formation of a stable conjugate (Aldrich and Reiner, 1972; Taylor, 1990), from which the enzyme usually can be reactivated through reaction with nucleophilic agents (Aldrich and Reiner, 1972; Chambers, 1992). In certain cases reactivability of these conjugates decreases with time due to a unimolecular process termed "aging" (Benschop and Keijer, 1966; Michel *et al.*, 1967). Aging is probably the major factor limiting the effectiveness of reactivation therapy, in cases of OP poisoning. Thus, understanding the detailed mechanistic pathways of aging is crucial for the development of efficient therapeutic strategies against human intoxication by OP agents such as certain insecticides and nerve agents.

For phosphate and phosphonate AChE inhibitors the pathways of both the phosphylation and the aging processes are well established (Segall *et al.*, 1993; Shafferman *et al.*, 1996a; Barak *et al.*, 1997; Ordentlich *et al.*, 1999; Millard *et al.*, 1999a; Viragh *et al.*, 2000). On the other hand, the nature of phosphonamido-AChE conjugates and their aging products was only recently investigated using site directed mutagenesis, enzyme kinetics and electrospray ionization mass spectrometry (ESI-MS; Barak *et al.*, 2000). Phosphylation of tabun and of its O-butyl analog was found to involve, as expected, displacement of cyanide from the phosphonocaynoamidate, yet the aging processes of the corresponding conjugates was only partially resolved. The aging of the butyl tabun-AChE conjugate was shown conclusively, by ESI-MS, to involve displacement of the dimethylamine moiety rather than elimination at the butoxy substituent. Yet, for the corresponding tabun conjugate, the macromolecular products of the two possible aging pathways (see Fig. 3) differ by 1 Da and therefore could not be unequivocally characterized by the ESI-MS method used (the accepted accuracy of ~100ppm precludes mass determination for over a 60000 Da protein with a single mass unit precision). The tryptic peptide bearing the active site of AChE was recently analysed by mass spectrometry as a strategy for direct elucidation of the mechanism of AChE inhibition by (1S,3S)-isomalathion (Doorn *et al.*, 2000).

A	Tryptic Peptides bearing the Active Site-Ser	Calculated Mass (Da)
TcAChE	^{193}TVTIFGE**S**AGGASVGMHILSPGSR^{216}	2331.18
HuAChE	^{178}LALQWVQENVAAFGGDPTSVTLFGE**S**AGAASVGMHLLSPPSR^{219}	4268.15

B

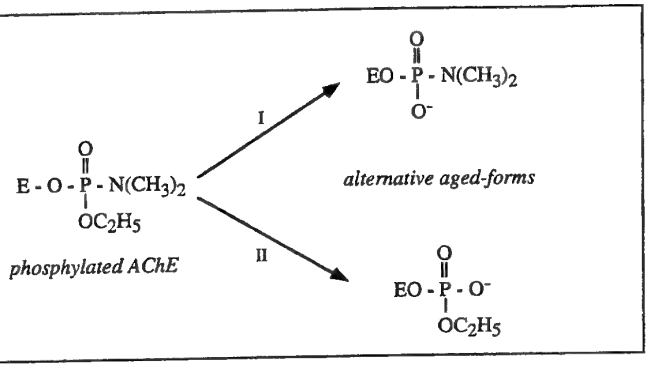

C		*phosphylated-AChE* calculated	measured	*aged-form* calculated I	calculated II	measured
Tabun	TcAChE	2466.21	2466.18	2438.20	2439.23	2439.17
	HuAChE	4403.20	4402.72	4375.20	4376.15	4375.70
Deuterated Tabun	TcAChE	2472.26	2472.32	2443.20	2439.23	2439.27
	HuAChE	4409.25	4408.92	4381.25	4376.15	4375.85

Figure 3: TcAChE and HuAChE Ser-active site peptides and their corresponding phosphoroamidyl-AChE conjugates. A. Sequence and mass of the Ser-active site peptides of TcAChE and of HuAChE generated by trypsin digestion. B. Scheme of alternative aging reaction pathways of the phosphoroamidyl-AChE conjugates. C. Table of calculated and measured molecular mass of the phosphylated active site Ser peptides following tryptic digestion of the corresponding TcAChE and HuAChE tabun-phosphylated and aged products.

In the present study we characterize the aging pathway of human acetylcholinesterase (HuAChE) with various OP agents, through a combined strategy involving tryptic digest of OP treated enzymes, stepwise elution of the peptide mixture by rapid ZipTip column fractionation, followed by MALDI-TOF/MS analysis. This methodology enabled accurate mass spectrometric peptide analysis for unequivocal assignment of phosphyl active site peptide adducts of modified AChEs from either *Torpedo californica* or human sources. It is concluded that this approach can be conveniently used for the determination of other OP-AChE conjugates and maybe applied for forensic studies aimed at identification of trace amounts of OP agents insecticides and other OP pollutants.

MATERIALS AND METHODS

Substrates and inhibitors - Acetylthiocholine iodide (ATC), toxogonine, paraoxon (p-nitrophenyl-diethyl phosphate) and 5:5'-dithiobis (2-nitrobenzoic acid) (DTNB) were purchased from Sigma. Generation of the alkyl N,N-dimethyl-phosphoramidocyanidates used in this study was carried out by modification of a previously published procedure (Holmstedt, 1951), using dimethylamidophosphoric dichloride and the appropriate alcohol. Phosphoroamidates were purified either by distillation (tabun, 72-74^{0}C/1.5mmHg) or by column chromatography (butyl analogue) to >95% purity (^{31}P NMR). Preparation of pinacolyl methylphosphonofluoridate (soman) was followed an accepted synthetic procedure using methylphosphonodifluoridate and alcohol (Monard and Quinchon, 1961). Generation of the ethyl *N,N*-dimethyl-d_6-phosphoroamidocyanidate used in this study was carried out by modification of a previously published procedure (Holmstedt, 1951), using *N,N*-dimethyl-d_6-amidophosphoric dichloride (prepared from *N,N*-dimethyl-d_6-amine hydrochloride and phosphorus trichloride), and ethanol. The hexadeutrio-phosphoroamidate was purified by distillation (89-92°C/25mmHg) to>95% purity (^{31}P NMR).

Recombinant HuAChE - Expression of recombinant HuAChE in a human embryonal kidney derived 293 cell line was described previously (Velan *et al.*, 1991a; Kronman *et al.*, 1992; Shafferman *et al.*, 1992a). Stable recombinant cell clone expressing high level of enzyme was established according to the procedure described previously (Kronman *et al.*, 1992), and the secreted enzyme in the cell supernatant was purified (over 90% purity) by affinity chromatography. TcAChE was a gift from Dr. I. Silman.

Kinetic studies and analysis of data - AChE activity was assayed according to Ellman *et al.* (Ellman *et al.*, 1961) (in the presence of 0.1 mg/ml BSA, 0.3mM DTNB 50mM sodium-phosphate buffer pH-8.0 and various concentrations of ATC), carried out at 27^{0}C and monitored by a Thermomax microplate reader (Molecular Devices).
Samples of inhibited-enzyme were prepared by mixing the enzyme (TcAChE or HuAChE) with an excess of one of the selected OP-inhibitor. Protein was separated from excess OP by ultrafiltration with centrisart column. The OP-enzyme conjugates were allowed to undergo aging from 24 to 72h. at 37°C.

AChEs proteolysis by trypsin - Five to ten μg of purified TcAChE or HuAChE were incubated in siliconized tubes at 37^{0}C for 2 h. in the presence of 20 μl of 50 mM Na^+ phosphate buffer, pH 8, 1 to 2 μg trypsin (Promega) and 20% acetonitrile (CH_3CN) (Merck). Following incubation, the tubes were evaporated to dryness in a Speed-vac centrifuge (Savant) and stored

at –20^{0}C until use. Glu-C, Chymotrypsin and Lys-C (Promega) proteolysis of HuAChE samples were similarly performed.

Sample preparation by ZipTip fractionation- Trypsinized AChE samples were suspended in 40 µl of 20% CH_3CN/0.1%TFA solution, and incubated at room temperature for 15 min. ZipTip (Millipore Co.) C-18 tips (for TcAChE fractionation) or C-4 tips (for HuAChE) were activated in 70%CH_3CN/0.1%TFA for 15 min, and then washed 5 times with 20 µl in 20% CH_3CN/0.1%TFA. The suspended AChE tryptic digests were adsorbed to the tips by 20 cycles of 10 µl aspirate and dispense. Stepwise elution was performed by 3 times 10 µl aspirate and dispense cycles into siliconized tubes containing 20 µl of different CH_3CN concentrations of (20%, 25%, 30%, 35%, 40%, 60% and 80%) in 0.1%TFA. MALDI-TOF/MS target was siliconized ("Sigmacot", Sigma) for 2-3 min, washed twice in double distilled water and allowed to dry at room temperature. Two µl of each elution fraction were applied to a MALDI-TOF/MS target well and allowed to dry in an oven at 37^{0}C. Two µl of 40% CH_3CN, 0.1%TFA saturated with α- cyano-4- hydroxycinnamic acid (cyano) matrix were added to each well and allowed to dry.

MALDI-TOF/MS analysis - Mass spectra were acquired on Micromass TofSpec 2E in positive ion reflectron mode, using source voltage of 20,000 volts, pulse voltage of 2600- 3000 and LASER intensity of 20%. External calibration using standard peptides was applied. Calculated monoisotopic mass for Ser active site bearing tryptic peptides were 2331.18 Da for TcAChE peptide (T^{193}-R^{216}), and 4268.15 Da for HuAChE (L^{178}-R^{219}) (Fig. 3A).

RESULTS AND DISCUSSION

Phosphorylation and phosphoroamidation reactions of AChEs proceed with different efficiencies and the properties of the resulting adducts vary in several respects. Phosphoryl-AChEs are usually stable to spontaneous reactivation, react quite rapidly with oxime reactivators and their propensity to undergo aging depends on branching of their alkoxy substituents (Michel *et al.*, 1967; Aldrich and Reiner, 1972; Segall *et al.*, 1993; Shafferman *et al.*, 1996a,b; Barak *et al.*, 1997b; Ordentlich *et al.*, 1999; Millard *et al.*, 1999a; Viragh *et al.*, 2000; Barak *et al.*,2000). On the other hand the stability of various phosphoramidyl-AChEs depends strongly on the nature of the phosphoramidyl moiety and varies from cases like methamidophos analogs that reactivate spontaneously (Langenberg *et al.*, 1988) to adducts with tabun like derivatives that react rather slowly with oxime reactivators. Also, aging of AChE adducts with alkyl N,N-dimethylphosphoroamidates was recently shown to proceed by a distinct pathway, which in the case of butyl-tabun was unequivocally demonstrated to involve replacement of the dimethylamino substituent (Barak *et al*, 2000). Since toxic phosphoroamidates like tabun are potential nerve agents while other derivatives like methamidophos are widely used as pesticides, further examination of the composition and properties of various phosphoramidyl-AChEs seems to be required.

In a recent study, ESI/MS of aged HuAChE adducts with both tabun and butyl- tabun showed a mass decrease of 28± 4 as compared to the non- aged adducts. This reduction in mass indicates that the aging of butyl-tabun-HuAChE involves the loss of dimethylamino group (-44 Da) concomitant with replacement by oxygen (+16 Da). As for the tabun conjugate, two alternative aging pathways could be considered: a. replacement of the dimethylamino moiety as in the butyl-tabun adduct - yielding a product with calculated molecular mass of 64808 Da; or b. elimination of the ethoxy moiety as in phosphate adducts such as diethylphosphoryl-AChE resulting in a product with calculated mass of 64807 Da (Barak *et al*, 2000). This small mass difference (~15 ppm) precludes an assignment of the actual aging product by the ESI-MS method used.

To achieve an unequivocal mass assignment of this aging product, mass analysis of proteolytic peptide mixture was considered, since the use of small fragments is bound to significantly improve the measurement accuracy. The MALDI-TOF/MS methodology was selected since this technology serves, at present, as the method of choice for accurate characterization of complex peptide mixtures, with an accuracy of less than 100 ppm (using external calibration, (Thomas *et al.*, 2000)). For a reliable measurement of 1 Da difference, the desired peptide mass should be, therefore, in the range of 1000-2500 Da. Accordingly, we have attempted to cleave the phospylated HuAChE enzyme in order to identify and determine such peptide bearing the phospylated active site Ser203. The potential use of a variety of proteases, such as Glu-C, Chymotrypsin, Lys-C, trypsin and their combination was examined, using MALDI-TOF/MS

analysis of the proteolytic digests (results not shown). Rather unexpectedly the various proteolytic digest experiments failed to produce resolvable peptides containing the active site serine, with the exception of the digest by trypsin (Fig. 3). Even in the case of the tryptic digest the peptide fingerprint was difficult to resolve. Thus, further fractionation of the proteolytic peptide mixture was needed for possible signal enrichment. In order to develop such a technique the AChE from *Torpedo Californica* (TcAChE) was used for which the resulting tryptic peptide containing the catalytic serine is anticipated to have a mass of 2331.18 Da (Fig. 3).

Direct application of the tryptic digest peptide mixture of untreated TcAChE resulted indeed in the identification of the expected peptide of 2331.19 Da, bearing the Ser catalytic site. However, as in the case of HuAChE, the observed peak signal was found to be weak (Fig. 4A) and irreproducible, probably due to ion suppression (Dai *et al.*, 1999a).

This well established phenomenon stimulated the development of various "sample preparation" methods, including matrix selection, mode of sample application on the target (Bundy and Fenselau, 1999) and sample cleanup (Dai *et al.* 1999b; Krause *et al.*, 1999). In the present study we approached the problem of sample preparation by developing a ZipTip stepwise elution method (see "Materials and Methods"). As seen in Fig. 4A-D, this method resulted in a dramatic signal enrichment and an almost exclusive appearance of the isotopically resolved desired peak, with the expected theoretical mass of 2331.18 Da (Fig. 4D and inset).

This approach was further tested with the well characterized aged product of butyl tabun inhibited AChE (Barak *et al.*, 2000) (Fig. 4E-H). The phosphorylated and aged peptides with the expected mass of 2494.26 Da and 2467.18 Da respectively, could be readily measured and exhibited isotopically resolved patterns only following stepwise elution, (see Fig. 4H and G, inset). This methodology was then applied to define the aging product of the tabun inhibited TcAChE. As seen in Fig. 3 aging through elimination of the ethoxy moiety should give rise to AChE- tabun product of 2438.20 Da (pathway I) while the elimination of the dimethylamino moiety should result in the formation of an 2439.23 Da tabun-AChE conjugate (pathway II). The MALDI-TOF/MS analysis of tryptic digest of TcAChE inhibited by tabun revealed the disappearance of the native catalytic serine bearing peptide (2331.17 Da) concomitantly with the appearance of two newly formed peaks with mass of 2466.18 and 2439.17 Da (Fig. 5 A,B). These two peaks could be assigned to the non-aged and aged forms of the tabun-inhibited TcAChE respectively. The mass of 2439.17 Da of the aged product suggests that aging of the TcAChE-tabun adduct proceeds via P-N bond scission since the alternative aging pathway should have resulted in generation of a product with an expected mass of 2438.20 (see Fig. 3). To verify that the measured 2439.17 Da peak indeed corresponds to the ethoxyphosphoryl-TcAChE, we analyzed adducts of TcAChE with paraoxon. In the case of paraoxon the initial diethoxy phosphoryl-TcAChE adduct can age only to the ethoxy phosphoryl-TcAChE and thus should have identical mass to that of the tabun aged product. Indeed, the observed mass of the aged form of paraoxon conjugate is 2439.13 Da as compared to the 2439.17 Da value observed for the aging product of tabun (Fig. 5B-C). These findings clearly demonstrate that the aging

pathway of the tabun-TcAChE conjugate proceeds through P-N bond scission (pathway II, Fig. 3).

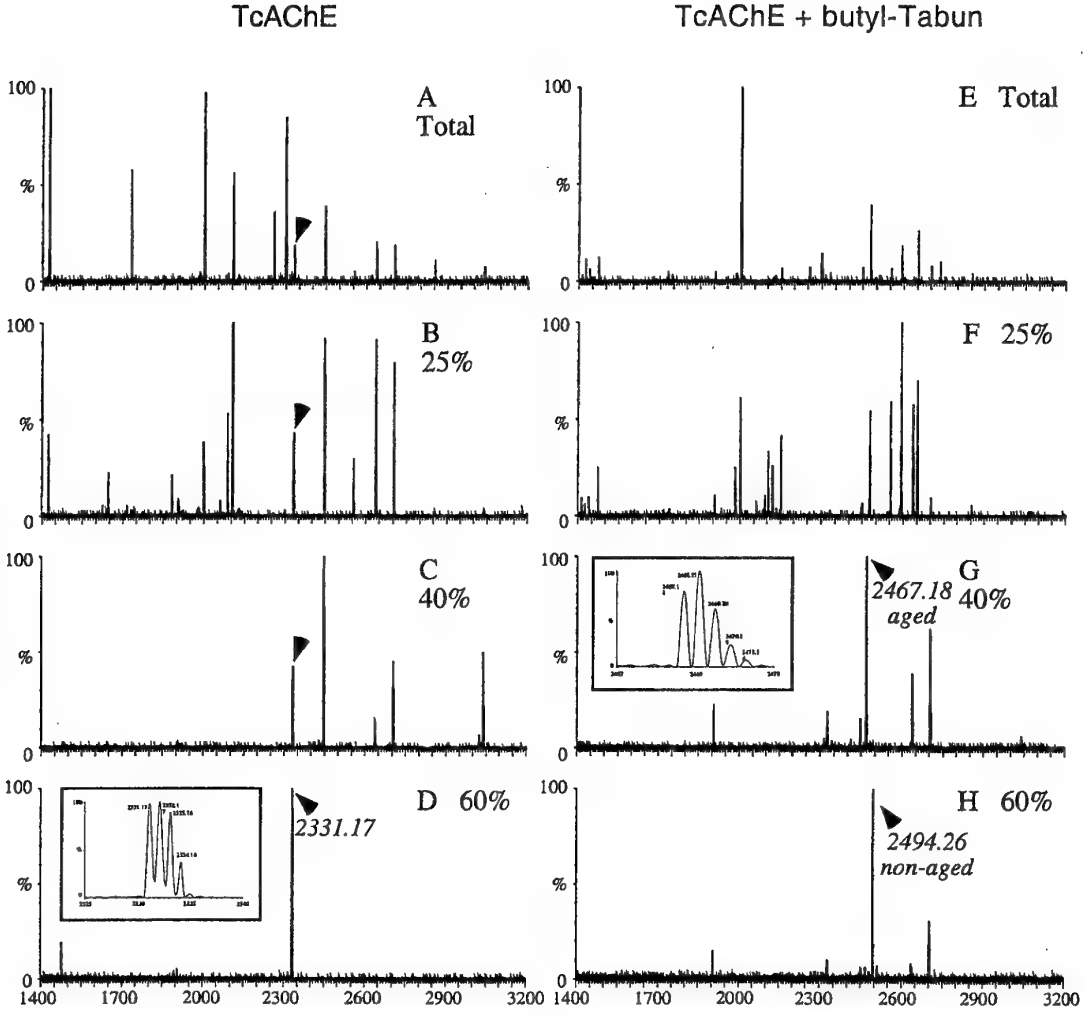

Figure 4: MALDI-TOF/MS spectra of tryptic digests of TcAChE and of its butyl tabun phosphylated conjugate following ZipTip stepwise elutions. 5 μg of free and butyl tabun phosphylated TcAChE enzymes were digested with 1 μg of trypsin (2 h, 37°C). The resulting peptide mixtures were adsorbed to ZipTip C-18 tips in 20%CH_3CN/0.1%TFA and eluted with increasing concentrations of CH_3CN as detailed in "Materials and Methods". Representative spectra of whole digest mixture before elution (total) and following the 25%, 40% and 60% CH_3CN elution of the native TcAChE (A-D) and of butyl tabun phosphylated TcAChE (E-H) are presented. Peptides bearing the active site serine, before and after reaction with butyl tabun are indicated with arrowheads. The isotopic resulotion of selected peaks is shown in inset (D,G).

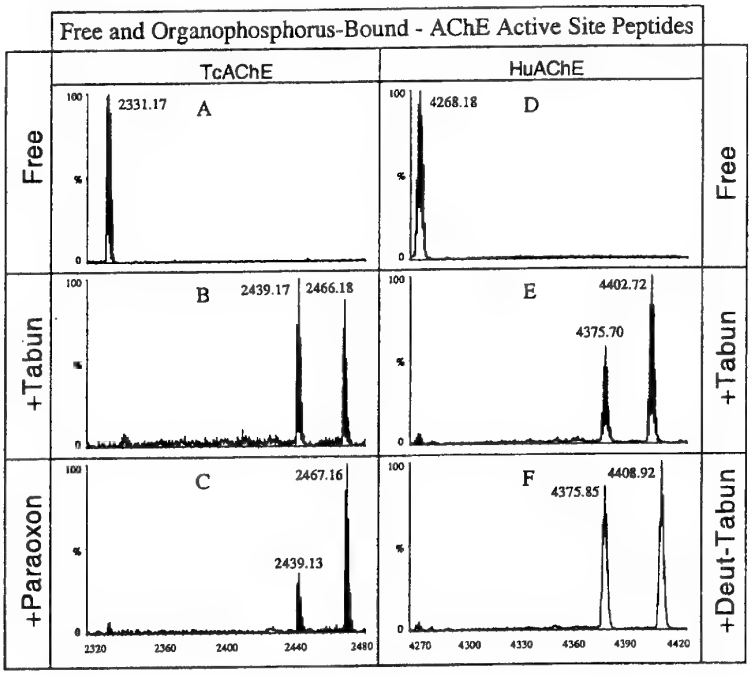

Figure 5: MALDI-TOF/MS spectra of tryptic digests of TcAChE or HuAChE before and after phosphylation by tabun, deuterated-tabun or paraoxon. 5 μg of free, tabun and paraoxon treated TcAChE were digested with 1 μg of trypsin. The resulting peptide mixtures were adsorbed to C-18 ZipTip and eluted step wise in CH_3CN as detailed in "Materials and Methods". Representative spectra of free TcAChE (A) tabun (B) and paraoxon (C) treated TcAChE are presented (60% CH_3CN eluted fractions). Similar experiments were performed with HuAChE with the following modifications: Ten μg of native, tabun and deuterated tabun treated HuAChE were digested with 2 μg of trypsin. The resulting peptide mixtures were adsorbed to ZipTip C-4, and eluted stepwise with CH_3CN as detailed in "Materials and Methods". Representative spectra of the native HuAChE (D) tabun (E) and deuterated tabun (F) treated HuAChE are presented (60% CH_3CN eluted fractions)

While the results with TcAChE demonstrate the applicability of the MALDI-TOF/MS methodology to phosphoramidate-AChE adducts and resolved the pathway of aging of tabun-TcAChE conjugate, the more relevant issue is the behavior of the analogous adducts with mammalian enzymes. Moreover there are documented instances of different interaction of active center inhibitors with TcAChE and mammalian enzymes like HuAChE and mouse AChE (Radic *et al.*, 1993; Ariel *et al.*, 1998). Upon treatment of HuAChE with tabun followed by tryptic digestion and ZipTip fractionation, two newly formed peaks with molecular mass of 4402.72 and 4375.70 were observed (Fig. 5E). The 4402.72 Da peak can be assigned to the non- aged form of the conjugate. Yet, due to the large size of the HuAChE tryptic Ser-peptide, the mass of the second peak, which presumably represent the aged product, could not provide a definite aging pathway assignment (see Fig. 3). To address this problem, we synthesized a hexadeuterio-tabun from the all-deuterio dimethylamine (see "Materials and Methods"). The non-aged adduct displayed, as expected, an increased mass of 6.05 Da, relative to the non-aged non-deuterated tabun-HuAChE (see Fig. 5E-F). According to Fig. 3, if now aging proceeds through pathway I, the aged fragment would gain an additional 6.05 Da, as compared to the

aged fragment arising by aging through pathway II. Since similar added mass (107.84±0.26) were detected for the aged forms obtained for deuterated tabun or tabun – HuAChE adducts, it is concluded that the aging of HuAChE proceeds through pathway II, namely loss of the dimethylamino moiety (Fig. 5 E-F). Experiments with tabun and hexadeutrio tabun were also performed with TcAChE. As in the case of HuAChE, the molecular masses of the phosphylated TcAChE Ser active site peptide differed by a mass of 6.14 Da (2466.18 and 2472.32) but following aging the corresponding two peptides had essentially identical masses (2439.17 and 2439.27). Taking together, these observations provide a definitive evidence that conjugates of both TcAChE or HuAChE with tabun, proceeds through P-N scission.

Table 3: MALDI-TOF/MS analysis of HuAChE[a] active site peptides conjugated to various OP agents

	OP-Agent	HuAChE-OP conjugate	Aged-Form
Soman	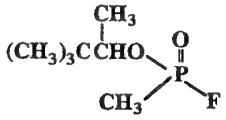 182.09 Da		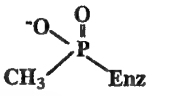 Calculated 4345.18 Da Measured 4345.18 Da
Methamido-phos	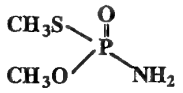 141.0 Da	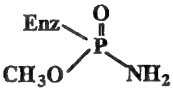 Calculated 4361.12 Da Measured 4361.28 Da	
Tabun	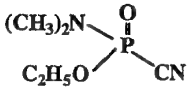 162.06 Da	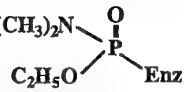 Calculated 4403.20 Da Measured 4402.72 Da	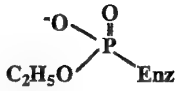 Calculated 4376.15 Da Measured 4375.70 Da
butyl-Tabun	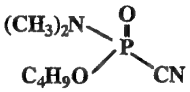 190.10 Da	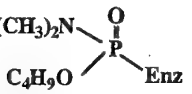 Calculated 4430.95 Da Measured 4430.95 Da	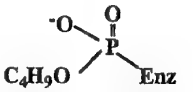 Calculated 4402.90 Da Measured 4402.90 Da
Deuterated-Tabun	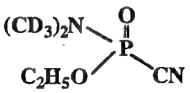 168.11 Da	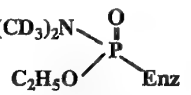 Calculated 4409.25 Da Measured 4408.92 Da	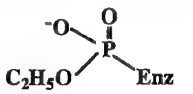 Calculated 4376.15 Da Measured 4375.85 Da

* The calculated and measured free HuAChE peptide mass are 4268.15 Da and 4268.48 Da, respectively

Another interesting question regarding AChE inhibition by phosphoroamidates is the nature of the reaction products with derivatives of methamidophos (Table 3). Previous studies, using

radiolabled methamidophos compounds demonstrated that the mechanism of Electric eel AChE inhibition by this ligand, proceeds through the loss of the methylthio moiety (Thompson and Fukato, 1982). In this work we applied our methodology for direct confirmation of the generality of this mechanism, using TcAChE as well as HuAChE. As seen in Fig. 6, only one new peak of 2424.18 Da (in TcAChE) or 4361.28 (in HuAChE), was detected, indicating the formation of AChE-methamidophos adducts in which the thiomethyl moiety is absent. In addition, the detection of the native peptides (2331.17 and 4268.18 in TcAChE and HuAChE respectively) following the processing of the fully inactive enzyme suggests that the enzyme undergoes spontaneous reactivation during sample preparation for MALDI-TOF/MS analysis. Spontaneous reactivation of the AChE-methamidophos adduct was observed and reported previously by De Jong *et al.*, (1982). Furthermore, it appears that the reactivation process does not include stable intermediates that could be detected by the MALDI-TOF/MS method, but rather proceeds in a single hydrolytic step.

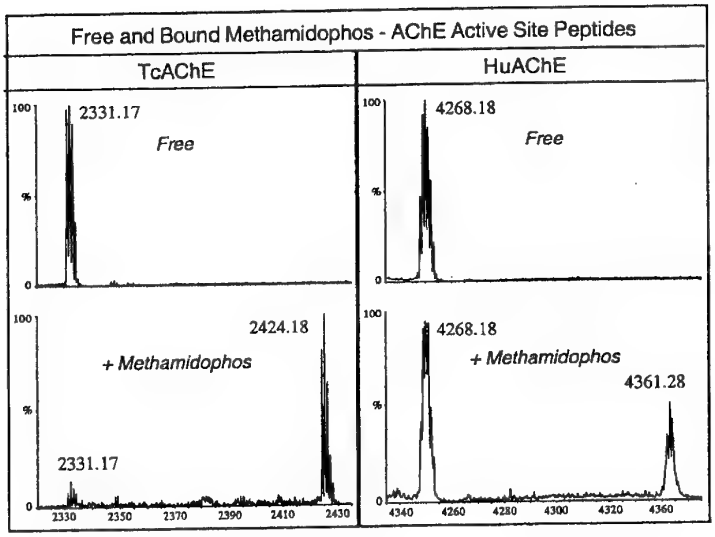

Figure 6: MALDI-TOF/MS spectra of tryptic digests of TcAChE or HuAChE before and after phosphylation by methamidophos. 5 μg of free, and methamidophos treated TcAChE and HuAChE were digested with trypsin as detailed in legend to Fig. 4. The resulting peptide mixtures were adsorbed to ZipTip and eluted stepwise in CH_3CN as detailed in "Materials and Methods". Representative spectra of 60% CH_3CN elutions of the free and methamidophos TcAChE and HuAChE treated enzymes are presented. The extent of spontaneous reactivation of the methamidophos-AChE adduct is demonstrated for HuAChE (due to a long time interval between incubation with inhibitor and tryptic digestion).

In this study we applied the method of MALDI-TOF/MS analysis of partially fractionated tryptic peptide mixtures for the determination of phosphoramide conjugates. Yet the relative facility of the experimental system and the ease of its application suggest that this method may be usefully applied for the unequivocal determination of HuAChE conjugates with other phosphorus derivatives like phosphates and phosphonates (see Table 3) and therefore may serve as a potent tool for other practical purposes like forensic studies or trace pollutant analyses.

IV. Engineering an Enzyme Mimic of Butyrylcholinesterase by Substitution of the Six Divergent Aromatic Acids in the Active Center of AChE.

INTRODUCTION

Acetylcholinesterase (AChE, EC 3.1.1.7) is a serine hydrolase whose function at the cholinergic synapse, is the rapid hydrolysis of the neurotransmitter acetylcholine (ACh). X-ray structures of AChEs from various sources (*Torpedo californica* - TcAChE; mouse - MoAChE; human – HuAChE; Drosophila - DAChE) show that the catalytic site is located near the bottom of a deep and narrow 'gorge', which penetrates halfway into the enzyme (Sussman *et al.*, 1991; Bourne *et al.*, 1995; Kryger *et al.*, 2000; Harel *et al.*, 2000). One of the striking features of this gorge is related to the presence of 14 aromatic residues, which line about 40% of its surface and which are highly conserved in enzymes from different species (Axelsen *et al.*, 1994). This complex array of aromatic residues was hypothesized to provide a guidance mechanism facilitating a two-dimensional diffusion of ACh into the active site (Axelsen *et al.*, 1994; Botti *et al.*, 1999; Koellner *et al.*, 2000) as well as for substrate accommodation (Ordentlich et al., 1993a; Vellom et al., 1993; Taylor and Radic, 1994; Barak et al., 1994; Botti *et al.*, 1999). Yet, butyrylcholineserase (BChE, acylcholine acyl hydrolase, EC 3.1.1.8), another type of cholinesterase found in vertebrates, catalyzes ACh hydrolysis as efficiently as AChE, although six of the active site gorge aromatic residues (72, 124, 286, 295, 297, 337 HuAChE numbering) are replaced by aliphatic amino acids (Harel *et al.*, 1992; Cygler *et al.*, 1993). On the other hand, AChE and BChE exhibit distinct substrate and inhibitor selectivities (Massoulie *et al.*, 1993) and some of the differences have been directly associated with the nature of the amino acids at each of these six positions (Shafferman *et al.*, 1992a; Ordentlich *et al.*, 1993a; Vellom *et al.*, 1993; Radic *et al.*, 1993; Barak *et al.*, 1994).

Early hypotheses (Jarv, 1984; ,Benschop and De Jong, 1988) and modeling experiments (Harel *et al.*, 1992; Barak *et al.*, 1992) indicated that the main functional difference between the AChE and BChE active sites is related to the structure of the acyl pocket, where residues corresponding to Phe295(*288*) and Phe297(*290*) are replaced by Leu and Val respectively. Indeed, studies of AChE by site directed mutagenesis and enzyme kinetics indicated that the acyl pocket residue Phe295 and to a lesser extent Phe297 determine specificity for phosphylating agents (Hosea *et al.*, 1995; Ordentlich *et al.*, 1996) and for the acyl moiety of substrates (Harel *et al.*, 1992; Ordentlich *et al.*, 1993a; Radic *et al.*, 1993; Vellom *et al.*, 1993), mainly by limiting the pocket size. Accordingly, BChE is more reactive than AChE toward bulky substrates like butyrylcholine (BCh) or organophosphorus inhibitors like diisopropyl phosphofluoridate (DFP) or paraoxon. In a similar manner, the about 5-fold higher affinity of BChE toward the active center inhibitor tacrine, as compared to that of AChE, can be related to the absence of an aromatic residue in position 337 (Tyr

in HuAChE and Ala in BChE) (Radic *et al.*, 1993; Loewenstein-Lichtenstein *et al.*, 1996; Ariel *et al.*, 1998).

These results as well as similar mutagenesis studies conducted on BChE (25,26) suggested that distinct substrate and inhibitor selectivity of the latter can be attributed mainly to a larger void at the active center and to a local structural modifications of the active center environment (Harel *et al.*, 1992; Ordentlich *et al.*, 1993a; Vellom *et al.* 1993; Gnatt *et al.*, 1994; Hosea *et al.*, 1995; Ordentlich *et al.*, 1996; Saxena *et al.* 1997a). However, this widely accepted view seems to be inconsistent with the finding that although the F295L AChE is almost as reactive as BChE toward butyrylthiocholine (BTC), its corresponding reactivity toward acetylthiocholine (ATC) is reduced relative to either wild type AChE or BChE (Ordentlich *et al.*, 1993a, Radic *et al.*, 1993). Further modification of the HuAChE acyl pocket, mimicking the composition in the HuBChE acyl pocket (the F295L/F297V enzyme), results in reactivity decrease toward both ATC and BTC compared to the F295L HuAChE (Taylor and Radic, 1994). In addition, recent examination of the stereoselectivity of the phosphonylation reaction of HuAChE active center mutants with soman isomers, suggests that although the AChE acyl pocket is an important determinant of the relative reactivity toward the P_S- and the P_R- diastereomers, the actual reactivity profiles of the acyl pocket mutant HuAChE, F295L/F297V, and the equine BChE toward soman are quite different (Ordentlich *et al.*, 1999).

In AChE residues Tyr72(*70*), Tyr124(*121*) and Trp286(*279*) are localized at or near the rim of the active center gorge and together with Asp74(*72*) and Tyr341(*334*) were shown to constitute the peripheral anionic subsite(s) (PAS) (Shafferman *et al.*, 1992b; Radic *et al.*, 1993; Barak *et al.*, 1994; Taylor and Radic, 1994). In BChE positions corresponding to 72, 124 and 286 are substituted by aliphatic amino acids, and consequently this enzyme is less reactive toward bisquaternary inhibitors like ambenonium and BW284C51, which bind to both the active center and the PAS or toward the PAS specific ligand fasciculin (Radic *et al.*, 1993; Vellom *et al.*, 1993; Radic *et al.*, 1994). Thus, the absence of aromatic residues at these positions makes the existence of a PAS on BChE questionable. Yet, affinity of BChE towards the peripheral ligand propidium was shown to be much higher than that of the MoAChE (Y72N/Y124Q/W286A) triple PAS mutant (Radic *et al.*, 1993). These studies as well as photoaffinity labeling studies (Schalk *et al.*, 1995; Nachon *et al.*, 1998) suggest that the ligand may bind at different loci in AChE and BChE. Thus the marked difference in affinities between AChE and BChE toward PAS ligands may not be related only to the absence of the three aromatic residues from the rim of the gorge (Masson *et al.*, 1996b). Moreover, the possible difference in the location of the PAS sites may be related also to the finding that modulation of catalytic activity at high substrate concentration, which is thought to involve substrate binding at the periphery, appears to be different for the two enzymes leading to substrate inhibition in AChE (Nachmansson and Wilson, 1951; Radic *et al.* 1991; Shafferman *et al.*, 1992b) and substrate activation in BChE (Cauet *et al.*, 1987 Masson *et al.*, 1996b, 1997, 1999).

In the present study, we further explore the differences between the functional architectures of AChE and BChE active centers, by systematic replacements of the relevant aromatic residues along the HuAChE active center gorge. Through comparison of the reactivities of single and multiple mutants

towards non-covalent inhibitors, we find that indeed the general architecture of the hexa-HuAChE mutant mimics the more spacious active center of BChE. Yet reactivities of the hexa-mutant toward certain covalent ligands such as substrates, transition state analogues and phosphonates reveal a significant functional impairment in the modified enzyme.

MATERIALS AND METHODS

Enzymes, reagents and inhibitor- Mutagenesis of AChE was performed by DNA cassette replacement into a series of HuAChE sequence variants, which conserve the wild type coding specificity (Soreq *et al.*, 1990a), but carry new unique restriction sites (Velan *et al.*, 1991a; Kronman *et al.*, 1992; Shafferman *et al.* 1992b). Generation of mutants W286A (*Trp279*), F295L(*Phe288*), F297V (*Phe290*), Y337A (*Phe330*) and the double mutant F295L/F297V was described previously (Ordentlich *et al.*, 1993a). Substitution of residues Y72N(*Tyr70*) and Y124Q(*Tyr121*) was carried out by replacement of the AccI-NruI and the NruI-NarI DNA fragments of the AChE-w4 variant (Shafferman *et al.* 1992b) with synthetic DNA duplexes, respectively. Generation of the double mutant Y72N/Y124Q was carried out by replacements of the AccI-DdeI as well as the DdeI-BstEII DNA fragments of the AChE-w3 variant (Shafferman *et al.* 1992b) with the respective fragments from the Y72N and Y124Q variants. The triple mutant Y72N/Y124Q/W286A was generated by inserting EcoRV-BstEII fragment carrying Y72N/Y124Q mutations into W286A AChE cDNA variant. The triple mutant F295L/F297V/Y337A was generated by replacement of the SalI-DdeI as well as the DdeI-Bsu36I DNA fragments of the neo-cat HuAChE expression vector (Velan *et al.*, 1993) with the respective fragments from the F295L/F297V and Y337A variants of AChE-w7 vector (Shafferman *et al.* 1992b). Construction of the hexa-mutant was carried out by ligation of the relevant DNA fragments from the two triple mutants variants (Y72N/Y124Q/W286A and F295L/F297V/Y337A), resulting in a DNA containing all six mutations (Y72N/Y124Q/W286A/F295L/F297V/Y337A), bounded by two unique restriction sites (EcoRV and Bsu36I) of the neo-cat vector (Velan *et al.*, 1993). Based on previously published genomic sequences of human BChE (Prody *et al.*, 1987; Arpagaus *et al.*, 1990), the complete coding cDNA sequence of BChE was reconstructed through ligation of PCR amplified exons. The full-length cDNA was inserted between the EcoRV-SalI sites, replacing the HuAChE sequences in the neo-cat -expression vector (Velan *et al.*, 1993). The sequences of all clones were verified by the ABI PRISM BigDye terminator reaction kit, using the ABI310 Genetic Analyzer (Applied Biosystems).

Procedures of transfection of human embryonal kidney-derived cell line (HEK-293) with expression vectors of recombinant enzymes (HuAChEs and HuBChE) and the generation of stable cell clones, expressing high levels of each of the various recombinant products, were described previously (Velan *et al.*, 1991a; Kronman *et al.*, 1992; Shafferman *et al.* 1992b). Acetylthiocholine iodide (ATC), butyrylthiocholine iodide (BTC), 5,5'-dithiobis (2-nitrobenzoic acid) (DTNB), ethyl(m-hydroxyphenyl)dimethylammonium chloride (edrophonium) di(*p*-allyl-N-dimethylamino-phenyl)-pentane-3-one (BW284C51), 1,10-bis(trimethylammonium)decane (decamethonium), 9-Amino-1,2,3,4-tetrahydroacridine hydrochloride hydrate (tacrine) and diisopropyl phosphorofluoridate (DFP) were purchased from Sigma. Synthetic (±)-huperzine-A was obtained from Calbiochem. m-(N,N,N-trimethylammonio)trifluoro-acetophenone (TMTFA) was prepared according to the procedure described by Nair *et al.* (1993).

Preparation of the racemic mixtures (45) of 2-butyl (IBMPF) and 1,2,2 trimethylpropyl (soman) methylphosphonofluoridates followed an accepted procedure using methylphosphonodifluoride and the appropriate alcohol. The P*s*C*s*-soman stereomer was prepared and purified as described before (Benschop *et al.*, 1984; Ordentlich *et al.*, 1999)

Determination of HuAChE Activity and Analysis of Kinetic Data - Activity of HuAChE enzymes was assayed according to Ellman *et al.* (in the presence of 0.1 mg/ml BSA, 0.3mM DTNB, 50mM sodium phosphate buffer pH-8.0 and various concentrations of ATC or BTC), carried out at 27°C and monitored by a Thermomax microplate reader (Molecular Devices). Enzyme concentration was determined by ELISA (Shafferman *et al.*, 1992a) and by active-site titration (Velan *et al.*, 1991a) using the P*s*C*s*-soman stereomer.

Michaelis-Menten constants (K_m) and the apparent first-order rate constants k_{cat} were determined according to the kinetic treatment described before (Shafferman *et al.*, 1992a,b). The apparent bimolecular rate constants k_{app} were calculated from the ratio k_{cat}/K_m. The behavior of either inhibition or activation at high substrate concentration can be described by Scheme 3 in which substrate molecule (S) binds to two different sites (Radic *et al.*, 1993). The dissociation constant for SE is K_{ss} and for SES is αK_{ss}, where α=1. Assuming that S binds to both E and ES, the parameter b reflects the efficiency with which the ternary complex SES forms product. If 0<b<1, there is substrate inhibition; if b>1, there is substrate activation and if b=1, the enzyme is said to have Michaelian behavior. K_m, K_{ss}, V_{max} and b were calculated by nonlinear curve fitting of Equation 1, using PRISM software (Graphpad).

Scheme 3:

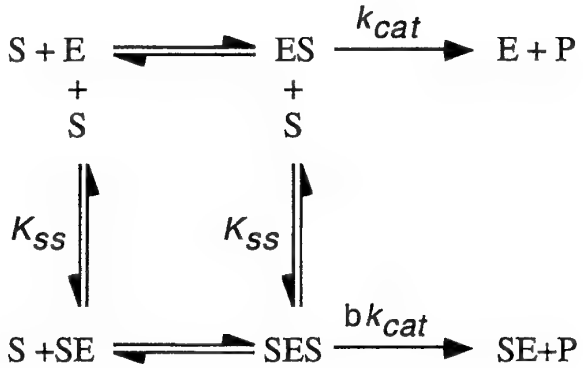

Equation 1:

$$v = \left(\frac{1 + b\,[S]/Kss}{1 + [S]/Kss}\right)\left(\frac{Vmax}{1 + Km\,[S]}\right)$$

Values of competitive inhibition constants (K_i) for the noncovalent inhibitors edrophonium, tacrine, huperzine A, BW284C51 and decamethonium were determined from the effects of various concentrations of the inhibitor on K_m and V_{max} of the enzyme - catalyzed hydrolysis of ATC. All the HuAChE enzymes examined formed rapid equilibria with the inhibitors, allowing for an immediate addition of increasing amounts of ATC to the enzyme - inhibitor mixture (preincubation of the enzymes with huperzine-A for 10 min, before addition of the substrate, or simultaneous mixing yielded the same results). The values of K_i were computed from the secondary plots of the apparent values of K_m (slopes of 1/V vs. 1/[S]) vs. concentrations of the respective inhibitors as described before (Ordentlich *et al.*, 1993a).

The apparent first order rate constants for the time-dependent inhibition of the wild type HuAChE mutants by TMTFA were determined by periodical measurement of the initial rate of substrate hydrolysis of aliquots taken from the reaction mixture. Following the kinetic treatment described by Nair *et al.* (1993, 1994) and assuming a two states inhibition mechanism, the values of k_{on} and k_{off} could be estimated from the linear plots of k_{obs} vs. inhibitor concentration, according to Equation 2.

Equation 2: $k_{obs} = k'_{on}\,[TMTFA] + k_{off}$.

Since in aqueous solution TMTFA is a mixture of the free ketone ($TMTFA_{ket}$) and the ketone hydrate ($TMTFA_{hyd}$), corrected values of the association rate constants were obtained from $k_{on} = k'_{on}(1+[TMTFA_{hyd}]/[TMTFA_{ket}])$, using the ratio of hydrated and ketone forms of TMTFA (62500) as determined by ^{19}F NMR (see Nair *et al.*, 1993). Direct measurements of k_{off} for WT-HuAChE, its hexa-mutant and HuBChE were determined from the rates of regeneration of enzymatic activity following removal of excess of free inhibitor by filtration through Centrisart C-4 microcentrifuge filters (Sartorius). The measured k_{off} values were in a good agreement with the calculated values.

Measurements of phosphylation rates, with HuAChE and its mutants, were carried out in at least four different concentrations of DFP, soman and IBMPF (I) and residual enzyme activity (E), at various time points, was monitored. The apparent bimolecular phosphylation rate constants (k_i) determined under pseudo-first order conditions, were computed from the slopes of the plots of ln(E) vs. time at different inhibitor concentrations. Rate constants under second order condition were determined from plots of ln{E/[Io-(Eo-E)]} versus time (Ordentlich *et al.*, 1999). Stereoselectivity of the enzymes towards various phosphonates, was determined by active-site titrations, comparing residual activities of enzymes inhibited by the appropriate racemic phosphonate to that of soman stereomer P*s*C*s* (Ordentlich *et al.*, 1993b).

Molecular Dynamics Simulation - All simulations were performed on an Octane Silicon Graphics workstation using the Dynamics execution and analysis modules of SYBYL 6.6 (Tripos 1999). AMBER all-atom parameter set was used throughout the simulations. The starting conformation of the wild type enzyme was obtained from the x-ray structure of the HuAChE-fasciculin complex model (Harel *et al.*, 2000, structure 1b41 on the Protein Data Bank) by removal of the ligand and relaxation of the contact regions. The essential water molecules W659 and W670 (Harel *et al.*, 2000) were retained throughout the simulations. Models of the HuAChE mutants were obtained by relaxation of the appropriately modified structures. One hundred and forty seven residues were involved in the simulation. Initial equilibrations at 300° K (20 ps) were followed by 160 ps of dynamics runs at 400° K with constrained main chain.

RESULTS

According to the molecular models of BChE proposed in the past (Harel *et al.*, 1992; Millard and Broomfield, 1992), out of about 30 residues lining the active site gorge, only 10 amino acids differ between HuAChE and HuBChE. Six of these changes involve substitutions of aromatic residues in HuAChE by non-aromatic residues in HuBChE (the other four, V73I*(71)*, S125T*(122)*, L289V*(282)*, S293T*(286)*, being conservative replacements). In order to further investigate whether this diminished "aromatic lining" of the BChE active site gorge is the main determinant of its distinct ligand selectivity, a HuAChE enzyme carrying appropriate replacements of all the six aromatic residues, has been generated (Y72N/Y124Q/W286A/F295L/F297V/Y337A). In addition, triple HuAChE mutants, with BChE–like replacements at the active center (F295L/F297V/Y337A) and the peripheral site (Y72N/Y124Q/W286A) were constructed. These multiple HuAChE mutants, together with the previously examined HuAChE derivatives carrying double and single aromatic residue replacements, were used to examine whether gradual "butyrylization" of HuAChE leads to increasingly BChE-like reactivity characteristics towards substrates, non-covalent and covalent inhibitors shown in Fig. 7.

Table 4: Kinetic parameters of hydrolysis of acetylcholine and butyrylcholine by HuBChE, HuAChE and its mutants

HuAChE Type	ATC K_m (mM)	ATC k_{cat} (x10^{-5}) (min^{-1})	ATC k_{cat}/K_m (x10^{-8}) ($M^{-1}xmin^{-1}$)	BTC K_m (mM)	BTC k_{cat} (x10^{-5}) (min^{-1})	BTC k_{cat}/K_m (x10^{-8}) ($M^{-1}xmin^{-1}$)
Wild Type	0.14	4.0	29	0.30	0.08	0.3
Y72N	0.14	5.4	38	0.14	0.09	0.7
Y124Q	0.19	4.5	24	0.16	0.25	1.5
W286A	0.25	4.1	16	0.20	0.27	1.4
F295L	0.25	1.0	4	0.04	0.26	6.5
F297V	0.78	1.5	1.9	0.25	0.60	2.7
Y337A	0.09	1.4	16	0.24	0.03	0.1
Y72N/Y124Q	0.14	4.1	29	0.25	0.20	0.8
F295L/F297V	1.3	0.5	0.4	0.42	0.43	1.2
Y72N/Y124Q/W286A	0.26	4.7	18	0.20	0.19	1.0
F295L/F297V/Y337A	2.9	0.8	0.3	0.90	0.55	0.6
Y72N/Y124Q/W286A/F295L/F297V/Y337A	4.7	0.8	0.2	3.3	1.5	0.5
HuBChE	0.04	0.5	13	0.05	1.1	22

*Values represent means of triplicate determinations with standards deviation not exceeding 20%.

Hydrolytic activity toward ATC and BTC - As already observed in the past wild type HuAChE and HuBChE display similar reactivity toward ATC, with bimolecular rate constants of $2.9 \cdot 10^9$ and $1.3 \cdot 10^9$ $M^{-1} \cdot min^{-1}$ respectively (see Table 4). No significant substrate selectivity of HuBChE is evident with respect to ATC and BTC, as the corresponding values of K_m and k_{cat} are similar for both substrates. On the other hand, HuAChE displays nearly 100-fold selectivity for ATC over BTC, with most of this reactivity decrease originating from the 50-fold difference between the corresponding values of k_{cat} (see Table 4).

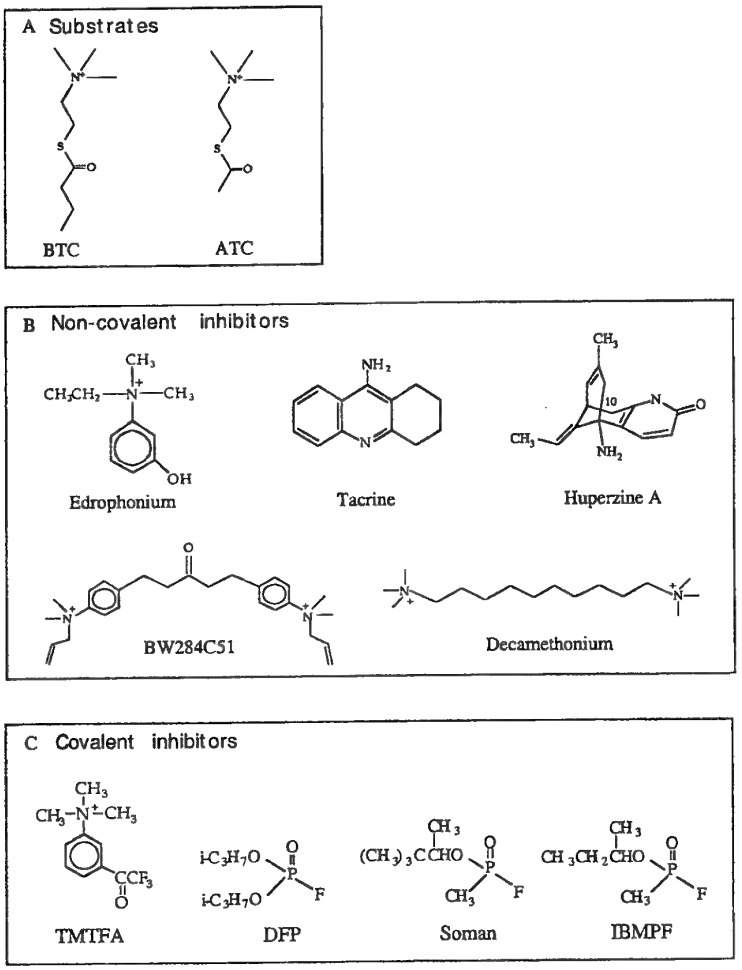

Figure 7: Chemical formulae of ligands used in this study.

The hexa-mutant HuAChE (Y72N/Y124Q/W286A/F295L/F297V/Y337A) exhibits low catalytic activity toward both ATC and BTC with bimolecular rate constants of $2 \cdot 10^7$ and $5 \cdot 10^7$ $M^{-1} \cdot min^{-1}$ respectively (see Table 4). In fact, catalytic activities (k_{app}) of the hexa-mutant HuAChE for ATC and BTC are approximately 65 and 45 fold lower respectively, than the corresponding values of HuBChE. It appears that this large difference in reactivity between the hexa-mutant and HuBChE is mainly associated with an increase in K_m values (4.7mM vs. 0.04mM for ATC and 3.3mM vs. 0.05mM for BTC). We note also that K_m values for both BTC and ATC of hexa-mutant HuAChE are higher (10-30 fold) than those determined for the wild type HuAChE enzyme. Furthermore, the k_{cat} values for hydrolysis of substrates by the hexa-mutant appear to be also affected relative to the wild type enzyme. For ATC we find a slight decrease (5 fold) but for BTC an increase (approx. 20 fold) in k_{cat} values relative to HuAChE.

The reactivity characteristics of the hexa-mutant HuAChE toward ATC are fully reproduced in the F295L/F297V/Y337A HuAChE and to a lesser extent in the double-mutant F295L/F297V. For both of these triple and double mutant enzymes a 9-20-fold increase of the K_m values and a 5-8-fold decrease of the k_{cat} values relative to the wild type HuAChE were observed. The hexa-mutant HuAChE and the triple and double active center mutants, also display similar catalytic activities toward BTC. The observation that reactivity toward substrates is determined predominantly by mutations at the active center is consistent with the lack of corresponding effects due to the multiple mutations at the PAS. Thus, the catalytic activities of the triple PAS mutant Y72N/Y124Q/W286A HuAChE toward ATC and BTC are comparable to those of the wild type enzyme.

In conclusion, with respect to ATC the values of the bimolecular rate constants (k_{app}) of the hexa-mutant or the F295L/F297V/Y337A HuAChEs are about 2-orders of magnitude lower than those of either the wild type HuAChE or the HuBChE enzymes. For BTC the values of k_{app} for these hexa- and triple-mutant HuAChEs are comparable to those of the wild type HuAChE and accordingly about 40-fold lower than that of HuBChE.

Substrate inhibition - Hydrolytic activities of HuAChE and HuBChE show different dependence on substrate concentration, with the former exhibiting substrate inhibition at [ATC] > 2mM, while for the latter, substrate activation has been reported at BTC concentration range of 20-40mM and substrate inhibition at [BTC] > 40mM (31,51). Effects of excess substrate on hydrolytic activity of HuAChE enzymes carrying single and multiple replacements of aromatic residues along the active site gorge were examined according to a kinetic model depicted in Scheme 3. The experimental values of factor b (see Scheme 3) are a measure of relative activity of the complexes ES and SES (b>1 demonstrates substrate activation while b<1 substrate inhibition).

As already shown before (Shafferman *et al.*, 1992b; Radic *et al.*, 1993), single replacements of residues Tyr72, Tyr124 and Trp286 at the periphery and of residue Phe295 at the active center affects secondary ATC binding to the enzyme (reflected in the values of K_{ss}) but has no effect on corresponding values of factor b (see Table 5). On the other hand, replacements of residues Phe297 and Tyr337 abolished substrate inhibition by ATC (Shafferman *et al.*, 1992b; Vellom et al., 1993).

Unlike the case of ATC, the secondary binding constant of BTC to the Y72N enzyme resembles that of the wild type HuAChE. In addition, substrate inhibition by excess of BTC is not abolished by replacement of Phe297.

Table 5: Kinetic parameters* for substrate inhibition/activation of HuBChE, HuAChE, and its mutants.

HuAChE Type	ATC		BTC	
	Kss (mM)	b	*Kss* (mM)	b
Wild Type	6±1	0.2±0.02	3±1	0.4±0.1
Y72N	21±8	0.3±0.1	2±0.6	0.5±0.1
Y124Q	15±3	0.2±0.1	11±3	0.1±0.1
W286A	16±8	0.3±0.1	30±10	0.4±0.1
F295L	28±3	0.3±0.1	20±2	0.1±0.02
F297V	1±0.5	0.9±0.1	50±10	0.4±0.1
Y337A	-	0.9±0.2	8±2	0.8±0.1
Y72N/Y124Q	20±7	0.3±0.1	24±4	0.1±0.1
F295L/F297V	-	1.0±0.1	-	1.0±0.1
Y72N/Y124Q/W286A	15±2	0.5±0.1	20±5	0.5±0.2
F295L/F297V/Y337A	-	1.0±0.1	-	1.0±0.2
Y72N/Y124Q/W286A/F295L/F297V/Y337A	-	0.9±0.2	-	1.0±0.1
HuBChE	4±1	1.9±0.2	1±0.2	2.4±0.2

*The kinetic parameters were determined according to Equation 1 (see Material and Methods).

In case of the F295/F297V and the F295/F297V/Y337A HuAChE mutants no substrate inhibition could be observed for both ATC and BTC (see Table 5; b = 1.0). The hexa-mutant HuAChE is also insensitive to substrate inhibition by ATC and BTC, at the concentration range tested, with similar b values. Notably, none of the mutant HuAChE enzymes exhibited a switch from substrate inhibition to substrate activation. In MoAChE substrate activation has been reported for the F297I enzyme (Radic *et al.*, 1993). Thus it appears that the structural features distinguishing between AChE and BChE with respect to substrate inhibition/activation are not dependent only on the aromatic residues lining the respective active site gorge. This observation is consistent with the b values (see Equation

1) reported for BChE mutants where aromatic residues have been introduced to mimic the AChE sequence (Masson *et al.*, 1996b; Saxena *et al.*, 1997a). In these cases substrate activation persisted in analogy to the wild type BChE.

Reactivity toward the AChE transition state analog TMTFA - The kinetics of AChE inhibition by TMTFA has been studied extensively since the AChE-TMTFA tetrahedral covalent adduct is believed to resemble the transition state of the acylation process (Nair et al., 1993, 1994; Ordentlich *et al.*, 1998). On the other hand, only very recently a comparable reaction with BChE has been described (Viragh *et al.*, 2000). Thus, comparison of TMTFA reactivities toward the wild type and certain mutant HuAChEs as well as HuBChE could shed new light on the effects of structural differences in the active center gorge on accommodating and covalently binding of substrates.

TMTFA was found to be a time dependent inhibitor of HuAChE and its mutants, as well as of HuBChE, showing linear dependence of the pseudo-first order rate constants of inhibition (k_{obs}) on inhibitor concentrations (Nair et al., 1993, 1994). The bimolecular rate constants k_{on} and the dissociation rate constants k_{off}, were calculated from the relation $k_{obs} = k_{on}[TMTFA]+k_{off}$ and corrected for hydration of the free ketone (see "Materials and Methods"). Values of k_{off} for the different enzymes were also determined directly by monitoring the regeneration of hydrolytic activity from the corresponding adducts and found to be in good agreement with those determined according to the above equation (see Table 6).

Comparison of TMTFA reactivities toward wild type HuAChE and toward HuBChE shows that while the values of k_{on} are practically equivalent ($1.9 \cdot 10^{11}$ and $1.7 \cdot 10^{11}$ $M^{-1} \cdot min^{-1}$ respectively), the dissociation rate constant (k_{off}) of HuBChE-TMTFA adduct is 66-fold higher than that of the corresponding HuAChE conjugate (see Table 6). The value of k_{on} for TMTFA inhibition of the hexa-mutant HuAChE is 170-fold lower than that of HuBChE and the corresponding value of k_{off} is 13-fold lower. Thus, "butyrylization" of the HuAChE active center both fails to reconstitute the functional environment of HuBChE necessary for high reactivity toward TMTFA, and impairs the corresponding functional architecture of HuAChE. While most of the impairment is due to mutations at the HuAChE acyl pocket (see Table 6), a small effect due to modifications at the PAS, could be observed (the value of k_{on} for the Y72N/Y124Q/W286A HuAChE is 3-fold lower than that for the wild type enzyme). Therefore the 190-fold decrease in the value of k_{on} for the hexa-mutant HuAChE, relative to that of the wild type enzyme, results predominantly from the triple replacements at the active center.

Table 6: Inhibition rate constants of HuBChE, HuAChE, and its mutants by the transition analogue TMTFA

HuAChE Type	TMTFA k_{on} [a] ($\times 10^{-9}$ M^{-1} min^{-1})	TMTFA k_{off} [a] ($\times 10^{4}$ min^{-1})	TMTFA Relative k_{on} (WT/mutant)	ATC Relative k_{app} [c] (WT/mutant)
Wild Type	190	6[b]	1	1
Y337A	250	5	0.8	1.8
F295L/F297V	4	20	50	73
Y72N/Y124Q/W286A	63	25	3	1.6
F295L/F297V/Y337A	6	55	32	97
Y72N/Y124Q/W286A/F295L/F297V/Y337A	1	30[b]	190	145
HuBChE	170	400[b]	1.1	2.2

[a] Values of k_{on} and k_{off} were determined from slope and intercept, respectively, of the plots of k_{obs} vs. five different concentrations of [TMTFA] (spanning the range of one order of magnitude), with correlation coefficients of at least 0.95 (see "Material and Methods").
[b] Values of k_{off} were determined from the rates of regeneration of hydrolytic activity following removal of free Inhibitor: WT-HuAChE= 4×10^{-4} min^{-1}; Y72N/Y124Q/W286A/F295L/F297V/Y337A=40×10^{-4} min^{-1} and HuBChE=300×10^{-4} min^{-1}.
[c] Values are according to results depicted in Table 1.

Multiple mutations at the HuAChE active center gorge appear to decrease the stability of the corresponding HuAChE-TMTFA conjugates (see Table 6). Yet the value of k_{off} for the hexa-mutant conjugate is merely 5-fold higher than that for the wild type HuAChE (and 13-fold lower than that for HuBChE), suggesting again that the active center environments participating in stabilization of the TMTFA tetrahedral intermediates with HuBChE and with hexa-mutant HuAChE are quite different.

Reactivity toward organophosphate inhibitors - While reactions of AChE with substrates and with TMTFA involve rapid formation of covalent tetrahedral intermediates, interaction of ChEs with organophosphate inhibitors like soman, IBMPF or DFP is thought to involve initial formation of a noncovalent complex with the tetrahedral species (Ordentlich *et al.*, 1996; Aldrich and Reiner, 1972; Main, 1976). Thus the inhibitory activity of these agents may further probe the influence of a modified AChE active center environment on the emergence of tetrahedral intermediates in reactions with substrates.

Reactivities of the bulky phosphate DFP toward the hexa-mutant HuAChE and toward HuBChE were found to be very similar and 150-166-fold higher than the corresponding activity toward the wild type HuAChE (Table 7). This reactivity enhancement toward DFP may result from the space-creating replacements at the acyl pocket (Ordentlich *et al.*, 1996) as well as from the replacements at the PAS. These findings are consistent with the recently reported x-ray structure of an aged AChE-DFP conjugate, where both the acyl pocket and part of the PAS seem distorted due to interaction

with the phosphoryl isopropoxy substituent (Millard *et al.*, 1999a). The notion that space creating mutations at both the HuAChE acyl pocket and the PAS result in a HuBChE-like binding environment for the bulky phosphoryl substituents, is consistent also with the stoichiometry of the hexa-mutant phosphonylation by racemic methylphosphonates. While the stoichiometry of reactions of HuBChE with racemic soman and IBMPF is 1:1 (indicating a relatively low stereoselectivity of this enzyme toward the corresponding phosphonate P*s*-diastereomers), equivalent reactions of both the wild type and the F295L/F297V/Y337A HuAChEs display 2:1 stoichiometry (see Fig. 8). However, reaction of the hexa-mutant HuAChE with IBMPF proceeds with 1:1 stoichiometry, indicating that the respective stereoselectivity of this enzyme is lower than that of the F295L/F297V/Y337A HuAChE, and may in fact be similar to that of HuBChE. Yet, the acyl pockets of HuBChE and of hexa-mutant HuAChE are not structurally equivalent, as indicated by the fact that the latter still displays 2:1 stoichiometry in reaction with the somewhat bulkier soman (see Fig. 8).

Table 7: Kinetic constants[a] of phosphylation reactions of HuBChE, HuAChE, and its mutants by DFP, soman, and IBMPF

HuAChE Type	k_i [a] (x10^{-4} M^{-1} min^{-1})		
	DFP	Soman	IBMPF
Wild Type	10 (1)[b]	10000 (1)	13000 (1)
Y72N/Y124Q	16 (0.6)	11000 (1)	15000 (1)
F295L/F297V	800 (0.01)	280 (36)	500 (26)
Y72N/Y124Q/W286A	30 (0.3)	13300 (0.8)	18000 (0.7)
F295L/F297V/Y337A	150 (0.07)	120 (85)	100 (130)
Y72N/Y124Q/W286A/F295L/F297V/Y337A	1500 (0.01)	50 (200)	290[c] (45)
HuBChE	1660 (0.01)	4000[c] (2.5)	4000[c] (3)

[a] Values were determined with five different concentrations of inhibitor (spanning the range of one order of magnitude) with standard deviation not exceeding 20%.
[b] The number in parentheses represents the ratio between the rate constant of WT-HuAChE to that of the rate constant of the corresponding mutant.
[c] Stoichiometry ratio of 1:1 was obtained by active site titration for the indicated mutants (for all other enzymes the stoichiometry ratio was 1:2).

In contrast to the nearly equivalent reactivities of the hexa-mutant HuAChE and the HuBChE toward DFP, the corresponding reactivities toward the two methyl-phosphonates soman and IBMPF were surprisingly different. For these organophosphate inhibitors we find a decrease in the hexa-mutant reactivity of 80 to 14 fold relative to HuBChE (note that corresponding decrease in reactivity relative to the wild type HuAChE is even greater, see Table 7). While affinities of HuAChE enzymes carrying replacements at the PAS toward the two methyl-phosphonates resemble those of the wild type enzyme, replacements at the active center result in 40-80 and 30-130 fold drop in the corresponding affinity for the F295L/F297V and the F295L/F297V/Y337A HuAChEs toward soman and IBMPF respectively. These results indicate that the relative destabilization of the hexa-mutant-HuAChE- methyl-phosphonate complexes (15 -200-fold as compared to wild type HuAChE or to HuBChE) is entirely due to mutations at the active center. These observations cannot be rationalized by an inferior accommodation of the phosphonyl methyl substituent in the more spacious acyl pocket, since a similarly composed acyl pocket in the HuBChE does not produce the same effect. Thus, unlike the case of DFP, accommodation of tetrahedral species with lower steric demands at the active center acyl pocket, seems to be different for the hexa-mutant HuAChE and for HuBChE. This difference appears to be common to the various tetrahedral species formed in the AChE active center either by noncovalent binding (methyl-phosphonates like soman or IBMPF) or through formation of covalent intermediates (substrates, TMFTA).

Reactivity toward noncovalent inhibitors - The functional architecture of HuAChE enzymes carrying multiple replacements of aromatic residues at the active center gorge and its possible resemblance to that of BChE, was further investigated through interactions with noncovalent inhibitors. Prototypical active center ligands like edrophonium, tacrine and huperzine A, as well as BW284C51 and decamethonium, the ligands bridging the active center and the PAS, were used to probe the changes in affinity resulting from removal of aromatic residues from the previously defined binding subsites (Ordentlich *et al.* 1993a; Barak *et al.*, 1994; see Table 8).

a. *Edrophonium*: Examination of the effects of single replacements of aromatic residues at the active center on enzyme reactivity toward edrophonium (Barak *et al.*, 1994; Ordenlich *et al.* 1995) indicated that only substitutions of Tyr337 and Phe297 by aliphatic residues had some effect on binding (8-fold and 6-fold respectively). The loss of reactivity toward edrophonium, observed for the hexa-mutant HuAChE, is 170-fold compared to the wild type HuAChE, and its inhibition constant is equivalent to that measured for HuBChE (Table 8). We note that most of this effect is contributed by the combined replacements of all the three aromatic residues at the active center, as manifested by the fact that the measured values of K_i for the F295L/F297V/Y337A and the Y72N/Y124Q/W286A HuAChEs are 53μM and 1.1μM respectively, while that of HuBChE is 50μM.

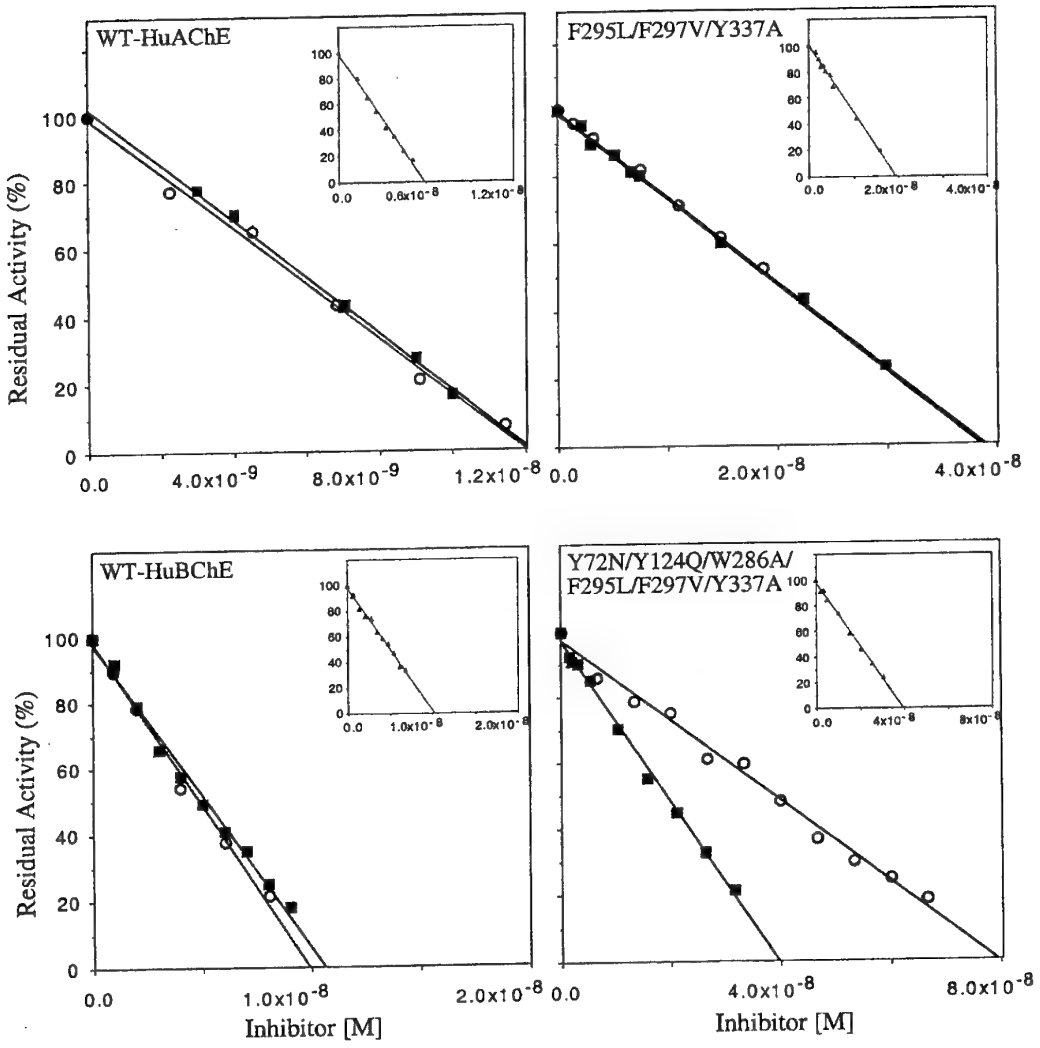

Figure 8: Comparison of active site titration profiles of HuAChE, the triple active center mutant F295L/F297V/Y337A, hexa-mutant of HuAChE and HuBChE with soman and IBMPF. For each enzyme preparation active site concentration was determined using the P*s*C*s*-soman stereomer which reacts in all cases with 1:1 stoichiometry (see inset). For both racemic soman (○) and racemic IBMPF (■) the wild-type HuAChE and its triple mutant display approximately stoichiometric ratios of 2:1 while the HuBChE exhibits a ratio of 1:1. In the case of the hexa-mutant of HuAChE the stoichiometric ratios for racemic soman and IBMPF are 2:1 and 1:1, respectively.

b. Tacrine: Previous studies with this active center inhibitor have shown that its binding is affected predominantly by residues of the HuAChE "aromatic patch" (Trp86, Tyr133, Tyr337) (Ariel *et al.*, 1998). In particular, replacement of the aromatic residue at position 337 by Ala increased the affinity of the resulting mouse (Radic *et al.*, 1993) and human (Ariel *et al.*, 1998) AChEs toward tacrine, and could partially account for the higher affinity of tacrine toward BChE (Ordentlich *et al.*, 1993a). Residue Tyr337 is substituted also in the multiple active center mutant HuAChEs (F295L/F297V/Y337A and hexa-mutant) and is probably contributing to the minor 5-fold increase in affinity of these enzymes for tacrine. Moreover, the values of dissociation constants for tacrine complexes with these HuAChE enzymes are practically equivalent to that with HuBChE (Table 8). This again suggests that the active center regions of the hexa-mutant HuAChE, probed by ligands like tacrine are quite similar to those in HuBChE. As could be expected from previous studies (Ariel *et al.*, 1998), replacement of aromatic residues at the PAS has no effect on tacrine binding.

c. *Huperzine A*: HuAChE reactivity toward this bulky inhibitor was previously shown to be affected significantly by replacements of active center residues which did not seem to be directly involved in the accommodation of this ligand (Ariel *et al.*, 1998; Ordentlich *et al.*, 1998). This may be exemplified by the large effects of mutation of the oxyanion hole residue Gly121 or the adjacent residue Gly122 on huperzine A binding (Ordentlich *et al.*, 1998). Therefore the relatively minor effects due to single replacements of aromatic residues at the active center or the PAS are difficult to explain in terms of specific interactions with the ligand. The exception is residue Tyr337, the replacement of which has been long known to lower affinity toward huperzine A (Ashani *et al.*, 1994; Saxena *et al.*, 1994), probably due to loss of cation-π interaction with the ligand amine moiety (Ariel *et al.*, 1998). Thus, the 1250-fold drop in affinity toward huperzine A of the F295L/F297V/Y337A HuAChE (Table 8), as compared to the wild type enzyme, seems to result mostly from the replacement at position 337. However, since replacements of aromatic residues at the PAS do not seem to affect reactivity toward huperzine A (e.g. Y72N/Y124Q/W286A HuAChE, see Table 8), the structural basis for the further decrease in affinity of the hexa-mutant toward this ligand is unclear. In any case, the dissociation constant of the huperzine A-hexa-mutant HuAChE complex is 25,000 fold higher then that of wild type HuAChE and only 8-fold higher than that of the corresponding complex with HuBChE. This underscores the similarity of the molecular environments of the hexa-HuAChE mutant and HuBChE as sampled by this ligand.

Table 8: Inhibition constants[a] of HuBChE, HuAChE, and its mutants by noncovalent ligands.

HuAChE Type	Edrophonium K_i (μM)	Huperzine A K_i (nM)	Tacrine K_i (nM)	Decamethonium K_i (μM)	BW284C51 K_i (nM)
Wild Type	0.3	16	57	4.6	10
Y72N/Y124Q	1.1	90	55	200	270
F295L/F297V	2.2	50	60	210	55
Y72N/Y124Q/W286A	1.1	30	35	260	8000
F295L/F297V/Y337A	53	20000	9	210	920
Y72N/Y124Q/W286A/F295L/F297V/Y337A	50	400000	12	360	170000
HuBChE	50	50000	12	2.5	14000

[a]Values were determined with five different concentrations of inhibitor (spanning the range of one order of magnitude) with standard deviation not exceeding 20%.

d. BW284C51: This bisquaternary ligand has long been known to display an over 3 orders of magnitude selectivity toward AChEs as compared to BChE (Aldrich and Reiner, 1972). It binds along the AChE active site gorge spanning the binding sites at the active center and the PAS (Barak *et al.*, 1994; Silman *et al.*, 1994). Indeed, the affinity of HuAChE enzymes toward this inhibitor is affected by perturbations at both the active center and the PAS with affinity decreases of 800-fold and 92-fold for Y72N/Y124Q/W286A and F295L/F297V/Y337A HuAChEs respectively. The corresponding affinity of the hexa-mutant HuAChE seems to reflect approximately the contributions of the structural changes at the two binding subsites. The hexa-mutant HuAChE is about 12-fold less reactive toward BW284C51 than the HuBChE. Since the structural motif of BW284C51 interacting with the AChE active center resembles edrophonium (Barak *et al.*, 1994), we may assume that the modified HuAChE active center and the active center of HuBChE contribute similarly to the overall affinity toward the ligand. Therefore, the somewhat different affinities of the hexa-mutant HuAChE and the HuBChE may originate from minor structural differences, which are not related to aromatic residues, along the active center gorge of the two enzymes.

e. *Decamethonium*: This bisquaternary ligand differs from BW284C51 in that it binds essentially with same affinity towards HuAChE and HuBChE ((Radic *et al.*, 1993) and Table 8). Nevertheless and unlike the other noncovalent ligands, the phenotype of the hexa-mutant is markedly different from that of HuBChE with respect to binding decamethonium. Yet, in line with the fact that this

ligand binds to the PAS (Harel *et al.*, 1993; Barak *et al.*, 1994; Bourne *et al.*, 1999) it is not surprising to find a substantial decrease in affinity of the Y72N/Y124Q, Y72N/Y124Q/W286A and of the hexa-mutant HuAChEs towards decamethonium (Shafferman *et al.*, 1992b; Millard and Broomfield, 1992 and Silman *et al.*, 1994, respectively). It is therefore quite clear that the binding modes of decamethonium to HuBChE and to HuAChE are different. In fact, such alternative binding was suggested in an earlier study where binding of decamethonium to BChE was modeled to bridge residues corresponding to Trp86 and Trp236 in AChE, which are well inside the gorge (Radic *et al.*, 1993). However it appears that mutations at the bottom of the gorge (F295L/F297V and F295L/F297V/Y337A) lead to a *decrease* in affinity towards decamethonium which could not be expected from either the models of the AChE-decamethonium complex (Radic *et al.*, 1993; Barak *et al.*, 1994) or x-ray structure of TcAChE and MoAChE-decamethonium complexes (Harel *et al.*, 1993; Bourne *et al.*, 1999). Finally, the effects of the mutations in the active center and the PAS are not additive and the various double, triple as well as the hexa-HuAChE mutants have similar inhibition constants for decamethonium (two orders lower than wild type HuAChE, Table 8). Thus, although these results reveal some intriguing features with respect to binding of decamethonium to HuAChE it appears that this ligand is currently not very useful to probe the active center differential characteristics of AChE and BChE.

DISCUSSION

Early sequence comparisons of AChE and BChE combined with the x-ray structure of TcAChE identified three inhibitor binding regions distinguishing the two enzymes (Chatonnet and Lockridge, 1989; Soreq and Zakut, 1990; Doctor et al., 1990). In AChE each of these regions is defined by a cluster of aromatic residues that seem uniquely disposed to accommodate the particular specificity requirements of the inhibitor, while in BChE the equivalent position bear aliphatic residues. One of these regions is located at the entrance to the active site gorge, about 15 Å away from the catalytic serine, and its composition is thought to affect primarily the ChE specificity toward bisquaternary ligands like BW284C51. The other two regions, the acyl pocket (Phe295; Phe297) and the hydrophobic subsite (containing Tyr337) are integral parts of the active center functional architecture, accommodating differentially ligands specific for AChE and BChE. The effects of residue substitutions at each of these regions have been investigated, mostly by single replacements (Harel *et al.*, 1992; Shafferman et al., 1992a; Ordentlich *et al.*, 1993a; Radic *et al.*, 1993; Vellom *et al.*, 1993; Barak *et al.*, 1994; Taylor and Radic, 1994; Loewenstein-Lichtenstein *et al.*, 1996; Masson *et al.*, 1996a; Saxena *et al.*, 1997a), leading to certain conclusions with regard to the structural and functional correspondence between the two cholinesterases: **a.** The difference in substrate specificity between AChE and BChE is predominantly due to a more open acyl pocket of the latter, accommodating more readily the larger acyl groups of butyrylcholine or benzoylcholine. **b.** The more open acyl pocket is responsible also for BChE specificity toward organophosphorus inhibitors like iso-OMPA or phosphates like DFP, DEFP and paraoxon, and for its greatly diminished stereoselectivity toward chiral phosphonates like soman or IBMPF. **c.** BChE selectivity toward tacrine and other aminoacridines as well as toward carbamates like bambuterol is predominantly due to the absence of an aromatic residue at the position equivalent to 337 of the hydrophobic subsite. Other bulky inhibitors like soman seem to sample similar hydrophobic environments in BChE and AChE. **d.** Absence of some aromatic residues at the PAS in BChE is probably responsible for its lower affinity, compared to AChE, towards bisquaternary ligands that bridge the active center and the rim of the gorge, such as BW284C51.

These conclusions are based mainly on single "space creating" mutations in AChEs as well as on "space reducing" mutations in BChE and are compatible with the generally accepted notion that interactions of substrates as well as of covalent and noncovalent inhibitors with AChE and BChE reveal nearly equivalent architectures of the respective active centers. Yet as mentioned earlier reactivity differences of BChE and of certain acyl pocket AChE mutants toward the substrates ATC or BTC (Ordentlich *et al.*, 1993a; Vellom *et al.*, 1993; Harel *et al.*, 1992) and certain stereoselective alkyl methylphosphonates (Hosea *et al.*, 1995; Ordentlich *et al.*, 1999) imply that active centers of AChE and BChE may not be as similar as thought before.

Examination of reactivity of the hexa-mutant HuAChE toward noncovalent inhibitors seems to indicate that the active center architecture of this enzyme indeed resembles that of HuBChE (Table 8). For the relatively small active center ligands like edrophonium or tacrine the ratio of the respective

inhibition constants of BChE and hexa-mutant HuAChE is 1. For the much bulkier huperzine A or the active center and PAS bridging ligand BW284C51 we find that while affinities of the hexa-mutant are 17,000 – 25,000 fold lower than those measured for HuAChE, they are only 8-12 fold different from those determined for HuBChE. In particular, affinities of the triple active center mutant F295L/F297V/Y337A, toward edrophonium, tacrine and huperzine A are very similar to those of HuBChE (Table 8). Thus, the multiple replacement of the active center aromatic residues Phe295, Phe297 and Tyr337 of HuAChE by the respective aliphatic residues Leu, Val and Ala of HuBChE does not affect the overall architecture of the active center but rather creates local voids that seem to be characteristic also to the corresponding architecture of HuBChE. In this modified HuAChE active center the positioning and function of residues, most important for ligand accommodation (like Trp86 or Tyr133 (Ordentlich *et al.*, 1995)), appear unchanged from those in the wild type HuAChE and HuBChE. Furthermore it appears that additional replacements of the three aromatic residues at the PAS by aliphatic residues do not seem to affect in a major way the accommodation of these noncovalent ligands at the active center.

In view of this conclusion it was rather surprising to find that the hexa-mutant HuAChE is about 40-140-fold less efficient than HuBChE or HuAChE, with respect to hydrolysis of both ATC and BTC. Most of the effect can be attributed to replacements of the three aromatic residues at the active center (Phe295, Phe297 and Tyr337). The discrepancy between the capability of the hexa-mutant HuAChE to accommodate noncovalent ligands in a HuBChE-like fashion and its inferior catalytic activity toward substrates may suggest that elements of the catalytic machinery have been affected by the multiple mutations. Several observations seem to be consistent with such a possibility. Removal of the steric constrains in the acyl pocket of HuAChE, by mutation of residue Phe295 to either alanine or leucine impart BChE-like catalytic activity to HuAChE toward BTC. However, substitution of additional aromatic residues leads to a decline of this activity and in the hexa-mutant the catalytic activity towards BTC resembles actually that of the wild type HuAChE (which is 50 fold lower than that of HuBChE). In addition, although the HuAChE and HuBChE enzymes are almost equally efficient catalysts of ATC hydrolysis, creation of a HuBChE-like void volume in the HuAChE active center lowers very significantly the catalytic activity towards ATC. Finally, the catalytic activity of the hexa-mutant HuAChE is very similar for ATC and BTC, irrespective of their size difference.

Further demonstration that the aromatic residue replacements affect the HuAChE catalytic machinery, while preserving the overall HuAChE (and HuBChE) active center architecture, is–provided by experiments with TMTFA, the prototypical AChE-transition state analog. The TMTFA molecule has been thoroughly investigated with respect to the structure of its tetrahedral adduct with TcAChE (Harel *et al.*, 1996) as well as to the kinetics of its reactions with various wild type and mutated AChEs (Nair *et al.*, 1994; Radic *et al.*, 1997; Ordentlich *et al.*, 1998). The accepted kinetic model of TMTFA reactivity indicates that the tetrahedral adduct is formed in a single kinetic step, and therefore the corresponding rate constant (k_{on}) is analogous to k_{app} (k_{cat}/K_m) of the catalytic process. Indeed, examination of the relative rate constant values in Table 6 shows analogous response of HuAChE reactivity, toward TMTFA and toward the substrate ATC, that culminates in the 150-fold decrease of

k_{app} for the hexa-mutant HuAChE catalytic activity, as compared to a 190-fold decrease of reactivity toward TMTFA. In addition, a 170-fold ratio of TMTFA k_{on} values for HuBChE and for the hexa-mutant HuAChE has been observed. Thus it appears that the difference in catalytic activity and in reactivity toward TMTFA, between both wild type HuAChE and HuBChE and the hexa-mutant HuAChE, is in the reduced ability of the latter to accommodate tetrahedral intermediates in the active center.

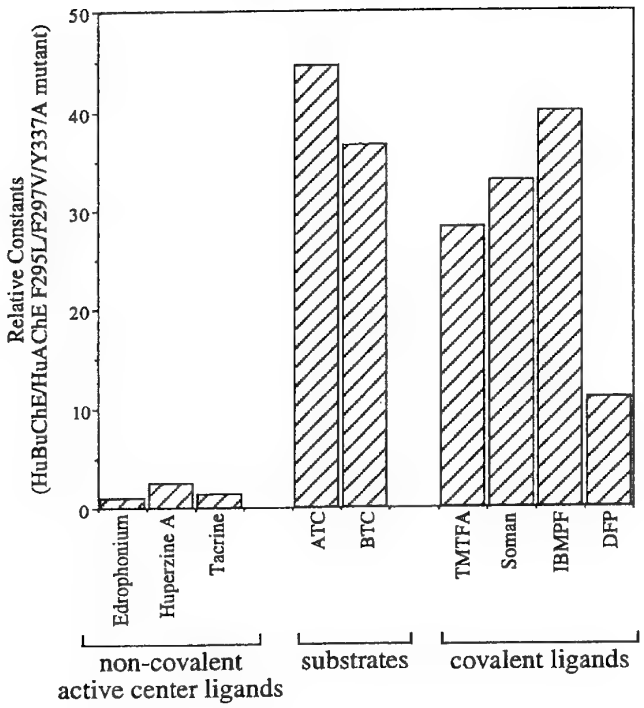

Figure 9: The relative reactivities of HuBChE and the triple active center mutant (F295L/F297V/Y337A) of HuAChE towards active center ligands. Shown are the relative values of: inhibition constants (K_i; see Table 8) for non-covalent inhibitors - edrophonium, huperzine A, and tacrine; of the apparent bimolecular rate constants for substrate hydrolysis of ATC and BTC (Table 4); and of the bimolecular rate constants of inhibition by the covalent ligands TMTFA, soman, IBMPF and DFP (see Tables 6,7).

The notion that the hexa-mutant HuAChE or more significantly the multiple active center mutants are impaired in their capacity to stabilize tetrahedral species in the active center, is consistent with the reactivity patterns of the HuAChE enzymes and of HuBChE toward methylphosphonates like soman or IBMPF. Unlike the substrates and TMTFA, the free phosphate molecules have tetrahedral geometry, and it was suggested that their reactivity toward ChEs is determined to a large extent by the stability of the corresponding noncovalent phosphate-ChE Michaelis complexes (Aldrich and Reiner 1972; Main, 1976; Ordentlich *et al.*, 1996). Accommodation of methylphosphonates by the HuAChE active center includes positioning of a methyl substituent in the acyl pocket in analogy to the acetyl methyl introduced in the tetrahedral intermediate of ATC or the trifluoromethyl substituent in the TMTFA-HuAChE adduct. The results demonstrate that the active center triple mutant HuAChE is impaired in reactivity toward soman and IBMPF to approximately the same extent as toward ATC or TMTFA (Table 6,7 and Fig. 9). Thus, the diminished ability of the active center modified HuAChE to accommodate tetrahedral species, as compared to that of the wild type HuAChE and that of HuBChE, is manifested for both covalently (tetrahedral intermediates of substrates and TMTFA) and non covalently bound (Michaelis complexes with methyl phosphonates) species.

The analysis presented above, underscoring the HuBChE-like ability of the hexa-mutant HuAChE to accommodate ligands as long as they do not present a tetrahedral geometry like that of methylphosphonates, suggests the involvement of the catalytic His447. In the tetrahedral intermediate with substrate this residue is thought to interact with both the choline oxygen and the O_γ-Ser203 as a part of its function in catalysis of the hydrolytic reaction (Barak *et al.*, 1997; Bencsura *et al.*, 1995; Shafferman *et al.*, 1996a). In the x-ray structure of the TcAChE adduct with TMTFA, participation of the analogous residue His440 in accommodation of the tetrahedral adduct, is clearly visible (Soreq and Zakut, 1990). In various modeling experiments of AChE-phosphate Michaelis complexes, the catalytic histidine was also implicated in interaction with the oxygen of the P-alkoxy substituent (Hosea *et al.*, 1995; Ordentlich *et al.*, 1996,1999). The precise juxtaposition of His447 was found to correlate with the facility of certain HuAChE-phosphonate conjugates to undergo a catalytic aging reaction (Barak *et al.*, 1993; Shafferman *et al.*, 1996a). It appears from all these studies that minor changes in orientation of the His447 side chain, resulting from mutations at the HuAChE active center, may interfere therefore with accommodation of tetrahedral species. Examination of whether impaired accommodation of tetrahedral species in the butyryl-like mutants correlates with enhanced mobility of the His447 side chain, was carried out by molecular simulation of residue motions at the active center (see "Materials and Methods"). The starting structure used in these experiments was taken from the x-ray structure of the HuAChE-fasciculin complex (Harel *et al.*, 2000). Following initial equilibration at 300°K the main chain was constrained and motions of the side chains were examined at 400°K. The results (see Fig. 10) seem to suggest that while in the wild type HuAChE the side chain of His447 maintains a similar average orientation as in the x-ray structure of HuAChE (Fig. 10A), in the F295L/F297V/Y337A and in the hexa-mutant HuAChEs (Fig. 10B,C) it tends to

assume a different average conformation. This mobility results in breaking of the H-bond with the catalytic Ser203 (Fig. 10B,C and Fig. 11). This conformational transition of His447 seems to be irreversible within the time scale of our simulations. While one should be careful about attributing any specific role to the altered His447 conformation, the enhanced His447 mobility in the two mutant enzymes is consistent

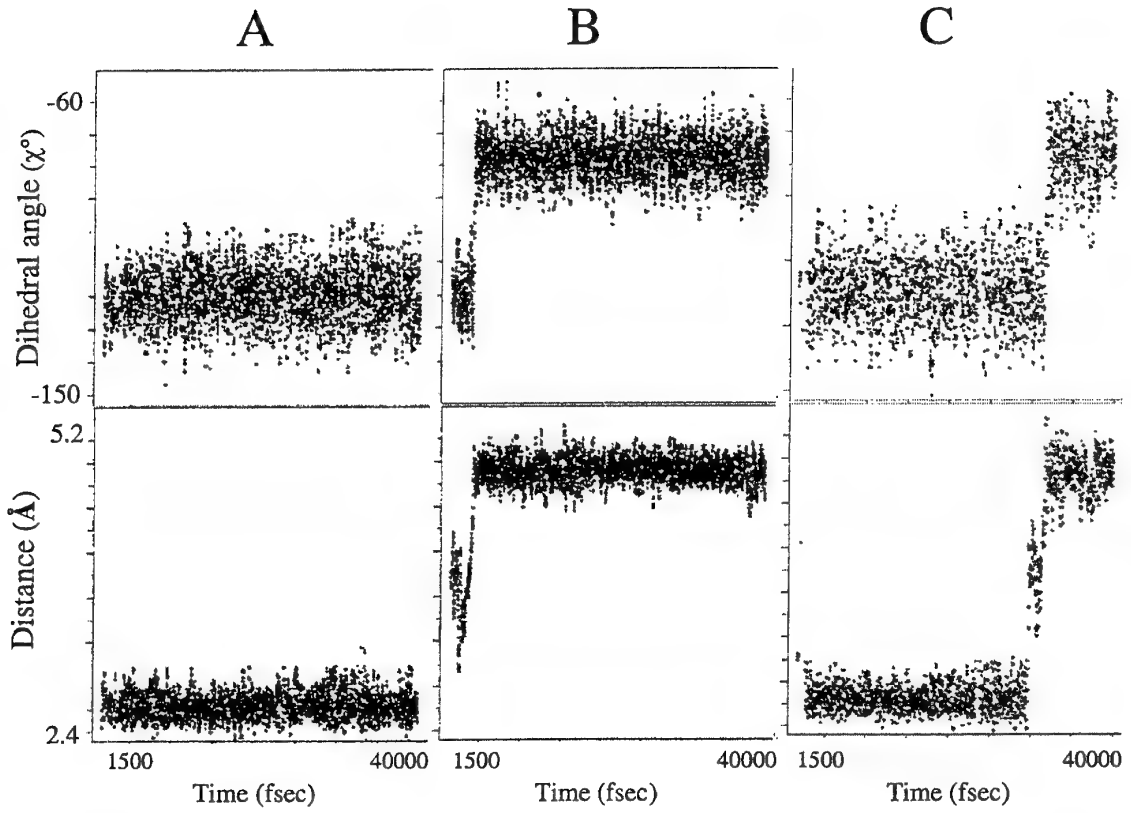

Figure 10: Examination of conformational mobility of the catalytic histidine side chain by molecular dynamic simulation. Depicted are 40ps. simulations performed on: A. wild-type HuAChE B. the triple active center mutant F295L/F297V/Y337A and C. the hexa-mutant Y72N/Y124Q/W286A/F295L/F297V/Y337A. Top panels - time dependence of the dihedral angle between the imidazolium moiety of His447 and the backbone (χ°). Lower panels – time dependence of the distance between $N\varepsilon_2$-His447 and γ-Ser203 (Å). Extension of simulation time (up to 160 ps.) did not result in any further changes of these conformational parameters.

with their impaired ability to accommodate tetrahedral species. In fact, such mobility of the catalytic histidine, in apparent response to steric changes in the active center has recently been observed in the x-ray structure of the TcAChE-VX conjugate (Millard *et al.*, 1999b). Steric changes due to multiple mutations at the HuAChE active center may also result in perturbation of its water structure (Koellner *et al.*, 2000). Specific water molecules in TcAChE and HuAChE were shown to play a major role in maintaining the orientation of His447 through the H-bond network (Ordentlich *et al.*, 1993b, 1996; Harel *et al.*, 2000).

If replacement of aromatic residues in the HuAChE active center produces a HuBChE-like architecture and at the same time alters the mobility of the catalytic histidine, the obvious question is why the same effect is not evident in HuBChE? It is reasonable to assume that in HuBChE an analogous perturbation to the positioning of the catalytic histidine is compensated by other interactions, yet an inquiry regarding the nature of these interaction as well as the residues participating in them is hardly possible without the x-ray structure of the enzyme. The results of the present study allude indeed to some differences in steric interactions within the active center, between the hexa-mutant HuAChE and HuBChE. These differences may be responsible for the small reactivity variations toward large ligands like huperzine A or BW284C51 and for the dissociation rate constants (k_{off}) values of the corresponding TMTFA adducts. In addition, while multiple mutations at the HuAChE active center gorge abolish substrate inhibition, the HuBChE-like phenotype of substrate-activation could not be achieved.

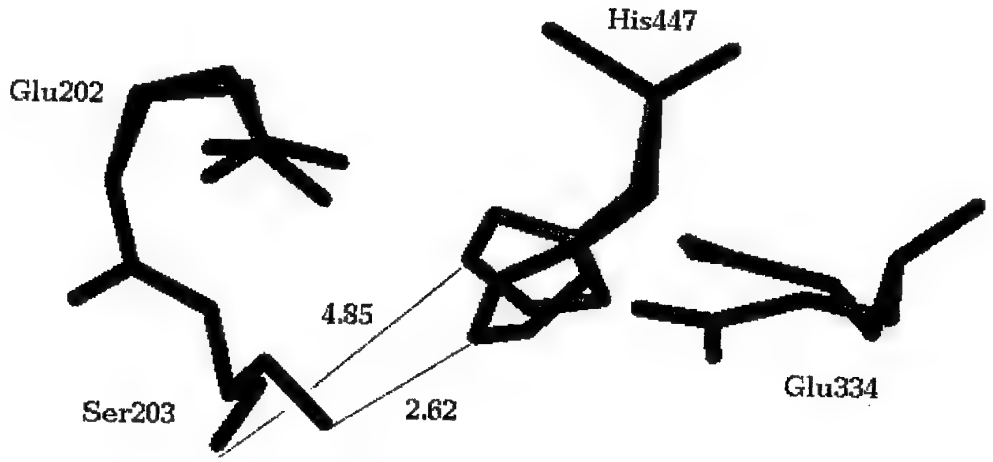

Figure 11: Potential modification of the optimal juxtaposition of the catalytic triad elements of the triple active center-mutant and the hexa-mutant HuAChEs. The relative positions of Glu-His-Ser in the wild type enzyme (yellow line) and in the mutant enzymes (blue line) as suggested by molecular dynamics simulations (see Fig. 10). Note that in the mutants devoid of the three active center aromatic residues, disruption of the H-bond interaction between the catalytic His and Ser is a consequence of displacement of the side chains of both of these residues, resulting in an increase of the $N\varepsilon_2$-His447 and $O\gamma$ of Ser203 distance from 2.62 Å in WT to 4.85 Å.

Another finding that suggests a somewhat different array of steric interactions with catalytic histidine in HuBChE, is the nearly equivalent reactivity of the hexa-mutant HuAChE and HuBChE with the organophosphate DFP. As with phosphonates these reactions involve initial noncovalent accommodation of the tetrahedral phosphate. Yet, in the case of DFP the substituent introduced into the acyl pocket is very large and may result in some distortion of the pocket in HuAChE. In fact, recent x-ray structure of the TcAChE-DFP adduct shows that the isopropoxy substituent pointing toward the acyl pocket distorts the main chains of both the acyl pocket and part of the peripheral site (Millard *et al.*, 1999). In the triple active center mutant HuAChE the accommodation of DFP seems to be impaired in a similar manner to that of other phosphate ligands, compared to HuBChE. Yet, during formation of the hexa-mutant HuAChE-DFP Michaelis complex introduction of the bulky substituent into the void volume of the active center gorge may compensate for the aromatic replacements with respect to the proposed mobility of His447.

In summary, comparison of reactivity profiles of the Y72N/Y124Q/W286A/F295L/F297V/Y337A hexa-mutant HuAChE and of HuBChE suggests that the active center overall architecture, which is responsible for noncovalent accommodation of ligands, is not very sensitive to local perturbations resulting from mutagenesis. Therefore the enzymatic characteristics of hexa-mutant HuAchE seem to be consistent with previous indications that AChE and BChE active centers differ predominantly in the volume of ligands they can accommodate. On the other hand, the precise juxtaposition of the catalytic residues (His and Ser) appears to be more sensitive to changes in the active center. Thus, the fact that the hexa-mutant HuAChE does not mimic the reactivity of HuBChE toward substrates and other covalent ligands may suggest that the catalytically productive orientation of the histidine in butyrylcholinesterase, is maintained by a somewhat different array of interactions than that in acetylcholinesterase.

V. Hierarchy of Post-Translation Modifications Involved in the Circulatory Longevity of Recombinant Bovine Acetylcholinesterase

INTRODUCTION

Protein clearance from the bloodstream is known to be a multifactorial process involving different removal pathways. These comprise kidney glomerular filtration, protease degradation, and active removal from the circulation via specific receptors for various determinants on the protein. Various characteristics of the protein, including protein size, subunit assembly, surface charge, hydrophobicity and carbohydrate contents/structure may therefore, play a role in determining its circulatory longevity (Ashwell and Harford, 1982; Drickamer, 1991). In recent years, special attention was focused on proteins such as acetylcholinesterase (AChE) and butyrylcholinesterase (BChE), which require long-term retention within the circulation to fulfill their therapeutic potential (Wolfe *et al.*, 1987; Ashani, *et al.*, 1991; Maxwell *et al.*, 1992; Raveh *et al.*, 1993; Kronman *et al.*, 1995; Chitlaru *et al.*, 1998; Saxena *et al.*, 1997b). Native serum-derived cholinesterases were found to reside in the circulation for long periods of time, whereas recombinant cholinesterases produced in tissue-culture systems are cleared from the circulation rather rapidly (Kronman *et al.*, 1995; Chitlaru *et al.*, 1998; Saxena *et al*, 1997b), suggesting that post-translation factors determine the circulatory behavior of these enzymes.

In the case of AChE, the contribution of appendiced carbohydrates to circulatory residence was demonstrated by the finding that bacterially generated recombinant AChE as well as N-Glycanase treated ChEs of animal cell origin, both being devoid of N-glycans, are cleared rapidly from the circulation of experimental animals (Fischer *et al.*, 1993 ; Kronman *et al.*, 1995). However, the pharmacokinetic profiles of an array of mutated recombinant human acetylcholinesterases (rHuAChEs) differing by the number of N-glycosylation sites (Kronman *et al.*, 1995), suggested that though N-glycosylation in itself does play a role in determining circulatory residence, the structural features of the N-glycans, rather than their actual number, play a decisive role in circulatory retention of ChEs. Amongst the glycan structural features affecting clearance, variations in the level of terminal sialylation are of particular importance because of the recognition and removal of undersialylated glycoproteins by the liver-specific asialoglycoprotein receptor (Weiss and Ashwell, 1989). Indeed, enzymatic removal of sialic acid moieties resulted in a catalytically active form of rHuAChE displaying accelerated elimination from the circulation (Kronman *et al.*, 1995), indicating that sialylation plays a pivotal role in determining the circulatory residence of rHuAChE. The importance of sialylation efficiency was further demonstrated by determining the clearance rates of various derivatives of rHuAChE, which differ one from another by their number of N-glycan side-chains. Based on direct measurement of the sialic acid content of each one of the examined forms of the enzyme, an inverse-linear relationship was found to exist between the number of unoccupied

sialic acid attachment sites, and the circulatory half-life values of the various enzyme forms (Kronman *et al.*, 1995). This line of studies served as a basis for the conversion of the rHuAChE molecule into its highly sialylated form (Chitlaru *et al.*, 1998) by the genetic modulation of the glycosylation machinery of AChE producer cell lines. Although highly sialylated rHuAChE was indeed retained in the circulation for extended periods of time, it was still cleared from the circulation more rapidly than serum-derived FBS-AChE or HuS-BChE (Kronman *et al.*, 1995; Chitlaru *et al.*, 1998; Saxena *et al.*, 1998b), suggesting that additional factors participate in determining the circulatory behavior of cholinesterases. In this context, it should be noted that cholinesterases can occur in multiple forms. Cell-bound AChEs consist of tetramers attached to membrane-anchored noncatalytic subunits such as the ColQ gene-encoded collagen-like tail, through the Proline Rich Attachment Domain (PRAD, (Bon and Massoulie, 1997) whereas secreted cholinesterases such as those residing in the circulation (e.g. FBS-AChE), are usually composed of soluble homo-tetramers. In contrast to the tetrameric serum-derived cholinesterases, recombinant cholinesterases produced in tissue-culture systems were found to consist mostly of dimers and monomers (Kronman *et al.*, 1995; Saxena, *et al.*, 1998b; Velan *et al.*, 1991b; Duval *et al.*, 1992; Mendelson *et al.*, 1998).

We have previously documented the cloning of the bovine acetylcholinesterase gene and developed systems for the high level production of recombinant bovine AChE (rBoAChE) in a human cell line (Mendelson *et al.*, 1998) . This recombinant enzyme displayed a distinct pharmacokinetic profile, which was characterized by its rapid removal from the circulation. In contrast, native serum-derived FBS-AChE with which rBoAChE shares an identical amino-acid sequence, was retained in the circulation for extended periods of time. Thus, two versions of the **same** protein, which differ in their post-translation processing only, exhibit markedly different pharmacokinetic behaviors and can therefore serve as a model system for inspection of post-translation factors involved in circulatory residence. This could not be achieved with the human recombinant enzyme due to the lack of an available native long-lived form of human AChE.

In the work presented in this report, we determined the effects of the various post-translation features of the recombinant bovine enzyme upon its circulatory behavior. Exhaustive MALDI-TOF analysis of derivatized N-glycans associated with both rBoAChE and native FBS-AChE allowed us to determine the exact structures of the carbohydrates of the respective enzymes. We found that the native and recombinant forms of bovine acetylcholinesterase differ in their glycan terminus occupancy. The efficient capping of glycans with either sialic-acid or with α-galactose, which characterized the native form of bovine AChE, were evaluated for their contribution to circulatory longevity. On the basis of this analysis, a genetic approach for the pharmacokinetic remediation of rBoAChE was designed and implemented. This line of studies was then followed by a series of experiments in which the effect of rBoAChE subunit assembly modulation on circulatory residence was examined. We demonstrate that a series of modulations can convert the rapidly cleared rBoAChE into a circulatory long-lived enzyme, exhibiting a pharmacokinetic profile, which is indistinguishable from that of the native fetal bovine serum acetylcholinesterase. Finally, by creating a large collection of carefully defined bovine AChE glycoproteins differing in the extent of glycan

sialylation and enzyme subunit oligomerization, we demonstrate that a hierarchic pattern of post-translation factors determines circulatory longevity.

MATERIALS AND METHODS

Cell culture techniques, enzyme production and purification of rBoAChE - Generation of HEK-293 cell lines stably expressing high levels of rBoAChE was described previously (Kronman *et al*. 1992; Mendelson *et al.*, 1998) . The generation of *in-vivo* highly sialylated rBoAChE was achieved by transfecting the recombinant sialyltransferase expressor HEK-293ST-2D6 cell line (see below) with the pBoAChE-nc vector followed by G418 selection to form rBoAChE stable producer cells. Purification of secreted rBoAChE, and the purification of FBS-AChE from calf serum (Biological Industries, Beth Haemek, Israel) were all described previously (Kronman *et al.* 1992; Mendelson *et al.*, 1998).

Generation of a HEK-293 master cell line expressing high levels of 2,6 sialyltransferase - Individual HEK-293 cell clones stably transfected with the pCEP4-α2,6ST plasmid carrying the rat ß-galactoside α 2,6-sialyltransferase gene (Chitlaru *et al.*, 1998), were tested for their ability to generate highly sialylated glycoproteins as follows: 96 well plates (Nunc, Maxisorp) were coated with decreasing amounts of cleared cell extracts (Chitlaru *et al.*, 1998) of the various clones (5-0.3μg/ml in carbonate buffer pH 9.6, 4h at 37^{0}C). Plates were then rinsed 3 times in 0.9% NaCl/0.05% Tween 20 and subjected to a consecutive series of incubations (1h at 37^{0}C each) in: (1) - 0.5% Tween 20/1% gelatin /PBS, (2) - biotinylated *Sambucus nigra* lectin (SNA , Sigma, 1 μg/ml in 0.5% Tween 20/PBS) and (3) - strepavidin-alkaline phosphatase conjugate (Sigma, 500 mU/ml in 0.5% Tween 20/PBS). Following each incubation step, plates were rinsed 3 times in 0.9% NaCl/0.05% Tween 20. Plates were developed and read in a Thermomax (Menlo Park, CA) as described before (Shafferman, *et al.*, 1992a). Optical density was plotted against bound cellular protein and cell-associated sialic acid levels (measured as mOD/μg protein) of the various clones were calculated. Clone HEK-293ST-2D6 displayed the highest level of sialic acid and subsequently served as the master cell line for expression and production of highly sialylated AChE.

Enzyme activity - AChE activity was measured according to Ellman *et al.* (1961). Assays were performed in the presence of 0.5 mM acetylthiocholine, 50 mM sodium phosphate buffer pH 8.0 0.1 mg/ml BSA and 0.3 mM 5,5'-dithiobis-(2-nitrobenzoic acid). The assay was carried out at 27^{0}C and monitored by a Thermomax microplate reader (Molecular Devices).

Pharmacokinetics - Clearance experiments in mice (3 to 6 ICR male mice per enzyme sample) and analysis of pharmacokinetic profiles were carried out as described previously (Kronman *et al.*, 1995). The study was approved by the local ethical committee on animal experiments. Residual

AChE activity in blood samples was measured and all values were corrected for background activity determined in blood samples withdrawn 1 hour before performing the experiment. The clearance patterns of the various enzyme preparations were usually biphasic and fitted to a bi-exponential elimination pharmacokinetic model ($C_t=Ae^{-k\alpha t}+Be^{-k\beta t}$) as described previously (Kronman *et al.*, 1995). This model enables determination of the parameters A and B which represent the fractions of the material removed from the circulation in the first-fast and second-slow elimination phases respectively, and $T_{1/2}\alpha$ and $T_{1/2}\beta$ which represent the circulatory half-life values of the enzyme in the fast and slow phases. The pharmacokinetic parameters MRT (mean residence time, which reflects the average length of time the administered molecules are retained in the organism) and CL (clearance, which represents the proportionality factor relating the rate of substance elimination to its plasma concentration (CL=dose/area under the concentration-time curve), (Rowland and Tozer,1989)) were independently obtained by analyzing the clearance data according to a noncompartmental pharmacokinetic model using the WinNonlin computer program (Laub and Gallo, 1996).

Release, recovery, purification and labeling of N-glycans - N-glycans of purified enzyme preparations (~100 ug protein) were released by N-glycosidase-F (Glyko, USA) treatment as described before (Kronman *et al.*, 1992). Deglycosylated protein was removed by ethanol-precipitation and glycans were recovered and purified from the supernatant as described by Kuster *et al.* (1997). To increase sensitivity (Anumula and Dhume, 1998; Okafo *et al.*, 1996, 1997) purified glycans were fluorescently labeled. Fluorescent labeling of purified glycans with 2-aminobenzamide (2-AB) was performed according to Bigge *et al.* (1995) using a commercial labeling kit (Glyko, USA). During the 2h labeling incubation, the temperature was kept at 55^{0}C to prevent heat-induced desialylation of the glycans.

Enzymatic modulation of N-glycans

A. Modulation of labeled N-glycans -

Sialic acid removal - Agarose-bound sialidase (0.04U, Sigma) was prewashed 5 times with water and incubated at room temperature for 16h with 2AB labeled N-glycans released from 1.5 -2.0 nmol AChE. Sialidase was removed by Eppendorf centrifugation. Desialylated N-glycans were vacuum dried, resuspended in 30 µl of water and stored at -20^{0}C until use. Glycans prepared in this manner were subjected to MALDI-TOF analysis or to further glycosidase treatments followed by MALDI-TOF analysis.

Removal of neutral monosaccharides - Desialylated 2AB-labeled N-glycans obtained from 0.05-0.07 nMole AChE (in 1 µl water), were incubated for 24h with 1 µl of bovine kidney fucosidase (1.3 U/ml, Glyko, USA), β-galactosidase (5 U/ml, Glyko, USA) or Green coffee bean α-galactosidase (0.5 U/ml, Sigma). Water was added to a final volume of 10 µl and samples were stored at -20^{0}C until analyzed by MALDI-TOF.

B. Modulation of AChE-bound N-glycans -

In vitro sialylation of rBoAChE - Pure rBoAChE (1.8 nmol) was incubated for 20 h at 37^{0}C in the presence of 2mU α2,6ST (Boehringer) and 100 nmoles of CMP-N-acetyl-neuraminic acid in 50mM NaCl (final volume = 800μl). I*n vitro* sialylated rHuAChE was extensively dialyzed against PBS for pharmacokinetics studies.

Removal of sialic acid from rBoAChE-bound N-glycans - AChE (100 nmol enzyme) in PBS was incubated for 16h with 1.2U of agarose-bound sialidase at room temperature. Sialidase was removed by Eppendorf centrifugation. Desialylated enzyme was dialyzed against PBS to remove free sialic acid.

α– galactosidase treatment of FBS-AChE - Highly purified FBS-AChE (6 nmol in PBS) was incubated for 5h at 37^{0}C with 8 units α-galactosidase, followed by extensive dialysis against PBS. To determine whether α-galactose removal proceeded to completion, a portion of the α-galactosidase treated enzyme was subjected to N-glycosidase-F treatment, 2AB labeling, and desialylation as detailed above, followed by MALDI-TOF analysis. Following AChE treatment with modifying glycosidases (sialidase or α-galactosidase), ChE activity was measured, to verify that enzyme integrity was not compromised by the treatment.

Esterification of sialic acids - To allow the concomitant measurement by MALDI-TOF analysis of both neutral and acidic glycans, the carboxylic groups of sialylated 2AB labeled glycans were converted into their neutral methylated forms by methyl iodide esterification, essentially as described by Kuster *et al* (1997). We note that in this procedure the 2AB moiety itself undergoes methylation and therefore both neutral and acidic glycans invariably display an increment in molecular mass of 14.015 kDa in addition to the increase in mass size resulting from sialic acid methylation in the case of acidic glycans. Esterified glycans were purified as described (Kuster *et al.,* 1997) and stored at -20^{0}C until MALDI-TOF analysis.

Mass spectrometry - Mass spectra were acquired on a Micromass TofSpec 2E reflectron time-of-flight (TOF) mass spectrometer. 2AB-labeled desialylated or 2AB-labeled esterified glycan samples, were mixed with an equal volume of freshly prepared DHB (10mg/ml in 70% acetonitrile) and loaded onto the mass spectrometer target. Routinely, 1 μl and 1 μl of glycan samples diluted 1:10 in water were subjected to analysis. Dried spots were recrystallized by adding 0.5 μl ethanol and allowed to redry. Neutral glycans were observed as $[M+Na]^+$ ions. 1 μl of peptide mixture (renin substrate, ACTH fragment 18-39, and angiotensin,10 pMole/μl all from Sigma) which served as a three-point external calibrant for mass assignment of the ions, was mixed with freshly prepared α-cyano-4-hydroxycinnamic acid (10 mg/ml in 49.5% acetonitrile; 49.5% ethanol; 0.001% TFA),

loaded on the mass spectrometer target and allowed to dry. All oligosaccharides were analyzed at 20 kV with a single-stage reflectron in the positive-ion mode. Between 100 and 200 scans were averaged for each of the spectra shown.

PRAD peptide synthesis - The PRAD peptide CLLTPPPPPLFPPPFFRG was synthesized manually in a T-bag by F-moc chemistry, as described (Houghten, 1985). The peptide was dialyzed against 0.05% TFA for 48hrs. Quality control of the peptide was performed by MALDI-TOF-MS, and its concentration was evaluated by its absorbance at 215 nm following reverse-phase HPLC.

In-vitro tetramerization of rBoAChE - Purified rBoAChE was incubated together with the synthetic PRAD peptide for 12-16h at room temperature, in the presence of 5mM phosphate buffer pH 8.0. In analytical tetramerization experiments designed for sucrose gradient analysis of tetramer formation, 0.12 nmol of rBoAChE (equivalent to 25U) were mixed with different ratios of the PRAD peptide as indicated, in a final volume of 70 µl.. Preparative tetramerization for the generation of milligram amounts of tetrameric rBoAChE for pharmacokinetic studies included 14.4 nmol of rBoAChE (equivalent to 3000U) which were incubated with 28.8 nmol PRAD peptide in a final volume of 2ml. Prior to administration to mice, *in-vitro* tetramerized rBoAChE was dialyzed extensively against PBS.

Sucrose density gradient centrifugation - Analytical sucrose density gradient centrifugation was performed on 5-25% sucrose gradients containing 0.1M NaCl/50 mM sodium phosphate buffer pH 8.0. For determination of the rHuAChE assembly status in the circulation of mice at various timepoints post-administration,10 µl samples removed from 5 mice, each injected with 1000U intravenously at T=0, were pooled and applied to sucrose gradients. Centrifugation was carried out in an SW41 Ti rotor (Beckman) for 26h at 160000 Fractions of 0.2 ml were collected and assayed for AChE activity. Alkaline phosphatase, catalase and β-galactosidase were used as sedimentation markers.

RESULTS

Characterization of the basic N-glycan structures associated with recombinant and native bovine AChE - To determine whether the differential pharmacokinetic patterns of FBS-AChE and its recombinant version expressed in a mammalian cell line (Mendelson *et al.*, 1998) can be correlated with the presence/absence of specific glycan structures, the N-glycans associated with the two enzymes were subjected to a detailed structural analysis by MALDI-TOF mass spectroscopy in conjunction with specific exoglycosidase digestions.

In a first series of studies, the glycans derived from rBoAChE and FBS-AChE were deacidified by sialidase treatment, and extensively analyzed in their nonsialylated form. This treatment which removes terminal sialic acids enables easy detection of the glycans by overcoming the inherent difficulty of analyzing negatively charged oligosaccharides by MALDI-TOF (Kuster *et al.*, 1997; Powell and Harvey, 1996; Papac *et al.*, 1996). To further increase sensitivity, N-glycans released by the N-glycosidase-F digestion, were fluorescently labeled with 2-AB ("Methods"). The analysis of N-glycans generated by this procedure provided the complete basic structure, branching/antennary typing and specific monosaccharide substitutions (e.g. fucosylation, presence of GalNAc) regardless of the terminal sialic acid occupancy status.

The MALDI-TOF spectra obtained for rBoAChE and FBS-AChE (Fig. 12A, Table 12), revealed that the oligosaccharide species associated with both enzymes are comprised of a large variety of 8-11 basic glycan structures, differing one from another both quantitatively in their relative abundance and qualitatively with respect to branching and monosaccharide substitutions. Based on molecular-weight matching, the basic structural identity of most of the glycans could be deduced. In some cases, an ambiguity remained due to equivalent masses of isomeric or anomeric monosaccharides. To resolve these ambiguities, desialylated glycan pools were subjected to a series of monosaccharide-specific exoglycosidase (α-galactosidase, β-galactosidase and fucosidase) treatments, and the resulting glycan products were subjected to MALDI-TOF analysis. Based on the molecular-weight shift of the trimmed glycans (Fig. 12, B-D) the structures of the entire spectrum of glycans could be deciphered unequivocally (Table 12). The relative abundance of the various oligosaccharide structures could thereby be determined, provided that these comprise more than 1% of the total glycan pool.

The analyses established that though the glycan pools of serum-derived FBS-AChE and 293-cell generated recombinant AChE, display a complex array of diverse structures, some general similarities between the two profiles can be found. In both enzymes, the vast majority of the oligosaccharides are of the complex type, the one notable exception being a hybrid glycan form

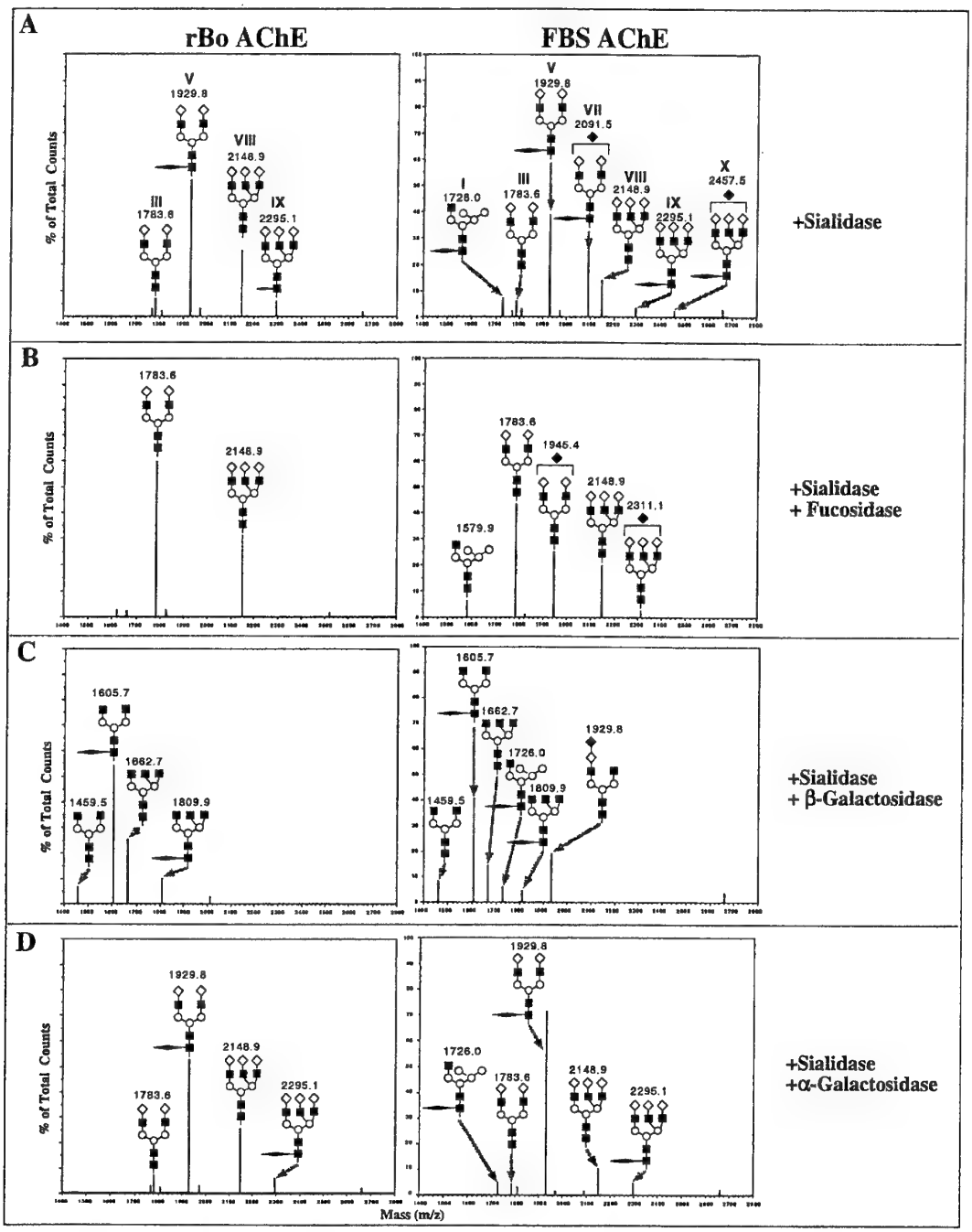

Figure 12: MALDI mass spectra of N-glycans associated with FBS-AChE and rBoAChE following desialylation. Purified N-glycans of FBS-AChE and rBoAChE were subjected to sialidase treatment and 2-AB labeling prior to MALDI-TOF analysis. Molecular weights and structural details are shown for the major glycan forms. Molecular weights represent monoisotopic masses of the respective $[M+Na]^+$ ions of the glycan species. *A*, without additional exoglycosidase digestion. *Roman numerals* refer to the peak designations ascribed to the various major forms in Table 12. *B*, after digest with bovine kidney fucosidase; *C*, after digestion with bovine testes β-galactosidase; *D*, after digestion with Green coffee bean α-galactosidase. *Solid square*, GlcNac; *open circle*, Man; *open diamond*, β-gal; *elongated diamond*, Fuc; *solid diamond*, α-gal.

Table 9 - Comparison of the basic glycan structures of desialylated rBoAChE and FBS-AChE

Peak Designation	Composition	Structure	MW [M+Na] +2AB	N-Glycan Abundance (% of Total)	
				rBoAChE (HEK-293 produced)	FBS-AChE *Native*
I	$(Man)_5(GlcNAc)_3(Fuc)$		1726.0	<0.8	6.8±0.3
II	$(Man)_3(GlcNAc)_4(\beta Gal)(Fuc)$		1767.8	2.5±0.5	1.8±0.4
III	$(Man)_3(GlcNAc)_4(\beta Gal)_2$		1783.6	6.9±1	5.5±0.8
IV	$(Man)_3(GlcNAc)_4(GalNAc)(Fuc)$		1809.9	2.1±0.4	2.5±0.4
V	$(Man)_3(GlcNAc)_4(\beta Gal)_2(Fuc)$		1929.8	52.4±4	38.3±3.2
VI	$(Man)_3(GlcNAc)_4(GalNAc)(\beta Gal)(Fuc)$		1971.8	2.4±0.4	1.7±0.4
VII	$(Man)_3(GlcNAc)_4(\beta Gal)_2(\alpha Gal)(Fuc)$		2091.5	<0.8	24.8±1.4
VIII	$(Man)_3(GlcNAc)_5(\beta Gal)_3$		2148.9	25.3±2	15±2.1
IX	$(Man)_3(GlcNAc)_5(\beta Gal)_3(Fuc)$		2295.1	5.9±2	3.3±0.26
X	$(Man)_3(GlcNAc)_5(\beta Gal)_3(\alpha Gal)(Fuc)$		2457.5	<0.8	2.2±0.4
XI	$(Man)_3(GlcNAc)_6(\beta Gal)_4(Fuc)$		2660.6	1.5±0.4	1±0.2
□GalNac ◆αGal ◇βGal ○Man ■ GlcNac ◄►Fuc					

Molecular weights, deduced structures, and relative abundances of enzymatically desialylated N-glycan structures associated with rBoAChE and FBS-AChE were determined from the MALDI-TOF spectra represented in Fig. 12.

(Table 12, peak I) which is present in FBS-AChE at relatively low frequencies. The most prevalent glycan structure in both rBoAChE and FBS-AChE is the biantennary fucosylated form, $(Man)_3$-$(GlcNAc)_4$-$(\beta\text{-gal})_2$-Fuc, (Table 12, peak V) which constitutes approximately 40-50 percent of the total glycans, and is present at approximately 7 to 10-fold higher levels than its nonfucosylated counterpart (Table 12, peak III). In both enzymes, 20-32% of the glycans are triantennary (Table 12, peaks VIII-X) while tetraantennary glycans are present at very low levels (Table 12, peak XI). Interestingly, the predilection towards fucosylated forms is apparent in biantennary but not trianntennary glycans. Low levels of glycans (4-5%) display masses (Table 12, peaks IV,VI) which allow their structures to be interpreted as biantennary forms which contain either a bisecting-GlcNAc residue or an outer-arm Gal to GalNAc substitution. Some of our MALDI structural data (not shown) suggest that most of these forms are of the latter type, though the presence of very low amounts (<1%) of GlcNac-bisected forms cannot be excluded.

Comparison of the various desialylated glycan structures and the abundances associated with the two forms of bovine AChE, revealed that the most significant difference with regard to the basic glycan structures, is the presence of high-levels (25-30 % of total glycans) of α-gal-containing oligosaccharides in the native FBS form of the enzyme and not in recombinant BoAChE. Though most of these forms are of the biantennary type (Fig. 12A and Table 12, peak VII), low levels (~2%) of triantennary glycans which carry α-gal are also present exclusively in the native enzyme (Fig. 12A and Table 12, peak X).

Determination of the sialylated glycan forms associated with recombinant and native bovine AChE - In view of the fact that the sialylation level of AChE was established to be important in determining its pharmacokinetic behavior (Kronman *et al.*, 1995; Chitlaru *et al.*, 1998) the glycans were subjected to a thorough MALDI-mediated determination of their terminal sialic acid occupancy. As mentioned earlier, MALDI-TOF analysis of sialylated oligosaccharides is inherently complicated by the fact that the sialic acid residues are frequently converted into charged ions which form salts with alkali metal ions, resulting in a multiple-peak spectrum which cannot be easily interpreted (Powell and Harvey, 1996). Moreover, scoring of sialic acid levels is difficult due to fragmentation of sialic-acid containing glycans in some cases (Kuster *et al.*, 1997). Although sialylated glycans can be monitored in the MALDI-TOF negative mode (Papac, *et al.*, 1996; Weikert *et al.*, 1999), the spectral data gathered in this manner does not include neutral oligosaccharide forms, precluding determination of the relative distribution of the various charged and noncharged glycans comprising the entire glycan pool. We therefore, quantitatively determined the sialic acid terminal occupancy of the bovine AChEs-derived glycans by a set of MALDI analyses carried out with glycans in which the negative charges of their sialic acid residues were neutralized by iodomethane-mediated esterification (Kuster *et al.*, 1997). The peaks of the neutralized glycans can be readily detected in the MALDI-TOF positive mode and assigned accurate masses, taking into account that the equimolar introduction of methyl groups into sialic acid residues results in a MALDI-recognizable constant increase of the molecular weight. Since conversion of acidic glycans into

neutral forms allows visualization of the entire range of N-glycans in the positive mode, the relative abundances of all the different glycan forms (sialylated as well as non-sialylated) comprising the glycan pool can be determined.

Inspection of MALDI-TOF spectra established that the major glycan forms and their relative abundances (Fig. 13A), are in excellent agreement with those detected by analysis of the desialylated glycans (Fig. 12). This indicates that the esterification process did not introduce any bias which may cause disproportionate detection of specific glycan structures. While the basic structures of the major glycans associated with FBS-AChE and rBoAChE are similar (with the notable exception of glycans containing terminal α-gal in FBS-AChE only, as mentioned above), the two preparations differ significantly in their sialic acid content. In the glycans of native FBS-derived protein, almost all of the β-gal moieties serve as acceptors for sialic acid (Fig. 13A1), in contrast to the glycans associated with the recombinant enzyme, of which a significant fraction terminates in uncapped β-gal (Fig. 13A2).

Considering the relative MALDI-scored abundances of the glycan forms, and based on the fact that bovine AChE possesses four utilized N-glycosylation sites (Mendelson *et al.*, 1998), it is possible to score the molar ratio of the various glycan forms with respect to their antennary terminal groups (Table 10). Thus, FBS AChE-associated glycans exhibit (per enzyme subunit) 7.3 sialylated termini, 1 terminal α-gal and only 0.3 termini ending in β-gal. In contrast, the recombinant version of the protein produced in HEK-293 cells is heavily undersialylated, exhibiting a molar ratio of 4.1 sialylated termini and 4.5 termini ending in β-gal, per enzyme subunit.

Taken together, the following conclusions can be drawn from the structural profiles of the carbohydrates released from the recombinant and native forms of bovine AChE: **(i)** Complex-type N-Glycans are associated with both recombinant and native BoAChE. The basic structures of the glycans and their relative abundances in the two enzyme preparations, are similar. **(ii)** The prevalent glycan structure in both cases is that of the biantennary type. **(iii)** Most of the glycans are core-fucosylated. **(iv)** A minority of the glycans carry a GalNAc residue while little or none contain bisecting GlcNAc. **(v)** A significant fraction of the biantennary glycans derived from the native FBS-AChE, display terminal α-Gal residues. This structure is not detected in the recombinant enzyme. **(vi)** FBS-AChE and rBoAChE differ sharply in their extent of terminal sialic-acid capping: while native FBS-AChE enzyme exhibits almost fully sialylated termini, the recombinant enzyme is markedly undersialylated.

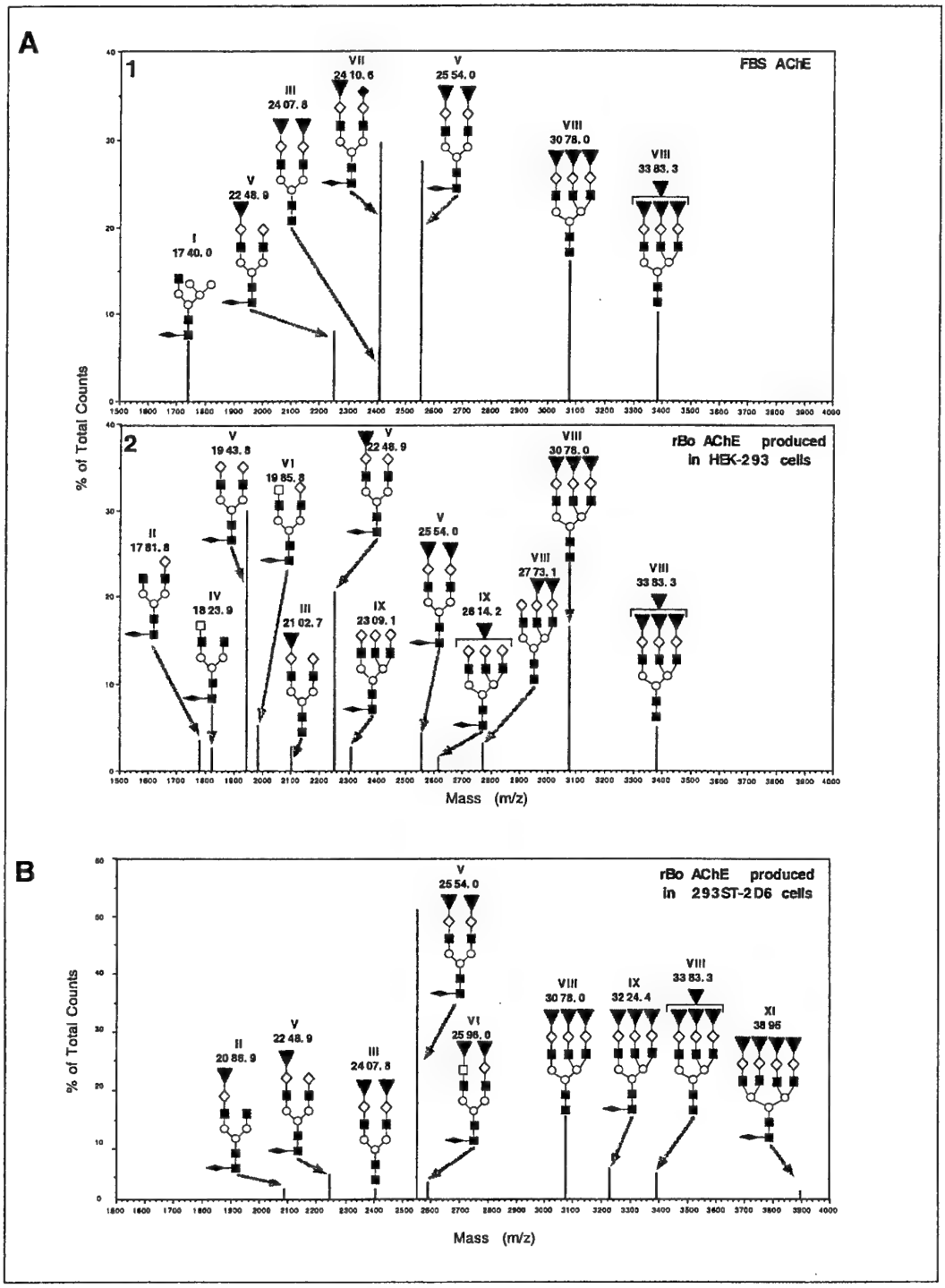

Figure 13: MALDI mass spectra of total N-glycan pools associated with FBS-AChE and rBoAChE produced by HEK-293 or 293ST-2D6 cells. Purified N-glycans of FBS-AChE and rBoAChE produced in HEK-293 cells (*A*) or in 293ST-2D6 cells (*B*) were subjected to 2-AB labeling and iodomethane-mediated esterification prior to MALDI-TOF analysis. Molecular weights and structural details are shown for the glycan forms. Molecular weights represent monoisotopic masses of the respective $[M+Na]^+$ ions of the glycan species. *Roman numerals* refer to the peak designations ascribed to the various major forms in Table 12. Note that an increase of 14.015 Da of all glycan species occurs due to the methylation of the common 2-AB moiety. *Solid square*, GlcNac; *open circle*, Man; *open diamond*, β-gal; *elongated diamond*, Fuc; *solid diamond*, α-gal. *Open square*, GalNAc; *inverted solid triangle*, sialic acid.

Table 10 - Terminal Occupancy of N-Glycans Associated with rBoAChE and FBS-AChE.

Structure	Molar Ratio (Structure/AChE subunit)	
	rBoAChE	FBS-AChE
Terminal sialic acid [1]	4.1	7.3
Terminal β-gal [2]	4.5	0.28
Terminal α-gal [3]	0	1.0
N-Glycans [4]	4	4
N-glycan termini [5]	9.1 [6]	8.9 [7]

(1) The molar ratio of total sialic acid (mol/mol AChE subunit) calculated from the MALDI-TOF spectra of FBS-AChE and rBo-AChE N-glycans (Fig. 13A) was 7.7 and 4.2, respectively. Note that one of the sialylated glycan forms (m/z = 3383.3 Da) contained 4 sialic acid residues per 3 glycan termini and therefore this structure includes a nonterminal sialic acid residue. The molar ratio of terminal sialic acids per AChE subunit was calculated as: [Total sialic acid ((mol/mol AChE subunit)] - [Nonterminal sialic acid ((mol/mol AChE subunit)] = [Terminal sialic acid ((mol/mol AChE subunit)].
(2) Calculated from the MALDI-TOF spectra of FBS-AChE and rBo-AChE (Fig. 13A).
(3) Calculated from the Table 12 and from the MALDI-TOF spectra of FBS-AChE and rBo-AChE (Fig. 13A).
(4) Bovine AChE contains 4 utilized N-glycosylation sites (Mendelson, 1998).
(5) Calculated from the frequencies of the various glycan forms in Table 12.
(6) rBoAChE contains glycan structures corresponding to peaks II, IV and VI (Table 12), which carry termini that are neither sialylated nor capped by β-gal. These forms contribute to the total N-glycan termini (9.1 mol/mol AChE subunit) a sum of 0.52 mole/AChE subunit.
(7) The apparent difference between the No. of N-glycan termini and the sum of terminal sialic acid, β-gal and α-gal , is accounted for by the presence of the structure corresponding to peak I in Table 12 (m/z = 1726.0). This hybrid structure possess none of these terminal moieties, yet contributes 6.8% glycan ends.

Assessment of the role of terminal α-galactosylation and sialylation on circulatory longevity - Since the two major differences between the N-glycans derived from native long-lived AChE and from the rapidly cleared recombinant enzyme are related to their terminal capping, we examined the effect of specific monosaccharide trimming of the intact FBS-AChE enzyme on its circulatory residence.

To examine the effect of sialic-acid removal on the pharmacokinetic behavior of FBS-AChE, the intact enzyme was subjected to extensive incubation in the presence of a large excess of sialidase (See "Materials and Methods"). A portion of the sialidase-treated glycoprotein was processed to allow MALDI-TOF inspection of the modified glycans, and the rest of the enzyme sample was tested for its pharmacokinetic behavior (Fig. 14A and Table 11). The MALDI-TOF spectrum of

the N-glycans released and purified after sialidase-treatment of FBS-AChE (Fig. 14A2) was found to be identical to the spectrum obtained following sialidase treatment on purified glycans from FBS-AChE (Fig. 12A). This verifies the complete and quantitative removal of sialic acid from the intact enzyme. Pharmacokinetic studies with sialidase-treated FBS-AChE (Fig. 14A1) clearly demonstrated that removal of sialic acid residues profoundly affected circulatory residence and precipitated enzyme removal from the bloodstream (Fig. 14A1 and Table 11), confirming that terminal sialylation is vital for cholinesterase maintenance in the circulation, as has been reported in previous studies (Douchet *et al.*, 1982; Kronman *et al.*, 1995; Chitlaru *et al.*, 1998; Saxena *et al.*, 1997b).

In contrast to the wealth of data concerning the possible effects of sialic-acid removal on the circulatory longevity of glycoproteins (Hossner and Billiar, 1981;Douchet *et al.*, 1982 Clarenburg, 1983; Thomas and Zamcheck, 1983; Lefort *et al.*, 1984; Vostal and McCauley, 1991; Kronman *et al.*, 1995; Saxena *et al.*, 1997b; Chitlaru *et al.*, 1998), there is very limited information on the involvement of α-gal capped glycans, in determining the circulatory behavior of glycoproteins. To examine this issue, the intact FBS-AChE enzyme was subjected to extensive α-galactosidase treatment (See "Materials and Methods"). Analysis of the glycans which were released from α-galactosidase treated FBS-AChE (Fig. 14B2), demonstrated a MALDI-TOF pattern similar to that obtained when the α-galactosidase treatment was performed on the glycans released from FBS-AChE (Fig. 12D). Thus, α-galactose can be completely removed from the intact FBS-AChE. The α-galactose removal from the enzyme did not affect the catalytic activity of the FBS-AChE and was not accompanied by other undesired glycosidase activities (Fig. 14B2). Inspection of the pharmacokinetic profile of FBS-AChE which was subjected to α-galactosidase treatment, demonstrated (Fig. 14B1 and Table 11), that in contrast to sialic-acid removal, α-gal removal did not accelerate FBS-AChE clearance and in fact exerted at most a very little effect on its pharmacokinetics. The $T_{1/2}\beta$ values for nontreated FBS-AChE and α-galactosidase treated FBS-AChE are indistinguishable (within the experimental error of the pharmacokinetic assay) with an apparent slight decrease in the Mean Residence Time (MRT, 1390 to 1150 minutes).

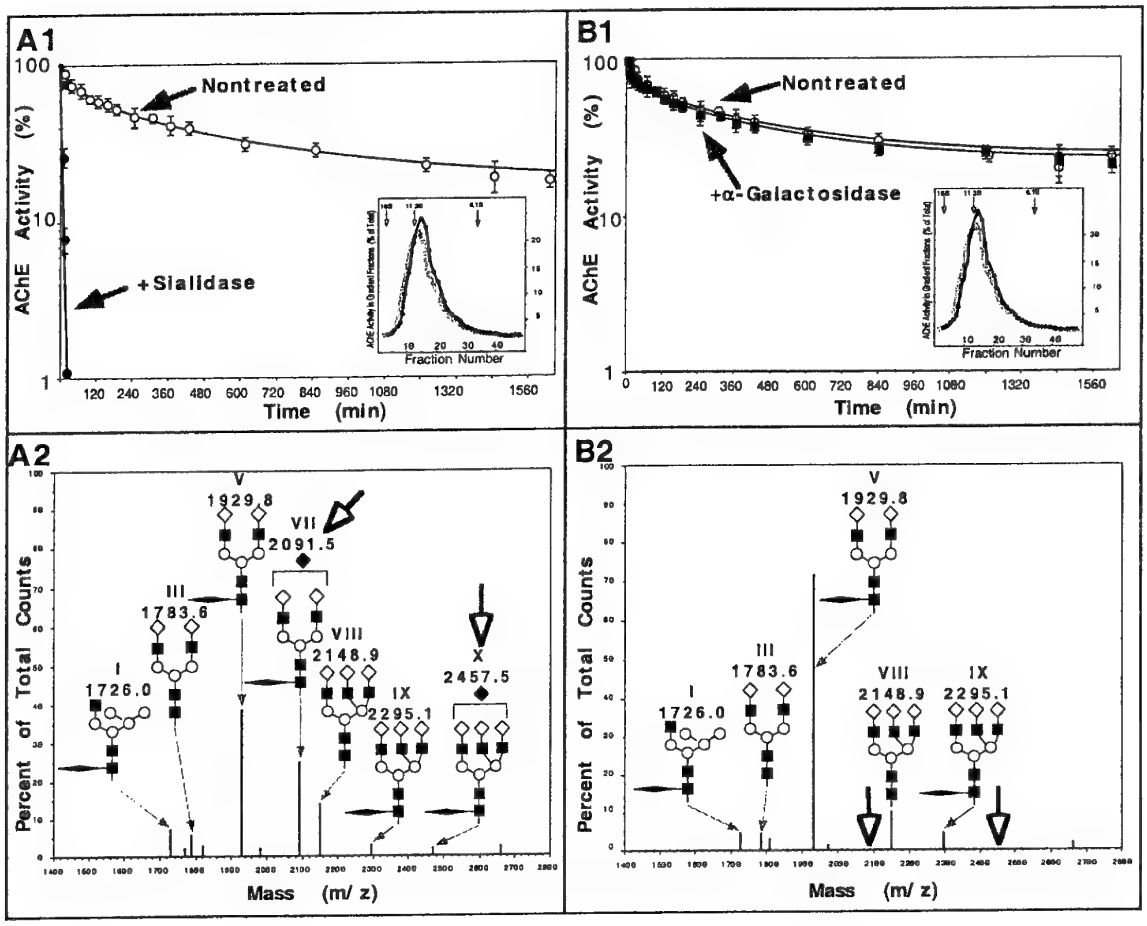

Figure 14: Effect of removal of sialic acid or α-galactose from intact FBS-AChE on its pharmacokinetic profile. Purified FBS-AChE or exoglycosidase-treated FBS-AChE was administered to mice (40μg/mouse in 0.2ml PBS). AChE values in samples removed immediately after injection were assigned a value of 100% and used for calculation of residual activity. Background cholinesterase levels in blood of pre-administered mice is less than 2 units/ml and was subtracted from the values obtained at the various time points. Exogenous AChEs were introduced at levels at least 30-fold higher than background level. *A1*, clearance profiles of sialidase-treated FBS-AChE (*filled circles*) and nontreated FBS-AChE (*open circles*). *Inset*, sucrose gradients of sialidase-treated (*black curve)* and nontreated enzymes *(shaded curve*) demonstrates retention of the tetrameric structure. *A2*, a portion of the sialidase-treated FBS-AChE was treated with *N*-glycosidase F, and glycans were purified, 2-AB labeled, and subjected to MALDI-TOF analysis. *B1*, clearance profiles of α-galactosidase-treated FBS-AChE (*shaded squares*) and non-treated FBS-AChE (*open circles*). *Inset*, sucrose gradients of α-galactosidase-treated (*black curve)* and nontreated enzymes *(shaded curve*) demonstrates retention of the tetrameric structure. *B2*, a portion of the α-galactosidase-treated FBS-AChE was treated with *N*-glycosidase F, and glycans were purified, 2-AB labeled, and subjected to MALDI-TOF analysis. Molecular weights and structural details are shown in *A2* and *B2* for the major glycan forms. Molecular weights represent monoisotopic masses of the respective $[M+Na]^+$ ions of the glycan species. *Open arrows* denote, respectively, the presence (peaks) and absence (expected locations of peaks) of α-gal-containing forms in *A2* (after sialidase treatment) and *B2* (after α-galactosidase treatment). *Solid square*, GlcNac; *open circle*, Man; *open diamond*, β-gal; *elongated diamond*, Fuc; *solid diamond*, α-gal.

Table 11 - Pharmacokinetic parameters of BoAChEs differing in their state of glycan sialylation and oligomerization.

Bovine AChE Source/Type	Treatment	A (% of total)	T1/2α (min)	B (% of total)	T1/2β (min)	Clearance (ml/hr/kg)	MRT (min)
HEK-293/recomb.	sialidase	100 *	3.5±0.4			1190	3.3
HEK-293/recomb.	-	78±6	4±0.6	23±4	29±7	302	57
HEK-293/recomb.	*in-vitro* sialylation	56±7	7.5±2	37±5	123±20	70	203
293ST-2D6/recomb.#	-	48±4	11±3	50±5	120±10	59	197
HEK-293/recomb.	*in-vitro* tetramerization	68±3	9±1	33±4	118±14	92	190
293ST-2D6/recomb.#	*in-vitro* tetramerization	35±6	30±10	67±2	965±40	6.5	1340
FBS/native	-	43±2	41±5	57±2	990±67	6.5	1390
FBS/native	α-galactosidase	44±8	50±8	54±9	930±90	7.5	1150
FBS/native	sialidase	100 *	3.5±0.3			1180	3.6

The circulatory clearance profiles of the various AChEs were determined as described ("Materials and Methods"). The biphasic pharmacokinetic curves were fitted to a of the form $C_t=Ae^{-k\alpha t}+Be^{-k\beta t}$. A and B represent the fractions of the material removed from the circulation in the first (fast) and second (slow) decay phases respectively. $T_{1/2}$ α and $T_{1/2}$ β represent the circulatory half-life values of the enzyme in the fast and slow phases, respectively. In all cases, the correlation coefficient was > 0.997. The clearance curves were also analyzed by fitting to a noncompartmental pharmacokinetic model for the calculation of Mean Residence Time (MRT) and Clearance using a Window-based program. Elimination half-life values calculated by noncompartmental analysis, coincided with the $T_{1/2}\beta$ values obtained by the biexponential elimination pharmacokinetic model. * : Sialidase-treated rBoAChE and FBS-AChE displayed a single-phase clearance profile, # : Recombinant BoAChE produced by the sialyltransferase expressor master cell line (See Results).

The effect of rBoAChE oversialylation on its pharmacokinetic behavior - HEK-293 cells, which serve as a production system for rBoAChE, are characterized by limited levels of sialyltransferase activity (Chitlaru *et al.*, 1998). This paucity is most pronounced for recombinant glycoproteins overexpressed at unusually high levels (Chitlaru *et al.*, 1998) in which case, the limitation in sialyltransferase activity of the cells preclude the production of recombinant proteins exhibiting fully sialylated glycans (Monica *et al.*, 1997). We have shown that this could be remedied by high-level sialyltransferase production resulting from the coexpression of a 2,6ST gene together with the gene encoding for the protein of interest (Chitlaru *et al.*, 1998). The finding that rBoAChE is pronouncedly undersialylated in comparison to FBS-AChE, and the fact that removal of the terminal sialic acid residues had a dramatic impact on clearance, prompted us to test the possibility of preventing rapid clearance of the recombinant bovine protein by expressing it in cell clones which display high levels of sialyltransferase activity.

(a) Generation of highly sialylated rBoAChE - The generation of a versatile cell line producing high levels of 2,6ST, which may serve for the production of fully sialylated glycoproteins, would require a reliable and rapid method for screening of cells which express high levels of sialyltransferase activity. The enzymatic method for detection of sialyltransferase activity by monitoring incorporation of radiolabeled sialic acid in the presence of soluble cell extract fractions (Weinstein *et al.*, 1982), is both cumbersome and not amenable with the simultaneous processing of many cell samples. Moreover, the measurement of high levels of cell-associated sialyltransferase activity, does not in itself demonstrate that glycans associated with these cells are indeed more efficiently sialylated. We therefore developed a solid-phase detection system based on a *Sambucus Nigra* Agglutinin (SNA) lectin-binding assay which scores the relative amounts of sialylated glycoprotein in cell extracts (See "Materials and Methods"). By utilizing this method, we could observe that individual cell clones isolated from a HEK-293 cell pool stably transfected with the rat 2,6ST gene, exhibited differing levels of glycoprotein-associated sialic acid (Fig. 15A). Extracts prepared from cells which were not transfected with the rat 2,6ST gene, failed to display significant SNA lectin affinity, in accordance with the low-level sialyltransferase activity, associated with these cells. Of all transfectant clones tested, clone 293ST-2D6 exhibited the highest levels of sialylated glycoproteins, commensurate with those scored in extracts of HuH7 cells (which, by virtue of their hepatic origin, possess very high levels of sialyltransferase activity). Clone 293ST-2D6 subsequently served as a host cell system for production of rBoAChE. Specific lectin probing of electroblotted recombinant AChE purified from HEK-293 and 293ST-2D6 cells demonstrated (data not shown) that the enzyme products of the two cell lines indeed differed markedly with respect to terminal occupancy of their glycans.

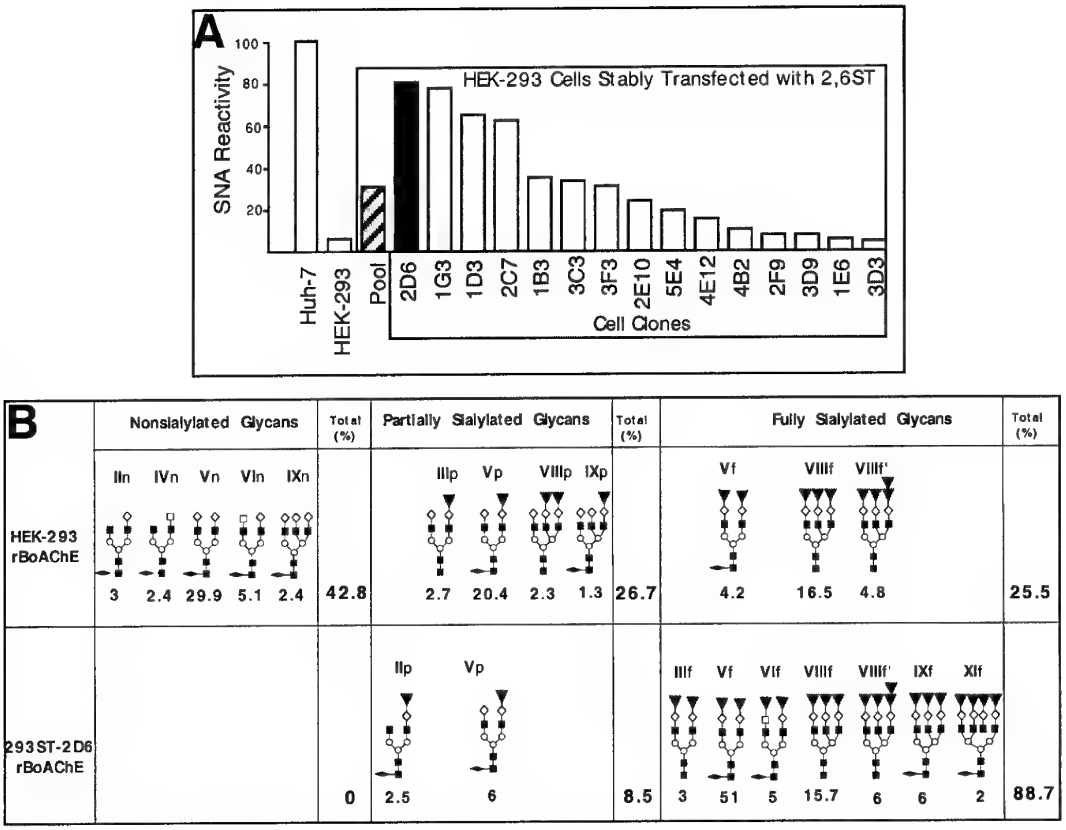

Figure 15: Generation of HEK-293 cell lines that allow expression of recombinant glycoproteins with high levels of sialylation. HEK-293 cells were stably transfected with the rat β-galactoside α2,6-sialyltransferase (*2,6ST*) gene, and sialic acid levels associated with individual cell clones were measured by *S. Nigra* agglutinin detection as described in "Methods". *A*, relative sialylation levels associated with the 2,6ST stably transfected cell pool (*striped*) and individual cell clones (*shaded*). The sialylation level determined for the HuH7 hepatic cell line was assigned a value of 100. The sialylation level of nontransfected HEK-293 cells is also shown. Cell clone 2D6 (*dark shading*) subsequently served as a cell host (assigned as 293ST-2D6) for transfection of rBoAChE expression vectors and recombinant protein production. *B*, glycan structures of rBoAChE produced by HEK-293 or 293ST-2D6 cells. Glycan structures were deduced from the mass spectral data shown in Fig. 13 and are classified according to their sialic acid occupancy. The various glycans are annotated by a Roman numeral that refers to the basic structures described in Fig. 12, followed by either "n" (indicates nonsialylated), "p" (indicates partially sialylated),or "f" (indicates fully sialylated). Where more than one fully sialylated form is present, the sialoforms are differentiated by a prime. The molecular weights of the monoisotopic masses of the respective $[M+Na]^+$ ions of the 2-AB labeled glycan species following iodomethane-mediated esterification are as follows: ***II*** *n* = 1781.8, ***II*** *p* = 2086.9, ***III*** p =2102.7, ***III*** f = 2407.8, ***IV*** n = 1823.9, ***V*** n = 1943.8, ***V*** p = 2248.9, ***V*** f= 2554.0, ***VI*** *n* = 1985.8, ***VI*** *f* = 2596.0, ***VIII*** *p* =2773.1, ***VIII*** *f* =3078.2 ***VIII*** *f'* =3383.1, ***IX*** *n* =2309.1, ***IX*** *p* =2614.2, ***IX*** *f* =3224.4, and ***XI*** *f* =3895.2. Note that methylation of the common 2-AB fluorescent moiety results in a molecular mass increase of 14.015 Da of all glycan species. Abundance values refer to the relative amount (% of total glycans) of each particular glycan species. *Solid square*, GlcNac; *open circle*, Man; *open diamond*, β-gal; *elongated diamond*, Fuc; *solid diamond*, α-gal. *Open square*, GalNAc; *inverted solid triangle*, sialic acid.

(b) Characterization of the glycan structures of oversialylated rBoAChE - MALDI-TOF structural analysis of N-Glycans recovered from recombinant BoAChE expressed in the 293ST-2D6 cells (Fig. 13B) established that the basic backbone structure of the N-glycans was not affected by the overexpression of the heterologous sialyltransferase gene. Close inspection of the glycan populations of the rBoAChE produced in the nonmodified and sialyltransferase-modified cells, could give the impression that some minor species are associated with the products of one cell line but not of the other (Fig. 15B). For instance, the tetraantennary form (Peak XIf) is represented as 2% of the total glycans in the enzyme of 293ST-2D6 cells only. However, the tetraantennary form actually is present in the nonmodified HEK-293 cell product as well, and can be detected if the glycan pool was subjected to sialidase treatment (Table 9, peak XI). It therefore follows, that the failure to observe this form in the glycan pool of the nonmodified cell-product, without prior treatment with sialidase (Fig. 15B, upper panel), is not due to its absence but rather to its distribution among multiple sialoforms (combinations of non-, mono-, di-, tri and/or tetrasialylated), each of which may be below detection level. Such careful inspection of the MALDI-TOF spectra, allows us to conclude that expression of the heterogeneous 2,6 sialyltransferase gene in the 293ST-2D6 cells did not introduce any alterations in the basic structure of the oligosaccharides comprising the glycan pool of rBoAChE.

MALDI-TOF analysis (Figs. 13B and 15B) established that the N-glycans of rBoAChE expressed in 293ST-2D6 cells are quantitatively capped with sialic acid residues (approximately 8.7 sialylated termini/enzyme subunit, and only 0.25 nonsialylated β-gal termini/enzyme subunit). This high extent of sialylation of glycan termini is similar to that of FBS AChE (compare Fig. 13B to Fig. 13A1). Alignment of the different forms comprising the glycan pools of the HEK-293 and 293ST-2D6 produced enzymes (Fig. 15B), revealed that while the ratio of [non-sialylated]:[partially-sialylated]:[fully-sialylated] glycans of the HEK-293 product was approximately 43:27:25, the corresponding values for the 293ST-2D6 product was 0:9:89. Notably, 92% of the most prevalent glycan species (Fig. 15B peak V) was not fully sialylated in the HEK-293 product, while in the 293ST-2D6 product over 89% of this glycan form is in its fully sialylated form. It is worth noting that the level of expression of rBoAChE in these cells is quite high (>50mg/liter). Taken together, these results clearly demonstrated that the coexpression at high levels of both sialyltransferase and rBoAChE, allows highly efficient sialylation of the various glycan forms associated with rBoAChE.

(c) Pharmacokinetic behavior of oversialylated rBoAChE - When subjected to pharmacokinetic studies the genetically modified-fully sialylated rBoAChE produced by the 293ST-2D6 cells demonstrated a significant increase in circulatory residence which is manifested by an increase in $T_{1/2}\beta$ from 29 to 120 min, and a greater than 3-fold increase in MRT from 57 to 197 min (Table 11). This increase was similar to that exhibited by HEK-293-produced rBoAChE which was sialylated *in-vitro* by commercial rat-liver α2,6ST (Table 11). Though the extent of glycan sialylation of rBoAChE from 293ST-2D6 cells is at least as high as that of FBS-AChE, the

residence time of the native enzyme (MRT = 1390 min) is still higher than that of the recombinant product. These results indicate that highly efficient sialylation can explain only in part, the elevated residence time of the native form of the enzyme.

Conversion of rBoAChE into stable tetrameric forms - Sucrose-gradient analyses of the fully sialylated rBoAChE produced by 293ST-2D6 cells (Fig. 16B1) established that the enzyme consists mainly of dimeric and monomeric forms of AChE catalytic subunits; the relative proportions of monomers, dimers and tetramers (G1:G2:G4) was approximately 40:50:10. This subunit assembly profile is similar to that of HEK-293 cell produced rBoAChE (Fig. 16A1), and is in sharp contrast to the native serum-derived BoAChE which consists of tetramers only (Ralston *et al.*, 1985; Mendelson *et al.*, 1998, see also Fig. 14). Since enzyme subunit assembly was not affected by glycan modification, it is clear that the partial improvement in circulatory residence exhibited by the 293ST-2D6 cell product, is a direct outcome of its improved sialylation.

In order to assess the contribution of the oligomerization status of BoAChE to its circulatory retention, an *in-vitro* system for the efficient generation of stable rBoAChE multimers was developed. To this end, we generated a synthetic peptide containing the ColQ Proline Rich Attachment Domain (PRAD), a region which was shown in the elegant studies of Bon and Massoulie (Bon and Massoulie, 1997; Bon *et al.*, 1997, see also Giles *et al.*, 1998) to be necessary and sufficient for efficient assembly of AChE tetramers *in-vivo,* via the C-terminal Tryptophan Amphiphilic Tail (WAT) domain of AChE (Simon *et al.*, 1998). The synthetic human PRAD peptide (Fig. 12A) was synthesized on the basis of the published sequence of the human ColQ protein (Ohno *et al.*, 1998) and in accordance with the defined boundaries of the attachment domains as established by deletion and site-directed mutagenesis studies (Bon *et al.*, 1997). The identity and purity of the synthetic peptide were confirmed by MALDI-TOF analysis (Fig. 17A, inset).

Incubation of the PRAD peptide with purified preparations of rBoAChE, resulted in a dose dependent oligomerization as detected by sucrose-gradient sedimentation assays (Fig. 17B). Assembled rBoAChE cosedimented at 11.3S with the catalase sedimentation marker, indicating that the oligomerized rBoAChE is in tetrameric form (Bon and Massoulie, 1997).

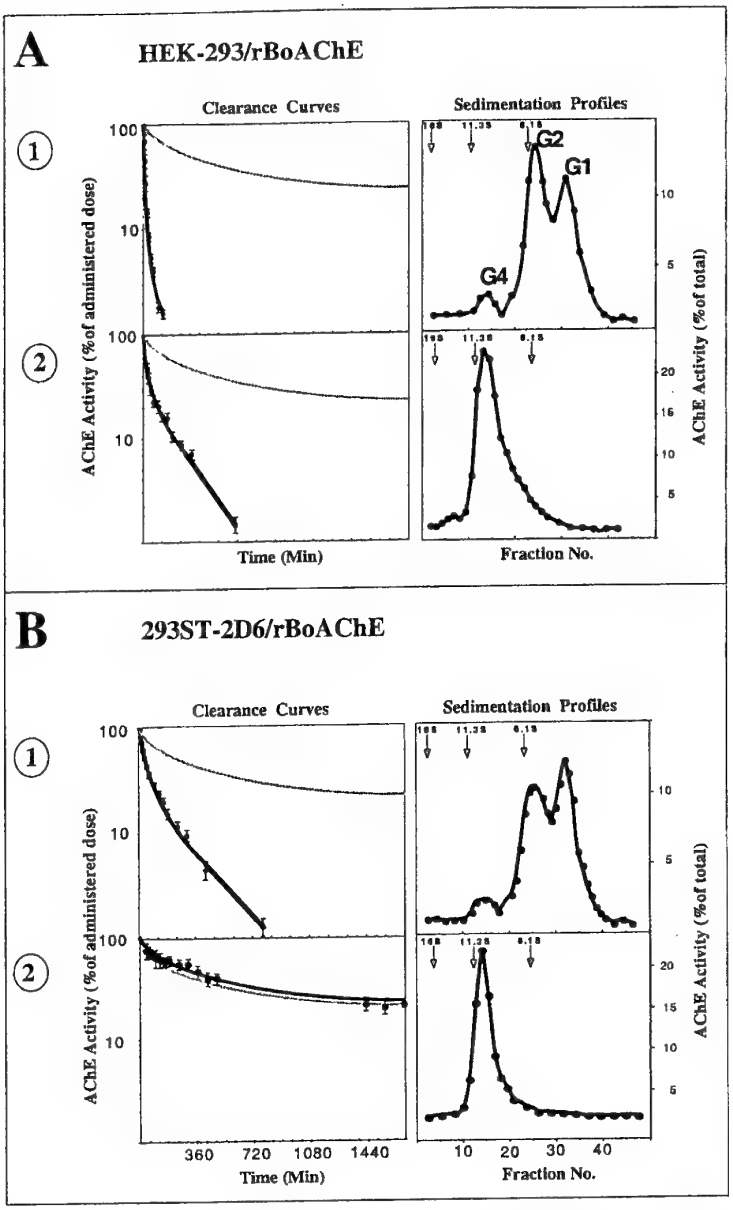

Figure 16: Pharmacokinetic profiles and subunit assembly status of rBoAChE produced by HEK-293 and 293ST-2D6 cells. *Left panels*, purified rBoAChE from HEK-293 cells before (*A1*) or after (*A2*) *in vitro* tetramerization in the presence of a synthetic peptide, representing the human Col-Q-derived PRAD or purified rBoAChE from 293ST-2D6 cells, before (*B1*) or after (*B2*) *in vitro* PRAD-mediated tetramerization, were administered to mice for determination of their circulatory clearance profiles and pharmacokinetic parameters as described in legend to Fig. 14 (see also Table 11). Elimination curves of the various rBoAChE preparations (*black circles*) are shown alongside the elimination curve of FBS-AChE (*gray curve*). *Right panel*, sucrose gradient sedimentation profiles of the corresponding rBoAChE preparations. *G1*, *G2*, and *G4* annotate the monomeric, dimeric, and tetrameric BoAChE peaks, respectively. *Arrows* denote the elution position of the sedimentation markers alkaline phosphatase (6.1S), catalase (11.3S),and β-galactosidase (16S) included in all samples.

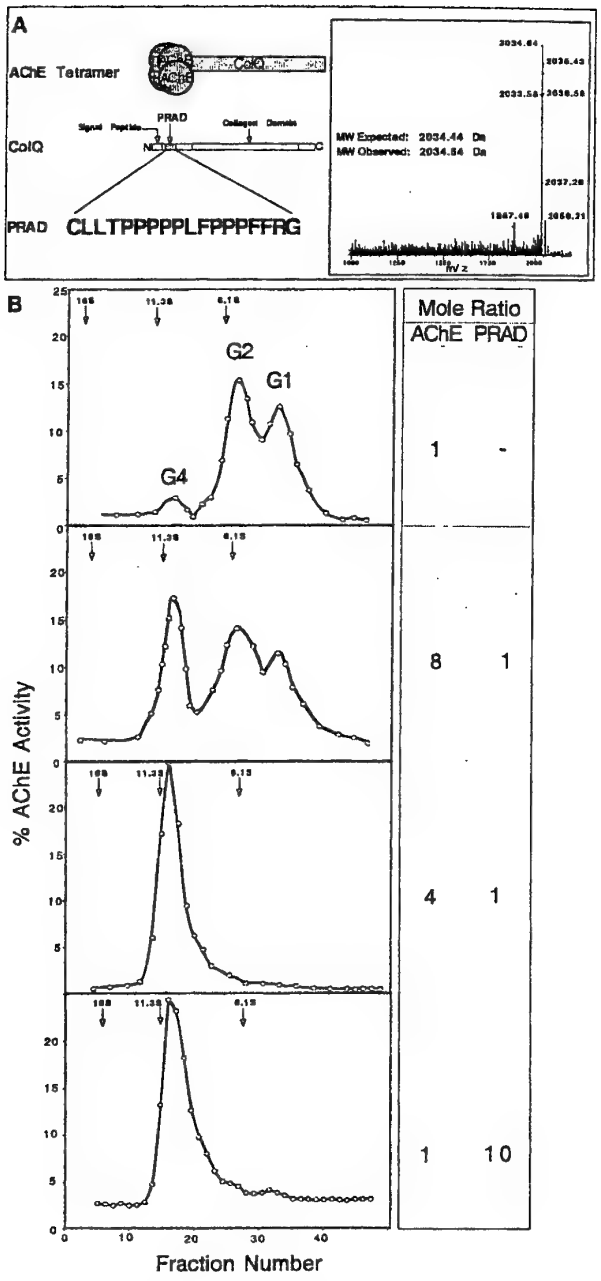

Figure 17: *In-vitro* PRAD-mediated tetramerization of rBoAChE. *A*, schematic representation of a membranal asymmetric AChE tetramer which is composed of the noncatalytic ColQ subunit and 4 catalytic AChE monomers. The amino acid sequence of human PRAD and its localization within the ColQ protein are shown. *Inset*, MALDI-TOF analysis of the pure synthetic human PRAD. *B*, recombinant BoAChE was incubated in the presence of PRAD, as described under "Methods" and subjected to sucrose gradient analysis. The molar ratios of AChE subunits and PRAD peptides included in each of the *in vitro* tetramerization reaction mixtures is shown (*right*). *G1*, *G2*, and *G4* annotate the monomeric, dimeric, and tetrameric BoAChE peaks, respectively. *Arrows* denote the elution position of the sedimentation markers alkaline phosphatase (6.1S), catalase (11.3S), and β-galactosidase (16S) included in all samples.

The PRAD-mediated *in-vitro* tetramerization process indeed followed faithfully the known stoichiometry of the ColQ/AChE assembly into heteromeric complexes of four catalytic and one noncatalytic subunit. Incubation of rBoAChE in the presence of PRAD at a lower molar ratio (PRAD:AChE=1:8) resulted in tetramerization of only part of the rBoAChE molecules. Incubation of rBoAChE in the presence of a large excess of PRAD peptide (PRAD:AChE = 10:1), resulted in

the formation of tetramers only; no other multimeric forms could be detected. Notably, the PRAD-mediated oligomerization process allowed the full conversion of both dimeric (G2) and monomeric (G1) forms into tetramers. No tetramerization could be detected when rBoAChE was incubated with an unrelated peptide comprising a commensurate number of amino acids. Furthermore, tetramerization via PRAD incubation did not occur with an AChE version lacking the C-terminal tail (not shown). Taken together, these results suggest that the tetramerization process faithfully reflects the physiological interaction between PRAD and WAT responsible for the generation of highly stable tetrameric forms of AChE (Massoulie *et al.*, 1999).

The *in-vitro* generated tetramers exhibited a high degree of stability, withstanding prolonged storage, several cycles of freezing-thawing, and extensive dialysis. This was further substantiated by our finding that following administration to mice, the enzyme retained its tetrameric configuration over long periods of time (not shown). Indeed, recently, the structure of a *Torpedo* AChE tetramer has been resolved by X-ray crystallography (Bourne *et al.*, 1999) and suggested that tetrameric forms of AChE are highly stable.

Tetramerization of either *Torpedo* or rat AChE by direct contact of proline rich domains and AChE subunits in a cell-free milieu was attempted in the past using polyproline rather than PRAD peptides. Efficient tetramerization occurred in the presence of cellular extracts which possibly contributed factors required for oligomeric assembly or in cells producing AChE which were cultured in the presence of polyproline (Bon *et al.*, 1997). The *in-vitro* tetramerization in the presence of a PRAD synthetic peptide and in the absence of additional assisting factors (such as cell extracts) reported here, may indicate that polyproline and *bona-fide* PRAD domains are not equivalent in their ability to promote tetramerization, the latter being a much more efficient oligomerization mediator. One should note however that the present study was conducted with the bovine version of AChE rather than the rat or *Torpedo* enzymes. The possibility that the bovine AChE is more prone for tetramerization than other AChE counterparts cannot be ruled out, yet there are no amino-acid sequence differences between the rat and bovine genes in their amphiphilic C-terminal tails which encompass the WAT domain interacting with PRAD (Legay *et al.*, 1993, Mendelson *et al.*, 1998).

Pharmacokinetics of rBoAChE tetramers - *In-vitro* PRAD-mediated tetramerization of the recombinant BoAChE produced by non-modified HEK-293 cells, (which promote limited levels of glycan sialylation only), displayed a significant pharmacokinetic improvement compared to the non-tetramerized enzyme (Fig. 16A2 and Table 11). Specifically, the biexponential $T_{1/2}\beta$ value increased from 29 to 118 min, and the MRT increased from 75 to 190 min. However, when fully-sialylated 293ST-2D6 cell-produced rBoAChE was subjected to *in-vitro* PRAD-mediated tetramerization, circulatory residence was increased in a much more pronounced manner, the $T_{1/2}\beta$ and mean residence time values for the tetramerized enzyme was 965 and 1340 minutes, respectively (Fig. 16B2 and Table 11). Most notably, following PRAD-mediated tetramerization, the fully sialylated rBoAChE displays a pharmacokinetic profile which was very similar to that observed for the long-lived native serum-derived BoAChE ($T_{1/2}\beta$ = 990 min; MRT = 1390 min). Thus, although enzyme

oligomerization in itself can increase the circulatory life-time of partially sialylated rBoAChE, its effect on circulatory longevity can be fully appreciated only when the enzyme is efficiently sialylated.

We have noted above, that in contrast to removal of terminal α-galactose residues from the FBS-AChE, which practically did not affect its circulatory life-time ($T_{1/2}\beta = 930$ min; MRT = 1150 min, Table 11), desialylation of the tetrameric FBS-AChE promoted its rapid clearance from the circulation ($T_{1/2}$ =3.5 min; MRT = 3.6 min). In view of the fact that protein oligomerization contributes to circulatory retention, one could have argued that the rapid clearance of desialylated FBS-AChE was actually caused by tetramer disassembly during the prolonged incubation in the presence of sialidase, required for complete removal of sialic acid from the intact protein. That this is not the case is clearly demonstrated by sucrose-gradient analyses (Figs. 14A1 and 14B1, insets) which show that the glycosidase-treated enzymes retained their tetrameric form, indicating that the differential effects of α-galactose and sialic acid removal cannot be attributed to tetramer dissociation, but are rather a direct outcome of the glycan modifications brought about by the respective enzymatic treatments. In line with the dramatic decrease in circulatory residence caused by desialylation of tetrameric FBS-AChE, we note that recombinant AChE tetramers also displayed a rapid removal rate following sialidase treatment, indistinguishable from that exhibited by the desialylated native enzyme. In fact, the pharmacokinetic profile of the desialylated tetrameric AChEs was identical to that obtained following desialylation of non-tetrameric AChE such as the recombinant versions produced by either HEK-293 cells or 293ST-2D6 cells.

DISCUSSION

Similar basic glycan structures are associated with recombinant HEK-293-produced and native serum-derived bovine acetylcholinesterase - Previous studies (Kronman *et al.*, 1995); Chitlaru *et al.*, 1998; Saxena *et al.*, 1997b) which were based on chemical determination of sialic acid, monosaccharide composition, charge and size distribution analyses and HPAEC-PAD profiling of oligosaccharides, allowed partial characterization of some features of the glycans associated with cholinesterases. For example, HPAEC-PAD analyses revealed that a complex array of glycan types which are differentially sialylated, are associated with recombinant acetylcholinesterase (Chitlaru *et al.*, 1998). In an other study, exoglycosidase-sequencing in conjunction with size-distribution chromatography allowed glycan structural analysis which was confined to the major species of the multiple forms associated with serum derived AChE (Saxena *et al.*, 1997b). Due to their limited power of resolution, these methodologies could not provide a comprehensive structural analysis of the entire spectrum of glycans, and therefore the biological significance of the findings was not entirely clear.

Here by MALDI-TOF profiling in conjunction with exoglycosidase mapping, we were able to determine the actual structures of essentially all the oligosaccharides comprising the glycan pools of both HEK-293-produced rBoAChE and serum-derived native bovine AChE. Though both enzyme species displayed an intricate array of glycan forms, common features of the two glycan pools could be established: (i) The rBoAChE and FBS-AChE associated glycans are of the complex type, displaying either biantennary (major species = $(Man)_3(GlcNAc)_4(\beta Gal)_2(Fuc)$) or triantennary structures (major species = $(Man)_3(GlcNAc)_5(\beta Gal)_3$), the most prevalent form being of the biantennary fucosylated type. While most of the glycan structures contained fucose, glycans exhibiting GalNAc were identified at very low levels (Table 12). (ii) With the exception of terminal monosaccharide occupancy, the basic structures of the oligosaccharides comprising both glycan pools were virtually identical (Fig. 12D). (iii) The relative abundances of the different basic structures of the glycans of both enzymes were similar (Table 12). The extent of similarity shared by the recombinant and native forms of AChE with respect to their basic N-glycans structures was remarkable considering the fact that they are pharmacokinetically-distinct and that they markedly differ in their origin. The recombinant enzyme originates from a human embryonic kidney cell line selected for its high expression of heterologous product. The native AChE is generated by fetal bovine cells of unknown origin. Since the probability that FBS-AChE is generated by fetal bovine kidney cells is low, this degree of glycan resemblance suggests that as long as the producer cells are equipped with sufficient amounts of necessary and appropriate elements of the glycosylation machinery, the glycan structures appended to a particular protein may be dictated to a considerable extent by the protein *per se*.

Table 12 - Structural Characteristics of N-Glycans Associated with rBoAChE and FBS-AChE

Glycan Characteristics	ENZYME SPECIES	
	rBoAChE (*recombinant*)	FBS-AChE (*native*)
Biantennary glycans	67%	74%
Multiantennary glycans	32%	22%
Fucosylated glycans	67%	82%
GalNAc-containing glycans	4.5%	4.2%
α–Gal-capped glycans	<0.8%	25% *
Glycan termini with exposed β–Gal	50%	3.2%

* - No glycans containing more than 1 α-gal residue could be detected. Due to the predominant biantennary nature of the α-gal containing glycans, this value is therefore equivalent to approximately 12% glycan termini occupancy by α-gal.

Oligosaccharides associated with the rapidly-cleared recombinant and the long-lived native bovine acetylcholinesterase diverge in their glycan-terminus occupancy - Comparison of the N-glycans derived from rBoAChE and FBS-AChE (Tables 10 and 15), revealed that the rBoAChE is pronouncedly undersialylated as compared to the FBS-AChE (in rBoAChE approximately 50% of the glycan termini exhibited an exposed β-gal while in FBS-AChE only 3.2% of the glycan termini exhibited an exposed β-gal). These results are not in agreement with those reported previously (Saxena *et al.*, 1997b) where on the basis of carbohydrate composition analysis of monosaccharides released from the glycans associated with FBS-AChE, it has been suggested that the long-lived FBS-AChE is heavily undersialylated and that half of the glycan termini associated with this enzyme are not capped by sialic acid. This discrepancy may be partly explained by the fact that in this study (Saxena *et al.*, 1997b), the number of potential N-glycosylation sites used to calculate termini occupancy was erroneously considered to be 5, rather than 4 (Mendelson *et al.*, 1998).

Inspection of the various glycans of rBoAChE, revealed that undersialylation is not random. We note a preferential sialylation of higher-branched (triantennary) glycans (Fig. 15B, peaks VIIIf and VIIIf'), as has been reported in other recombinant expression systems as well (Legay *et al.*,1993). Nevertheless, since the triantennary forms comprise a relatively low sub-population of the total glycans of rBoAChE, there is an overall state of undersialylation of the glycans associated with this enzyme.

Glycans containing α-gal are not present on rBoAChE yet in the native FBS-AChE enzyme constitute 25-30% of the total glycan pool. These are mostly of the biantennary form, though triantennary glycans exhibiting α-gal were also detected (Fig. 12A peaks VII and X). The lack of α-gal-containing glycans in the recombinant enzyme produced by cells of human origin (HEK-293) is in full accordance with the well-documented fact that humans, Old World primates, and anthropoid apes, lack the glycosyltransferase activity required for α-gal appendage (Galili *et al.*, 1998).

The role of cell and protein-specific factors in determining glycan forms of BoAChE - The marked difference in the composition of the glycan termini suggests that cellular factors are decisive in determining the nature of terminal glycosylation, as is indeed manifested by the correlation between the low abundance of sialyltransferases in HEK-293 cells (Chitlaru *et al.*, 1998) and the poor sialylation of rHuAChE (Kronman *et al.*, 1995; Chitlaru *et al.*, 1998) or of rBoAChE produced in these cells (Mendelson *et al.*, 1998). Nevertheless, that terminal glycosylation is not determined solely by cell-specific elements but also by protein-related factors is substantiated by the findings that other recombinant proteins expressed in HEK-293 cells show a glycosylation pattern distinctly different from that found for rBoAChE. For example, the major glycan forms of recombinant Protein C produced in HEK-293 cells, carry an outer-arm fucose in addition to the core fucose, and contain high levels of Gal to GalNAc substitutions (Yan *et al.*, 1993). In the case of rBoAChE, glycan structures carrying more than 1 fucose were undetected, while Gal to GalNAc substitutions were identified on less than 5 percent of the glycans (Table 12). The low level of GalNac-terminating glycans in HEK-293-produced rBoAChE, is significant with respect to circulatory longevity, since terminal GalNAc may serve as an acceptor for the appendage of sulphate groups. SO_4-terminating glycans were described for pituitary hormones such as LH and TSH, where they ensures the necessary oscillatory nature of the pituitary endocrine effect, by the rapid removal of the hormones from the bloodstream via a specific hepatic clearance receptor (Fiete *et al.*, 1991,1998). The lack of high levels of GalNAc in rBoAChE, precludes a significant role for this epitope in the removal of rBoAChE.

Do α-galactosylated glycans affect circulatory longevity of glycoproteins? - The possible effect of α-gal residues on the circulatory residence of therapeutic glycoproteins is a matter of debate (Galili, 1993; Borrebaeck *et al.*, 1993; Borrebaeck, 1999; Junghans, 1999). Previous studies concerning the pharmacokinetic behavior of tissue-type plasminogen activator (t-PA), have indicated that recombinant glycoforms which contained α-galactose moieties in their carbohydrate chains exhibited a significantly longer mean residence time in the circulation of chimpanzees, than those which lacked such structures (Tanigawara *et al.*, 1990). However, the effect of α-gal removal on clearance of t-PA was not examined experimentally, and therefore the correlation of α-gal containing glycans with long-lived protein species may be no more than circumstantial. Here, we find that

quantitative removal of terminal α-gal did not significantly alter FBS-AChE clearance (Fig. 14B1), indicating that α-gal does not provide pharmacokinetic advantage to the administered enzyme.
In the case of t-PA, the authors attributed the protective effect of α-gal to the presence of high levels of anti α-gal antibodies in the circulation of some primates (apes, old world monkeys, and humans). It was suggested that these antibodies may interact with the glycoprotein in such a manner so that recognition sites in the liver may be obstructed, leading to reduction in hepatic uptake rates. One should note that the pharmacokinetic behavior of FBS-AChE in rodents (Figs. 14A1, 14B1) which lack antibodies against α-gal is similar to that found in primates such as rhesus monkeys (Maxwell *et al.*, 1992), suggesting that at least in the case of FBS-AChE, antibodies against α-gal do not appear to play any role in determining circulatory lifetime.

Increasing cellular sialyltransferase levels results in the generation of highly sialylated rBoAChE glycans with improved pharmacokinetic performance - The generation of a master cell line, 293ST-2D6, expressing stable high-levels of recombinant sialyltransferase (Fig. 15A), enabled us to examine whether increased sialylation of rBoAChE enhanced its circulatory retention to levels which are comparable to those of FBS-AChE. Inspection of the glycans associated with the sialyltransferase-modified cell product (Fig. 15B, lower panel) established that these are shifted to higher molecular weights, as compared to the glycans from rBoAChE produced by nonmodified HEK-293 cells, and that only 8.5% of the glycans are undersialylated. This fraction is composed of the monosialylated biantennary fucosylated glycan (peak Vp) and its immature precursor form lacking a galactose (peak IIp). The latter is refractive to further sialylation due to its immature nature. This glycan species may correspond to the sialylation-refractive glycan forms observed by us in human rAChE using the HPAEC-PAD detection system (Chitlaru *et al*, 1998), but which could not then be accurately quantified nor assigned a definitive structure, due to the limitations of the detection system employed.
Examination of the pharmacokinetic behavior of the highly sialylated rBoAChE, revealed that this glycoprotein resided in the circulation for considerably longer periods of time ($T_{1/2}\beta$ = 120 min, MRT = 197 min) than the undersialylated enzyme produced in nonmodified HEK-293 cells ($T_{1/2}\beta$ = 29 min, MRT = 57 min). However, the extended residence time exhibited by this glycoprotein still falls short of the corresponding retention values exhibited by the native FBS-AChE ($T_{1/2}\beta$ = 990 min, MRT = 1390 min) indicating that factors other than glycan sialylation are also important for the extension of the circulatory life-time.

***In-vitro* tetramerization of BoAChE and its effect on circulatory longevity -** In contrast to the rBoAChE which was characterized by the predominant presence of dimeric and monomeric forms, naturally occurring forms of AChE, whether circulatory or membrane-bound, are arranged in multimeric complexes (Taylor, *et al.*, 1981; Younkin *et al.*, 1982; Ralston *et al.*, 1985; Atack *et al.*, 1987; Stieger *et al.*, 1989; Mendelson *et al.*, 1998). Dimerization of catalytic subunits of AChE occurs invariably by covalent disulfide bridging involving cysteine residues situated in the C terminal domains of the enzyme (Velan *et al.*, 1991a). Dimers further assemble into stable quaternary complexes which represent the main form of circulatory acetylcholinesterase, as is the case of serum-derived fetal bovine AChE. In several occasions monomeric subunits of AChE have been reported (Lazar and Vigny, 1980; Atack, *et al.*, 1987), but their origin as breakdown products of multimeric forms could not be ruled out (Rotundo and Fambrough, 1979; Vignay *et al.*, 1979; Allmand *et al.*, 1981; Lockridge and LaDu, 1982). The nonphysiological dimeric and monomeric configurations of cell culture-generated AChE has been reported to characterize other versions of recombinant cholinesterases as well. For example, recombinant preparations of rat or *Torpedo* AChE produced in COS cells (Bon and Massoulie, 1997, Bon *et al.*, 1997), human butyrylcholinesterase from CHO cells (12) and human AChE from HEK-293 cells (Velan *et al.*, 1991a, Kronman *et al.*, 1995), all consist of mainly dimers of catalytic units and only of negligible fractions of tetramers. The subunit assembly state of AChE does not affect the catalytic ability of the enzyme, nor does it influence directly the production rates of recombinant versions of the enzymes produced in various cell culture systems (Velan *et al.*, 1991a). Recombinant forms of AChE are consistently characterized by a short circulatory residence time when administered to experimental animals (Kronman *et al.*, 1995, Chitlaru *et al.*, 1998, Saxena *et al.*, 1998b, Mendelson *et al.*, 1998), while the naturally occurring forms of serum-derived tetrameric AChEs possess a long circulatory residence time. These observations suggested that the oligomerization status of AChE may play an important role in the pharmacokinetic properties of the corresponding enzymes. Yet, the overriding pharmacokinetically deleterious effect of glycan undersialylation and the inability to control the oligomerization state of AChE precluded until now the full appreciation of the role of oligomerization in circulatory retention. For example, Saxena *et al.* (1998b), conducted a comparative pharmacokinetic study between various acetylcholinesterases differing in the extent of their tetramer/dimer content but this study was not conclusive since the various AChE forms inspected differed not only in their oligomerization status. Similarly, in an earlier study in our laboratory (Kronman *et al.*, 1995), no clear-cut correlation between the oligomerization state of various human recombinant AChEs produced in HEK-293 cells and their circulatory clearance rate could be shown. It was therefore important to develop a system which allows one to control both the degree of glycan sialylation and the extent of enzyme subunit oligomerization. This could now be achieved thanks to the pioneering studies of Bon *et al* (Bon and Massoulie,1997 , Bon *et al.*, 1997) which have established that coexpression of AChE and the ColQ Proline Rich Attachment Domain (PRAD) in COS cells resulted in the generation of stable secreted AChE tetramers.

Here we show that *in vitro* tetramerization by purified PRAD is **sufficient** for the process of tetramer assembly. This is an extension of the original system developed by Giles *et al.* (1998). Most notably the stoichiometry of the PRAD-AChE association (Fig. 17B) reflects faithfully the known molar ratio of 1xColQ/4xAChE within the membranal quaternary complexes of AChE, confirming their tetrameric nature and the expected presence of a single PRAD peptide in the asymmetric complex (Simon et al., 1998). The strict 4 to 1 ratio for tetramerization of AChE was also indirectly suggested by coexpression experiments in COS cells (Bon and Massoulie, 1997) in which it was found that a 4 to 1 ratio of plasmid DNA in the cotransfection mixture is required for generation of tetramers. It should be noted that *in-vitro* oligomerization in the presence of PRAD, led to efficient tetramerization not only of rBoAChE dimers (G2), but also of monomeric (G1) forms (Fig. 17B).

The studies presented here, clearly show that tetramerization prevents the fast removal of recombinant BoAChE from the circulation (Fig. 16 and Table 11). Most notably, the pharmacokinetic values of the tetramerized enzyme were improved to the extent that the efficiently sialylated recombinant AChE displays a pharmacokinetic profile which is virtually indistinguishable from that of its native serum-derived counterpart.

Inspection of the state of assembly in the circulation following administration of fully tetramerized enzyme, failed to reveal the presence of dimers or monomers, even after long periods of time (not shown), suggesting that removal from the circulation does not involve an intermediate stage in which the tetramer is dissociated into dimers or monomers.

The observation that the oligomerization status contributes to the serum residence time of AChE suggests a simple explanation for the scarcity of naturally occurring dimeric forms of circulating AChE, since the only population of AChE molecules which survive in the circulation over long periods of time are those arranged into tetrameric complexes. Alternatively, the relatively low amounts of tetramerized AChEs in recombinant cell production systems, may reflect the lack of a selection process which allows the preferential accumulation of the tetramerized enzyme population.

Why are tetramers more stable in the circulation? This may reflect a simple size-exclusion phenomenon: high molecular weight complexes are not amenable to glomerular filtration while dimers and monomers of relatively low hydrodynamic volume are removed efficiently from the circulation by the kidneys. Alternatively, the assembly of enzyme subunits into tetrameric forms may mask some epitopes which contribute to the clearance of the enzyme subunit. The possible involvement of such protein-related elements in cholinesterase removal from the circulation is at present a subject of study in our laboratory.

What is the interplay between sialylation and tetramerization in determining circulatory longevity ? - In Fig. 18A we depict in a schematic manner, the contribution of both glycan sialylation and enzyme tetramerization to the pharmacokinetic behavior of rBoAChE. Conversion of the partially sialylated non-assembled enzyme (Fig. 18A-b) into either its fully sialylated form (Fig. 18A-e), or into its tetramer configuration (Fig. 18A-c), results in a significant increase in the circulatory life-time of the enzyme, yet, these enzyme forms still are cleared more rapidly than the native serum-derived form of bovine acetylcholinesterase. Only when the partially sialylated non-assembled recombinant enzyme has been subjected to both improvement in the level of terminal sialylation as well as tetramerization (Fig. 18A-f), does the modified product remain in the circulation for periods of time which are comparable to the native enzyme (Fig. 18B). However, these two factors do not operate by simple rules of additivity in their contribution to protein longevity. This is exemplified by the fact that both assembled and non-assembled enzyme forms which are totally devoid of sialic acid are removed in an equally rapid manner within minutes, from the circulation (Compare Figs. 18A-d, and 18B-g to Fig. 18A-a). Thus, tetramerization in itself cannot pharmacokinetically rescue totally asialylated enzyme, and in fact does not contribute in any measurable way to its circulatory retention. Conversely, partial sialylation does result in improved circulatory retention of non-tetramerized AChE, as can be observed by comparing the pharmacokinetic properties of rBoAChE and sialidase-treated rBoAChE (compare Fig. 18A-a to 22A-b). Thus, glycoprotein sialylation plays an overriding role in circulatory retention, and a minimal level of sialylation is required for manifestation of the role of other factors such as subunit assembly, in determining circulatory longevity. This fundamental aspect of glycan sialylation probably reflects the high efficiency of the hepatic asialoglycoprotein-receptor mediated removal system which evolved to allow the rapid turnover of immature glycoproteins from the circulatory system (Ashwell and Harford, 1982). Yet, we note that some low levels of asialylated glycan termini can be tolerated, as indicated by the observation that removal of terminal α-gal moieties which we show to result in the exposure of β-gal residues, did not significantly affect circulatory residence (Fig. 18B-h). Since following α-galactosidase treatment of FBS-AChE, 1 glycan terminus per enzyme subunit (~12% of the total glycan termini) carries an uncapped β-gal, one must assume that elimination from the circulation of rBoAChE by the hepatic asialoglycoprotein receptor requires more than one exposed β-gal residue per AChE subunit. This is in accordance with the observations of Ashwell and Morell (1974), that clearance via the asialoglycoprotein receptor is strongly dependent upon the density of the appended terminal-galactose residues. One should however keep in mind that the slightly lower MRT value exhibited by the α-galactosidase treated enzyme may indeed reflect the fact that this enzyme is approaching the threshold of circulatory tolerance for asialoglycoproteins.

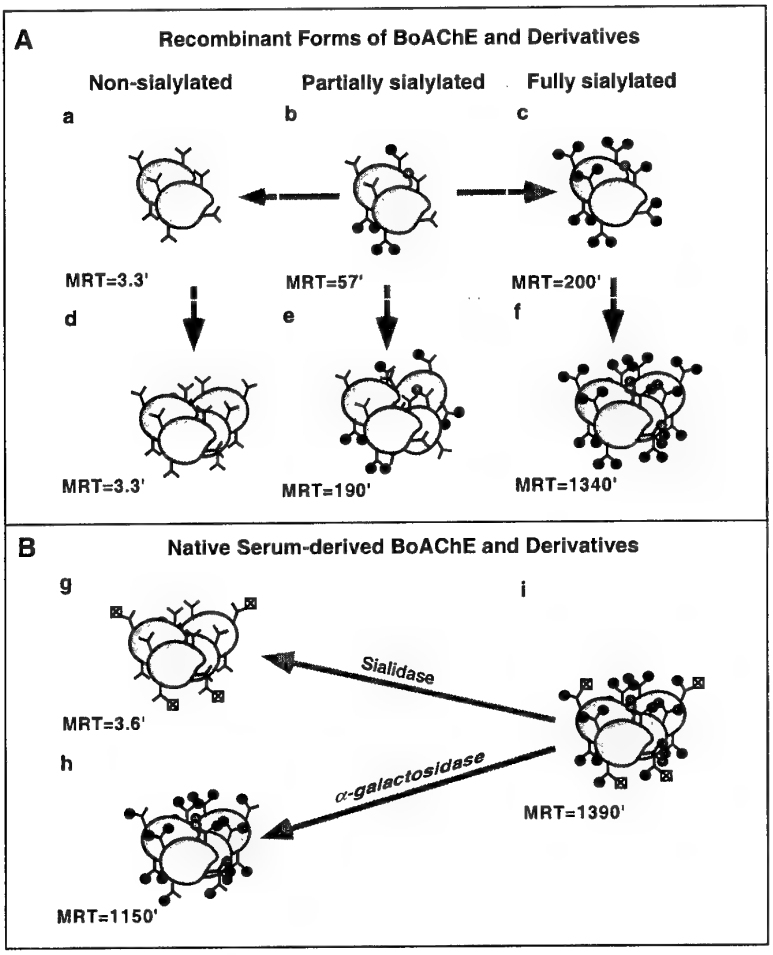

Figure 18: Schematic presentation of the interplay between occupancy of N-glycan termini by sialic acid or α-galactose and tetramerization to the circulatory longevity of the BoAChE glycoprotein. Schematic structures and MRT values of rBoAChE and FBS-AChE before and after various treatments. *A*, Recombinant BoAChE: *a*, produced by HEK-293 cells and desialylated by enzymatic treatment with sialidase; *b*, nonmodified recombinant BoAChE produced by HEK-293 cells; *c*, recombinant BoAChE in its fully sialylated form following *in vitro* sialyltransferase treatment or expression in the genetically engineered 293ST-2D6 cells; *d-f*, each of these three rBoAChE sialoforms (*a-c*) were treated with PRAD to generate their respective tetrameric forms. *B*, FBS-FBS-AChE: *g*, native enzyme subjected to sialidase treatment; *h*, native enzyme subjected to α-galactosidase treatment; *i*, native FBS-AChE. Note that form *g* still bears α-gal termini. *Dotted circles*: sialic acid; *Crossed squares*, α-galactose.

Concluding remarks - AChE possesses a valuable therapeutic potential, by virtue of its high affinity to organophosphorus poisons. Its use as an efficient bioscavenger has been advanced by the development of recombinant production systems (Fischer *et al.*, 1993; Kronman *et al.*, 1992) and the identification of catalytically favorable mutations (Taylor and Radic, 1994; Ordentlich *et al.*, 1996;

Shafferman *et al.*, 1996b,c; Millard *et al.*, 1998; Ordentlich *et al.*, 1999). Yet the short circulatory residence time of the various recombinant AChE preparations represents one of the factors which preclude the development of an efficient acetylcholinesterase-based recombinant bioscavenger and the formulation of a method for the pharmacokinetic improvement of the enzyme represents a major biotechnological challenge. In the present study we show that a delicate hierarchy of post-translation-related components can indeed determine circulatory residence time, and that when these factors are combined judiciously in their optimized configurations, one can reconstitute into the rBoAChE mold, all the elements which would promote its circulatory longevity. This study can serve as a basis for the generation of a therapeutically efficient bioscavenger based on recombinant human acetylcholinesterase, as well as generation of other pharmacokinetically long-lived biomolecules, and suggests a mode of operation for unraveling cellular processes and biochemical factors involved in circulatory longevity.

VI. Effect of Human Acetylcholinesterase Subunit Assembly on its Circulatory Residence

INTRODUCTION

The propensity of some proteins to be retained for extended periods of time in the circulation, while others are rapidly directed towards clearance pathways, has major consequences for biological functions such as immunological responses and endocrine regulation as well as for the generation of therapeutically efficient biomolecules. Among the latter, in recent years special attention was focused on the enzymes acetylcholinesterase (AChE) and butyrylcholinesterase (BChE), whose therapeutic potential requires their long-term retention within the circulation (Wolfe *et al.*, 1987; Ashani, *et al.*, 1991; Broomfield *et al.*, 1991; Maxwell *et al.*, 1992; Raveh *et al.*, 1993; Kronman *et al.*, 1995; Saxena *et al.*, 1997b, Chitlaru *et al.*, 1998).

Elimination of circulating proteins is an intricate process involving a variety of removal mechanisms. Specific characteristics of the circulating protein, including protein size, surface charge, hydrophobicity, and the presence of specific amino-acid and carbohydrate epitopes, may be decisive in determining its circulatory longevity. In addition to clearance systems which are based on protein elimination via kidney glomerular filtration or protease degradation, different receptor-based systems which recognize and bind to protein-related epitopes, are responsible for the active removal of the protein from the bloodstream (Ashwell and Harford, 1982; Drickamer, 1991).

In the case of AChE, the contribution of appendiced carbohydrates to circulatory residence was demonstrated by the finding that bacterially generated recombinant AChE as well as N-Glycanase treated ChEs of animal cell origin, both being devoid of N-glycans, are cleared rapidly from the circulation of experimental animals (Fischer *et. al*, 1993; Kronman *et al.*, 1995). However, the pharmacokinetic profiles of an array of mutated rHuAChE differing by the number of N-glycosylation sites (Kronman *et al.*, 1995), suggested that though N-glycosylation in itself does play a role in determining circulatory residence, the structural features of the N-glycans, play a decisive role in circulatory retention of ChEs. In particular, we have shown that the capping of N-glycan β-galactose residues with sialic acid, is required for long-term retention of the protein, and that an inverse-linear relationship exists between the number of exposed β-galactose residues in association with a given form of recombinant human acetylcholinesterase (rHuAChE), and its circulatory life-time. In accordance with these findings, we demonstrated (Chitlaru *et al.*, 1998) that circulatory residence can be extended by generating rHuAChE or recombinant bovine acetylcholinesterase (rBoAChE) in a modified cell line which expresses high levels of recombinant 2,6 sialyltransferase, and thus allows improved sialylation of the coexpressed recombinant AChE products. However, we noted that though the enzyme produced in the sialyltransferase-modified cells displays increased

retention, it is still removed from the circulation more rapidly than native serum-derived ChEs. The inability of the modified enzyme to be retained in the circulation over long periods of time in a manner comparable to that of native serum-derived ChEs, may be an outcome of specific sugar-related epitopes or other post-translation factors. Specifically, the more rapid clearance of recombinant ChEs may result from the fact that recombinant cholinesterases produced in the HEK-293 as well as in other cell systems, characteristically display a state of subunit assembly which differs from that of circulatory long-lived native serum-derived enzyme. While the recombinant enzyme is mostly in dimeric and monomeric form, the native serum derived enzyme is almost exclusively assembled into tetramers. The failure of recombinant ChEs to assemble efficiently into tetramers may accelerate their removal from the circulation. This indeed was recently shown to be the case for bovine acetylcholinesterase (Kronman *et al*, 2000). However, unlike the bovine enzyme, natural human tetrameric circulating acetylcholinesterase are not known to exist, and whether the assembly of the human enzyme subunits into tetrameric forms confers any pharmacokinetic advantage to this enzyme, is yet not clear.

In the present study, we first employ refined MALDI-TOF analyses to allow an accurate determination of the glycan structures of rHuAChE produced by HEK-293 and sialyltransferase overexpressor 293ST-2D6 cell lines, and assess quantitatively the contribution of N-glycan terminal sialylation to the elimination of rHuAChE from the circulation. In addition, by utilizing rHuAChE mutants which fail to form intersubunit disulfide bridges, or by inducing *in-vitro* tetrameric assembly by the ColQ-derived Proline Rich Attachment Site (PRAD, Bon and Massoulie, 1997; Bon *et al.*, 1997; Giles *et al.* 1998, Kronman *et al.* 2000), as well as by employing highly enriched dimeric enzyme preparations, we conduct a comparative pharmacokinetic analysis of an array of uniformly assembled rHuAChEs. These various oligomeric preparations which differ one from another in their enzyme subunit organization were prepared in different cellular backgounds to probe also the combined effect of sialylation and subunit assembly on clearance. Thus, we determine a rank order for monomeric, dimeric and tetrameric rHuAChEs which are either highly-sialylated, partially-sialylated or totally asialylated, with respect to their ability to reside in the circulation. Finally, we demonstrate that by combining efficient sialylation with induction of high order oligomerization, it is possible to confer the recombinant HuAChE with unprecedented circulatory residence abilities.

MATERIALS AND METHODS

Cell Culture - Generation of HEK-293 cell lines stably expressing high levels of rHuAChE (Soreq *et al.*, 1990 was described previously (Kronman *et al.*, 1992). Generation of *in-vivo* highly sialylated rHuAChE (wild type and C580A) was achieved by expressing of the wild-type or mutated HuAChE genes in the genetically modified 293ST-2D6 cells which stably express a recombinant rat Golgi-version of 2,6 sialyltransferase (Chitlaru *et al.*, 1998, Kronman *et al.*, 2000). Both HEK-293 and 293ST-2D6 cells were cultured in DMEM supplemented with 10% FCS.

Enzyme Production, Purification and Quantitation - Recombinant AChE was produced in large scale by HEK-293 or 293ST-2D6 cells (10^8-109 cells/liter) cultured in tissue culture multitrays (Lazar *et al.*, 1993). Following the establishment of the anchor dependent cultures, the cells were fed with production media (containing 10% AChE depleted fetal bovine serum). Conditioned media harvested from confluent stationary cell cultures consistently contained higher proportions of tetramerized AChE (G4-between 10-15%; G2-between 70-80%; G1-between 5-20%, such as preparation 4 in Table 14) than that of young subconfluent cultures of producer cells (such as preparation 8 in Table 14) which are characterized by very high levels of dimers (G2>95% , Velan *et al.*, 1991a, Lazar *et. al.* 1993 and unpublished data).

Purification of secreted rHuAChE was performed by affinity chromatography to sepharose-bound procainamide as described previously (Kronman *et al.*, 1992, 1995). AChE activity was measured according to Ellman *et al.* (1961). Assays were performed in the presence of 0.5 mM acetylthiocholine, 50 mM sodium phosphate buffer pH 8.0 0.1 mg/ml BSA and 0.3 mM 5,5'-dithiobis-(2-nitrobenzoic acid). The assay was carried out at 27°C and monitored by a Thermomax microplate reader (Molecular Devices) as described previously (Shafferman *et al.*, 1992a).

Pharmacokinetics - Clearance experiments in mice (3 to 6 ICR male mice per enzyme sample) and analysis of pharmacokinetic profiles were carried out as described previously (Kronman *et al.*, 1995). Residual AChE activity in blood samples was measured and all values were corrected for background activity determined in blood samples withdrawn 1 hour before performing the experiment. The clearance patterns of the various enzyme preparations were usually biphasic and fitted to a bi-exponential elimination pharmacokinetic model ($C_t=Ae^{-k\alpha t}+Be^{-k\beta t}$) as described previously (Kronman *et al.*, 1995). This model enables determination of the parameters A and B which represent the fractions of the material removed from the circulation in the first-fast and second-slow elimination phases respectively, and $T_{1/2}\alpha$ and $T_{1/2}\beta$ which represent the circulatory half-life values of the enzyme in the fast and slow phases. The pharmacokinetic parameters MRT (mean residence time, which reflects the average length of time the administered molecules are retained in the organism) and CL (clearance, which represents the proportionality factor relating the rate of substance elimination to its plasma concentration (CL=dose/area under the concentration-time curve) were independently obtained by analyzing the clearance data according to a noncompartmental pharmacokinetic model using the WinNonlin computer program (Laub and Gallo, 1996).

Release, Recovery, Purification and Labeling of N-Glycans- N-glycans of purified enzyme preparations (~100 ug protein) were released by N-glycosidase-F (Glyko, USA) treatment as described before (Kronman *et al.*, 1992). Deglycosylated protein was removed by ethanol-precipitation and glycans were recovered and purified from the supernatant as described by Kuster *et al.* (1997). To increase sensitivity (Okafo *et al.*, 1996, 1997; Anumula and Dhume, 1998) purified glycans were fluorescently labeled. Fluorescent labeling of purified glycans with 2-aminobenzamide (2-AB) was performed according to Bigge *et al.* (1995) using a commercial labeling kit (Glyko, USA). During the 2h labeling incubation, the temperature was kept at 55^{0}C to prevent heat-induced desialylation of the glycans.

Enzymatic Modulation of N-Glycans.

Sialic Acid Removal.- Agarose-bound sialidase (0.04U, Sigma) was prewashed 5 times with water and incubated at room temperature for 16h with 2AB labeled N-glycans released from 1.5 -2.0 nmol AChE. Sialidase was removed by Eppendorf centrifugation. Desialylated N-glycans were vacuum dried, resuspended in 30 µl of water and stored at -20^{0}C until use. Glycans prepared in this manner were subjected to MALDI-TOF analysis or to further glycosidase treatments followed by MALDI-TOF analysis.

For the generation of asialylated rHuAChE preparations (C580A-HuAChE monomeric, wt enzyme and *in-vitro* tetramerized enzyme) for pharmacokinetic study, a similar procedure was employed except that 100nmoles of AChE were incubated for 16 h with 1.2 U of agarose-bound sialidase. The preparations of AChEs devoid of terminal sialic acid residues were extensively dialyzed against PBS prior to administration to animals for the efficient removal of free sialic acid.

Removal of Neutral Monosaccharides- Desialylated 2AB-labeled N-glycans obtained from 0.05-0.07 nMole AChE (in 1 µl water), were incubated for 24h with 1 µl of bovine kidney fucosidase (1.3 U/ml, Glyko, USA), β-galactosidase (5 U/ml, Glyko, USA) or Green coffee bean α-galactosidase (0.5 U/ml, Sigma). Water was added to a final volume of 10 µl and samples were stored at -20^{0}C until analyzed by MALDI-TOF.

Esterification of Sialic Acids- To allow the concomitant measurement by MALDI-TOF analysis of both neutral and acidic glycans, the carboxylic groups of sialylated 2AB labeled glycans were converted into their neutral methylated forms by methyl iodide esterification, essentially as described by Kuster *et al.* (1997). We note that in this procedure the 2AB moiety itself undergoes methylation and therefore both neutral and acidic glycans invariably display an increment in molecular mass of 14.015 kDa in addition to the increase in mass size resulting from sialic acid methylation in the case

of acidic glycans. Esterified glycans were purified as described (Kuster et al., 1997) and stored at -20^{0}C until MALDI-TOF analysis.

Mass Spectrometry - Mass spectra were acquired on a Micromass TofSpec 2E reflectron time-of-flight (TOF) mass spectrometer. 2AB-labeled desialylated or 2AB-labeled esterified glycan samples, were mixed with an equal volume of freshly prepared 2,5-dihydroxybenzoic acid (DHB, 10mg/ml in 70% acetonitrile) and loaded onto the mass spectrometer target. Routinely, 1 μl and 1 μl of glycan samples diluted 1:10 in water were subjected to analysis. Dried spots were recrystallized by adding 0.5 μl ethanol and allowed to redry. Neutral glycans were observed as $[M+Na]^+$ ions. 1 μl of peptide mixture (renin substrate, ACTH fragment 18-39, and angiotensin, 10 pMole/μl all from Sigma) which served as a three-point external calibrant for mass assignment of the ions, was mixed with freshly prepared α-cyano-4-hydroxycinnamic acid (10 mg/ml in 49.5% acetonitrile; 49.5% ethanol; 0.001% TFA), loaded on the mass spectrometer target and allowed to dry. All oligosaccharides were analyzed at 20 kV with a single-stage reflectron in the positive-ion mode. Between 100 and 200 scans were averaged for each of the spectra shown.

PRAD Peptide Synthesis- The PRAD peptide CLLTPPPPPLFPPPFFRG was synthesized manually in a T-bag by F-moc chemistry, as described previously (Houghten, 1985). The peptide was dialyzed against 0.05% TFA for 48hrs. Quality control of the peptide was performed by MALDI-TOF-MS, and its concentration was evaluated by its absorbance at 215 nm following reverse-phase HPLC.

In-vitro Tetramerization of rHuAChE - Previous studies by Giles *et al.* (1998), demonstrated that rHuAChE can be tetramerized by a PRAD derived peptide. The conditions used in the present study for tetramerization of sialylated or nonsialylated rHuAChE were based on incubation of the affinity chromatographically purified rHuAChE with the synthetic PRAD peptide for 12-16h at room temperature, in the presence of 5mM phosphate buffer pH 8.0. In analytical tetramerization experiments designed for sucrose gradient analysis of tetramer formation, 0.06 nmol of rHuAChE (equivalent to 25U) were mixed at different mole ratios with the PRAD peptide [AChE/PRAD: 10/1, 4/1, 1/4] in a final volume of 70 μl. Preparative tetramerization for the generation of milligram amounts of tetrameric rHuAChE for pharmacokinetic studies included 14.4 nmol (equivalent to 6000U) of rHuAChE (mostly dimeric) which were incubated with 28.8 nmol PRAD peptide in a final volume of 2ml. Prior to administration to mice, *in-vitro* tetramerized rHuAChE was dialyzed extensively against PBS.

Sucrose Density Gradient Centrifugation. - Analytical sucrose density gradient centrifugation was performed on 5-25% sucrose gradients containing 0.1M NaCl/50 mM sodium phosphate buffer pH 8.0. Centrifugation was carried out in an SW41 Ti rotor (Beckman) for 26h at 160000 Fractions of 0.2 ml were collected and assayed for AChE activity. Alkaline phosphatase, catalase and β-galactosidase were used as sedimentation markers. For determination of the rHuAChE assembly status in the circulation of mice at various timepoints post-administration, 10 μl samples removed from 5 mice, each injected with 1000U intravenously at T=0, were pooled and applied to sucrose gradients.

RESULTS AND DISCUSSION

Comparison of the N-glycans associated with rHuAChE produced by HEK-293 cells and sialyltransferase-modified HEK-293 cells - Previously (Kronman *et al.*, 1995), we found that the terminal sialylation of the N-glycans appended to the cholinesterase plays a decisive role in determining the circulatory behavior of cholinesterases. This result prompted us to generate the novel 293ST-2D6 cell line (Chitlaru *et al.*, 1998, Kronman *et al.*, 2000) engineered to overexpress a heterologous Golgi-associated α-2,6 sialyltransferase gene (Weinstein et al., 1982) which acts upon cotransfected glycoproteins and generates highly sialylated glycoforms (Kronman *et al.*, 2000). Examination of rHuAChE produced by HEK-293 cells and sialyltransferase-modified HEK-293 cells by high-pH anion-exchange chromatography pulsed amperometric detection (HPAEC-PAD), revealed that in the latter case the glycans were sialylated to a greater extent (Chitlaru *et al.*, 1998). However, this method did not allow accurate quantitative evaluation of the sialylation extent nor elucidation of the precise glycan structures associated with the rHuAChE product. In the present study we decipher the entire spectrum of N-glycan forms associated with rHuAChE produced from the different cell lines by employing refined MALDI-TOF techniques. Recently, we used this technique successfully to analyze N-glycans structures of bovine AChE (Kronman *et al.*, 2000).

To allow visualization by MALDI-TOF of the entire range of N-glycans associated with rHuAChE, 2-aminobenzamide labeled glycans were converted to neutral forms by two different methods. In the first mode, sialic acid residues were removed from the purified N-glycans to form a non-charged glycan pool which can be readily analyzed by MALDI-TOF at very low quantities and in a highly reproducible manner, (S.D. $\leq$ 2%) (however by this method we obviously lose all information regarding the state of sialylation of the various glycan forms). In an alternative mode of operation, the glycans were subjected to an esterification procedure in which sialic acid residues were converted to their noncharged methyl-ester forms. Utilizing this method, the relative quantities and structures of *both* sialylated as well as nonsialylated glycan forms can be determined within a single MALDI-TOF spectrum. However, since this procedure entails some loss in sensitivity as well as a lower level of reproducibility (S.D. $\leq$ 10%), the data gathered using this protocol, was validated by comparing it to the data acquired by MALDI-TOF analysis of desialylated glycans. Accordingly, the relative amounts of the different sialylated and nonsialylated esterified glycan forms was considered to be accurate, when the sum of sialoforms corresponding to each of the basic glycan structures, coincided with the relative quantity of the corresponding glycan structures determined for desialylated glycans.

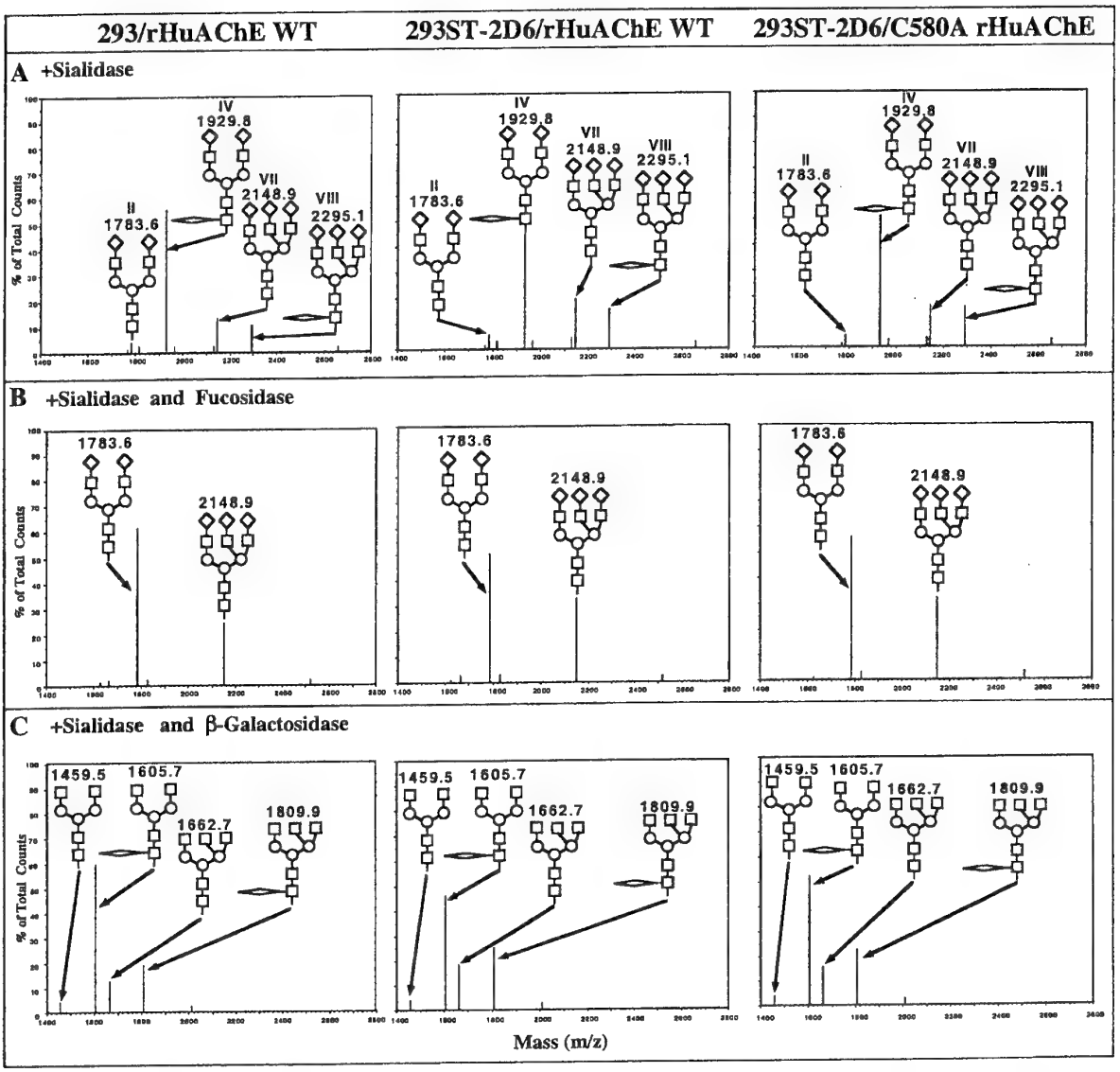

Figure 19: MALDI mass spectra of N-glycans associated with recombinant forms of human AChE following desialylation. N-glycans purified from wild type (WT) rHuAChE produced in 293 cells or 293ST2D6 cells or from the mutated C580A rHuAChE generated in 293ST2D6 cells were subjected to sialidase treatment and 2-AB labeling prior to MALDI-TOF analysis. Molecular weights and structural details are shown for the major glycan forms. Molecular weights represent monoisotopic masses of the respective [M + Na]+ ions of the glycan species. (A) without additional exoglycosidase digestion. Roman numerals refer to the peak designations assigned to the various major forms in Table 13. (B) after digestion with bovine kidney fucosidase, (C) after digestion with bovine testes β-galactosidase.

□GlcNac;○Man;◇ β-Gal;◁▷Fuc

Table 13: Comparison of the basic glycan structures of desialylated WT rHuAChE and C580A-rHuAChE

Abbreviation		Structure	MW $(M+Na)^+ + 2AB$	N-Glycan Abundance (% of Total)		
				HEK-293 produced rHuAChE	293ST2D6 produced rHuAChE	293ST2D6 produced C580A
I	NG1A2F		1767.8	1.68±0.2	1.55±0.4	1.0±0.2
II	NA2		1783.6	4.89±0.8	5.2±0.6	4.6±0.5
III	NG2(GalNac)A2F		1809.9	3.2±1.0	3.6±0.5	<0.8
IV	NA2F		1929.8	56.0±4.1	49.0±4.8	51.0±4.6
V	NG1(GalNAc)A2F		1971.8	3.3±0.76	3.9±0.7	2.9±0.8
VI	NA2BF		2132.6	3.0±0.45	4.6±1	4.1±1
VII	NA3		2148.9	13.6±1.0	18.8±0.9	16.3±1.1
VIII 10	NA3F		2295.1	11.2±1.6	14.5±1.9	15.9±2.1
IX	NA4F		2660.6	2.2±0.29	2.8±0.8	3.3±1.0

□ GlcNAc ○ Man ■ GalNAc ◇ Gal ◁ Fuc

Inspection of the MALDI-TOF profiles of desialylated glycans of rHuAChE produced by HEK-293 cells and sialyltransferase-modified 293ST-2D6 cells revealed that in both cases the corresponding glycan pools comprise an array of varied glycan structures (Fig. 19A). Subsequent exoglycosidase-treatment of the glycans (Fig. 19 B, C) allowed us to determine the exact structures of the different glycans (Table 13). In both cases, the major glycan species (49-56% of total glycans) corresponds to the complex-type biantennary fucosylated form (Table 13, peak IV). Triantennary glycans (25-33% of the total glycans) consist of similar amounts of fucosylated and nonfucosylated species (Table 13, peaks VII and VIII). Higher-branched glycans (Table 13, peak IX), bisecting glycans (Table 13, peak VI), and GalNAc-containing glycans (Table 13, peaks III and V) are present in both preparations at low levels only.

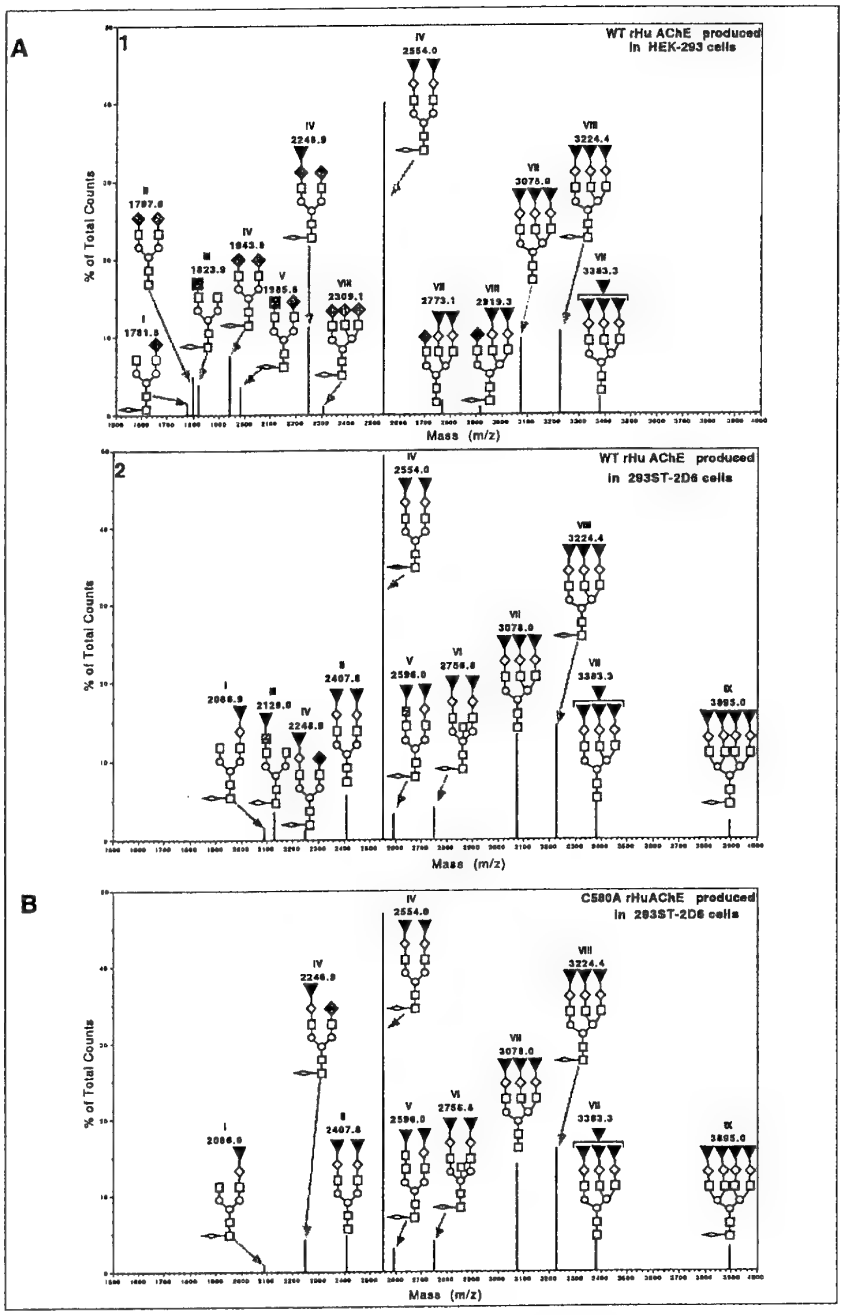

Figure 20: MALDI mass spectra of total N-glycan pools associated with WT rHuAChE produced by HEK-293 or 293ST-2D6 cells and C580A-AChE produced by 293ST-2D6 cells. (A) Purified N-glycans of WT AChE produced in HEK-293 cells (A1) or in the genetically modified 293ST-2D6 cells (A2), and (B) C580A-AChE generated in 293ST–2D6 cells, were subjected to 2-AB labeling and iodomethane-mediated esterification prior to MALDI-TOF analysis. Molecular weights and structural details are shown for the glycan forms. Molecular weights represent monoisotopic masses of the respective [M + Na]+ ions of the glycan species. Roman numerals refer to the peak designations of the various major forms in Table 13. Note that an increase of 14.015 Da of all glycan species occurs due to the methylation of the common 2-AB moiety.

□GlcNac;○Man;◇ β-Gal;⊠ GalNAc;⌔Fuc; ▼ sialic acid.

Terminally exposed (nonsialylated) b-Gal and GalNAc residues are shadowed.

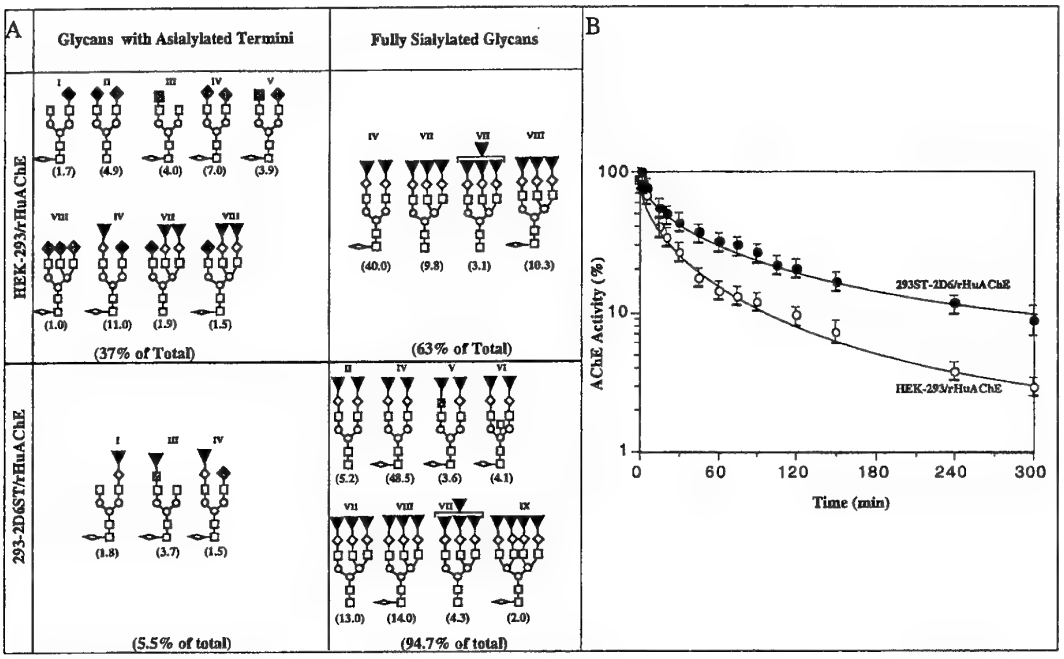

Figure 21: Glycan structures and pharmacokinetic profiles of rHuAChE produced by HEK-293 or 293ST-2D6 cells. A. Glycan structures were deduced from the mass spectral data shown in Fig. 20, and classified according to their sialic acid occupancy. The various glycans are annotated by a Roman numeral which refers to the basic structures described in Fig. 19. The molecular weights of the monoisotopic masses of the respective [M + Na]+ ions of the 2AB labeled glycan species following iodomethane-mediated esterification are as follows: **I**(asialylated) = 1781.8, **I**(sialylated)= 2086.9, **II**(asialylated) = 1797.6, **II** (sialylated)= 2407.8, **III**(asialylated) = 1823.9, **III**(sialylated) = 2129.0, **IV**(asialylated) = 1943.8, **IV**(partially sialylated) = 2248.9, **IV**(sialylated) = 2554.0, **V**(asialylated) = 1985.8, **V**(sialylated) = 2596.0, **VI** (sialylated) = 2756.8, **VII** (partially sialylated) = 2773.1, **VII** (fully sialylated) = 3078.0, **VII** (hyper-sialylated)= 3383.3 , **VIII** (asialylated) = 2309.1, **VIII** (partially sialylated) = 2919.3, **VIII** (fully sialylated) = 3224.4, **IX** (sialylated) = 3895.0. Note that methylation of the common 2-AB fluorescent moiety results in an increase of 14.015 Da of all glycan species. Abundance values refer to the relative amount (% of total glycans) of each particular glycan species. **B**. Purified AChE from HEK-293 cells (filled circles) or from 293ST-2D6 cells (empty circles) was administered to mice (40 μg/mouse in 0.2 ml PBS). AChE activity values in samples removed immediately after injection were assigned a value of 100% and used for calculation of residual activity. Background cholinesterase levels in blood of pre-administered mice is less than 2 units/ml and was subtracted from the values obtained at the various time points. Exogenous AChEs were introduced at levels that are at least 30-fold higher than background level.

□GlcNac;○Man;◇ β-Gal;⧖ GalNAc; <>Fuc; ▼ sialic acid.

Terminally exposed (nonsialylated) β-Gal and GalNAc residues are shadowed.

Examination of the MALDI-TOF spectra of esterified glycans of rHuAChE produced by HEK-293 cells (Fig. 20A1) and sialyltransferase-modified 293ST-2D6 cells (Fig. 20A2), revealed that the two glycan pools differ significantly only in their state of sialylation. While only 63% of the glycans associated with the enzyme product of nonmodified HEK-293 cells are fully sialylated (Fig. 21A, upper panel), nearly 95% of the glycans associated with the rHuAChE of 293ST-2D6 cells display full sialylation (Fig. 21A, lower panel). Only 5.5-5.7 % of the glycans (Fig. 21A, peaks I and III) consist of immature forms lacking a GlcNac moiety, and therefore are refractive to further sialylation.

Taken together, these results clearly establish that the sialyltransferase-modified 293ST-2D6 cell line promotes highly-efficient sialylation of rHuAChE coexpressed at high levels. Furthermore, sialylation-refractive glycans are present at low levels only, suggesting that incomplete sialylation is probably not the main reason for the fact that highly-sialylated rHuAChE are cleared more rapidly than native serum-derived cholinesterases (Table 13, see also Chitlaru *et al.*, 1998).

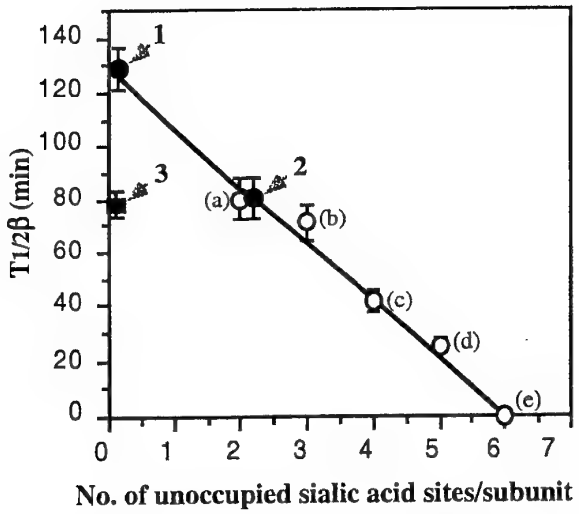

Figure 22: Relationship between the circulatory residence time of WT rHuAChE produced by HEK-293 or 293ST-2D6 cells and of C580A AChE produced by 293ST-2D6, and their degree of sialic acid occupancy. The T1/2β time values of WT rHuAChE produced by (1) 293ST-2D6 or (2)HEK-293 cells and (3) monomeric C580A AChE produced by 293ST-2D6, were plotted against the number of unoccupied glycan termini as calculated from the by MALDI-TOF analysis data (Fig. 21A). This type of relationship was first reported by us (Fig. 5 in Kronman *et al.*, 1995,) for rHuAChE preparations consisting mostly of *dimeric* forms of: (a), WT rHuAChE, (b), D61N rHuAChE, (c), S541N rHuAChE, (d), D61N/S541N rHuAChE and (e) sialidase-treated WT rHuAChE, which differ in their sialic acid content. In this previous study, estimation of the number of unoccupied glycan termini was based on the assumption (Kronman *et al*, 1995) that the N-glycans associated with HEK-293 AChE are mainly of a biantennary type. Note that the predicted extrapolated T1/2β value for fully sialylated dimeric forms of rHuAChE of approximately 130 min., is in excellent agreement with the value determined for highly sialylated rHuAChE produced by 293ST-2D6 cells (1).

In an earlier study (Kronman *et al.*, 1995), we assumed that the predominant forms of the glycans appended to various rHuAChE enzymes produced in HEK-293 cells were of the biantennary type. Based on this assumption, and on the chemical quantitation of sialic acid of an array of rHuAChE mutants which differ in their state of sialylation, a value representing the number of glycan termini which are not occupied by sialic acid residues was calculated. This allowed us to find an inverse-linear relationship between the number of asialylated glycan termini per enzyme subunit, and the residence time of the different rHuAChE forms examined. Using the refined MALDI-TOF technique for glycan analysis, we can now determine accurately the actual number of glycan termini per enzyme subunit, and their extent of sialic acid capping. First, we find that the actual average number of N-glycan termini per AChE subunit (containing three utilized N-glycosylation sites) is 6.4. Furthermore, we could establish (Fig. 21A) that 2.2 glycan termini per enzyme subunit of rHuAChE produced by the nonmodified HEK-293 cells are devoid of sialic acid, while only 0.21 glycan termini per enzyme subunit of rHuAChE produced by the sialyltransferase-modified 293ST-2D6 cell line, do not contain terminal sialic acid moieties (of these, only 0.045 glycan termini per enzyme subunit of the highly sialylated rHuAChE, contain exposed galactose which can serve for sialic acid capping). When we now introduce the accurately-determined values of asialylated glycan termini (Fig. 21A) of the two forms of wild-type rHuAChE (from 293ST-2D6 and nonmodified HEK-293 cells) on a graph (Fig. 22) redrawn on the basis of the previously described relationship (Fig. 5 in Kronman *et al.*, 1995) between T1/2β and the number of asialylated glycan termini, we find that: (a) the experimental values determined here, are in good agreement with the values derived from the previously determined slope of the linear relationship, and (b) the T1/2β of ~130 min observed for the rHuAChE produced by the sialyltransferase-modified cells is indeed very close to the predicted value extrapolated for fully sialylated molecules.

The fact that the T1/2β of rHuAChE produced by the sialyltransferase-modified 293ST-2D6 cell line, is in accordance with the value predicted for an enzyme devoid of unoccupied sialylation sites, substantiates our conclusion that extension of circulatory residence by improved sialylation has reached an upper limit, and that post-translation related factors other than glycan sialylation impose a limitation on its ability to reside in the circulation for longer periods of time, in a manner similar to that of native cholinesterases.

Circulatory residence of rHuAChE is affected by its state of assembly - Naturally occurring circulatory and membrane-bound cholinesterases are assembled as multimeric complexes (Lockridge *et al.*, 1979; Taylor *et al.*, 1981; Younkin *et al.*, 1982; Ralston *et al.*, 1985; Atack *et al.*, 1987; Mendelson *et al.*, 1998; Stieger *et al.*, 1989). Homodimers of enzyme subunits, formed by covalent disulfide bonding of cysteine residues located at the C-terminal end of the enzyme, are further assembled into quaternary forms. Examination of fetal bovine acetylcholinesterase by sucrose-gradient analysis reveals that this circulatory long-living enzyme

is arranged entirely in the tetrameric configuration. In contrast, recombinant cholinesterases produced in various cell culture systems contain variable amounts of tetramers, dimers and monomers (Velan *et al.*, 1991a; Duval *et al.*, 1992; Kronman *et al.*, 1995; Saxena *et al.*,1998b; Mendelson *et al.*, 1998). For example, human recombinant AChE produced in HEK 293 or 293ST-2D6 cells exhibits at the most 5-15% tetramers and >60% dimers of AChE subunits, suggesting that the inability of recombinant human cholinesterase to assemble efficiently into stable tetramers may contribute to its relatively rapid removal from the circulation. We have recently shown (Kronman *et al.*, 2000) that indeed, in the case of bovine AChE, the aptitude of the native fetal serum-derived enzyme to reside for prolonged time in the circulation depends not only on its sialylation level but also on its tetrameric quaternary configuration. It should be noted that unlike in the case of the bovine enzyme, human native circulatory AChE counterparts, are not available and therefore the impact of tetramerization cannot be directly probed by comparison to a serum-resident enzyme of human origin.

To establish whether tetrameric forms of rHuAChE can exhibit a significant pharmacokinetic advantage, inspection of the subunit assembly state of administered rHuAChE was carried out. Recombinant AChE was injected into mice and blood samples withdrawn at various time points were applied to sucrose gradients to determine the state of assembly of the residual enzyme (Fig. 23A). The clearance study was performed with mice which were administered a high dose of 1000 AChE units/mouse instead of the standard dose of 100 unit/mouse (Kronman *et al.*, 1995, Chitlaru *et al.*, 1998) of highly sialylated rHuAChE preparation produced by the 293ST-2D6 cell line. The rHuAChE used was purified from the cell conditioned media of confluent stationary cells, containing a higher (10-15%), than usual proportion of tetramers (see "Materials and Methods"). This high input dose was necessary in view of the fact that approx. 60% of the injected activity is cleared from the circulation in the fast phase of the removal process (Kronman *et al.*, 1995) yielding a residual activity which probably be too low for accurate analysis of blood samples by sucrose-gradient sedimentation. It should be noted that the use of a fully sialylated preparation is required for this type of experiment since, as shown previously, the effect of *N*-Glycan undersialylation on clearance of AChE from the circulation, overrides any other potential factor contributing to circulatory longevity (Chitlaru *et al.*, 1998).

The pharmacokinetics of the individual oligoforms were followed by their deconvolution from the sedimentation profiles obtained at the various time points (Fig. 23A). An enrichment in the relative amount of rHuAChE tetramers at each successive time point was clearly observed (Fig. 23B), indicating that the tetrameric form of the enzyme was being removed at a much slower rate than the dimers and monomers. Thus, while the tetrameric form constitutes only ~12% of the input enzyme, they constitute 65% and almost 100% of the circulatory enzyme at 9 hrs and 24 hrs post-injection, respectively (Fig. 23B).

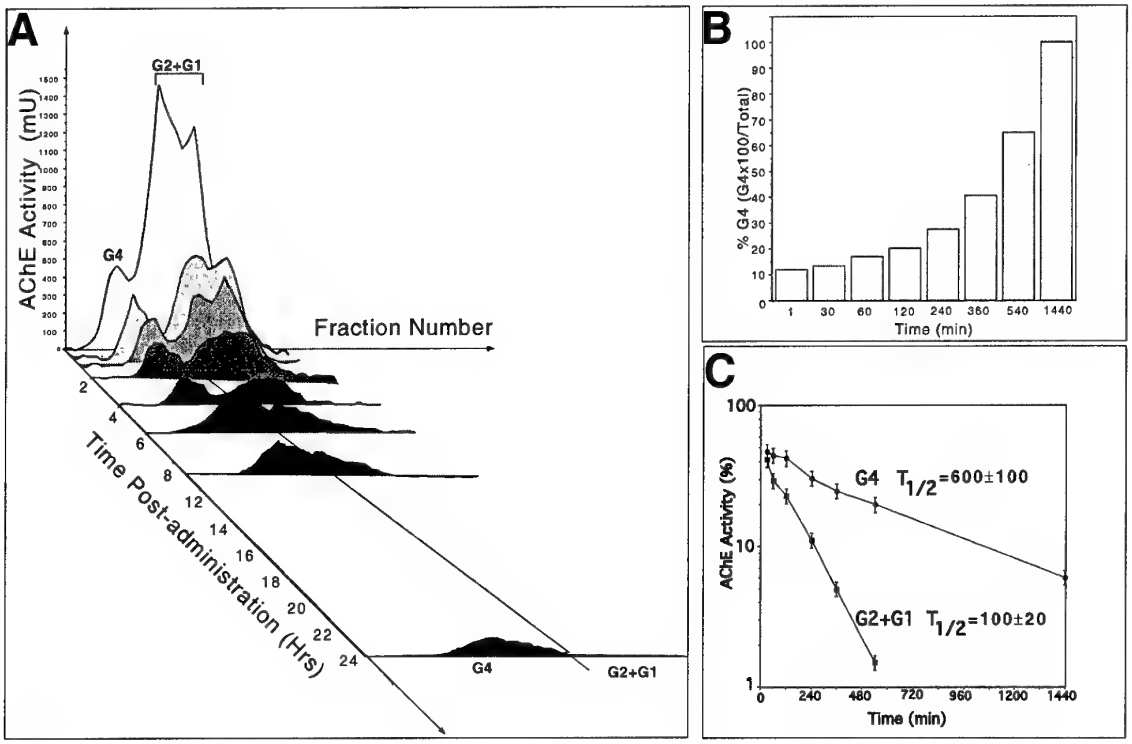

Figure 23: Enrichment of the tetrameric AChE fraction in the circulation following its administration to mice. A purified heterogeneous (with respect to its subunit assembly status) rHuAChE preparation produced in 293ST-2D6 cells, containing 12% tetramers and 88% dimers/monomers, was administered to 5 mice (1000U/mouse, Table 14, preparation 6). At the indicated time points post-administration, 10µl samples were withdrawn from each mouse , pooled and subjected to oligomeric status determination by sucrose gradient centrifugation. A: AChE sedimentation profiles in the blood samples; B: Percentage of the tetrameric AChE fraction (G4) in the blood samples. Note that the input material (time = 1min post-administration) contains only 12% tetramers while the sample 24 hrs post-administration consists entirely of tetrameric (G4) forms. C: Exponential activity decay curves calculated individually for the tetrameric fraction (G4) and the combined monomeric/dimeric fractions (G1+G2).

Plotting of the residual AChE activity of the tetrameric form against the time elapsed since enzyme administration, allowed us to estimate the pharmacokinetic profile of the tetrameric form of rHuAChE (Fig. 23C). Accordingly, the slow phase half-life time (T1/2β) was found to be 600±100 min. Though this type of evaluation of the circulatory behavior of the multimeric forms of rHuAChE, clearly indicated that the tetrameric form of the enzyme is retained in the bloodstream much more efficiently than monomers and dimers, the poor resolution of the peaks representing the dimeric and monomeric forms of the enzyme, precluded determination of individual pharmacokinetic profiles for these two forms. Yet we may establish from this experiment that the combined pharmacokinetic profile of rHuAChE dimers and monomers

exhibited a $T_{1/2}\beta$ value of 100±20 min. Furthermore, although difficult to quantitate, a clear-cut enrichment of the dimeric fraction as compared to the monomeric fraction is observed. For example, at 9 hrs post-administration the monomeric portion is virtually undetectable while dimeric AChE can still be observed (Fig. 23A).

To confirm the results obtained in these experiments, and to accurately determine the pharmacokinetic behavior of AChE with respect to its subunit assembly, we set up a system for inspection of homogenous preparations of the various rHuAChE oligomeric forms.

Pharmacokinetic profile of monomeric and dimeric rHuAChE - To determine the pharmacokinetic behavior of non-assembled rHuAChE, the C580A mutated enzyme (Velan *et al.*, 1991b) which is impaired in its ability to form the interchain disulfide bridge necessary for enzyme dimerization, was expressed at high levels in the sialyltransferase-modified 293ST-2D6 cell line and in HEK-293 cells. In view of the demonstrated impact of glycosylation, and in particular, sialylation on the pharmacokinetics of AChE, identical glycan repertoires are a prerequisite for conducting a pharmacokinetic comparison between the dimeric WT and monomeric C580A AChEs. Analysis of the N-glycans appended to the enzyme product revealed that the basic structures (Fig. 19), relative abundances (Table 13), and most importantly, the degree of sialylation (Fig. 20) of C580A-HuAChE, are indeed indistinguishable from those of the wild-type rHuAChE.

When administered to mice, the highly sialylated C580A enzyme was cleared from the circulation more rapidly than highly sialylated wild-type enzyme (Table 14 and Fig. 25). Specifically, the slow-phase half-life ($T1/2\beta$) value, and mean residence time (MRT) for C580A-HuAChE were 80±6 and 110 minutes, respectively (Table 14, Prep. 3) as compared to 133±9 and 195 minutes, respectively, in the case of the wild type dimeric enzyme (Table 14, Prep. 6). Since both the fully sialylated C580A-HuAChE and the dimeric wild type enzyme are virtually indistinguishable in their N-glycosylation (Fig. 19 and 2, Table 13), the apparent differences in their circulatory residence is most probably an outcome of the difference in their subunit assembly. It appears therefore, that the non-assembled monomeric form of the enzyme is more readily removed from the circulation, than assembled forms of the enzyme. Indeed, plotting the $T1/2\beta$ value of highly sialylated C580A against the number of unoccupied sialic acid sites/enzyme subunit (Fig. 22), reveals that in this case the $T1/2\beta$ value deviates from the linear relationship observed in the past between the number of unoccupied glycan termini and the clearance rates of the other differently sialylated forms of the enzyme examined. It should be noted that all the AChE sialoforms used for the pharmacokinetic studies which generated the

Table 14: Pharmacokinetic parameters of recombinant HuAChEs differing in their level of sialylation and state of assembly

Enzyme type	Prep No.	State of Assembly	Sialylation status	A (% of total)	$T_{1/2}\alpha$ (min)	B (% of total)	$T_{1/2}\beta$ (min)	Clear-ance (ml/hr /kg)	MRT (min)
Monomer (C580A)	1	G1 >99%	Asialylated *	100(c)	3.5±0.2	-	-	1170	3.6
	2		Partially sialylated**	65±3	3.8±0.7	35±2	50±8	199	73
	3		Fully sialylated ***	75±6	5.9±1.5	28±4	80±6	138	110
Dimer (Wild type)	4	G2>95%	Asialylated	100(c)	3.3±0.15	-	-	1210	3.5
	5	G4 = 15%; G2+G1= 85%	Partially sialylated	74±5	7.3±0.7	25±1.5	80±4	124	102
	6	G4 = 12%; G2+G1= 88%	Fully sialylated(a)	59±4	14±2	42±3	133±9	93	195
	7	G2>95%	Fully sialylated(b)	62±4	13±2.5	40±3	129±8	99	186
Tetramer (Wild type + PRAD peptide)	8	G4 >99%	Asialylated	100(c)	3.5±0.18	-	-	1185	3.5
	9		Partially sialylated	55±6	6.9±2	46±4	129±13	83	194
	10		Fully sialylated	59±4	30±5	40±4	595±40	13	740

The circulatory clearance profiles of the various AChEs were determined as described ("Materials and Methods"). Asialylated rHuAChEs (*) were obtained by *in vitro* desialylation of 293ST-2D6 cell-produced rHuAChEs. Partially sialylated rHuAChEs (**) were produced in HEK-293 cells. Fully Sialylated rHuAChEs (***) were produced in the genetically modified 293ST-2D6 cells overexpressing a sialyltransferase gene (Chitlaru *et al.*, 1998, Kronman et al., 2000). The biphasic pharmacokinetic curves were fitted to an equation of the form $C_t=Ae^{-k\alpha t}+Be^{-k\beta t}$. A and B represent the fractions of the material removed from the circulation in the first (fast) and second (slow) decay phases respectively. $T_{1/2}\ \alpha$ and $T_{1/2}\ \beta$ represent the circulatory half-life values of the enzyme in the fast and slow phases, respectively. In all cases, the correlation coefficient was > 0.997. The clearance curves were also analyzed by fitting to a noncompartmental pharmacokinetic model for the calculation of Mean Residence Time (MRT) and Clearance using a Window-based program. Elimination half-life values calculated by noncompartmental analysis, coincided with the $T_{1/2}\beta$ values obtained by the biexponential elimination pharmacokinetic model. G4, G2, G1 = Tetrameric, dimeric, and monomeric forms, respectively. and (b) refer to different conditioned media harvesting regimens of the producer cells for the generation of (a) preparations containing different distributions of oligoforms (S of a dense (stationary) culture; (b) - Conditioned media of a young (logarithmical growing) subconfluent culture. (c) - Sialidase-treated AChE displays a single-phase clearance profile. see Materials and Methods): (a) - Conditioned media

inverse-linear relationship (Fig. 22) were composed mainly of dimers. It is also worth noting that this difference between the monomers and dimers become less pronounced with partially sialylated products derived from HEK-293 cells (Table 14 preparations 2 and 5), and is completely abolished when the enzyme glycans are totally devoid of sialic acid residues (Table 14, Preparations 1 and 4).

Pharmacokinetic profile of *in-vitro* generated tetrameric rHuAChE - Tetrameric forms of AChE are encountered as post-synaptic complexes localized in neuromuscular junctions. In these complexes, subunit multimerization and membranal anchorage of AChE is mediated by the ColQ protein (the non-catalytic AChE subunit, Duval *et al.*, 1992; Ohno *et al.*, 1998; Krecji *et al.*, 1997). Recognition and tetramerization of AChE depends on the Proline Rich Attachment Domain (PRAD) of ColQ which recruits four AChE subunits by interacting with their C terminal regions (Bon and Massoulie, 1997; Bon *et al.* 1997; Feng *et al.*, 1999). The ability of a synthetic peptide comprising the PRAD region of ColQ to promote *in-vitro* assembly of rAChE subunits into tetramers, was shown recently (Giles *et al.*, 1998, Kronman *et al.*, 2000). Incubation of rHuAChE in the presence of synthetic PRAD peptide resulted in the quantitative conversion of the mostly-dimeric preparation to tetrameric form (Fig. 24); no residual monomeric or dimeric forms could be detected. The reaction appears (Fig. 24B) to follow the 1:4 [PRAD]/[AChE] stoichiometry implied by the tetrameric nature of the AChE multimeric complex. As reported for the bovine AChE tetramers (Kronman *et al.*, 2000), the *in-vitro* PRAD generated tetramers of recombinant human AChE are highly stable withstanding prolonged dialysis and several cycles of freezing and thawing. Furthermore, the *in-vitro* tetramerization reaction can be scaled up for the generation of sufficient amounts of tetrameric AChE to enable pharmacokinetic studies. The fact that human AChE possesses the ability to tetramerize efficiently into soluble complexes by PRAD mediated *in-vitro* tetramerization is of particular interest, since native circulating HuAChE tetrameric forms of acetylcholinesterase have not been reported, and the only tetrameric AChE complexes known in humans are the neuromuscular membrane-bound forms of the enzyme.

Tetramerization of ChE subunits mediated by the ColQ protein has been shown to involve the C terminal region of the enzyme (Simon *et al.*, 1998, Blong *et al.*, 1997, Altamirano and Lockridge, 1999) which contains the Tryptophan Amphiphilic Tail (WAT) domain, directly recognizing and interacting with the PRAD of ColQ. In line with these reports, we find that incubation in the presence of PRAD of a truncated AChE form (ΔC rHuAChE, Kryger *et al.*, 2000) lacking the C terminal region, did not result in any detectable tetramer formation (Fig. 24B).

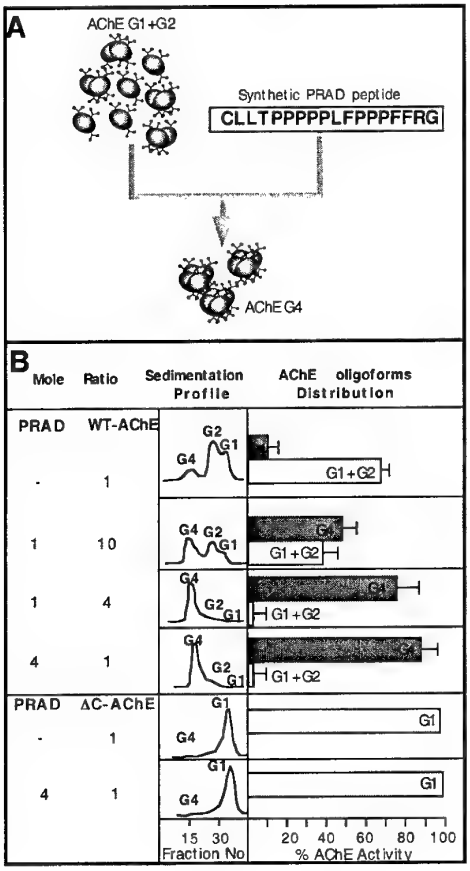

Figure 24: ***In-vitro*** **PRAD-mediated tetramerization of rHuAChE.** A: Schematic description of the tetramerization process mediated by the ColQ-derived synthetic PRAD peptide. The peptide was synthesized according to the published sequence of the human ColQ gene (Ohno et al., 1998) as described in Materials and Methods. Note that both monomers and dimers may be recruited by PRAD into tetrameric quaternary complexes. B: AChE subunit assembly status determined by sucrose gradient analysis following incubation of purified HEK-293-rHuAChE in the presence of a highly uniform synthetic PRAD preparation at the molar ratios presented in the left panel. The sedimentation profiles of the various reactions are presented in the middle panel. The percentage of tetrameric (G4) and residual monomeric/dimeric fraction (G1+G2) following each of the reactions is represented in the right panel histograms. Note that no tetramerization occurs with the truncated ΔC version of AChE which lacks the WAT domain required for interaction with PRAD (Bon et al., 1997; Altamirano and Lockridge, 1999).

Highly sialylated rHuAChE produced by 293ST-2D6 cells was subjected to *in-vitro* PRAD-mediated tetramerization and its pharmacokinetic behavior was monitored (Fig. 25B). The enzyme was retained in the circulation for considerably longer periods of time than either dimeric or monomeric forms of rHuAChE (Fig. 25B). The T1/2β, and MRT values of tetrameric rHuAChE (Table 14, Prep. 9) are 595 and 740 minutes, respectively, and thus the tetrameric form of the enzyme displays roughly a 4-fold and 7-fold increase in circulatory retention over pure fully sialylated_dimeric and monomeric forms of rHuAChE, respectively. Notably, the $T_{1/2}\beta$ value (595 minutes) of highly-sialylated rHuAChE uniformly tetramerized by interaction with the synthetic PRAD peptide, is very similar to that estimated for the tetrameric fraction of the heterogeneous preparation of highly sialylated rHuAChE (Fig. 23C, $T_{1/2}\beta$=600 min). The agreement in the values obtained by the two independent experimental approaches is remarkable in view of the fact that the mechanism of assembly of the tetramers of the heterogeneous population derived from the 293ST-D6 cells is unknown and such tetramers most probably do not include PRAD-like peptides. Similarly, in the case of the bovine AChE, we have recently shown that native serum-derived tetramers and *in-vitro* generated bovine rHuAChE tetramers obtained by incubation with PRAD exhibit identical circulatory residence time. This identical pharmacokinetic behavior strengthen the notion that tetramerization *per-se* is the factor which confers long-term circulatory residence.

The relationship between N-glycan sialylation and oligomerization in establishing the HuAChE residence time in the circulation - Taken together, the pharmacokinetic experiments performed with differently assembled forms of rHuAChE clearly establish that the complexation of enzyme subunits into forms of higher order, contributes significantly to their ability to reside in the circulation for long periods of time. We observe a clear direct correlation between the pharmacokinetic characteristics of the different preparations (Fig. 25, see also the clearance parameters in Table 14) and their multimerization state. These observations are consistent with the recently reported results obtained with the bovine version of AChE (both recombinant and native fetal bovine serum (FBS)) whose residence in the circulation was shown to be affected by subunit assembly and sialylation. These two elements were shown to exert their pharmacokinetic influence in a hierarchical manner, sialylation being the overriding factor (Kronman *et al.*, 2000).

In this report, we find that circulatory longevity of human AChE follows a simple tetramer>dimer>monomer rule. Yet, as in the case of the bovine enzyme, this rule is manifested in a sialylation dependent manner as indicated by the following observations: **(i)** sialidase treatment of recombinant human AChEs which differ in their oligomerization state, leads to their equally rapid clearance from the circulation within minutes (Table 14 Preparations 1, 4, 8), **(ii)** partially sialylated forms such as those produced by HEK-293 cells exhibit only a modest increase in retention time upon assembly of the monomers to dimers and of dimers to tetramers (note the MRT of 73 min, 102 min and 194 min, for preparations 2, 5 and 9 in Table 14), **(iii)**

dimeric forms of fully sialylated AChE (produced in 293ST-2D6 cells) are retained in the circulation significantly longer than fully sialylated monomeric forms or partially sialylated dimeric forms, and (**iv**) a dramatic synergistic pharmacokinetic effect is observed upon tetramerization of **fully** sialylated rHuAChE (note MRT=740 min in Table 14, Preparation 10, see also Fig. 25).

While sialylation prevents clearance by blocking the recognition of glycoproteins by the liver asialoglycoprotein receptor (Weiss and Ashwell, 1989), the mechanism by which circulatory residence time is enhanced through multimerization is not entirely clear. On the one hand, large multimeric complexes are known to be retained due to the size-exclusion which limits the glomerular filtration removal process operating in the kidneys (Renkin and Gilmore, 1973). It has been reported that proteins smaller than 70 kDa are effectively removed from the circulation by the kidneys (Koths and Halenbeck, 1985; Knauf *et al.*, 1988). This would imply that glomerular filtration affects equally dimers and tetramers and cannot explain the dramatic

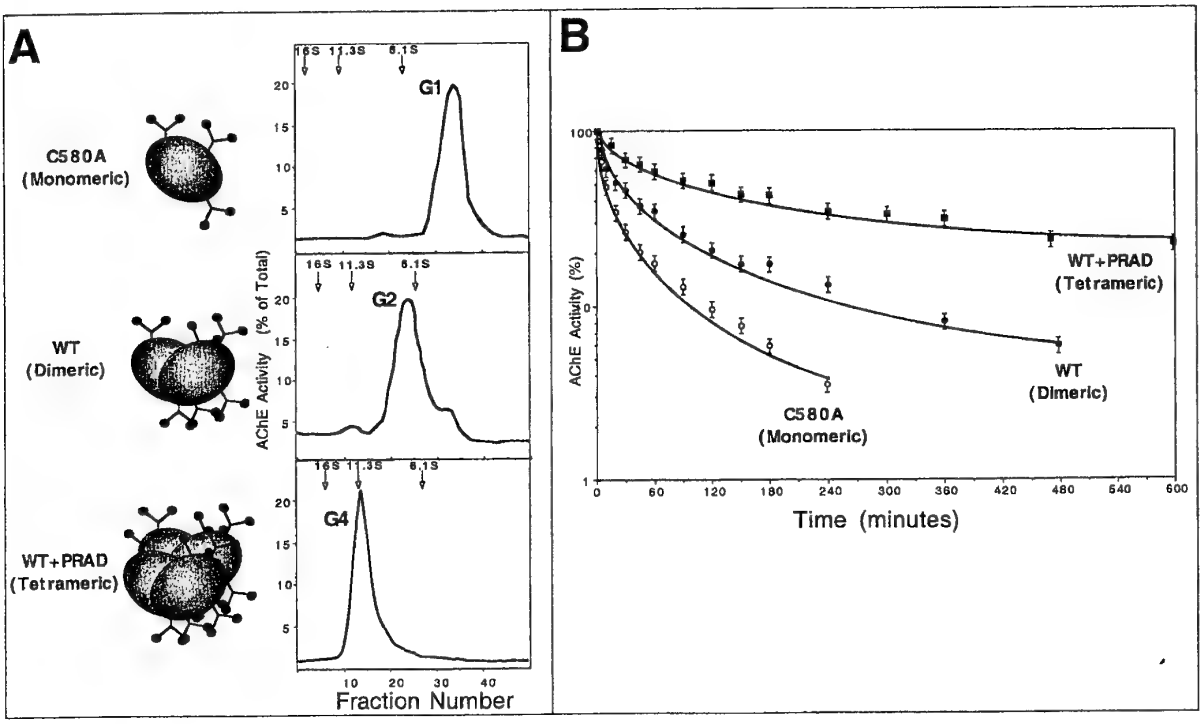

Figure 25: Pharmacokinetic behavior of monomeric, dimeric and tetrameric homogenous preparations of fully sialylated rHuAChE. A: Schematic representation and sucrose gradient sedimentation profiles of the three homogenous preparations of AChE representing a discrete subunit-assembly form: **monomeric** C580A AChE, **dimeric** WT AChE (>95% dimers), and **tetrameric** AChE (obtained by preparative complexation with PRAD). B: Circulatory clearance profiles of the three preparations in mice. See Table 14 for a detailed presentation of the pharmacokinetic parameters deduced from the curves.

difference in the removal rates of the two forms since both dimeric and tetrameric AChE exceed the 70 kDa cut-off limit (MW of dimeric and tetrameric rHuAChE are approximately 140 and 280 kDa, respectively). On the other hand, assembly of catalytic subunits into tetramers, may mask clearance-mediating amino-acid epitopes such as those involved in the removal of other glycoproteins (Warshawsky *et al.*, 1993; FitzGerald *et al.*, 1995; Collen *et al.*, 1991; Horn *et al.*, 1995; Berryman and Bensadoun, 1995). The possible epitope-masking effect of tetramerization is compatible with the recently published crystal structure of AChE tetramers (Bourne *et al.*, 1995). The proposed structure implies a highly regulated and stable architecture of the subunits in which certain domains of all four AChE molecules participating in a tetramer are sequestered within the quaternary structure. The possible involvement of such epitopes as a third circulatory residence factor (in addition to sialylation and oligomerization) participating in the clearance of AChE, is also implied from the difference between the pharmacokinetic behavior of fully-sialylated tetrameric forms of bovine AChE (Kronman *et al.*, 2000) and human AChE (human enzyme, MRT= 740 min, bovine enzyme, MRT = 1340 min). It should be noted in this context that all of the divergent amino-acids between the human and bovine AChEs are located at the surface of the molecules and are mostly situated within two distinct topological clusters (Mendelson *et al.*, 1998), and thus, they may confer different patterns of interaction with other proteins. The possible involvement of amino acid epitopes in the clearance of AChE is currently under study in our laboratory.

The therapeutic use of recombinant enzymes of human genetic origin, generated in human heterologous cell culture systems (e.g. HEK-293 or 293ST-D6), entails a significant immunogenic advantage. Yet, the paucity of a long-lived form of human AChE represented a serious concern for the development of a recombinant bioscavenger of human origin. The significant enhancement of the circulatory residence time of rHuAChE by combined genetic oversialylation and biochemical tetramerization presented in this report, represents therefore a significant step towards the development of a therapeutically-relevant formulation which will allow the exploitation of the bioscavenging abilities of AChE. These studies may serve as a basis for the generation of genetically modified cultured cells, with a high potential for promoting both sialylation and tetramerization for the high level expression of a circulatory long-lived AChE product or for the improvement pharmacokinetic performance of other recombinant glycoproteins of therapeutic value, the use of which may have been complicated by their short residence time.

VII. Overloading and removal of N-glycosylation targets on human acetylcholinesterase - Effects on glycan composition and circulatory residence time

INTRODUCTION

The distinctive residence-time courses of different proteins in the circulation are determined by a set of parameters which characterize the proteins and affect their susceptibility to diverse elimination systems. These parameters include primary traits (e.g. protein size, charge, hydrophobicity and the presence of specific amino-acid epitopes) as well as post-translation processing-related characteristics such as side-chain carbohydrate appendage and enzyme subunit assembly. More often, protein removal is mediated by more than one mechanism (Smedsrod and Einarsson, 1990; Narita *et al.*, 1995; Szkudlinski *et al.*, 1995; van der Kaaden *et al.*, 1995). The intricate pattern of coexistent elimination processes confer a typical pharmacokinetic profile characterizing the protein.

Acetylcholinesterase (AChE, EC 3.1.1.7), an enzyme which plays a crucial role in the termination of nerve impulse transmission, is mostly present in the form of cell-bound catalytic hetero-oligomers which are tethered to postsynaptic cells through structural noncatalytic subunits (Massoulie *et al.*, 1993, 1998). In the fetal stage, soluble homo-tetrameric acetylcholinesterase can be found at appreciable levels in the circulation as well (Ralston *et al.*, 1985), while in adults, circulating acetylcholinesterase is substituted by the homo-tetrameric form of the related enzyme, butyrylcholinesterase (BChE). The biological role of circulating cholinesterases and the stage-dependent occurrence of the acetylcholinesterase and butyrylcholinesterase, are yet poorly understood.

Previous studies have demonstrated the therapeutic potential of plasma-derived cholinesterases as efficient bioscavengers of organophosphate compounds. In addition to their high reactivity towards this group of toxic agents, the native forms of cholinesterases were retained in the circulation of experimental animals for extended periods of time, exhibiting mean residence times of more than 1000 minutes (Raveh *et al.*, 1993; Saxena *et al.*, 1997b; Kronman *et al.*, 2000). In contrast, recombinant human or bovine AChE, produced in stably transfected cell lines of the human embryonal kidney 293 (HEK-293) cell line, were eliminated from the bloodstream of experimental animals within much shorter periods of time (mean residence times of recombinant human (Kronman *et al.*, 1995; Chitlaru *et al.*, 2001) and of recombinant bovine (Kronman *et al.*, 2000; Mendelson *et al.*, 1998) AChEs are approximately 100 and 60 minutes, respectively). Glycan processing and enzyme assembly were both found to be decisive factors in determining the circulatory fate of acetylcholinesterases (Kronman *et al.*, 1995, 2000; Chitlaru *et al.*, 1998, 2001). Specifically, the inefficient terminal sialylation of the N-glycans appended to the recombinant AChEs, contributed greatly to the rapid elimination of these forms

of the enzyme. Indeed, genetic modulation of AChE producer cell lines by the introduction of heterologous α-2,6 sialyltransferase, resulted in the generation of efficiently sialylated recombinant AChE, which resided in the circulation for extended periods of time (Kronman et al., 2000; Chitlaru *et al.*, 1998). Likewise, induction of enzyme subunit oligomerization, by the *in-vitro* complexation of recombinant bovine or human AChE together with a synthetic Col-Q-derived Proline Rich Attachment Domain (PRAD) peptide, also resulted in the formation of recombinant AChEs with improved pharmacokinetic performances. N-glycan sialylation and subunit assembly of the recombinant enzymes acted in an hierarchical manner with respect to circulatory residence time.

The biological activity of many proteins is influenced by N-glycosylation (Goochee and Monica, 1990; Goochee *et al.*, 1991). In some cases N-glycans are directly involved in catalytic activity (Smith *et al.*, 1990; Wittwer and Howard, 1990; Takeuchi *et al.*, 1990), while in other cases they determine the ability of the respective proteins to be retained in the circulation. Acetylcholinesterases provide an attractive system for exploring the effect of N-glycan loading on glycoprotein pharmacokinetics since their enzymatic activity of is not impaired by N-glycan modulation (Mutero and Fournier, 1992; Fischer *et al.*, 1993; Velan *et al.*, 1993). Human acetylcholinesterase carries three N-glycosylation consensus (Asn-X-Ser/Thr) sequences (Prody *et al.*, 1987) , all of which are utilized in the recombinant version of the enzyme (Velan *et al.*, 1993). We have reported previously (Kronman *et al.*, 1995), the generation of a series of glycosylation-variants of recombinant human AChE, which are either underglycosylated or overglycosylated. The preliminary pharmacokinetic analyses of the various glycosylation-variants of recombinant human acetylcholinesterase (rHuAChE) did not reveal any appreciable effect of the number of glycans, on the circulatory half-life time of the corresponding forms of the enzyme. However, these recombinant enzymes were both deficient in sialic acid capping and were composed of a mixed population of monomers, dimers and tetramers, therefore, a possible effect of glycosylation levels on pharmacokinetics may have been masked by the overriding deleterious effect of incomplete glycan sialylation and enzyme subunit assembly.

In the present study, we perform a pharmacokinetic study of sixteen different post-translationally processed recombinant human AChE forms which define an array of variations in number of N-glycosylation sites, in terminal sialylation, and in subunit assembly. By exploiting matrix-assisted laser desorption ionization-time-of-flight (MALDI-TOF) mass spectrometry high resolution analysis, which enables detailed AChE-associated carbohydrate structural determination, we establish that all the different AChE glycoforms carry N-glycans of similar structures. This allows us to determine the specific contribution of AChE N-glycosylation level and its concerted effect with other post-translation modifications to circulatory longevity.

MATERIALS AND METHODS

Cell culture techniques, enzyme production and purification of rHuAChE and its derivatives - The generation of HEK-293 cell lines stably expressing high levels of wild type rHuAChE, N350Q hypoglycosylated rHuAChE, and the D61N or D61N/S541N hyperglycosylated variants of rHuACHE, were described previously (Kronman e*t al.*, 1992, 1995; Velan e*t al.*, 1993). The generation of *in-vivo* highly sialylated rHuAChE (wild type and glycosylation mutants) was achieved by stably expressing the wild type or mutated human acetylcholinesterase genes in the genetically modified 293ST-2D6 cells that express high levels of heterologous 2,6-sialyltransferase (Chitlaru *et al.*, 1998; Kronman et al., 2000). Cells were cultured in DMEM (Dulbecco's modified Eagle's medium) supplemented with 10% (w/v) FBS. Purification of secreted rHuAChE by affinity chromatography on procainamide columns was described previously (Kronman *et al.*, 1992, 1995). All the mutated versions of rHuAChE under study, exhibit catalytic properties indistinguishable from those of the wild-type enzyme.

Enzyme activity - AChE activity was measured according to Ellman *et al.* (1961). Assays were performed in the presence of 0.5 mM acetylthiocholine, 50 mM sodium phosphate buffer pH 8.0 0.1 mg/ml BSA and 0.3 mM 5,5'-dithiobis-(2-nitrobenzoic acid). The assay was carried out at 27^{0}C and monitored by a Thermomax microplate reader (Molecular Devices).

Pharmacokinetics - Clearance experiments in mice (3 to 6 ICR male mice per enzyme sample) and analysis of pharmacokinetic profiles were carried out as described previously (Kronman *et al.*, 1995). The study was approved by the local ethical committee on animal experiments. Residual AChE activity in blood samples was measured and all values were corrected for background activity determined in blood samples withdrawn 1 hour before performing the experiment. The clearance patterns of the various enzyme preparations were usually biphasic and fitted to a bi-exponential elimination pharmacokinetic model ($C_t=Ae^{-k\alpha t}+Be^{-k\beta t}$) as described previously (Kronman *et al.*, 1995). This model enables determination of the parameters A and B which represent the fractions of the material removed from the circulation in the first-fast and second-slow elimination phases respectively, and $T_{1/2}\alpha$ and $T_{1/2}\beta$ which represent the circulatory half-life values of the enzyme in the fast and slow phases. The pharmacokinetic parameters MRT (mean residence time, which reflects the average length of time the administered molecules are retained in the organism) and CL (clearance, which represents the proportionality factor relating the rate of substance elimination to its plasma concentration (CL=dose/area under the concentration-time curve, (Rowland and Towzer, 1989)) were independently obtained by analyzing the clearance data according to a noncompartmental pharmacokinetic model using the WinNonlin computer program (Gabrielsson and Weiner, 1999). Circulatory half-life values calculated by non-compartmental analysis, were in all cases

in good agreement with the $t_{1/2}\beta$ values derived from the biexponential elimination pharmacokinetic model.

Release, recovery, purification and labeling of N-glycans - N-glycans of purified enzyme preparations (~100 ug protein) were released by N-glycosidase-F (Glyko, USA) treatment as described before (Kronman *et al.*, 1992). Deglycosylated protein was removed by ethanol-precipitation and glycans were recovered and purified from the supernatant as described by Kuster *et al.* (1997). To increase sensitivity (Okafo *et al.*, 1996, 1997; Anumula and Dhume, 1998) purified glycans were fluorescently labeled. Fluorescent labeling of purified glycans with 2-aminobenzamide (2-AB) was performed according to Bigge *et al.*, (1995) using a commercial labeling kit (Glyko, USA). During the 2h labeling incubation, the temperature was kept at 55^0C to prevent heat-induced desialylation of the glycans.

Removal of sialic acid from labeled N-glycans - Agarose-bound sialidase (0.04U, Sigma) was prewashed 5 times with water and incubated at room temperature for 16h with 2AB labeled N-glycans released from 1.5 -2.0 nmol AChE. Sialidase was removed by Eppendorf centrifugation. Desialylated N-glycans were vacuum dried, resuspended in 30 µl of water and stored at -20^0C until use. Glycans prepared in this manner were subjected to MALDI-TOF analysis or to further glycosidase treatments followed by MALDI-TOF analysis.

Esterification of sialic acids - To allow the concomitant measurement by MALDI-TOF analysis of both neutral and acidic glycans, the carboxylic groups of sialylated 2AB labeled glycans were converted into their neutral methylated forms by methyl iodide esterification, essentially as described by Kuster *et al* (1997). We note that in this procedure the 2AB moiety itself undergoes methylation and therefore both neutral and acidic glycans invariably display an increment in molecular mass of 14.015 kDa in addition to the increase in mass size resulting from sialic acid methylation in the case of acidic glycans. Esterified glycans were purified as described (Kuster *et al.*, 1997) and stored at -20^0C until MALDI-TOF analysis.

Mass spectrometry - Mass spectra were acquired on a Micromass TofSpec 2E reflectron time-of-flight (TOF) mass spectrometer (Kuster *et al.*, 1997; Rudd *et al.*, 1997; Mechraf and Novotny, 1998). 2AB-labeled desialylated or 2AB-labeled esterified glycan samples, were mixed with an equal volume of freshly prepared DHB (10mg/ml in 70% acetonitrile) and loaded onto the mass spectrometer target. Routinely, 1 µl and 1 µl of glycan samples diluted 1:10 in water were subjected to analysis. Dried spots were recrystallized by adding 0.5 µl ethanol and allowed to redry. Neutral glycans were observed as $[M+Na]^+$ ions. 1 µl of peptide mixture (renin substrate, adrenocorticotropic hormone fragment 18-39, and angiotensin,10 pMole/µl all from Sigma) which served as a three-point external calibrant for mass assignment of the ions, was mixed with freshly prepared α-cyano-4-hydroxycinnamic acid (10 mg/ml in 49.5%

acetonitrile; 49.5% ethanol; 0.001% TFA), loaded on the mass spectrometer target and allowed to dry. All oligosaccharides were analyzed at 20 kV with a single-stage reflectron in the positive-ion mode. Between 100 and 200 scans were averaged for each of the spectra shown. The N-glycan structure assignment was confirmed by inspecting the MALDI-TOF spectra of the various preparations following step-wise exoglycosidase trimming (Kuster *et al.,* 1997; Kronman *et al.*, 2000).

In-vitro tetramerization of rHuAChE - Previous studies by Giles *et al.* (1998) demonstrated that rHuAChE can be tetramerized by a PRAD-derived peptide. The synthesis and quality control of the human version of the PRAD peptide of the sequence CLLTPPPPPLFPPPFFRG was described previously (Kronman *et al.*, 2000). Preparative tetramerization for the generation of milligram amounts of tetrameric wild-type and glycosylation-variants of rHuAChE for pharmacokinetic studies included 14.4 nmol of rHuAChE (equivalent to 3000U) which were incubated with 28.8 nmol PRAD peptide in a final volume of 2ml. Prior to administration to mice, *in-vitro* tetramerized rHuAChEs were dialyzed extensively against PBS.

Sucrose density gradient centrifugation - Analytical sucrose density gradient centrifugation was performed on 5-25% sucrose gradients containing 0.1M NaCl/50 mM sodium phosphate buffer pH 8.0. Centrifugation was carried out in an SW41 Ti rotor (Beckman) for 26h at 160,000*g*. Fractions of 0.2 ml were collected and assayed for AChE activity. Alkaline phosphatase, catalase and β-galactosidase served as sedimentation markers.

RESULTS

Generation of rHuAChE glycoforms harboring increasing numbers of N-glycans and exhibiting various degrees of sialylation and subunit assembly - The general strategy for determining the role of the number of N-glycans on the retention of rHuAChE in the circulation is based in the present report on structural and pharmacokinetic studies involving a series of site-directed glycosylation mutated versions of human AChE (Fig. 26, see also (Kronman *et al.*, 1995)). The mutant enzymes N350Q, D61N, and D61N/S541N contain 2, 4 and 5 appended N-glycans respectively, as opposed to the wild-type enzyme which carries three N-glycans (Prody *et al.*, 1987; Velan *et al.*, 1993). These forms of rHuAChE, as well as the wild type enzyme were produced in human embryonic kidney (HEK) cells of the 293 line. In these cells, all the potential native or engineered N-glycosylation sites on rHuAChE, conforming to the consensus Asn-Xaa-Thr/Ser sequence, are utilized (Kronman *et al.*, 1995). Conversely, disruption of a potential glycosylation site, such as in the case of N350Q results in the complete abrogation of N-glycan appendage at the corresponding position (Velan *et al.*, 1993). We have documented in the past that HEK-293 cells do not contain sufficient amounts of sialyltransferase activity and therefore the N-glycans of rHuAChE produced in high

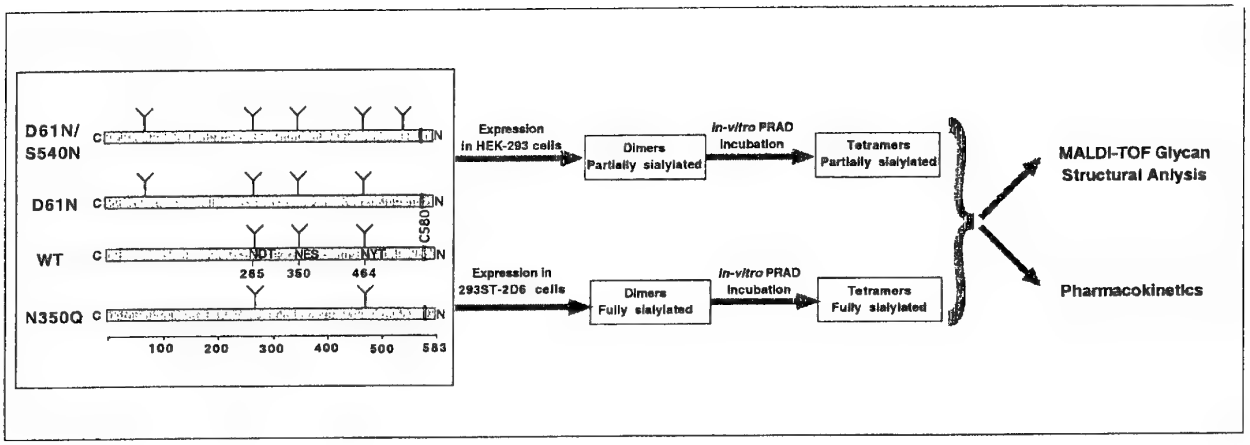

Figure 26: The various forms of rHuAChE under study: experimentation scheme. N350Q, D61N and D61N/S540N are site directed mutated forms of rHuAChE containing 2, 4 and 5 N-glycosylation sites, respectively, as indicated by schematic biantennary structures. The WT form contains 3 glycosylation sites at the indicated amino acid sequences. The cysteine residue at position 580, responsible for the generation of dimers is indicated as a double bar marked C580. The 4 differently glycosylated AChE forms were expressed in HEK-293 and 293ST-2D6 cells for the generation of partially or fully sialylated dimeric versions of recombinant enzyme, respectively. In turn, each version of enzyme was subjected to tetramerization by *in-vitro* incubation with the ColQ-derived PRAD peptide. All the forms of rHuAChE were subjected to a detailed pharmacokinetic study paralleled by a quantitative structural analysis of their N-glycans.

levels by these cells are inefficiently sialylated (Chitlaru *et al.,* 1998). The undersialylated state of HEK-293 cell-produced AChE results in the exposure of N-glycan terminal Gal residues which are efficiently recognized by the liver asialoglycoprotein clearance receptor, therefore negatively affecting the ability of the enzyme to be retained in the circulation for extended periods of time (Kronman *et al.*, 1995, 2000; Chitlaru *et al.*, 1998). To remedy the suboptimal sialylation level of HEK-293-produced rHuAChE, the various mutated forms of rHuAChE which differ in their number of appended N-glycans, were expressed also in the genetically modified 293ST-2D6 cells (Chitlaru *et al.*, 1998; Kronman *et al.*, 2000) which produce high amounts of recombinant α2,6 sialyltransferase (Fig. 26). Indeed, the various glycosylation mutants produced in the modified 293ST-2D6 cells display nearly fully sialylated glycans (Fig. 27A), as established by MALDI-TOF structural analysis of the corresponding glycan pools (see below).

In addition to efficient terminal sialylation, the subunit assembly state of AChE positively affects its ability to be retained in the circulation (Chitlaru *et al.*, 1998; Kronman *et al.*, 2000). We have previously shown that it is possible to generate highly homogenous preparations of rHuAChE tetramers *in vitro*, utilizing a synthetic peptide representing the Proline Rich Association Domain (PRAD) of the ColQ protein (Bon and Massoulie, 1997; Bon *et al.*, 1997; Giles *et al.,* 1998; Chitlaru *et al.*, 1998; Kronman *et al.*, 2000) which represents the membrane-anchored noncatalytic subunit of AChE multimers encountered at the post-synaptic membranes of the neuro-muscular junctions (Hall, 1973; Rosenberry and Richardson, 1977; Vignay *et al.*, 1983; Rotundo *et al.*, 1997). The array of rHuAChE glycosylation forms differing in their number of N-glycans were therefore subjected to PRAD-mediated *in vitro* tetramerization (Fig. 26). All the glycosylation variants of rHuAChE, regardless of their degree of terminal sialylation (partially sialylated produced in HEK-293 cells or fully sialylated produced in 293ST-2D6 cells) were equally amenable to tetramerization and stable tetrameric preparations could be generated with all AChE forms (Fig. 27C). Thus, for the present study, sixteen forms of rAChE were generated differing in: **(i)** the number of glycosylation sites (2, 3, 4, and 5 N-glycans), **(ii)** the extent of sialylation (expressed in HEK-293 or 293ST-2D6 cells) and **(iii)** the subunit assembly status (mixed populations consisting mostly of dimers, or fully tetrameric preparations generated by incubation with the PRAD peptide).

MALDI-TOF structural analysis of N-glycans released from the various rHuAChE glycoforms - In order to determine the degree of similarity of the N-glycan pools associated with the different versions of rHuAChE glycoforms under study, the structures and relative quantities of the N-glycans derived from the various enzyme forms (Fig. 26), were compared by MALDI-TOF analysis. These analyses included the resolution of the basic features of the appended N-glycans such as the class (complex, hybrid or high mannose glycans), branching (number of antennae GalNAc, fucose, bisecting GlcNAc), as well as determination of their level

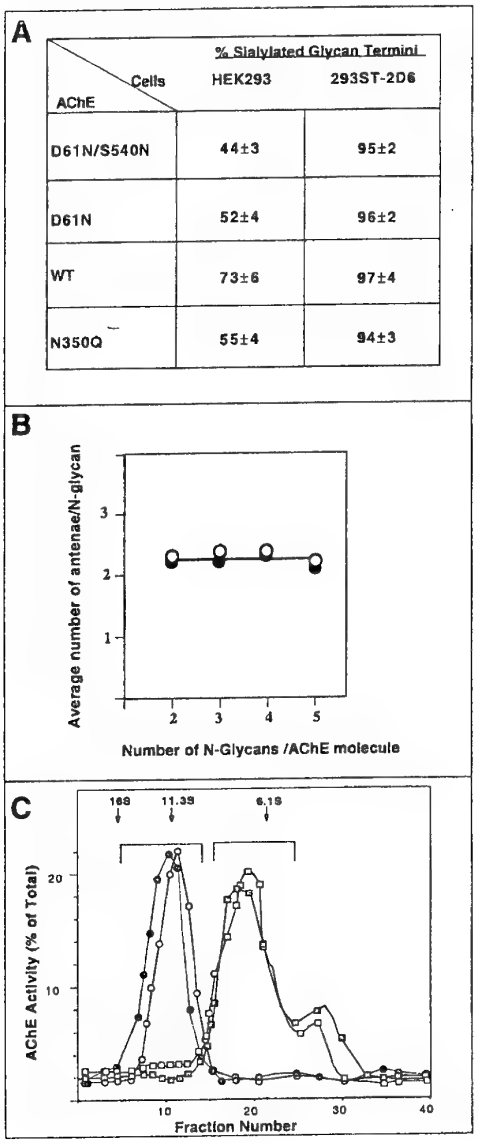

Figure 27: Characterization of glycan capping and branching, and enzyme subunit assembly state of the various forms of rHuAChE under study. A: Percentage of sialylated termini in the glycan pools associated with the various AChE forms, calculated from the frequencies of individual glycan structures detected by the MALDI-TOF analysis (see Table 15 and Fig. 29). Note the almost complete sialylation of the glycans associated with the 293ST-2D6 cell-generated AChEs. **B**: The average number of glycan antennae per glycosylation site calculated for each of the rHuAChE glycoforms under study (based on the data presented in Table 16), were plotted against the number of N-glycan attachment sites of the corresponding enzyme species. Note that in all cases, regardless of the cell production system, all glycoforms carry a nearly identical average number of glycan antennae. **C**: Sucrose gradient sedimentation assay of AChEs before and after PRAD mediated *in-vitro* tetramerization. All mutated rHuAChE forms under study, regardless of their N-glycan terminal sialylation status, tetramerized efficiently in the presence of the PRAD peptide; shown are examples for the diglycosylated N350Q rHuAChE (gray squares-before, and gray circles-after PRAD treatment) and pentaglycosylated D61N/S540N rHuAChE (open squares-before, and open circles-after PRAD treatment). Arrows denote the elution position of the sedimentation markers alkaline phosphatase (6.1S), catalase (11.3S), and β-galactosidase (16S) included in all samples.

of terminal glycan sialylation (Kronman et al., 2000; Kuster *et al.*, 1997).

MALDI-TOF analyses following enzymatic removal of glycan terminal sialic acid residues (Fig. 28 and Table 15) established that the N-glycans associated with all the different rHuAChE forms belong to 11 discrete classes which vary in their branching and monosaccharide substitutions, ranging from partially galactosylated biantennary to fully galactosylated tetraantennary complex-type forms. The relative abundance of the different glycan forms are similar in all the species of rHuAChE, regardless of the number of N-glycans appended per enzyme subunit (2, 3, 4 or 5 glycans) and of the recombinant production system (HEK-293 cells or 293ST-2D6 cells). In all cases, the overall N-glycan branching was found to be nearly identical (Fig. 27B) and the most prevalent form was found to be the biantennary core-fucosylated structure (Table 15, form IV). The N-glycan structural similarity observed for the various rHuAChE forms reflects the N-glycan biosynthetic abilities of the HEK-293 cells and their propensity for the generation of biantennary complex glycan structures on heterologous recombinant proteins (Smith *et al.*, 1992; Yan *et al.*, 1993). Similar N-glycans were found to be associated with recombinant bovine acetylcholinesterase produced in the same cell systems (Kronman *et al.*, 2000).

Although the various AChE forms were mostly found to contain highly similar glycans, some minor structural differences between the glycan repertoires of the various mutated AChEs were observed, such as the unequal occurrence of N-glycans exhibiting outer-arm GalNAc residues (Table 15, form V). These structures were mainly encountered in the mutated D61N and D61N/S541N AChE versions and to a lesser extent also in the 293ST-2D6 produced N350Q mutant which contains only two of the three native glycosylation sites. The relatively low abundance of these GalNAc terminated glycans as well as the observation that they are fully capped with sialic acid when expressed in the sialyltransferase 293ST-2D6 coexpressor cell line (see below), suggest that they probably do not play a role in determining pharmacokinetic behavior differences among the various AChE forms.

Examination of terminal glycan sialylation by MALDI-TOF analysis of iodomethane-mediated esterified glycans (Fig. 29, Table 16) clearly established that although exhibiting glycans of highly similar basic structure, the various AChE glycoforms generated by HEK-293 cells differ one from another in the extent of terminal glycan sialylation (Table 16). A clear relation is observed between the level of non-sialylated glycan termini and the number of N-glycans appended to the various mutants. Thus the HEK-293 cell generated triglycosylated (wild type, WT), tetraglycosylated (D61N) and pentaglycosylated (D61N/S541N) AChEs are characterized by 1.8, 4.7, and 6.0 nonsialylated glycan termini per enzyme subunit., respectively, reflecting the limited ability of the HEK-293 cell glycosylation machinery to efficiently sialylate an increasing number of glycan termini (Kronman *et al.*, 1995). In contrast, expression of the various rHuAChE glycoforms in the sialyltransferase-modified 293ST cells, resulted in the generation of glycans which equally display almost fully sialylated glycan termini

Table 15: Comparison of desialylated Glycan Structures of WT and Glycosylation Mutants of rHuAChE

Molecular masses, deduced structures and relative abundances of the enzymatically desialylated N-glycan structures were determined from the MALDI-TOF spectra represented in Fig. 28. Results represent the average ±S.D. obtained from the analysis of at least three independent N-glycan preparations.

	Structure	MW $(M+Na)^+$+2AB	N350Q (2 Glycans)		WT (3 Glycans)		D61N (4 Glycans)		D61N/S541N (5 Glycans)	
			HEK-293	293ST2D6	HEK-293	293ST2D6	HEK-293	293ST2D6	HEK-293	293ST2D6
I		1767.8	2.7±0.4	<0.8	1.68±0.2	1.55±0.4	3.5±0.6	2.4±0.4	3.1±0.4	3.6±0.6
II		1783.6	8.0±0.9	11.6±1.2	4.9±0.8	5.2±0.6	9.9±1.1	14.1±2.0	12.8±1.1	3.4±0.5
III		1809.9	1.4±0.2	<0.8	3.2±1.0	3.6±0.5	1.9±0.3	1.3±0.2	2.9±0.4	8.0±0.6
IV		1929.8	47.7±4	29.5±3.2	56.0±4.1	49.0±4.8	26.4±2.1	19.2±1.8	25.2±1.9	28.7±2.2
V		1971.8	7.4±0.8	12.7±1.1	3.3±0.8	3.9±0.7	19.8±2.1	24.1±2.6	17.7±1.3	18.9±1.1
VI		2132.6	4.1±0.4	7.1±0.9	3.0±0.4	4.6±1.0	3.0±0.5	5.5±0.6	12.9±1.0	5.4±0.5
VII		2148.9	13.9±1.4	24.9±2.9	13.6±1.0	18.8±0.9	21.3±2.2	23.9±2.4	10.5±0.5	9.3±0.7
VIII		2295.1	8.6±0.7	10.7±1.1	11.2±1.6	14.5±1.9	9.4±1.0	5.4±0.7	10.6±0.9	9.6±0.7
IX		2336.5	<0.8	<0.8	<0.8	<0.8	<0.8	<0.8	<0.8	4.0±0.5
X		2498.5	<0.8	<0.8	<0.8	<0.8	<0.8	<0.8	<0.8	2.4±0.3
XI		2660.6	2.0±0.3	3.5±0.3	2.2±0.3	2.8±0.8	4.8±0.4	3.9±0.3	4.2±0.4	5.1±0.5
			□GlcNAc ○Man ■GalNAc ◇Gal —Fuc							

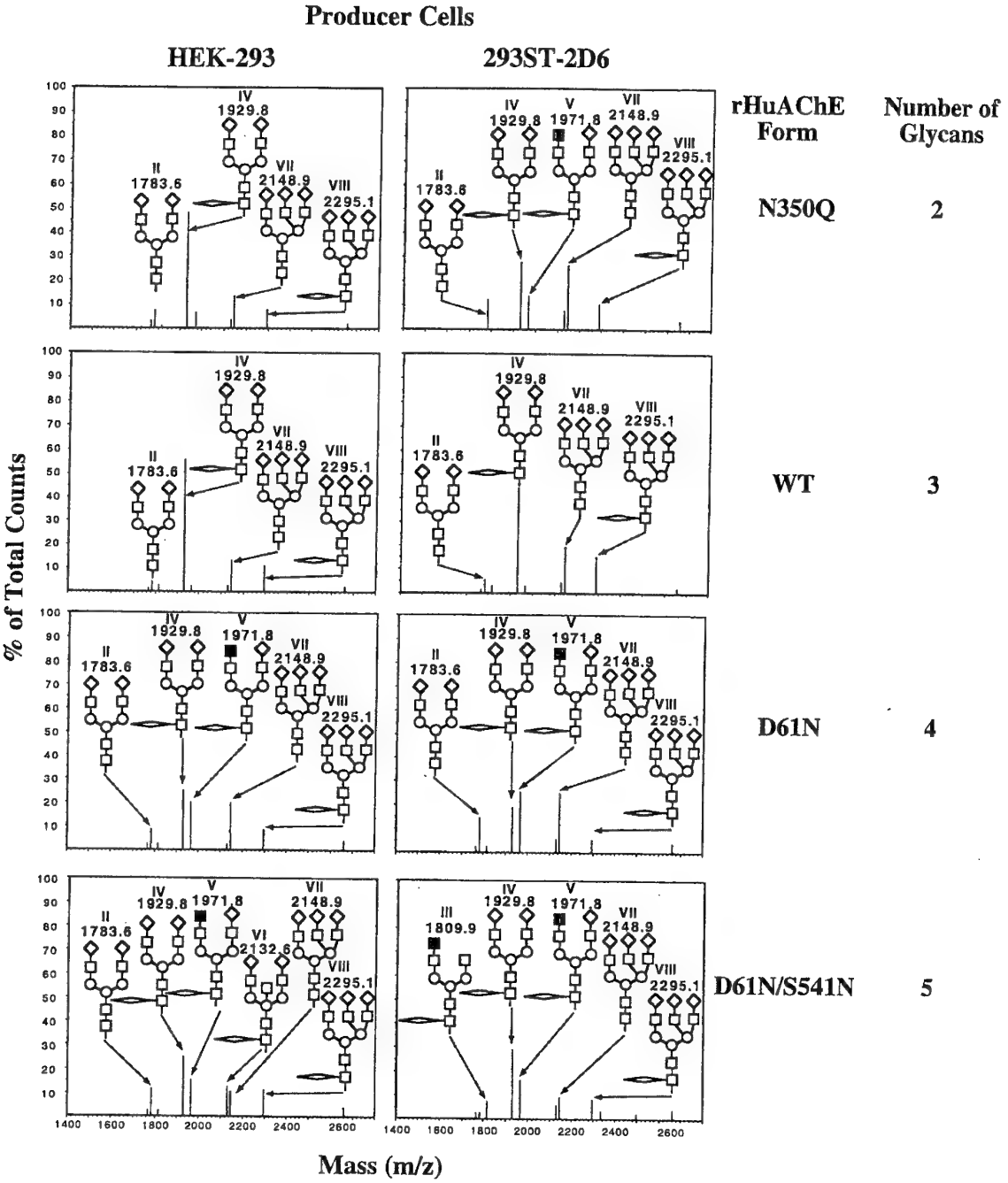

Figure 28: MALDI-TOF mass spectra of desialylated N-glycans released from WT and glycosylation mutant forms of rHuAChE Purified N-glycans of the indicated various rHuAChEs were subjected to sialidase treatment and 2-AB labeling prior to MALDI-TOF analysis. Molecular weights and schematic structures are shown for the major glycan forms. Molecular weights represent monoisotopic masses of the respective $[M+Na]^+$ ions of the glycan species. *Roman numerals* refer to the peak designations ascribed to the various major forms in Table 15. *Square*, GlcNac; *circle*, Man; *diamond*, β-Gal; *elongated diamond*, Fuc; *dark square*, α-Gal

(0.2-0.6 nonsialylated termini/AChE molecule, Table 16) regardless of the number of appended N-glycans. Thus, the efficient correction of the sialic acid capping by the expression of the various mutated AChE forms in the sialyltransferase genetically modified 293ST-2D6 cell line resulted in the generation of a set of enzymes which carry highly similar N-glycans with respect to their basic structures and terminal sialic acid capping, and differ one from another only in the actual number of appended N-glycans. These can now serve for conducting a meaningful study of the involvement of the number of glycosylation sites in determining the pharmacokinetic behavior of AChEs.

Pharmacokinetics of rHuAChE glycoforms: the combined effect of N-glycosylation, terminal sialylation and oligomerization in determining the circulatory retention of AChE - The entire array of rHuAChEs differing in their number of N-glycans, both in their partially or fully sialylated configurations (produced by HEK-293 or 293ST-2D6 cells, respectively) were subjected to a pharmacokinetic study before or after *in vitro* PRAD-mediated tetramerization. The various forms were administered to mice and their clearance rates were determined by measuring the residual AChE activity in blood samples withdrawn at different times post-administration. The parameters characterizing the pharmacokinetic performance of each rHuAChE glycoform were calculated according to the biphasic decay and the noncompartmental circulatory elimination models (Table 17 and Figs. 30 and 31). Inspection of the mean residence times (MRTs) of the various enzyme forms establishes that an increase in the number of appended N-glycans contributes to the ability of the enzyme to be retained in the circulation, yet the manifestation of this contribution clearly depends both on the level of glycan terminal sialylation and the subunit assembly state of the enzyme. Thus, within each of the four categories of rHuAChE enzyme forms under study, **i**-undersialylated/nonassembled, **ii**-undersialylated/tetramerized,, **iii**-sialylated/nonassembled, and **iv**-undersialylated/tetramerized, (Table 17), the presence of increasing numbers of N-glycans on the different mutants appears to affect their pharmacokinetic behavior according to a different pattern, as detailed below.

Comparison of the pharmacokinetics of the various AChE glycoforms, which are partially sialylated and nonassembled (category **i**, Table 17), revealed that the triglycosylated WT enzyme resides in the circulation for significant longer periods of time (MRT WT undersialylated/nonassembled =102 min) than the diglycosylated N350Q form (MRT N350Q undersialylated/nonassembled=67 min). However, a further increase in the number of appended N-glycans resulted in a decrease in their circulatory residence in a progressive manner, the triglycosylated WT, tetraglycosylated D61N, and pentaglycosylated D61N/S541N versions of rHuAChE, displayed MRTs of 102 min, 46 min, and 25 min, respectively. This decline in circulatory residence, which accompanies the increase in the number of appended glycans, is

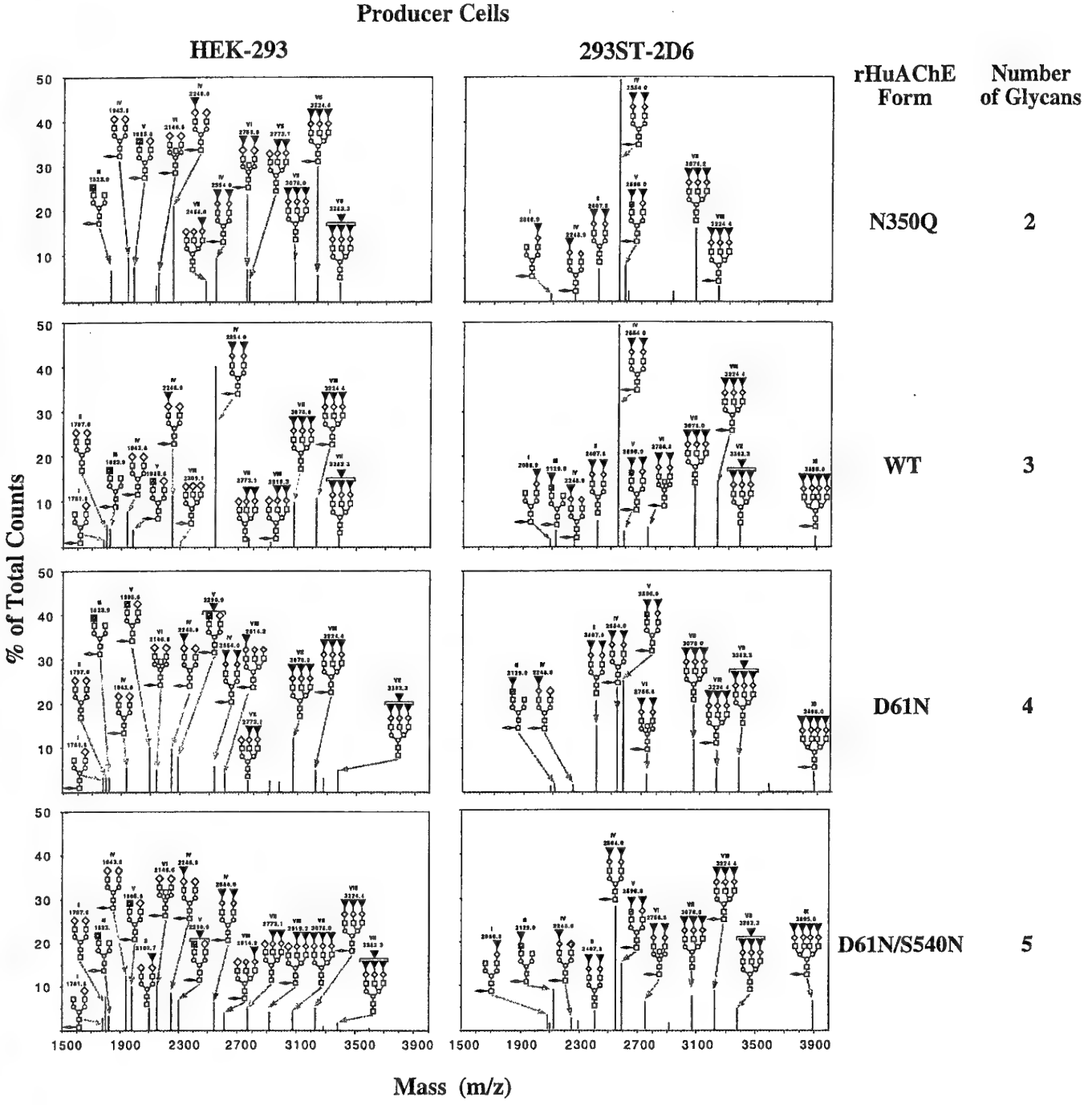

Figure 29: MALDI-TOF mass spectra of the esterified N-glycans pools released from WT and glycosylation mutant forms of rHuAChE Purified N-glycans of the indicated various rHuAChEs were subjected to 2-AB labeling and iodomethane-mediated esterification prior to MALDI-TOF analysis. Molecular weights represent monoisotopic masses of the respective [M+Na]+ ions of the glycan species. *Roman numerals* refer to the peak designations ascribed to the various major forms in Table 15. Note that an increase of 14.015 Da of all glycan species occurs due to the methylation of the common 2-AB moiety. *Square,* GlcNac; *circles,* Man; *diamond,* β-Gal; *elongated diamond,* Fuc; *dark square,* α-Gal; *inverted dark triangles,* Sialic acid.

Table 16: Structural branching and sialylation state of N-glycans released from WT and glycosylation-mutant forms of rHuAChEs generated in HEK-293 and 293ST-2D6 cells

The data were calculated on the basis of the frequencies of the individual glycan structures detected by MALDI-TOF analysis (Figs. 28 and 29).

Producer Cells	AChE Form	No. of glycans/ AChE molecule	Average No. of antennae/ AChE molecule	Sialylated termini/ AChE molecule	Non-sialylated termini/ AChE molecule
HEK-293	N350Q	2	4.5	2.5	2.0
	WT	3	6.8	5.0	1.8
	D61N	4	9.8	5.1	4.7
	D61N/S541N	5	10.7	4.7	6.0
293ST-2D6	N350Q	2	4.6	4.3	0.3
	WT	3	7.2	7.0	0.2
	D61N	4	9.5	9.1	0.4
	D61N/S541N	5	11.0	10.4	0.6

Table 17: Pharmacokinetic Parameters of WT and mutated versions of rHuAChE differing in their number of appended N-glycans, level of terminal sialylation and subunit oligomerization state.

Category	rHuAChE status	AChE glycoform	No. of glycans	A (% of total)	$T_{1/2}\alpha$ (min)	B (% of total)	$T_{1/2}\beta$ (min)	Clearance (ml/hr/kg)	MRT (min)
i	undersialylated, nonassembled[a]	N350Q	2	55±3	8.4±1	33±3	54±4	176	67
		WT	3	74±5	7.3±0.7	25±1.5	80±4	124	102
		D61N	4	76±11	4.6±0.3	34±4	44±3	227	46
		D61N/S541N	5	78±5	3.9±1	34±5	25±7	370	25
ii	undersialylated, tetramerized[b]	N350Q	2	45±7.2	6.7±2.6	56±8.5	60±10	107	87
		WT	3	55±6	6.9±2	46±4	129±13	83	194
		D61N	4	77±2.5	4.5±0.5	25±3	71±4	232	85
		D61N/S541N	5	72±7	4.0±0.6	29±3	75±6	228	82
iii	sialylated, nonassembled[c]	N350Q	2	67±9	21±4	26±7.2	120±22	88	132
		WT	3	58±4	14±1	42±2	133±9	93	195
		D61N	4	52±5.5	11.8±3	46±3.6	129±13	65.5	190
		D61N/S541N	5	60±7	13±2	38±7	133±15	68	201
iv	sialylated, tetramerized[d]	N350Q	2	52±10	29±8	49±10	158±22	44	201
		WT	3	59±4	30±5	40±4	595±40	13	740
		D61N	4	58±9	40±8	43±4.5	760±50	11	1055
		D61N/S541N	5	40±3.4	22±7	58± 4	713±85	9.8	1020

a - Produced in nonmodified HEK-293 cells.

b- Produced in nonmodified HEK-293 cells and subjected to *in-vitro* PRAD-mediated tetramerization.

c - Produced in sialyltransferase-coexpressor 293ST-2D6 cells.

d- Produced in sialyltransferase-coexpressor 293ST-2D6 cells and subjected to *in-vitro* PRAD-mediated tetramerization.

fully compatible with the relatively high number of N-glycan terminating with exposed Gal residues in the tetraglycosylated and pentaglycosylated HEK-293 produced preparations (Table 16).

All of the various rHuAChE glycoforms under study, including those which carry additional N-glycans were efficiently converted into enzyme tetramers (Fig. 27C), testifying to the fact that the appended N-glycans do not obstruct contact-zone interactions required for the efficient generation of stable tetrameric forms (Morel *et al.*, 2001) and in line with the reported spatial architecture of AChE tetramers determined by X-ray crystallography (Bourne *et al.*, 1995). All the enzyme forms belonging to this category (undersialylated/tetramerized) exhibited prolonged circulatory residence in comparison to their nonassembled counterparts (compare MRTs of the corresponding rHuAChE glycoforms of categories **i** and **ii**, Table 17). Pharmacokinetic profiling of this group of enzyme forms (category **ii,** Table 17), demonstrated that, as in the previous category (category **i**), an increase in MRT value is promoted by the addition of a third glycan (MRT $N350Q_{undersialylated/tetramerized}$ = 87 min; $WT_{undersialylated/tetramerized}$ = 194 min), and that this increase is not further improved by the presence of a fourth or fifth glycan appendage. However, unlike in the case of the nonassembled enzyme forms, the MRTs of the two hyperglycosylated forms of the enzyme are similar (MRT $D61N_{undersialylated/tetramerized}$=85 min; MRT $D61N/S541N_{undersialylated/tetramerized}$=82 min). In this case, the positive pharmacokinetic effect of tetramerization mitigates the deleterious effect of asialoglycoprotein receptor-mediated circulatory removal, resulting in the equal residence of the tetra and penta-glycosylated AChEs.

The pharmacokinetic influence of the number of appended N-glycans is most apparent in the case of fully sialylated forms of AChEs. Fully sialylated tri- tetra- and pentaglycosylated AChEs in their nonassembled form (category **iii,** Table 17), are equally retained in the circulation for considerably longer periods of time than diglycosylated N350Q rHuAChE ($MRT_{sialylated/nonassembled}$ of WT, D61N, and D61N/S541N =195min, 190min and 201min, respectively; $MRT_{sialylated/nonassembled}$ N350Q = 132 min). Following their tetramerization, a dramatic pharmacokinetic effect was observed for the fully sialylated rHuAChE glycoforms (category **iv,** Table 17). The fully sialylated tetramers display MRT values which increase proportionally to the number of N-glycans within the 2-4 glycan/subunit range ($MRT_{sialylated/tetramerized}$ of N350Q, WT, and D61N =201min, 740min and 1055min). The high MRT exhibited by the mutated tetraglycosylated form represents a 10 fold increase in the circulatory residence as compared to the unmodified wild-type enzyme (category **i,** MRT WT $_{undersialylated/nonassembled}$ =102min) and a 40% increase over the WT enzyme in its fully modified state. This latter effect is only observed upon full sialylation and tetramerization emphasizing the requirement of optimal sialylation and subunit assembly for assessment of the pharmacokinetic role of N-glycan appendage. Addition of a fifth glycan at amino-acid 541, such as in the case of the D61N/S541N mutant, does not further improve pharmacokinetics

(category **iv**, MRT $WT_{sialylated/tetramerized}$ =1020min), suggesting that the four glycans in the D61N mutant are sufficient to confer this unprecedently high circulatory residence to rHuAChE.

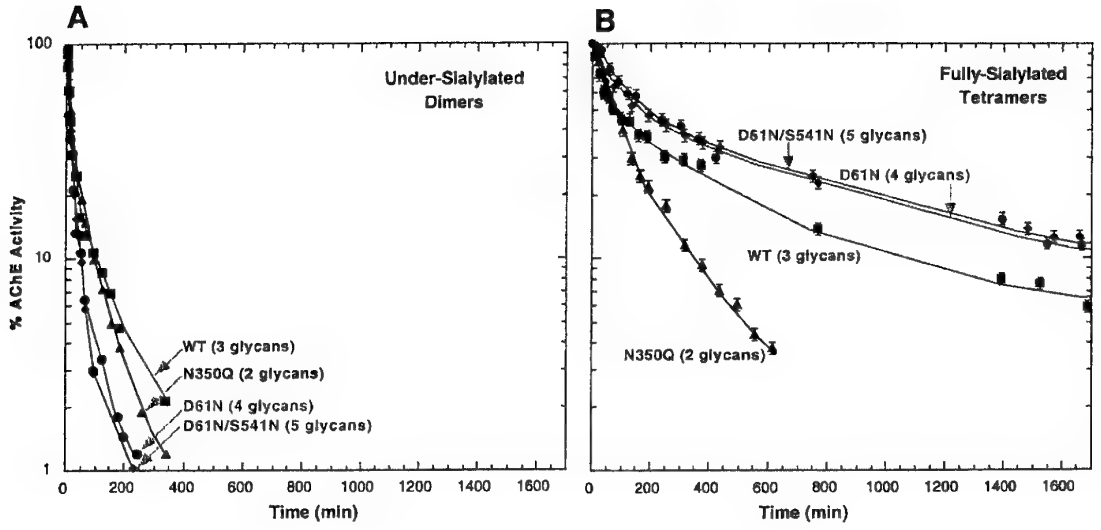

Figure 30: Comparison of the circulatory elimination profiles of WT and mutated forms of rHuAChE Purified preparations (100 U) of WT and mutated forms of rHuAChE, generated in HEK-293 cells (exhibiting undersialylated N-glycans) or 293ST-2D6 cells (exhibiting fully sialylated glycans), were administered to 3-6 ICR male-mice (per enzyme sample) before (dimeric) or after (tetrameric) *in-vitro* PRAD-mediated tetramerization. The residual AChE activity in the circulation was assayed at the indicated time points post administration; circulatory removal curves were determined for all the AChE forms and the derived pharmacokinetic parameters are presented in Table 17. **A**: HEK-293 generated AChEs, **B**: 293ST-2D6 cell generated AChEs following PRAD treatment. *triangle*, N350Q; *squares*, WT; *circle*, D61N; *diamond*, D61N/S541N. Error bars represent the standard deviation.

DISCUSSION

Examination of an array of fully processed rHuAChE enzyme forms which are efficiently sialylated and assembled into their tetrameric forms, revealed that the number of appended glycans influences their ability to reside in the circulation over extended periods of time (Fig. 31, Fully sialylated tetramers). Thus, di- tri and tetraglycosylated rHuAChE exhibit mean residence time values of 200, 740 and 1055 mins, respectively. The mean residence time of the fully processed tetraglycosylated D61N rHuAChE (1055 min), is of the same magnitude as that of FBS-AChE (MRT = 1340min, (Kronman et al., 2000)), with which it shares the same number of appended glycans at corresponding locations (Mendelson *et al.*, 1998). Structural examination of FBS-AChE carried out previously (Kronman et al., 2000), demonstrated that this native enzyme which physiologically resides in the circulation, occurs entirely in a fully sialylated tetrameric form. Conversely, the wild-type human AChE, which possesses only three N-glycans, is not encountered as a native circulatory enzyme but rather as a post-synaptic or erythrocyte-associated membrane anchored complex.

The manner in which the N-glycosylation load, terminal N-glycan sialylation and subunit oligomerization act together in determining the residence time of the enzyme (Fig. 31), clearly suggests that a multifactorial mechanism is involved in the removal of AChE from the circulation and that these multiple factors exert their influence in a hierarchical manner. Terminal N-glycan sialylation is the governing factor in this hierarchy; since totally desialylated forms of AChE are cleared rapidly from the circulation within minutes in an equal manner, regardless of their oligomerization state and their number of appended N-glycans (Chitlaru *et al.*, 1998; Kronman *et al.*, 2000, and data not shown). The dominant position of sialylation is reflected also by the observation that under partial sialylation conditions, increasing the number of N-glycans both on dimers and tetramers has a deleterious rather than advantageous effect on AChE residence time (Fig. 31, Undersialylated dimers, Undersialylated tetramers). In this case, increasing the number of N-glycans on the enzyme surface results in a quantitative increase in the amount of terminal Gal residues which serve as highly potent clearance epitopes. This situation was responsible for our inability in the past to assign a positive pharmacokinetic role for the rHuAChE N-glycan number (Kronman *et al.*, 1995), since in this previous study, rHuAChE forms were prepared in HEK-293 cells which possess only limited sialyltransferase activity, and therefore suffered from pronounced undersialylation. Inefficient enzyme assembly, which represents a second factor in the hierarchical AChE multifactorial elimination pathways (Chitlaru et al., 1998), may be remedied by PRAD-mediated tetramerization, yet in itself, is not sufficient for enabling the increased number of glycans to fully exert their pharmacokinetic effect (Fig. 31, Undersialylated tetramers). Rather, the full manifestation of the circulatory longevity promoted by quantitative N-glycosylation, requires a pre-existing state of highly efficient tetramerization and sialylation of the enzyme.

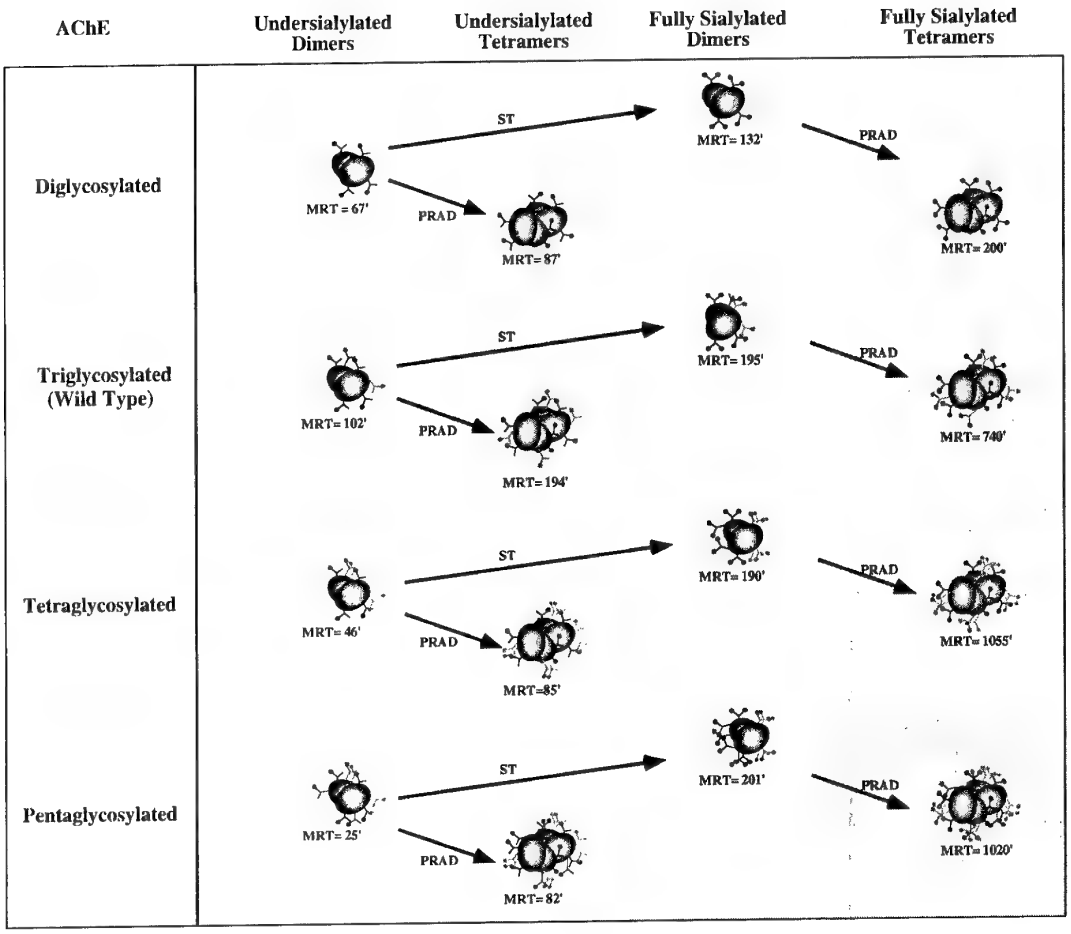

Figure 31: Schematic representation of the combined effect of the number of appended N-glycans, N-glycan sialic acid capping and oligomerization state on the circulatory retention of rHuAChE All 16 forms of AChE under study are depicted as globular spheres representing the AChE subunit. Bifurcated extensions protruding from the spheres represent N-glycans. The circles terminating some of these bifurcated extensions represent sialic acid moieties. Diglycosylated, Tetraglycosylated and Pentaglycosylated, refer to the N350Q, D61N, and D61N/S541N rHuAChE mutants, respectively. Undersialylated dimers are generated by expression in HEK-293 cells, while fully sialylated dimers are generated in the sialyltransferase expressor 293ST-2D6 cell system, and denoted by ST. The *in-vitro* quantitative tetramerization is denoted by PRAD. MRT refers to the mean residence times of the various rHuAChE forms. Decrease or increase in MRTs are indicated by a change to lighter or darker backgrounds, respectively (the darker the background, the higher the MRT).

The role of glycosylation in determining the circulatory residence of glycoproteins has been examined in many systems (Welply, 1991; Opdenakker *et al.*, 1993; Rademacher *et al.*, 1988). Clearance of erythropoietin, tissue plasminogen activator, interferon, and various hormones (Fukuda *et al.*, 1989; Smedsrod and Einarsson, 1990, Sareneva et al., 1993; Rao Thotakura and Blithe, 1995) depends on removal pathways which involve glycan recognition. In the case of erythropoietin, tissue plasminogen activator and sex hormone binding globulin, removal of glycan side-chains enhanced protein residence in the circulation of experimental animals (Fukuda *et al.*, 1989; Smedsrod and Einarsson, 1990; Cousin *et al.*, 1998). However, in most if not all of these cases, the appended glycans were either suboptimally sialylated, or consisted of high-mannose forms, and consequently served as excellent substrates for highly potent hepatic removal systems. The removal of glycans, as it was carried out in these studies, may serve therefore to evaluate the contribution of the specific glycan processing of these proteins to circulatory residence, rather than allow any definite conclusion regarding the role of glycan loading *per-se,* on circulatory retention. In this respect, these reported results are similar to those documented for glycosylation mutants of rHuAChE produced in the HEK-293 cell system, where addition of glycans had a clear adverse pharmacokinetic effect, due to the increase of pharmacokinetic unfavorable uncapped glycan termini (present study and (Kronman *et al.*, 1995)). In the present study, by ensuring optimal processing of the N-glycans and by maximizing other post-translation modifications, rHuAChE served to directly assess the effect of the actual number of N-glycans on its pharmacokinetic performance.

The improved pharmacokinetic performance exhibited by AChE carrying an increased number of appended N-glycans may be a consequence of one or more of the following phenomena: **(i)** interference with glomerular filtration, **(ii)** decreased susceptibility to plasma residing proteolytic enzymes and/or improved thermostability of the molecule conferred by surface-bound glycans, and **(iii)** a clearance-epitope masking effect exerted by glycan-promoted shielding,.

All the forms of rHuAChE under study possess a molecular weight greater than the kidney filtration cut-off threshold (approx, 70kDa, (Kanwar, 1984)) and therefore it is unlikely that N-glycosylation exerts its effect via prevention of kidney glomerular filtration. Furthermore, the addition of a single glycan (average MW=2.5 kDa) per enzyme subunit contributes insignificantly to the overall mass of the tetrameric molecule (MW>280 kDa). N-glycosylation introduces into the AChE molecule surface an increase in negative charge, due to the presence of the terminal sialic acid residues. This increase in the negative charge may also affect the elimination in the kidneys, yet we noted that a mutated version of rHuAChE in which seven negatively charged surface amino-acids have been replaced by neutral amino-acid moieties (Shafferman *et al.*, 1994) did not exhibit any variation in its pharmacokinetic performance (not shown), strongly suggesting that the surface charge does not play a significant role in the circulatory residence of AChE.

Table 18: Stability of rHuAChE glycoforms in murine plasma

Purified rHuAChEs (0.25-0.3 Units/ml) were incubated in the presence of murine plasma at 37°C. At the indicated time points, samples were examined for residual enzyme activity. Enzyme activity is expressed as percent of input activity measured immediately following enzyme dilution in plasma. Note that within the time range of 0.5-6 hrs, enzyme activity remained constant within experimental error, at levels similar to input values. Decrease in activity at 24 hrs. was similar for all rHuAChE glycoforms.

	Residual AChE activity (%) Time (hrs)						
AChE form	**0.5**	**1.0**	**2.0**	**3.0**	**4.0**	**6.0**	**24.0**
N350Q	95±3	96±3	95±4	97±3	95±4	97±3	70±8
WT	94±5	96±4	94±5	97±2	95±4	96±3	74±9
D61N	95±4	97±3	95±3	97±2	96±3	94±5	71±6
D61N /S541N	96±2	94±5	96±4	95±2	97±3	95±4	73±5

It is also unlikely that the observed effects of N-glycosylation reported here, are due to protection of the AChE molecule against deleterious proteolytic blood-borne activities, since incubation in murine plasma at 37°C of all the AChE glycoforms under study, did not result in any detectable loss of enzyme activity, within the time-frame relevant to pharmacokinetic profiling (Table 18). Moreover, even when prolonged *in-vitro* incubation in the presence of murine serum (≥24 hrs.), did have some effect on enzyme activity, it affected equally all the various AChE glycoforms.

The most likely interpretation of the observed pharmacokinetic improvement upon N-glycan addition is therefore, the masking of clearance epitopes. Such epitopes are exposed when glycosylation sites are removed, like in the case of the N350Q mutant which exhibits a pharmacokinetic behavior inferior to that of the wild-type enzyme regardless of its sialylation and oligomerization state (Fig. 31). It is worth noting that a possible involvement of amino-acid epitopes in the clearance rate of AChE has been suggested by the observation that fully sialylated and tetramerized human and bovine AChE, both of which carry four glycans per enzyme subunit, differ in their circulatory retention rate (MRT-human rAChE=1055min; MRT-

bovine rAChE=1340min, (Kronman *et al.*, 1995; Chitlaru *et al.*, 1998) and this report). These two versions of AChE differ in their primary amino-acid sequence only by 34 residues (Mendelson *et al.*, 1998); yet these residues are clustered in 3 divergence patches which are all located on the surface of the molecule, and therefore may form unique surface-related epitopes which might serve as ligands for protein removal. Furthermore, the existence of surface-related clearance epitopes was substantiated by the observation that a pharmacokinetically beneficial epitope-sheathing effect is promoted by polyethylene glycol conjugation to the widely dispersed lysine residues on the AChE surface (Cohen *et al.*, 2001).

It may therefore follow, that a further increase in the circulatory retention of the human version of AChE may be achieved by introducing additional N-glycosylation consensus signals to the tetraglycosylated rHuAChE at appropriate positions which will mask the surface-related epitopes which promote clearance. It should be noted that in the present study, addition of a fifth glycosylation site at position 541 (D61N/S541N rHuAChE), failed to provide any detectable pharmacokinetic advantage over the tetraglycosylated D61N rHuAChE (Table 17) It is possible that this position is situated at too far a distance from any circulatory elimination epitope and therefore cannot provide effective shielding. Further studies, which examine the pharmacokinetic effect of introduction of additional glycosylation sites in proximity to the human/bovine divergent amino-acid surface clusters, are presently being carried out at our laboratory.

The findings reported here have practical biotechnological implications with regard to the development of a prophylactic or post-exposure bioscavenger of OP poisons. The series of studies documented here and in previous reports (Kronman *et al.*, 1995, 2000; Chitlaru *et al.*, 1998) establish that at least three post-translation modifications, N-glycosylation, glycan sialylation and subunit assembly state, are involved in an hierarchical manner in determining the clearance rate of exogenously administered recombinant glycoproteins. The ability to modulate these three parameters by recombinant DNA engineering manipulations, may allow one to favorably tailor the circulatory residence times not only of AChEs, but also of other biomolecules with therapeutic potential.

VIII. Effect of Chemical Modification of Recombinant Human Acetylcholinesterase by Polyethylene Glycol on its Circulatory Longevity

INTRODUCTION

Acetylcholinesterase (AChE, EC 3.1.1.7) plays a pivotal role in the cholinergic system where it functions in the rapid termination of nerve impulse transmission. The high reactivity of the enzyme toward organophosphorus (OP) compounds, suggests that exogenous cholinesterase can serve as an effective therapeutic agent in the prophylaxis and treatment of OP-poisoning. Indeed the successful exploitation of the scavenging potential of administered cholinesterase has been demonstrated in rodents and in non-human primates (Wolfe *et al.*, 1987; Broomfield *et al.*, 1991; Doctor *et al.*, 1992; Maxwell *et al.*, 1992; Raveh *et al.*, 1993). The use of human AChE as an efficient bioscavenger has been advanced by the development of recombinant production systems (Kronman *et al.*, 1992; Lazar *et al.*, 1993; Fischer *et al.*, 1993) and the introduction of catalytically favorable mutations (Millard *et al.*, 1995; Ordentlich *et al.*, 1996; Shafferman *et al.*, 1996b,c; Hosea *et al.*, 1996). Yet, the short circulatory residence time of the various recombinant AChE (Kronman *et al.*, 1995; Saxena *et al.*, 1997, 1998; Mendelson *et al.*, 1998) preparations represents one of the factors which precludes the development of an efficient acetylcholinesterase-based recombinant bioscavenger, and the formulation of a method for the pharmacokinetic improvement of the enzyme is a major biotechnological challenge.

The circulatory fate of AChE is dictated by a delicate hierarchy of post-translation-related determinants (Kronman *et al.*, 1995, 2000; Chitlaru *et al.*, 1998, 2001). Pharmacokinetic studies showed that the concomitant oligomerization of AChE catalytic units and sialylation of AChE oligosaccharides exert a synergistic effect upon circulatory longevity of AChE. Based on these studies, circulatory short-lived recombinant AChEs (of human or bovine origin) can be converted into circulatory long-lived species by genetic engineering of the producer cells which brings about full sialylation of AChE together with biochemical treatment which induce tetramerization of the enzyme product (Chitlaru *et al.*, 1998, 2001; Kronman *et al.*, 2000). The observation that the successful alterations of protein size and surface significantly increased AChE circulatory residence, suggests that other modifications such as appendage of polymers by chemical modification of the protein surface may improve circulatory retention.

Several recombinant proteins have been exploited as potent therapeutic agents following the enhancement of their pharmacological performance by chemical modification of protein surface by natural or synthetic polymers (for review see Lundblad and Bradshaw, 1997; DeSantis and Jones, 1999). These include mainly polyethylene glycol (PEG), but also dextrans, heparin, albumin, polyvinylpyrrolidone and other polymers (for review see Monfardini and Veronese,

1988). PEG is the most widely used polymer for protein modification due to its lack of toxicity, the relatively simple chemistry required for its covalent binding to proteins, and its commercial availability. Abuchowski and coworkers (Abuchowski *et al.*, 1977) were the first to show that extension of circulatory residence of bovine liver catalase can be achieved by polyethylene glycol (PEG) conjugation. Since then, several studies demonstrated the therapeutic improvement of recombinant proteins by PEG-conjugation (e.g. Hershfield *et al.*, 1987; Knauf *et al.*, 1988; Clark *et al.*, 1996; Veronese *et al.*, 1996; Chapman *et al.*, 1999). It is believed that PEG attachment to proteins extends their circulatory residence through interference with protein removal pathways including kidney glomerular filtration, proteolytic degradation, as well as in active clearance via specific receptors (Harris, 1992; Zalipsky and Lee, 1992; Sakane and Pardridge, 1997). One of the limitations of protein PEG-conjugation is that it may lead to loss of biological activity (Monfardini and Veronese, 1998).

In view of the fact that AChE is one of the most efficient biocatalysts, with well characterized effects of various post-translational modifications on pharmacokinetic behavior (Kronman *et al.*, 1995, 2000; Saxena *et al.*, 1997, 1998; Mendelson *et al.*, 1998; Chitlaru *et al.*, 1998, 2001), it was interesting to use this promising therapeutic bioscavenger molecule as a target for studies of PEG modifications. Here we demonstrate, for the first time, the successful generation of PEG-conjugated rHuAChE, which fully retains its enzymatic activity and reactivity towards organophosphates. Most notably, the modification of HuAChE by PEG improves the pharmacokinetic properties of rHuAChE to the extent that its circulatory longevity surpasses all other known recombinant or native serum-derived forms of AChE.

MATERIALS AND METHODS

Generation of C-terminus truncated HuAChE, enzyme production and purification - Truncation of the C-terminus (a substitution of the last 40 amino acids with a pentapeptide, ASEAP) of the T-subunit of human AChE (Soreq *et al.,* 1990), was preformed by DNA cassette replacement (Shafferman *et al.,* 1992a), as described recently (Kryger *et al.,* 2000). The DNA coding sequences for the truncated HuAChE (ΔC-HuAChE) was inserted into a tripartite expression vector expressing also the reporter gene *cat* and the selection marker *neo* (Velan *et al.,* 1991; Kronman *et al.,* 1992). Generation of stably transfected HEK-293 cell lines expressing high levels of rHuAChE and purification of the secreted enzyme was performed as described previously (Velan *et al.,* 1991a; Kronman *et al.,* 1992).

MALDI-TOF analysis of glycans - N-glycans of ΔC-HuAChE (~100 μg protein) were purified, 2AB labeled and converted into their neutral methylated forms by methyl iodide esterification, as described previously (Kronman *et al.,* 2000). Mass spectra of 2AB-labeled esterified ΔC-HuAChE glycans were acquired on a Micromass TofSpec 2E reflectron time-of-flight (TOF) mass spectrometer. Samples of 1 μl of glycan samples diluted 1:10 in water were mixed with an equal volume of freshly prepared 2,5-dihydroxybenzoic acid (10mg/ml in 70% acetonitrile) and loaded onto the mass spectrometer target. Dried spots were recrystallized by adding 0.5 μl ethanol and allowed to dry again. Glycans were observed as $[M+Na]^+$ ions. 1 μl of peptide mixture (renin substrate, ACTH fragment 18-39, and angiotensin, 10 pMole/μl all from Sigma) which served as a three-point external calibrant for mass assignment of the ions, was mixed with freshly prepared α-cyano-4-hydroxycinnamic acid (10 mg/ml in 49.5% acetonitrile; 49.5% ethanol; 0.001% TFA), loaded on the mass spectrometer target and allowed to dry. All oligosaccharides were analyzed at 20 kV with a single-stage reflectron in the positive-ion mode. Between 100 and 200 scans were averaged for each of the spectra shown.

Sucrose density gradient centrifugation - Analytical sucrose density gradient centrifugation was performed on 5-25% sucrose gradients containing 0.1M NaCl/50mM sodium phosphate buffer pH 8.0. Centrifugation was carried out in an SW41 Ti rotor (Beckman) for 26h at 160000g. Fractions of 0.2 ml were collected and assayed for AChE activity. Alkaline phosphatase, catalase and β-galactosidase were used as sedimentation markers.

PEG-conjugation reaction and analysis of the products - Attachment of PEG chains to primary amines in rHuAChE was performed using succinimidyl propionate activated methoxy PEG (SPA-PEG; Shearwater polymers, Inc.). Purified ΔC-HuAChE (1-5μM) was incubated with PEG-5000 or PEG-20000 in 50mM phosphate buffer pH 8.0 for 2 hours at room temperature. There is a significant variance in the extent of the modification and the distribution of the modified products depending on the particular preparation of activated PEG used and the molar ratio of AChE to PEG in the conjugation reaction. A specific set of conjugation conditions and PEG preparation resulting in relatively homogenous products (no more than 3 differently PEG-conjugated forms) was chosen for this study. To generate the PEG-AChE conjugates analyzed in this study, PEG was added at a ratio of 5:1(low ratio) or 25:1 (high ratio) $[PEG]_0/[AChE\ primary\ amines]_0$. The modified products were dialyzed extensively against phosphate buffer saline (PBS). Samples of the proteins were resolved on 7.5% SDS-polyacrylamide gels, electrotransfered onto nitrocellulose and subjected to Western-blot analysis using mouse polyclonal anti-HuAChE antibodies (Shafferman *et al.*, 1992a).

Enzyme activity and reaction with inhibitors - AChE activity was measured according to Ellman *et al.* (Ellman *et al.*, 1961). Assays were performed in the presence of 0.5 mM acetylthiocholine, 50 mM sodium phosphate buffer pH 8.0, 0.1 mg/ml BSA and 0.3 mM 5,5'-dithiobis-(2-nitrobenzoic acid). The assay was carried out at 27°C and monitored by a Thermomax microplate reader (Molecular Devices). K_m values of HuAChE and PEG-HuAChE for acetylthiocholine were obtained from Lineweaver-Burk plots and k_{cat} calculations were based on active-site titration (Shafferman *et al.*, 1996a). Interactions of HuAChE or PEG-HuAChE with the AChE-specific inhibitors edrophonium, propidium, BW284C51, snake-venom toxin - fasciculin-II and with the organophosphate compound diisopropylfluorophosphate (DFP) were analyzed as described previously (Ordentlich *et al.*, 1996).

Pharmacokinetics - Clearance experiments in mice (3 to 6 ICR male mice per enzyme sample) and analysis of pharmacokinetic profiles were carried out as described essentially previously (Kronman *et al.*, 1995). The study was approved by the local ethical committee on animal experiments. Mice were injected with the various rHuAChE preparations (40μg/mouse in 0.2 ml PBS). Residual AChE activity in blood samples was measured and all values were corrected for background hydrolytic activity in the blood (using samples withdrawn 1 hour before performing the experiment). AChE activity values in samples removed immediately after injection were assigned a value of 100% and used for calculation of residual activity. Background cholinesterase levels in blood of pre-administered mice were less than 2 units/ml. The clearance patterns of the various enzyme preparations were usually biphasic and fitted to a bi-exponential elimination pharmacokinetic model ($C_t=Ae^{-k\alpha t}+Be^{-k\beta t}$) as described previously (Kronman *et al.*,

1995). This model enables determination of the parameters A and B which represent the fractions of the material removed from the circulation in the first-fast and second-slow elimination phases respectively, and $T_{1/2}\alpha$ and $T_{1/2}\beta$ which represent the circulatory half-life values of the enzyme in the fast and slow phases. The pharmacokinetic parameters MRT (mean residence time, which reflects the average length of time the administered molecules are retained in the organism) and CL (clearance, which represents the proportionality factor relating the rate of substance elimination to its plasma concentration (CL=dose/area under the concentration-time curve), were independently obtained by analyzing the clearance data according to a noncompartmental pharmacokinetic model using the WinNonlin computer program (Laub and Gallo, 1996).

RESULTS AND DISCUSSION

Selection of the HuAChE oligoform for study - AChE is found in multiple molecular forms that are the outcome of alternative splicing events and post-translational organization into multi-subunit structures (Velan *et al.,* 1991b). The recombinant wild type enzyme produced in various heterologous systems is comprised of a mixed population of oligomeric forms (monomers, dimers and tetramers) (Velan *et al.,* 1991b). Recently we have demonstrated that not only glycosylation and sialylation (Kronman *et al.,* 1995; Chitlaru *et al.,* 1998) but also the oligomerization state of the enzyme (Kronman *et al.,* 2000; Chitlaru *et al.,* 2001) plays an important role in determining its circulatory fate. Therefore, in order to assess the possible effects of chemical modification of rHuAChE by PEG on the longevity of the resulting modified enzyme it was essential to use homogenous preparations with respect to post-translation modification of both carbohydrates and subunit assembly. Accordingly we have selected a monomeric form of AChE (ΔC-HuAChE) devoid of the C-terminal sequences corresponding to residues 544-583. These sequences were replaced by the pentapeptide ASEAP, to generate a derivative of the H-subunit AChE (Fig. 32A; Kryger *et al.,* 2000). Since the ΔC-HuAChE form does not include the C-terminal cysteine (C580), which forms the interchain disulfide bonds between catalytic subunits (Velan *et al.,* 1991b), this enzyme preparation is monomeric. The use of ΔC-HuAChE for this study had additional potential advantages: a) Unlike the monomeric HuAChE C580A mutant, the truncated ΔC-HuAChE monomer does not carry the amphiphilic WAT domain (Simon *et al.,* 1998; Altamirano and Lockridge., 1999) involved in the *noncovalent* association of AChE subunits. This ensures that the ΔC-HuAChE monomeric enzyme preparation will not be contaminated with residual higher oligomeric form (Velan *et al.,* 1991b) and compare HuAChE C580A to ΔC-HuAChE in Fig. 32C); b) Since masking of a part of the surface of the enzyme by intersubunit interactions is not possible in ΔC-HuAChE we can expect that the entire surface of the enzyme will be accessible to PEG; c) The 3D structure of ΔC-HuAChE was recently determined by X-ray crystallography (Kryger *et al.,* 2000) permitting precise spatial localization of the potential lysine targets for PEG-conjugation (Fig. 32B); d). The truncated ΔC-HuAChE form contains only seven rather than ten lysines (see Fig. 32A). This could be useful in reducing the complexity of the population of PEG modified enzymes, and may be advantageous for future analysis.

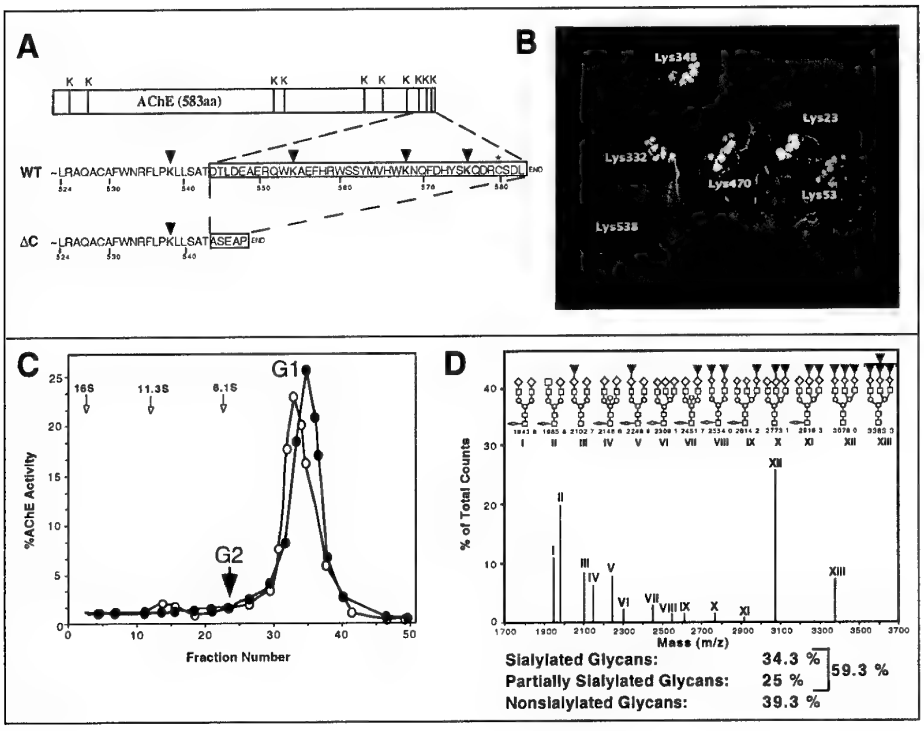

Figure 32: Generation and characterization of a C-terminus deleted recombinant version of HuAChE. **(A)** Schematic representation of distribution of lysine (K) along the HuAChE sequence and the C-termini sequences of the WT- and ΔC-rHuAChE forms. Lysine residues are marked by arrows and cysteine-580 in the WT form, responsible for intermolecular bridging is marked by an asterisk. Note the clustering of lysines at the C-terminus of WT-HuAChE. **(B)** Location of lysine residues within the three-dimensional structure of ΔC-HuAChE (Kryger *et al.*, 2000). **(C)** Sucrose-gradient sedimentation profiles of ΔC-rHuAChE (full circles) and C580A-rHuAChE (open circles). G1 – sedimentation position of the monomeric form of AChE; G2 - expected sedimentation position of the dimeric form. Arrows denote the sedimentation positions of the markers: alkaline phosphatase (6.1S), catalase (11.3S), and β-galactosidase (16S) included in the samples. **(D)** MALDI-TOF analysis of total N-glycans of ΔC- rHuAChE produced by HEK-293 cells. Purified N-glycans were subjected to 2-AB labeling and iodomethane-mediated esterification prior to MALDI-TOF analysis. Molecular weights represent monoisotopic masses of the respective $[M + Na]^+$ ions of the glycan species. Note that an increase of 14.015 Da of all glycan species occurs due to the methylation of the common 2-AB moiety. The abundance of sialylated partially sialylated and nonsialylated forms was calculated from the relative peak amplitude of each glycan form.

□GlcNac: ○ Man: ◇ β-Gal: ⌯ Fuc: ▼ sialic acid.

The gene encoding for the truncated enzyme (ΔC-HuAChE) was introduced into HEK-293 cells, and stably transfected cell clones producing high levels of the truncated enzyme were established as described previously (Kronman *et al.,* 1992; Velan *et al.,* 1991b). MALDI-TOF analysis of the N-glycans attached to the ΔC-HuAChE expressed in HEK-293, demonstrate that only 60% of the N-glycan are sialylated (Fig. 32D). Similar levels of partial sialylation were observed for other recombinant AChEs expressed at high levels in HEK-293 cells (Chitlaru *et al.,* 1988, 2001; Kronman *et al.,* 2000). The biological activity of ΔC-HuAChE is essentially identical to that of the wild-type enzyme as judged by the catalytic characteristics as well as its reactivity towards noncovalent or covalent active center or peripheral site ligands (Table 19 and Ordentlich *et al.,* 1996; Shafferman *et al.,* 1996b; Velan *et al.,* 1991).

Modification of ΔC-HuAChE by PEG - The amino-acid residues to which a PEG chain is attached is determined by the method used for the activation of the PEG precursor (Zalipsky, 1995; Francis *et al.,* 1998). For the studies described here we used succinimidyl-propionate activated methoxy-PEG. This monovalent version of activated PEG is directed to lysine residues and terminal amines, and forms a stable amide linkage with the conjugated protein. Inspection of the ΔC-HuAChE 3D structure reveals that all of its seven lysine residues are located on the enzyme surface (Fig. 32B). Only one of these lysines (Lys 348) is adjacent to the entrance to the 'catalytic gorge'. To generate modified AChE preparations differing in the number and in the size of attached PEG molecules, we tested various incubation conditions of ΔC-HuAChE with PEG-5000 or PEG-20000 (see Materials and Methods). Modulation of PEG attachment to AChE is possible by altering the reaction conditions (e. g. molar concentration, pH) and the molar ratio of activated PEG to AChE. Under certain conditions high PEG occupancy levels (multiplicity of up to 8 discrete forms, as judged by SDS-PAGE) can be achieved. However this entails a high level of heterogeneity, which complicates the accurate determination of the impact that the product size has on the pharmacokinetic performance. In this study, therefore, we chose a set of conjugation conditions which results in PEG-modified AChE-preparations that are characterized by a relatively high degree of homogeneity with respect to the number of different PEG-AChE products (no more than 3 differently PEG-conjugated species within one preparation, as judged by SDS-PAGE).

Fig. 33 demonstrates the unique migration pattern of discrete bands of the PEG-AChE products generated under the various conditions. At low or high molar ratios of PEG to primary ΔC-HuAChE amines used here (see Materials and Methods), a minimal mixture not exceeding 2-3 discrete polypeptide bands for reaction mixture was obtained. Incubation of the 66kDa ΔC-HuAChE molecule with PEG-5000 at the lower ratio of PEG to primary amines resulted in PEG-AChE products with apparent molecular weights of 84 and 98kDa (Fig. 33A Prep. A,

bands 1', 2') while incubation with the same PEG-5000 at a higher ratio of PEG to primary amines resulted in the generation of modified enzymes with an apparent molecular weight of 113 and 127kDa (Fig. 33A Prep. B, bands 3', 4'). These results indicate that increasing the PEG to AChE ratio leads to a higher level of lysine occupancy by PEG. Incubation of ΔC-HuAChE with PEG of higher molecular weight (PEG-20000) resulted in the generation of a similar ladder of larger products of 119, 160, 213 and 250 kDa where again the apparent molecular weight depended on the molar ratio of PEG to ΔC-HuAChE (Fig. 33A Prep. C and D).

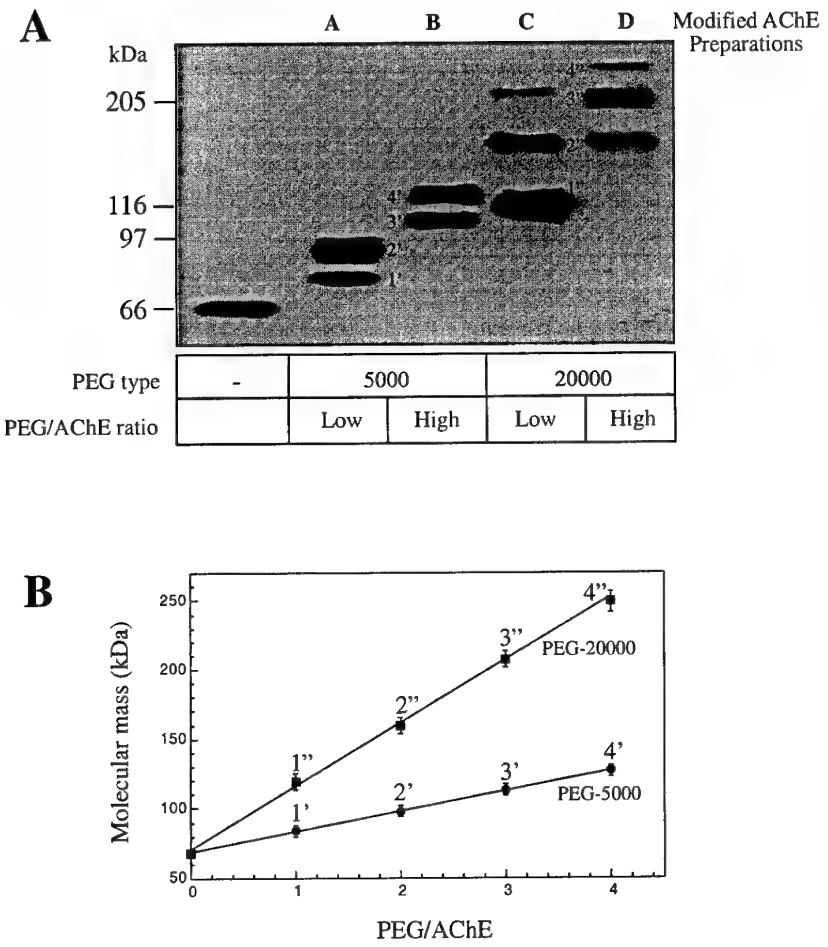

Figure 33: Analysis of PEG-AChE products. HuAChE was modified by PEG–5000 or PEG–20000 as indicated, at two PEG:AChE primary amines ratios (preparations A, C –low ratio; B, D – high ratio) **(A)** Western blot analysis of PEG-HuAChE preparation (A-D) using mouse polyclonal anti-HuAChE antibodies. Individual bands depicted in these preparations are marked 1'-4' for AChE-PEG-5000 and 1"-4" for AChE-PEG-20000. **(B)** Correlation between the apparent molecular weight of each of the individual PEG-AChE products and the expected number of PEG units attached per AChE molecule. (determined from three independent experiments; correlation coefficients > 0.99).

The apparent molecular weights of the individual products in each preparation appear to differ from their nearest neighbors by similar mass units. For example, the increase in molecular weight between band 1' and 2' is similar to the apparent mass increase between polypeptides 2' and 3' or between 3' and 4' (Fig. 33). This is also the case for the products that were generated using PEG-20000 (bands 1" to 4" in Fig. 33). This uniform discrete increase in mass between neighboring bands on a gel is interpreted as a progressive attachment of single PEG subunits (Fig. 33B). Accordingly, under these conditions, the number of PEG units conjugated to each AChE molecule can vary between 1 to 4 in correlation with the initial ratio of PEG to AChE in the reaction mixture, independently of the size of the PEG used. We note that PEG-conjugation under different conditions can generate less homogenous AChE preparations with more than 4 PEG units attached per HuAChE molecule (see Materials and Methods). It is not unlikely that under the conditions selected for study, the PEG appendage occurs preferentially at some modification–prone sites (see below). Indeed, the phenomenon of incomplete PEG-conjugation of all potential targets on proteins, under various conditions, is quite common (Davis *et al.*, 1981; Knauf *et al.*, 1988; Clark *et al.*, 1996; Veronese *et al.*, 1996). In a recent study by Clark and coworkers (Clark *et al.*, 1996) PEG-conjugation of the growth hormone did not exceed 70% occupancy of the potential attachment sites. While some of the sites of the growth hormone are more reactive than others, a well defined correlation between reactivity to PEG and the surface accessibility of the amino acids or their involvement in intramolecular interactions could not be established.

Enzymatic characterization of PEG-HuAChE molecules - A major problem associated with PEG-modification of proteins is that in many instances it leads to loss of biological activity. For example, loss of 72% and 92% of catalytic activity was documented for PEG-adenosine deaminase and PEG-asparaginase, respectively (Davis *et al.*, 1981; Kamisaki *et al.*, 1981). The deleterious effect of PEG modification on activity is believed to be mainly attributed to the attachment of the PEG chains at critical sites on the target molecule, but also to other factors such as harsh coupling condition or modification of surface charge at the attachment site. To assess the effect of PEG modification on ΔC-HuAChE, detailed kinetic studies were performed with enzyme modified with the larger PEG moiety (PEG-20000; Preparations C and D; Fig. 33A). The K_m and the k_{cat} values of the modified enzymes were indistinguishable, within the experimental error, from those of the non-modified enzyme (Table 19). Likewise, the inhibition constants (K_i) for the classical non-covalent active-site inhibitor edrophonium or the covalent organophosphate DFP were similar to those of the nonmodified AChE (Table 19). It was quite interesting to find that even ligands such as propidium, and the bis-quaternary inhibitor BW284C5, that bind to the peripheral anionic site at the entrance to the active site gorge (Shafferman *et al.*, 1992b; Barak *et al.*, 1994; Radic *et al.*, 1994; Masson *et al.*, 1996; Rosenbary *et al.*, 1996), displayed an affinity to the highly PEG-conjugated HuAChE similar to that of nonmodified HuAChE (Table 19). Likewise, the substrate inhibition constant K_{ss}

representing the dissociation of a second substrate from the peripheral site (Shafferman *et al.*, 1992b; Barak *et al.*, 1994; Radic *et al.*, 1994; Masson *et al.*, 1996; Rosenbary *et al.*, 1996), of the PEG-ΔC-HuAChE and of the nonmodified enzyme were similar (Table 19). Remarkably, modification of the lysine residues by PEG-conjugation did not affect the affinity of the 'three-finger' peptide snake-venom fasciculin-II, which binds tightly to the peripheral site of AChE and occludes the portal of the active center gorge (Table 19). Unlike the other peripheral inhibitors (e.g. propidium or BW284C5) which are small molecules, fasciculin is a bulky polypeptide of 61 amino-acids and its attachment to HuAChE involves extensive surface contacts, as recently elucidated from the X-ray crystallography of the ΔC-rHuAChE /fasciculin-II complex (Kryger *et al.*, 2000). The fact that binding of fasciculin to AChE is not impaired by PEG implies that the long PEG chains do not wrap around the enzyme, but rather remain in an extended configuration. It should be noted, that one of the seven ΔC-rHuAChE lysine residues, Lys348, is located within the HuAChE surface interaction domain of fasciculin-II (Kryger *et al.*, 2000). Since PEG-conjugation, under the conditioned used, does not appear to reduce fasciculin-II binding it is possible that this particular lysine residue does not readily serve as a substrate for PEG modification. It may be interesting to note that Lys348 is located in close proximity to the N-glycosylation site Asn350. Altogether, it appears that PEG-conjugation of ΔC-HuAChE, can be compatible with maintenance of full enzymatic activity with no apparent effect on reactivity toward various ligands or on the scavenging potential of toxic agents exemplified by the organophosphate diisopropylfluorophosphate (DFP).

Table 19: Comparison of catalytic properties and inhibition constants towards various inhibitors of non-modified and PEG-modified ΔC-AChE*

		AChE Preparations		
		Non-Modified	**Prep. C** (PEG-20000 low ratio)	**Prep. D** (PEG-20000 high ratio)
Kinetic parameters	K_m (mM)	0.09±0.01	0.09±0.01	0.09±0.01
	k_{cat} (10^5 x min^{-1})	3.9±0.2	4.0±0.2	3.9±.01
	k_{app}(10^8 x $M^{-1}min^{-1}$)	43±2	44±4	43±3
	K_{ss} (mM)	9±2	6±2	10±3
Inhibition Constants	**Edrophonium** (K_i ,μM)	0.8±0.2	0.8±0.2	0.8±0.2
	Propidium (K_i ,μM)	1.0±0.3	0.6±0.2	0.7±0.3
	BW284C51 (K_i ,nM)	8±1	10±2	6±1
	Fasciculin (K_i ,nM)	0.8±0.1	0.7±0.2	1.1±0.3
	DFP (k_i, 10^{-4} x $M^{-1}min^{-1}$)	57±4	58±3	51±2

* Values are means ± S.D. for at least three independent experiments

Pharmacokinetic behavior of PEG-HuAChE - The pharmacokinetic characteristics of the different PEG-AChE preparations (Fig. 34A and Table 20) clearly demonstrate that in all cases circulatory residence is significantly improved by PEG conjugation. The most pronounced effect was observed following modification of ΔC-HuAChE with either PEG-5000 or PEG-20000 at the higher PEG to AChE ratio (Prep B and Prep D respectively; Fig. 34A). In the latter case, the MRT was 50 times longer than that of the non-modified enzyme (2100 min. and 42 min. respectively; Table 20). Such a high MRT value in ICR mice, exceeds by far any previously reported value for any type of AChE or BChE molecules from either recombinant, native or serum derived origin (the maximal MRT values for serum derived human BChE, horse BChE or the fetal bovine AChE is about 1400 min ; Kronman *et al.*, 1995; Saxena *et al.*, 1997b).

Table 20: Pharmacokinetic parameters of non-modified and PEG-modified AChEs

	Pharmacokinetic parameters					
AChE Preparations	**A** (% of total)	**$T_{1/2}\alpha$** (min)	**B** (% of total)	**$T_{1/2}\beta$** (min)	**Clearance** (ml/hr/kg)	**MRT** (min)
Non-modified	74±8	3.6±0.6	26±2	44±3	170.4	42±3
Prep. A (PEG-5000 low ratio)	56±9	29±6	43±3	390±50	14.2	510±70
Prep. B (PEG-5000 high ratio)	46±3	28±5	64±3	540±70	13.2	740±80
Prep. C (PEG-20000 low ratio)	35±3	32±5	65±5	750±130	12	950±120
Prep. D (PEG-20000 high ratio)	23±4	35±15	76±3	1550±120	4.3	2100±200

The circulatory clearance profiles of the various AChEs were determined as described ("Materials and Methods"). A, B, $T_{1/2}\alpha$ and $T_{1/2}\beta$ represent the fractions of the material removed from the circulation and half-life values of the first (fast) and second (slow) decay phases, respectively. In all cases, the correlation coefficient was > 0.99. The clearance curves were also analyzed by fitting to a noncompartmental pharmacokinetic model for the calculation of Mean Residence Time (MRT) and Clearance using a Window-based program.

It appears that the extension of circulatory longevity by PEG-conjugation can be attributed both to the number and size of PEG subunits attached to the enzyme. In an attempt to determine the quantitative relationship between the MRT and the molecular weight of the PEG-modified enzyme we computed the "average" apparent molecular weight for each of the preparations. To this end we determined the relative abundance of PEG-conjugated products in a given preparation by subjecting its SDS-PAGE western blots profile to densitometric analysis. For example, preparation A (Fig. 33A) is composed of two products with apparent molecular weights of 84kDa and 98kDA. The larger product comprises 73% of the preparation, and the number of PEG molecules attached to each product according to Fig. 33B, allows us to determine that the "average" apparent molecular weight of the preparation is 94 KDa, with an average number of 1.7 attached PEG units to ΔC-HuAChE molecule. In the same way, the "average" apparent molecular weight and the average number of PEG for preparation B, C and D was determined to be 120kDa /3.5, 138kDa/1.5 and 203kDa/2.9 respectively. Using these computed "average" values we find (Fig. 34B) that the MRT is linearly dependent on the *overall* apparent molecular weight of the PEG-conjugated-HuAChE preparation. The finding of

the linear relationship in Fig. 34B suggests that the factor determining the circulatory time of AChE, is not the number of the modified sites *per se* but the actual increase in molecular size as a consequence of the PEG-conjugation. Thus, it appears that in principle attachment of a single very large PEG unit to HuAChE may be as efficient as PEG-conjugation of all potential lysines by smaller PEG subunits.

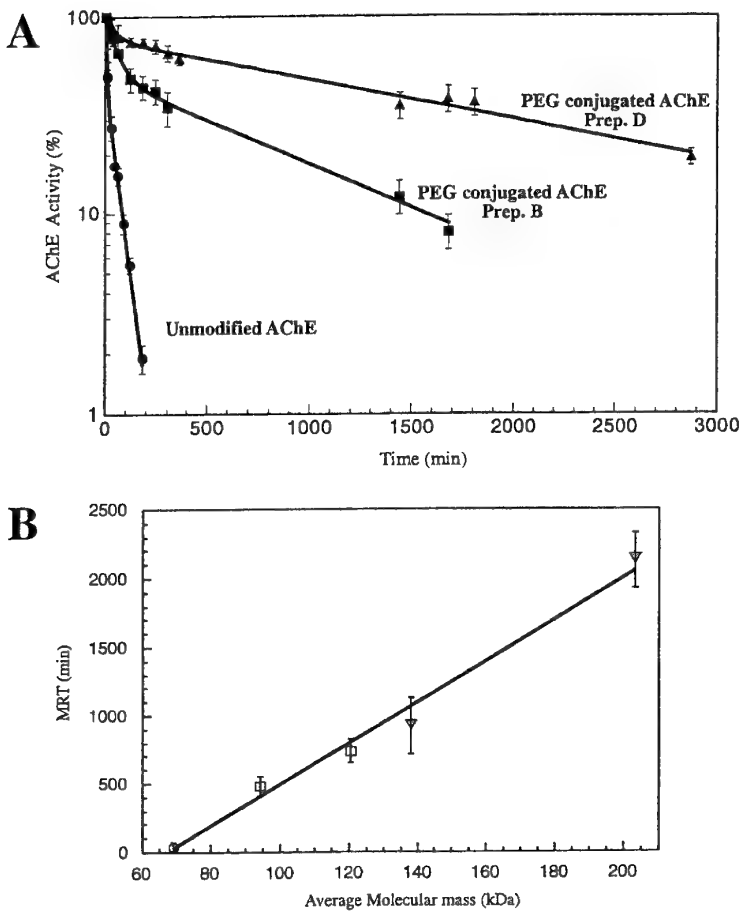

Figure 34: Pharmacokinetic profiles of non-modified and PEG-modified AChE. (A) Clearance profiles of non-modified AChE (ΔC-rHuAChE), AChE modified by PEG-5000 (Prep. B) or PEG-20000 (Prep. D). The various exogenous rAChEs were introduced into mice at levels that are at least 30-fold higher than background level (see methods for details). **(B)** Correlation of the mean residence time (MRT) and the "average" molecular weight of the PEG-AChE preparation. Circle - non-modified HuAChE, squares-HuAChE-PEG-5000 preparations A,B and triangles – HuAChE-PEG-20000 preparations C,D. The MRT values of the various preparation (Table 20) was plotted against the calculated (see text for details) "average" apparent molecular weight of each preparation (correlation coefficient was 0.991).

Several studies with superoxide dismutase addressed the issue of the effect of size and number of PEG modifications on the pharmacokinetics. While some of these studies argued that the number of PEG molecules linked to SOD has an important role in its pharmacokinetic performance (Boccu *et al.,* 1982), other studies showed that the predominant factor is the molecular size of the modified enzyme (Nakaoka *et al.,* 1997). Another study documented that the circulatory residence time of PEG-modified-interleukin-2 correlates with the size of the modified proteins rather than with the number of PEG molecules attached (Knauf *et al.,* 1998). Our study clearly shows that in the case of recombinant HuAChE, the principal determinant that governs the improvement in the circulatory profile of PEG-HuAChE proteins is their overall size. Although a direct correlation was observed between circulatory residence time and molecular size of PEG-HuAChE, one should be careful in concluding that this linear relationship will be maintained for PEG-HuAChE molecules with further higher levels of PEG occupancy than that tested here.

One of the more striking findings of this work is that a very substantial extension in circulatory residence could be achieved even with the *partially* sialylated ΔC-HuAChE and furthermore that such an extension can be achieved by the attachment of a relatively limited number of PEG molecules. Recently, we have shown that while oligomerization can increase circulatory MRT of recombinant human or bovine AChE, the MRT values depend on a delicate interplay between oligomerization and the extent of glycan variability (Kronman *et al.,* 2000; Chitlaru *et al.,* 2001). Thus the completely desialylated tetramers, dimers or monomers of HuAChE had very short MRTs (~3.5 min). The partially sialylated (60% sialylated N-glycan termini) monomeric ΔC-HuAChE (66kDa), dimeric (130kDa) and tetrameric (~ 260kDa) HuAChE display MRT values of 42, 102 and 190 min, respectively (Table 20 and Kronman *et al.,* 1995; Chitlaru *et al.,* 2001). On the other hand the fully sialylated tetramers and dimers of HuAChE had MRTs of 700 min and 190 min, respectively. It was therefore quite unexpected that limited PEG-conjugation of the *partially* sialylated ΔC-HuAChE (resulting in "average" apparent molecular weights of 94kDa or 138kDa (preparations A and C)) exhibit high MRTs of 500 to 900 minutes. This is even more striking in view of the fact that these MRTs are in the same range as those determined for the much larger tetramers in their *fully* sialylated form. These results suggest that PEG-conjugation can compensate in a very efficient manner for both oligomerization and more significantly, also for undersialylation. This observation can be exploited to overcome one of the main hurdles for generating recombinant human AChE as a therapeutic drug with extended longevity.

IV. KEY RESEARCH ACCOMPLISHMENTS

1. Development of a method for analysis of OP-AChE active center peptide conjugates by Matrix Assisted Laser Desorption/Ionization-Time of Flight Mass Spectrometry (MALDI-TOF/MS).

2. Determination of the interactions of phosphoroamidate OP-agents with the AChE active center, through kinetic studies with rHuAChE and various mutants combined with mass spectrometric analysis of the respective adducts.

3. Demonstration that the "aging" of AChE conjugates with tabun and its derivatives proceeds through replacement of the dialkylamine at the phosphyl moiety. These studies demonstrated that while AChE adducts with phosphonates and phosphoroamidates are similar the respective aging mechanisms are different and involve somewhat different participation of the active center catalytic elements.

4. Demonstration that multiple replacements of aromatic residues at the HuAChE active center alter the molecular architecture in a predictable manner. Namely, replacement of the 6 aromatic residues distinguishing the active center of HuAChE from that of HuBChE yielded mutant HuAChE with noncovalent binding characteristics similar to those of HuBChE.

5. Evidence of involvement of aromatic residues in the HuAChE active center in stabilization of the functional juxtaposition of the catalytic triad.

6. Determination (by extensive lectin analysis in conjunction with exoglycosidase trimming) that rHuAChE carries at most very low amounts of appended O-glycan side-chains, not exceeding 1-2 O-glycans units per 30 enzyme subunit molecules. Demonstration by MALDI-TOF analysis of rHuAChE tryptic digest products, that threonine 504 does not serve as a site for O-glycan appendage. These findings provide evidence that O-glycosylation does not play any significant role in determining the pharmacodynamic properties of human acetylcholinesterase.

7. Establishment of a reproducible and quantitative method for structural analysis of the entire array of N-glycans appended to cholinesterase enzymes, by MALDI-TOF/MS.

8. Demonstration of a high degree of similarity between the backbone structures of the glycans of native and recombinant bovine acetylcholinesterase, and a significant difference in their

glycan capping by α-galactose and sialic acid residues. Terminal α-galactose are totally absent from recombinant enzyme.

9. Pharmacokinetic profiling of different species of the enzyme, together with MALDI-TOF analysis of the N-glycans in conjunction with directed deglycosylation of specific terminal monosaccharides determined that capping by sialic acid, but not α-galactose, contributes to the circulatory residence of bovine cholinesterases.

10. Establishment of a method for the selection of individual genetically engineered cell clones which exhibit high levels of recombinant sialyltransferase activity, based on a solid-phase *S. nigra* agglutinin lectin-binding detection system. This method allowed the selection of a recombinant HEK-293-based cell clone expressing high levels of sialyltransferase, which can serve for the coexpression of bovine or human cholinesterase, as well as other recombinant proteins.

11. Determination by pharmacokinetic analysis that highly sialylated recombinant enzyme produced by the sialyltransferase-expressor cell clone, resides in the circulation for longer periods of time than non-modified partially sialylated rBoAChE.

12. Development of a quantitative method for the *in-vitro* assembly of recombinant bovine acetylcholinesterase enzyme subunits into tetramers, using a synthetic peptide containing the human ColQ Proline Rich Attachment Domain.

13. Generation of an array of different forms of recombinant bovine acetylcholinesterase, differing both in their levels of glycan sialylation and subunit assembly (monomers, dimers tetramers), with mean circulatory residence times ranging from 3.5 minutes up to 1390 minutes. These studies established the hierarchical nature of the post-translation-related factors which determine the pharmacokinetic behavior of cholinesterases, and served as a basis for the generation of a recombinant product displaying a pharmacokinetic profile which is indistinguishable from that of native serum cholinesterase.

14. Generation of an array of different forms of recombinant human acetylcholinesterase, differing both in their levels of glycan sialylation and subunit assembly (monomers, dimers tetramers), with mean circulatory residence times ranging from 3.6 minutes up to 740 minutes. These studies established that the circulatory retention of the human AChE is governed in an hierarchical manner by the same set of post-translation-related factors which determine the pharmacokinetic behavior of bovine AChE.

15. Generation of an array of glycosylation-mutants of recombinant human acetylcholinesterase, displaying different numbers (2,3,4, or 5) of appended N-glycans, as well as differing in their levels of glycan sialylation and subunit assembly (monomers, dimers tetramers). These studies established the contribution of glycan loading to the circulatory longevity of human AChE which may display a mean residence time value of up to 1055 minutes in the case of overglycosylated fully-sialylated tetramerized forms of the enzyme.

16. Generation of chemically modified recombinant human acetylcholinesterase carrying polyethylene-glycol (PEG) side-chains attached to lysine residues. These studies established that the chemical modification of the enzyme allows its long-term residence within the circulation, and that at a ratio of 4:1 of attached PEG to :rHuAChE, a mean residence time value of over 2,100 minutes is attained, exceeding the circulatory retention values of any other known form of recombinant or native serum-derived AChE reported to date. This study allowed us to determine that AChE PEGylation can efficiently compensate for suboptimal oligomerization or sialylation of the enzyme, and may therefore serve as a basis for the development of a therapeutically efficient recombinant human AChE-based OP bioscavenger.

V. REPORTABLE OUTCOME

List of publications of full papers related to the current contract

Kronman, C., Chitlaru, T., Elhanany, E., Velan, B. and Shafferman, A. (2000). Hierarchy of post-translation modifications involved in the circulatory longevity of glycoproteins: Demonstration of concerted contributions of glycan sialylation and subunit assembly to the pharmacokinetic behavior of bovine acetylcholinesterase. *J. Biol. Chem.* **275**, 29488-29502

Kryger, G., Harel, M., Giles, K., Toker, L., Velan, B., Lazar. A., Kronman, C., Barak, D., Ariel, N., Shafferman, A., Silman, I. and Sussman, J.L. (2000). Structures of recombinant native and E202Q mutant human acetylcholinesterase complexed with the snake-venom toxin fasciculin-II. *Acta Cryst.* **D56**,1385-1394

Barak, D., Ordentlich, A., Kapaln, D., Barak, R., Mizrahi, D., Kronman, C., Segall, Y., Velan, B. and Shafferman, A. (2000). Evidence for P-N bond scission in phosphoroamidate nerve agent adducts of human acetylcholinesterase. *Biochemistry*, **39**, 1156-1161

Malany, S., Sawai, M., Sikorski, R.S., Seravalli, J., Quinn, D.M., Radic, Z., Taylor, P., Kronman, C., Velan, B. and Shafferman, A. (2000). Transition state structure and rate determination for the acylation stage of acetylcholinesterase catalyzed hydrolysis of (acetylthio)choline. *J. Am. Chem. Soc.*, **121**, 9883-9884

Chitlaru, T., Kronman, C., Velan, B. and Shafferman, A. (2001). Effect of human acetylcholinesterase subunit assembly on its circulatory residence. *Biochem. J.* **354**, 613-625.

Cohen, O., Kronman, C., Chitlaru, T., Ordentlich, A., Velan, B. And Shafferman, A.(2001) Effect of chemical modification of recombinant human acetylcholinesterase by polyethylene glycol generates an enzyme with exceptional circulatory longevity. *Biochem. J.* **357**, 795 802.

Elhanany, E., Ordentlich, A., Dgany, O., Kaplan, D., Segall, Y., Barak, R., Velan, B. and Shafferman, A. (2001). Resolving pathways of interaction of covalent inhibitors with the active site of acetylcholinesterases: MALDI-TOF/MS analysis of various nerve agent phosphyl adducts. *Chem. Res. Toxicol.*, **14**, 912-918.

Kaplan, D., Ordentlich, A., Barak, D., Ariel, N., Kronman, C., Velan, B. and Shafferman, A. (2001). Does "butyrylization" of acetylcholinesterase through substitution of the six divergent

aromatic amino acids in the active center gorge generate an enzyme-mimic of butyrylcholinesterase. *Biochemistry,* **40**, 7433-7445.

Chitlaru, T., Kronman, C., Velan, B. and Shafferman, A. (2002). Overloading and removal of N-glycosylation targets on human acetylcholinesterase - effects on glycan composition and circulatory residence time. *Biochem. J.,* **363**, 619-631.

Shafferman, A., Barak, D., Ordentlich, A., Ariel, N., Kronman, C., Kaplan, D. and Velan, B. (2002). Structural and functional correlates of human acetylcholinesterase mutants for evaluation of Alzheimer's disease treatments. *Mapping and Progress of Alzheimer's and Parkinson's Disease*, Eds. Mizuno, Y. , Fisher, A. and Hanin, I. (Plenum Publishing Corp.) **51**, 187-192.

Shafferman, A., Ordentlich, A., Barak, D., Kronman, C., Ariel, N., Chitlaru, T., Mendelson, I., Marcus, A., Lazar, A., Segall, Y. and Velan, B. (2002). Bioengineering of optimal hydrolytic and pharmacodynamic properties into recombinant AChE OP-bioscavengers. *Proceedings of Medical Defense Bioscience Review,* Published on CD.

Sussman, J.L., Millard, C.B., Gillilan, R.E., Koellner, G., Kryger, G., Harel, M., Greenblatt, H.M., Ordentlich, A., Barak, D., Shafferman, A. and Silman, I. (2002). Crystal structures of conjugates of AChE with nerve agents at atomic resolution. *Proceedings of Medical Defense Bioscience Review,* Published on CD.

Shafferman, A., Chitlaru, T., Ordentlich, A., Velan, B. and Kronman, C. (2002). A complex array of post-translation modifications determines the circulatory longevity of AChE in a hierarchical manner. *Cholinergic Mechanisms*. In press.

Chitlaru, T., Kronman, C., Lazar, S., Zeliger, N., Velan, B. and Shafferman, A. (2002). Effect of post-translation modifications of human acetylcholinesterase on its circulatory residence. *Cholinergic Mechanisms*. In press.

Cohen, O., Kronman, C., Chitlaru, T., Ordentlich, A., Velan B. and Shafferman A. (2002). Generation of pharmacokinetically improved recombinant Human Acetylcholinesterase by polyethylene glycol modification. *Cholinergic Mechanisms*. In press.

Elhanany, E., Ordentlich, A., Dgany, O., Kaplan, D., Segall, Y., Barak, R., Velan, B. and Shafferman, A. (2002). MALDI-TOF/MS analysis of tabun-AChE conjugate: A tool for resolution of "aging" pathway. *Cholinergic Mechanisms*. In press.

Kaplan, D., Ordentlich, A., Barak, D., Ariel, N., Kronman, C., Velan B. and Shafferman, A. (2002). Attempts to engineer an enzyme-mimic of Butyrylcholinesterase by substitution of the six divergent aromatic amino acids in the active center of AChE. *Cholinergic Mechanisms*. In press.

Kronman, C., Chitlaru, T., Zeliger, N., Lazar, S., Lazar, A., Zilberstein, L., Velan, B. and Shafferman, A. (2002). Some basic rules governing oligosaccharide-dependent circulatory residence of glycoproteins are revealed by MALDI-TOF/MS mapping of the multiple N glycans associated with recombinant bovine acetylcholinesterase . *Cholinergic Mechanisms*. In press.

Ordentlich, A., Barak, D., Ariel, N., Kronman, C., Kaplan, D., Velan, B. and Shafferman, A. (2002). Surprising findings from the functional analysis of Human AChE adducts of Alzheimer's disease drugs. *Cholinergic Mechanisms*. In press.

List of publications of abstracts and presentations related to the current contract

Barak, D., Ordentlich, A., Kronman, C., Ariel, N., Segall, Y., Velan, B. and Shafferman, A. (2000). Site directed mutagenesis of the oxyanion hole residues unravels the unique AChE structural features contributing to the enzyme affinity towards OP-agents. In: *Bioscience 2000 Abstract Book* p.27.

Chitlaru, T., Kronman, C., Seliger, N., Lazar, A., Zilberstein, L., Velan, B. and Shafferman, A. (2000). A general method for screening cell lines for glycosyltransferase activities and its application for the conversion of recombinant bovine acetylcholinesterase to its fully sialylated form. In: *Bioscience 2000 Abstract Book* p. 30.

Kronman, C., Chitlaru, T., Seliger, N., Lazar, A., Zilberstein, L., Velan, B. and Shafferman, A. (2000). Some basic rules governing oligosaccharide-dependent circulatory residence of glycoproteins are revealed by MALDI-TOF mapping of the multiple N-glycans associated with recombinant bovine AChE. In: *Bioscience 2000 Abstract Book* p. 38.

Ordentlich, A., Barak, D., Kaplan, D., Barak, R., Mizrahi, D., Kronman, C., Segall, Y., Velan, B. and Shafferman, A. (2000). Formation and aging of human AChE conjugates with tabun: new mechanistic insights. In: *Bioscience 2000 Abstract Book* p. 45.

Ordentlich, A., Barak, D., Kronman, C., Benschop, H.P., De Jong, P.A., Ariel, N., Barak, R., Segall, Y., Velan, B. and Shafferman, A. (2000). Lessons learned by use of stereomers of soman - an organophosphate inhibitor with two chiral centers on the functional architecture of human acetylcholinesterase. In: *Bioscience 2000 Abstract Book* p. 46.

Chitlaru, C., Kronman, C., Zeliger, N., Lazar, S., Velan, B. and Shafferman, A. (2001). Generation of a pharmacokinetically improved recombinant version of acetylcholinesterase by modulations of post-translation protein processing. *International Symposium on Applications of Enzymes in Chemical and Biological Defense Abstract Book*, p. 23-24

Kronman, C., Chitlaru, T., Elhanany, E., Velan, B. and Shafferman, A. (2001). Glycan composition analysis of acetylcholinesterase by MALDI-TOF: Implications for improvement of its pharmacokinetic behavior. In: *The 66th meeting of the Israel Chemical Society Abstract Book,* p. 125

VI. CONCLUSIONS

Understanding reaction pathways of phosphylation, reactivation and 'aging' of AChE with toxic organophosphate compounds, is both a biochemical and pharmacological challenge. While AChE adducts with phosphonates and phosphates are known to age through scission of the alkoxy C-O bond, the aging path for adducts with phosphoroamidates (P-N agents) like the nerve agent N,N-dimethyl-phosphoncyanoamidate (tabun), is not clear. Here we report that conjugates of tabun and of its butyl analog (butyl-tabun) with the E202Q and F338A human AChEs (HuAChEs), age at similar rates to that of the wild type enzyme. This is in marked contrast to the large effect of these substitutions on the aging of the corresponding HuAChE adducts with phosphates and phosphonates, suggesting that a different aging mechanism may be involved. Both tabun and butyl-tabun appear to be similarly accommodated in the active center, as suggested by molecular modeling and by kinetic studies of phosphylation with a series of HuAChE mutants (E202Q, F338A, F295A, F297A, F295L/F297V). Electrospray ionization mass spectrometric analysis (ESI-MS) of the aging process of HuAChE adducts with the two P-N agents, shows for both cases a mass decrease of 28±4 Da. Due to the nature of the alkoxy substituent such mass decrease can be unequivocally assigned to loss of the dimethylamino group for the butyl-tabun conjugate. For the corresponding tabun conjugate, the macromolecular products of the two possible aging pathways differ only by 1 Da, and therefore could not be unequivocally characterized by the ESI-MS method. A more sensitive mass detection method - Matrix Assisted Laser Desorption Ionization Mass Spectrometry (MALDI-TOF/MS) was applied. Tryptic digests of phosphylated *Torpedo californica* AChEs, ZipTip peptide fractionation and MALDI-TOF/MS analysis enabled reproducible signal enrichment of the isotopically resolved peaks of organophosphoroamidate-conjugate of the AChE active site Ser peptide. The results unequivocally demonstrate, for the first time, that the pathway of tabun adducts of AChEs proceeds through P-N bond scission.

In the past we have demonstrated that modifications of functional subsites like the H-bond network, the acyl pocket, the aromatic patch or the oxyanion hole, have specific effects on phosphylation and aging, either enhancing or diminishing the OP-scavenging capacity of the modified enzyme. Correlation of these effects with respect to certain OP-agents showed an overlap between functional trends due to specific modifications. One of the practical implications of such analyses, with respect to design of future scavenger, could be that modification of the acyl pocket may be combined with other replacements at the active center to further enhance the OP-scavenging potential. A blueprint for assessing the contributions of multiple aromatic replacements, combined with those at the acyl pocket (Phe295, Phe297), was provided by the different amino acid composition of the gorge linings in AChE and BChE, since the two enzymes exhibit similar reactivity toward ACh as well as toward various OP-

agents. To investigate how this particular structural variability affects reactivity of the respective HuAChEs toward OP-agents, gradual replacement of up to all the 6 aromatic residues in HuAChE by the corresponding residues in HuBChE, was carried out.

For most of the prototypical noncovalent active center and peripheral site ligands, like tacrine edrophonium or BW284C51, the hexa-mutant HuAChE displayed a reactivity phenotype closely resembling that of HuBChE. These results support the accepted view that the active center architectures of AChE and BChE differ mainly by the presence of a larger void space in BChE, Nevertheless, reactivity of the hexa-mutant HuAChE toward the substrates acetylthiocholine and butyrylthiolcholine, and OP-agents like soman IBMPF and DFP is about 45-170-fold lower than that of HuBChE. Most of this reduction in reactivity can be related to the combined replacements of the three aromatic residues at the active center - Phe295, Phe297, Tyr337.We propose that the hexa-mutant HuAChE, unlike BChE, is impaired in its capacity to accommodate certain tetrahedral species in the active center. This impairment may be related to the enhanced mobility of the catalytic histidine His447, which is observed in molecular dynamics simulations of the hexa-mutant and the F295L/F297V/Y337A HuAChE enzymes but not in the wild type HuAChE. Evidently such conformational destabilization of His447 should be avoided in further design of OP-bioscavenger through concerted perturbations of the HuAChE active center functional architecture.

The use of rHuAChE as a therapeutic bioscavenger of organophosphorus agents, is impeded by its relatively rapid clearance from the circulation, as compared to native serum-derived cholinesterases. Effective exploitation of the bioscavenging potential of rHuAChE therefore requires the generation of a modified version of the enzyme exhibiting extended circulatory residence.

Previous studies have established that increasing the sialylation occupancy of the N-glycans appended to rHuAChE, either by biochemical incorporation of sialic acid or by coexpression of the α2,6 sialyltransferase gene, results in a concomitant increase in the circulatory residence of the recombinant protein. However, circulatory retention of highly sialylated rHuAChE is still lower than that of serum-derived cholinesterases, indicating that other factors, other than high efficient glycan sialylation are also required for the circulatory longevity of cholinesterases. To define determine whether these factors are related to glycan structure, we performed an extensive structural study of the glycans appended to rBoAChE and its native serum-derived counterpart, FBS-AChE. This detailed analysis, allowed us to determine the precise structures and relative abundance of the various glycan forms associated with these two forms of bovine acetylcholinesterase, and allowed us to examine the possible role of specific glycan structures in determining pharmacokinetic behavior. Based on these studies, we conclude that sialic acid capping efficiency is the only glycan-structure-associated factor which may account for the differential pharmacokinetic behaviors of the native and recombinant forms of the enzyme. In contrast to the abundance of N-glycans attached to HuAChE, it appears that very low levels, if any, of O-glycans are appended to the recombinant enzyme.

Further studies allowed us to determine that enzyme assembly of the catalytic subunits of rBoAChE into tetramers serves as a contributing factor to the extension of circulatory retention, yet this effect is most pronouncedly manifested in highly sialylated recombinant enzyme. The concomitant optimization of both glycan sialylation and enzyme tetramerization results in the generation of rBoAChE, which resides in the circulation for long periods of time, indistinguishably from that of the native form of the enzyme. Based on these findings, we were able to determine that enzyme sialylation and subunit assembly contribute to circulatory retention of rBoAChE in an hierarchical manner, glycan sialylation being the overriding factor.

Extensive pharmacokinetic profiling of human acetylcholinesterase forms differing in their state of sialylation, and subunit oligomerization, in conjunction with MALDI-TOF analyses of glycan structures, allowed us to determine that the circulatory residence of the human form of acetylcholinesterase is governed in an hierarchical manner by the same set of rules established for the bovine version of the enzyme. Extension of these studies allowed us to establish the role of glycan loading in determining the circulatory fate of human AChE, and to define its contribution to circulatory residence within the hierarchical pattern of post-translation-related rules determining circulatory longevity.

Chemical modification of human acetylcholinesterase was evaluated as a means for generating an enzyme with improved pharmacodynamic properties. In a set of experiments, we monitored the effect of polyethylene-glycol (PEG) attachment to rHuAChE on the catalytic and pharmacokinetic properties of the enzyme. Under optimized conditions, the chemically-modified enzyme exhibited unaltered catalytic performance yet was retained in the circulation for extremely long periods of time, exceeding the circulatory residence values of all other recombinant or native serum-derived human cholinesterases reported to date. Moreover, efficient PEG-conjugation allowed long-term retention of enzyme forms exhibiting suboptimal oligomerization and sialylation as well, affirming its notable impact on the pharmacokinetic properties of the enzyme.

Taken together, these studies suggest a mode of operation for unraveling cellular processes and biochemical factors involved in circulatory longevity that provides a basis for the generation of a therapeutically efficient bioscavenger based on recombinant human acetylcholinesterase.

REFERENCES

Abuchowski, A., McCoy, J. R., Palczuk, N. C., Van Es, T. and Davis, F.F. (1977). Effect of covalent attachment of polyethylene glycol on immunogenicity and circulating life of bovine liver catalase. *J Biol. Chem.* **252**, 3582-3586

Aldrich, W.N., and Reiner, E., (1972). Enzyme Inhibitors as Substrates, (Neuberger, A. and Tatum, E.L. Eds.), North-Holland Publishing Co.; Amsterdam.

Allmand, P., Bon, S., Massoulie, J. and Vigny, M. (1981). The quaternary structure of chicken acetylcholinesterase and butyrylcholinesterases; effect of collagenase and trypsin. *J. Neurochem.* **36,** 860-867

Altamirano, C.V. and Lockridge, O. (1999). Conserved aromatic residues of the C-terminus of human butyrylcholinesterase mediate the association of tetramers. *Biochem.* **38**, 13414-13422

Anumula, K.R. and Dhume, S.T. (1998). High resolution and high sensitivity methods for oligosaccharide mapping and characterization by normal phase high performance liquid chromatography following derivatization with highly fluorescent anthranilic acid. *Glycobiology* **8,** 685-694

Ariel, N., Ordentlich, A., Barak, D., Bino, T., Velan, B. and Shafferman, A. (1998). The "aromatic patch" of three proximal residues in the human acetylcholinesterase active centre allows for versatile interaction modes with inhibitors. *Biochem. J.* **335,** 95-102

Arpagaus, M., Kott, M., Vatsis, K.P., Bartels, C.F., La Du B.N. and Lockridge, O. (1990). Structure of the gene for human butyrylcholinesterase. Evidence for a single copy. *Biochemistry* **29**, 124-131

Ashani, Y., Grunwald, J., Kronman, C., Velan, B. and Shafferman, A. (1994). Role of tyrosine 337 in the binding of huperzine A to the active site of human acetylcholinesterase. *Molec. Pharmacol.* **45**, 555-560

Ashani, Y., Shapira, S., Levy, D., Wolfe, A.D., Doctor, B.P. and Raveh, L. (1991). Butyrylcholinesterase and acetylcholinesterase prophylaxis against soman poisoning in mice. *Biochem Pharmacol.* **41,** 37-41

Ashwell, G. and Harford, J. (1982). Carbohydrate-specific receptors. *Ann. Rev. Biochem.* **51,** 531-554

Ashwell, G. and Morell, A.G. (1974). The role of surface carbohydrates in the hepatic recognition and transport of circulating glycoproteins. *Adv. Enzymol. Relat. Areas Mol. Biol.* **41**, 99-128

Atack, J.R., Perry, E.K., Bonham, J.R. and Perry, R.H. (1987). Molecular forms of butyrylcholinesterase in human neocortex during development and degeneration of the cortical cholinergic system. *J. Neurochem.* **48,** 1845-1850

Axelsen, P.H., Harel, M., Silman, I. and Sussman, J.L. (1994). Structure and dynamics of the active site gorge of acetylcholinesterase: synergistic use of molecular dynamics simulation and X-ray. *Protein Sci.* **3,** 188-197

Barak, D., Ariel, N., Velan, B. and Shafferman, A. (1992). in *Multidisciplinary Approaches to ChE Functions* (Shafferman, A. and Velan, B. Eds.) pp. 177-183, Plenum

Barak, D., Kronman, C., Ordentlich, A., Ariel, N., Bromberg, A., Marcus, D., Lazar, A., Velan, B., and Shafferman, A. (1994). Acetylcholinesterase peripheral anionic site degeneracy conferred by amino acid arrays sharing a common core. *J. Biol. Chem.* **264**, 6296-6305

Barak, D., Ordentlich, A., Segall, Y., Velan, B., Benschop, H.P., De Jong, L.P.A. and Shafferman, A. (1997a). Carbocation mediated processes in biocatalysts - contribution of aromatic moieties. *J. Am. Chem. Soc.*, **119**, 3157-3158

Barak, R., Ordentlich, A., Barak, D., Fischer, M., Benschop, H.P., De Jong, L.P.A., Velan B. and Shafferman, A. (1997b). Direct determination of the chemical composition of acetylcholinesterase phosphonylation products utilizing electrospray-ionization spectroscopy. *FEBS Lett.* **407**, 347

Barak, D., Ordentlich, A., Segall, Y., Velan, B., Benschop, H.P., De Jong, L.P.A. and Shafferman, A. (2000). Evidence for P-N bond scission in phosphoroamidate nerve gent adducts of human acetylcholinesterase. *Biochemistry* **39**, 1156-1161

Bencsura, A., Enyedy, I. and Kovach, I.M. (1995). Origins and diversity of the aging reaction in phosphonate adducts of serine hydrolase enzymes: what characteristics of the active site do they probe? Biochemistry **34,** 8989–8999

Benschop, H.P. and De Jong, L.P.A. (1988). Nerve agent stereoisomers: analysis, isolation and toxicology. *Acc. Chem. Res.* **21**, 368-374

Benschop, H.P. and Keijer, J.H. (1966). The mechanism of aging of phosphonylated cholinesterases. *Biochim. Biophys. Acta* **128,** 586

Benschop, H.P., Konings, C.A.G., Van Genderen, J. and De Jong, L.P.A (1984). Isolation, anticholinesterase properties, and acute toxicity in mice of the four stereoisomers of the nerve agent soman. *Toxicol. Appl. Pharmacol.* **72,** 61-74

Berryman, D.E., and Bensadoun, A. (1995). Heparan sulfate proteoglycans are primarily responsible for the maintenance of enzyme activity, binding and degradation of lipoprotein lipase in Chinese hamster ovary cells. *J. Biol. Biochem. 270,* 24525-24531

Bigge, J.C., Pate, T.P., Bruce, J.A., Goulding, P.N., Charles, S.M. and Parekh, R.B. (1995). Nonselective and efficient fluorescent labeling of glycans using 2-amino benzamide and anthranilic acid. *Anal. Biochem.* **230**, 229-238

Blong, R.M., Bedows, E., and Lockridge, O. (1997). Tetramerization domain of human butyrylcholinesterase is at the C-terminus. *Biochem. J. 327,* 747-757.

Boccu, E., Velo, G.P. and Veronese, F.M. (1982). Pharmacokinetic properties of polyethylene glycol derivatized superoxide dismutase. Pharmacol. Res. Commun. **14**, 113-120

Bon, S. and Massoulie, J. (1997). Quaternary associations of acetylcholinesterase. I. Oligomeric associations of T subunits with and without the amino-terminal domain of the collagen tail. *J. Biol. Chem.* **272,** 3007-3015

Bon, S., Coussen, F. and Massoulie, J. (1997). Quaternary associations of acetylcholinesterase. II. The polyproline attachment domain of the collagen tail. *J. Biol. Chem.* **272,** 3016-3021

Borrebaeck, C.A.K., Malmbourg, A.C. and Ohlin, M. (1993). Does endogenous glycosylation prevent the use of mouse monoclonal antibodies as cancer therapeutics? *Immunology Today* **14,** 477-480

Borrebaeck, C.A.K. (1999). Human monoclonal antibodies: the emperor's new clothes? *Nature Biotechnology* **17,** 621

Botti, S.A., Felder, C., Lifson, S., Sussman, J.L. and Silman, I. (1999). A modular treatment of molecular traffic through the active site of cholinesterase. *Biophys. J.* **77,** 2430-2450

Bourne, Y., Taylor, P. and Marchot, P. (1995). Acetylcholinesterase inhibition by fasciculin: crystal structure of the complex. *Cell* **83,** 503-512

Bourne, Y., Grassi, J., Bougis, P.E. and Marchot, P. (1999). Conformational flexibility of the acetylcholinesterase tetramer suggested by x-ray crystallography. *J. Biol. Chem.* **274,** 30370-30376

Broomfield, C.A., Maxwell, D.M., Solana, R.P., Castro, C.A, Finger, A.V. and Lenz, D.E. (1991). Protection by butyrylcholinesterase against organophosphorus poisoning in nonhuman primates. *J. Pharmacol. Exp. Ther.* **259**, 683-698

Bundy, J. and Fenselau, C. (1999). Lectin-based affinity capture for MALDI-MS analysis of bacteria. *Anal. Chem.* **71,** 1460-1463.

Cadogan, J.I.G., Eastlick, D., Hampson, F. and Mackie, R.K. (1969). The reactivity of organo-phosphorus compounds. Part XXIV. Acidic hydrolysis of dialkyl methylphosphonates. *J. Chem. Soc.* **B**, 144-146

Cauet, G., Friboulet, A. and Thomas, D. (1987). Substrate activation and thermal denaturation kinetics of the tetrameric and the trypsin-generated monomeric forms of horse serum butyrylcholinesterase. *Biochem. Cel l Biol.* **65,** 529-35

Chambers, H.W. (1992). Organphosphorus compounds: An overview. *In* Organophosphates, Chemistry, Fate and Effects (Chambers, J. E. and Levi, P. E. Eds.), pp. 3-17, Academic Press, New York.

Chapman, A.P., Antoniw, P., Spitali, M., West, S., Stephens, S. and King, D.J. (1999). Therapeutic antibody fragments with prolonged in vivo half-lives. *Nature Biotech.* **17**, 780-783

Chatonnet, A. and Lockridge, O. (1989). Comparison of butyrylcholinesterase and acetylcholinesterase. *Biochem. J.* **260,** 625-634

Chitlaru, T., Kronman, C., Zeevi, M., Kam, M., Harel, A., Ordentlich, A., Velan, B. and Shafferman, A. (1998). Modulation of circulatory residence of recombinant acetylcholinesterase through biochemical or genetic manipulation of sialylation levels. *J. Biol. Chem.* **336**, 647-658

Chitlaru, T., Kronman, C., Velan, B. and Shafferman, A. (2001). Effect of human acetylcholinesterase subunit assembly on its circulatory residence. *Biochem. J.* **354**, 613-625

Clarenburg, R. (1983). Asialoglycoprotein receptor is uninvolved in clearing intact glycoproteins from rat blood. *Am. J. Physiol.* **244,** G247-G253

Clark, R., Olson, K., Fuh, G., Marian, M., Mortensen, D., Teshima, G., Chang, S., Chu, H., Mukku, V., Canova-Davis, E., Somers, T., Cronin, M., Winkler, M. and Wells, J.A. (1996). Long-acting growth hormones produced by conjugation with polyethylene glycol. *J. Biol. Chem.* **271**, 21969-21977

Cohen, O., Kronman, C., Chitlaru, T., Ordentlich, A., Velan, B. and Shafferman, A. (2001). Chemical modifications of recombinant human acetylcholinesterase by polyethylene glycol generates an enzyme with exceptional circulatory longevity. *Biochem. J.* **357**, 795-802

Collen, D., Lijnen, H.R., Vanlinthout, I., Kieckens, L., Nelles, L., and Stassen, J.M. (1991). Thrombolytic and pharmacokinetic properties of human tissue-type plasminogen activator variants, obtained by deletion and/or duplication of structural/functional domains, in a hamster pulmonary embolism model. *Thrombosis and Haemostasis* **65,** 174-180

Cousin, P., Dechaud, H., Grenot, C., Lejeune, H. and Pugeat, M. (1998). Human variant sex hormone-binding globulin (SHBG) with an additional carbohydrate chain has a reduced clearance rate in rabbit. *J. Clin. Endocrin. Metabolism* **83**, 235-240

Coyle, J.T., Price, D.L. and DeLong, M.R. (1983). Alzheimer's disease: A disorder of cortical cholinergic innervation. *Science* **219,** 1184-1190

Cygler, M., Schrag, J.D., Sussman, J.L., Harel, M., Silman, I., Gentry, M.K. and Doctor, B.P. (1993). Relationship between sequence conservation and three-dimensional structure in large family of esterases, lipases, and related proteins. *Protein Sci.* **2,** 366-382

Dai, Y., Li, L., Roser, D. C., and Long, S. R. (1999a). Detection and identification of low- mass peptides and proteins from solvent suspensions of *escherichia coli* by high performance liquid chromatography fractionation and matrix-assisted laser desorption ionization mass spectrometry. *Rapid Commun. Mass Spectrom.* **13,** 73-78

Dai, Y., Whittal, R. M. and Li, L. (1999b). Two-layer sample preparation: A method for MALDI-MS analysis of complex peptide and protein mixtures. *Anal. Chem.* **71,** 1087-1091

Davis, S., Abuchowski, A., Park, Y.K. and Davis, F.F. (1981). Alteration of the circulating life and antigenic properties of bovine adenosine deaminase in mice by attachment of polyethylene glycol. *Clin. Exp. Immunol.* **46**, 649-652

De Jong, L.P.A. and Wolring, G. Z. (1978). Reactivation and aging of cyclopentyl methylphosphonylated acetylcholinesterase in the presence of some 1-alkyl-2-hydroxyiminomethyl-pyridinium salts. *Biochem. Pharmacol.* **27**, 2911-2917

De Jong, L.P.A., Wolring, G.Z. and Benschop, H.P. (1982). Reactivation of acetylcholinesterase inhibited by methamidophos and analogous (Di)Methylphosphoramidates. *Arch. Toxicol.* **49,** 175-18

De Jong, L. P. A., Verhagen, M. A. A., Langenberg, J. P., Hagedorn, I., Loffler, M. (1989). The bispyridinium-dioxime Hlo. A potent reactivator of acetylcholinesterase inhibited by the stereoisomers of tabun and soman. *Biochem. Pharmacol.* **38**, 633-640

DeSantis, G. and Jones, J.B. (1999). Chemical modification of enzymes for enhanced functionality. *Curr. Opin. Biotech.* **10**, 324-330

Doctor, B.P., Chapman, T.C., Christner, C.E., Deal, C.D., De La Hoz, D.M., Gentry, M.K., Ogert, R.A., Rush, R.S., Smyth, K.K. and Wolfe, A.D. (1990). Complete amino acid sequence of fetal bovine serum acetylcholinesterase and its comparison in various regions with other cholinesterases. *FEBS Lett.* **266,** 123-127

Doctor, B.P., Blick, D.W., Gentry, M.K., Maxwell, D.M., Miller, S.A., Murphy, M.R. and Wolfe, A.D. (1992). Acetylcholinesterase: a pretreatment drug for organophosphate toxicity. In: Multidisciplinary Approaches to Cholinesterase Functions. (Shafferman A. and Velan B. Eds.), pp. 277-286, Plenum Pub. Co., New York

Doorn, J. A., Gage, D. A., Schall, M., Talley, T. T., Thompson, C. M. and Richardson, R. J. (2000). Inhibition of acetylcholinesterase by (1S,3S)- Isomalathion proceeds with loss of thiomethyl: Kinetic and mass spectral evidence for an unexpected primary leaving group. *Chem. Res. Toxicol.* **13,** 1313-1320

Douchet, J.C., Masson, P. and Morelis, P. (1982). Elimination de la cholinesterase humaine purifee injectee an rat. *Trav. Sci.* **3,** 342-347

Drickamer, K. (1991). Clearing up glycoprotein hormones. *Cell* **67,** 1029-1032

Duval, N., Krejci, E., Grassi, J., Coussen, F., Massoulie, J., and Bon, S. (1992). Molecular architecture of acetylcholinesterase collagen-tailed forms; construction of glycolipid-tailed tetramer. *EMBO J.* **11,** 3255-3261

Ellman, G.L., Courtney, K.D., Andres, V. and Featherstone, R.M. (1961). A new and rapid colorimetric determination of acetylcholinesterase activity. *Biochem Pharmacol.* **7,** 88-95

Feng, G., Krecji, E., Molgo, J., Cunningham, J.M., Massoulie, J., and Sanes, J.R. (1999). Effect of enzyme preparations on in situ an in vitro degradation and in vivo digestive characteristics of mature cool-season grass forage in beef steers. *J. Cell Biol.* **144,** 1349-1360

Fiete, D., Srivastava, V., Hindsgaul, O. and Baenziger, J.U. (1991). A hepatic reticuloendothelial cell receptor specific for SO_4-GalNAc beta 1,4GlcNAc beta 1,2Man alpha that mediates rapid clearance of lutropin. *Cell* **67,** 1103-1110

Fiete, D.J., Beranek, M.C. and Baenziger, J.U. (1998). A cysteine-rich domain of the "mannose" receptor mediates GalNAc-4-SO_4 binding. *Proc. Natl. Acad. Sci. USA* **95,** 2089-2093

Fischer, M., Ittah, A., Liefer, I. and Gorecki, M. (1993). Expression and reconstitution of biologically active human acetylcholinesterases from *E. Coli. Cell. Mol. Neurobiol.* **13,** 25-38

FitzGerald, D.J., Fryling, C.M., Zdanovsky, A., Saelinger, C.B., Kounnas, M., Winkles, J.A., Strickland, D., and Leppla, S. (1995). Pseudomonas exotoxin-mediated selection yields cells with altered expression of low-density lipoprotein receptor-related protein. *J. Cell Biol.* **129,** 1533-1541

Francis, G.E., Fisher, D., Delegado, C., Malik, F., Gardiner, A. and Neale, D. (1998). PEG-conjugation of cytokines and other therapeutic proteins and peptides: the importance of biological optimization of coupling techniques. *Inter. J. Hemato.* **68**, 1-18

Fukuda, M.N., Sasaki, H., Lopez, L. and Fukuda, M. (1989). Survival of recombinant erythropoietin in the circulation: the role of carbohydrates. *Blood* **73**, 84-89

Gabrielsson, J.L. and Weiner, D.L. (1999). Methodology for pharmacokinetic/pharmacodynamic data analysis. *Pharm. Sci. Technol. Today.* **2**, 244-252

Galili, U. (1993). Interaction of the natural anti-gal antibody with alpha-galactosyl epitopes: a major obstacle for xenotransplantations in humans. *Immunol. Today* **14,** 480-482

Galili, U., Shohet, S.B., Kobin, E., Stults, C.L.M. and Macher, B.A. (1998). Man, apes and old world monkeys differ from other mammals in the expression of alpha-galactosyl epitopes on nucleated cells. *J. Biol. Chem.* **263,** 17755-17762

Giles, K., Ben-Yohanan, R., Velan, B., Shafferman, A., Sussman, J.L., and Silman, I. (1998). In: *Structure and Function of Cholinesterases and Related Proteins* (Doctor, B.P., Taylor, P., Quinn, D.M., Rotundo, R.L. and Gentry, M.K., Eds) p442, Plenum Publishing Corp. New York.

Gnatt, A., Loewenstein, Y., Yaron, A., Schwarz, M. and Soreq, H. (1994). Site-directed mutagenesis of active site residues reveals plasticity of human butyrylcholinesterase in substrate and inhibitor interaction. *J. Neurochem.* **62,** 749-755

Goochee, C.F. and Monica, T. (1990). Environmental effects on protein glycosylation. *Bio/Technology* **8**, 421-427

Goochee, C.F., Gramer, M.J., Andersen, D.C., Bahr, J.B. and Rasmussen, J.R. (1991). The oligosaccharides of glycoproteins: bioprocess factors affecting oligosaccharide structure and their effect on glycoprotein properties. *Bio/Technology* **9**, 1347-1355

Hall, Z.W. (1973). Multiple forms of acetylcholinesterase and their distribution in endplate and non-endplate regions of rat diaphragm muscle. *J. Neurobiol.* **4**, 343-361

Hall, C. R. and Inch, T. D. (1990). Phosphorus stereochemistry: mechanistic implications of the observed stereochemistry of bond forming and breaking processes at phosphorus in some 5- and 6-membered cyclic phosphorus esters. *Tetrahedron* **36**, 2059-2095

Harel, M., Sussman, J.L., Krejci, E., Bon, S., Chanal, P., Massoulie, J. and Silman, I. (1992). Conversion of acetylcholinesterase to butyrylcholinesterase: modeling and mutagenesis. *Proc. Natl. Acad. Sci. USA.* **89,** 10827-10831

Harel, M., Schalk, I., Ehret-Sabatier, L., Bouet, F., Goeldner, M., Hirth, C., Axelsen P.H., Silman, I. and Sussman, J.L. (1993). Quaternary ligands binding to aromatic residues in the active-site gorge of acetylcholinesterase. *Proc. Natl. Acad. Sci. U S A.* **90**, 9031-9035

Harel, M., Quinn, D.M., Nair, H.K., Silman, I. and Sussman, J.L. (1996). The x-ray structure of a transition state analog complex reveals the molecular origins of the catalytic power and substrate specificity of acetylcholinesterase. *J. Am. Chem. Soc.* **118**, 2340-2346

Harel, M., Kryger, G., Rosenberry, T.L., Mallender, W.D., Lewis, T., Fletcher, R.J., Guss, J.M., Silman, I. And Sussman, J.L. (2000). Three dimensional structures of Drosophila melanogaster acetylcholinesterase and of its complexes with two potent inhibitors. *Protein Sci.* **9,** 1063-1072

Harris, J.M. (1992). Introduction to biotechnical and biochemical applications of poly(ethylene glycol). In:Poly(Ethylene Glycol) Chemistry, Biotechnical and Biomedical Applications. (J. M. Harris, Ed.), pp. 1-14. Plenum Press, New York

Hershfield, M.S., Buckeley, R.H., Greenberg, M.L., Melton, A.L., Schiff, R., Hatem, C., Kurtzberg, J., Matkert, M.L., Kobayashi, A.L. and Abuchowski, A. (1987). Treatment of adenosine deaminase deficiency with polyethylene glycol-modified adenosine deaminase. *N. Engl. J. Med.* **316**, 589-596

Holmstedt, B. (1951). Synthesis and pharmacology of (dimethylamino)ethoxyphosphoryl cyanide-allied anticholinesterase compounds containing the N-P bond. *Acta Physiol. Scand.* **46,** 11445

Horn, I.R., Moestrup, S.K., van den Berg, B.M.M., Pannekoek, H., Nielsen, M.S., and van Zonneveld, A-J. (1995). Analysis of the binding of pro-urokinase and urokinase-plasminogen activator inhibitor-1 to the low density lipoprotein receptor-related protein using a Fab fragment selected from a phage-displayed Fab library. *J. Biol. Chem.* **270**, 11770-11775

Hosea, N.A., Berman, H.A. and Taylor, P. (1995). Specificity and orientation of trigonal carboxyl esters and tetrahedral alkylphosphonyl esters in cholinesterases. *Biochemistry* **34,** 11528-11536

Hosea, N. A., Radic, Z., Tsigelny, I., Berman, H., Quinn, D. M. and Taylor, P. (1996). Aspartate 74 as a primary determinant in acetylcholinesterase governing specificity to cationic organophosphonates. *Biochemistry* **35,** 10995-11004

Hossner, K.L. and Billiar, R.B., (1981). Plasma clearance and organ distribution of native and desialylated rat and human transcortin: species specificity. *Endocrinology* **108,** 1780-1786

Houghten, R.A. (1985). General method for the rapid solid-phase synthesis of large numbers of peptides: specificity of antigen-antibody interaction at the level of individual amino acids. *Proc. Natl. Acad. Sci. USA* **82**, 5131-5135

Jarv, J. (1984). Stereochemical aspects of cholinesterase catalysis. *Bioorg. Chem.* 12, 259-278.

Junghans, R.P. (1999). Anti-gal antibodies - where's the beef? *Nature Biotechnology* **17,** 938

Kamisaki, Y., Wada, H., Yagura, T., Matsushima, A. and Inada, Y. (1981). Reduction in immunogenicity and clearance rate of Escherichia coli L-asparaginase by modification with monomethoxypolyethylene glycol. *J. Pharmacol. Exp. Therapeut.* **216**, 410-414

Kanwar, Y.S. (1984). Biology of disease: biophysiology of glomerular filtration and proteinuria. *Lab. Invest.* **51**, 7-21

Keijer, J.H. and Wolring, G.Z. (1969). Stereospecific aging of phosphonylated cholinesterases. *Biochim. Biophys. Acta* **185**, 465-468

Knauf, M.J., Bell, D.P., Hirtzer, P., Luo, Z. P., Young, J.D. and Katre, N. V. (1988). Relationship of effective molecular size to systemic clearance in rats of recombinant interleukin-2 chemically modified with water-soluble polymers. *J. Biol. Chem.* **263**, 15064-15070

Koellner, G., Kryger, G., Millard, C.B., Silman, I., Sussman, J.L. and Steiner, T. (2000). Active-site gorge and buried water molecules in crystal structures of acetylcholinesterase from *Torpedo californica*. *J. Mol. Biol.* 296, 713-735.

Koths, K., and Halenbeck, R. (1985). In: *Cellular and Molecular Biology of Lymphokines* (Sorg, C. and Schimple, A., Eds) pp 779-783, Academic Press, New York.

Krause, E., Wenschuh, H., and Jungblut, P. R. (1999). The dominance of arginine-containing peptides in MALDI-Derived tryptic mass fingerprints of proteins. *Anal. Chem.* **71**, 4160-4165

Krecji, E., Thomine, S., Boschetti, N., Legay, C., Sketelj, J., and Massoulie, J. (1997). The mammalian gene of acetylcholinesterase-associated collagen. *J. Biol. Chem.* **272,** 22840-22847

Kronman, C., Velan, B., Gozes, Y., Leitner, M., Flashner, Y., Lazar, A., Marcus, D., Sery, T., Grosfeld, H., Cohen, S. and Shafferman, A. (1992). Production and secretion of high levels of recombinant human acetylcholinesterase in cultured cell lines: microheterogeneity of the catalytic subunit. *Gene* **121**, 295-304

Kronman, C., Velan, B., Marcus, D., Ordentlich, A., Reuveny, S. and Shafferman, A. (1995). Involvement of oligomerization, N-glycosylation and sialylation in the clearance of cholinesterases from the circulation. *Biochem. J.* **311**, 959-967

Kronman, C., Chitlaru, T., Elhanany, E., Velan, B. and Shafferman, A. (2000). Hierarchy of post-translation modifications involved in the circulatory longevity of glycoproteins: Demonstration of concerted contributions of glycan sialylation and subunit assembly to the pharmacokinetic behavior of bovine acetylcholinesterase. *J. Biol. Chem.* **275**, 29488-29502

Kryger, G., Giles, K., Harel, M., Toker, L., Velan, B., Lazar, A., Kronman, C., Barak, D., Ariel, N., Shafferman, A., Silman, I. and Sussman, J.L. (1998). 3D structure at 2.7 Å resolution of native and E202Q mutant human acetylcholinesterases complexed with fasciculin-II. In: Structure and Function of Cholinesterases and Related Proteins . (Eds. Doctor, B.P., Quinn, D.M., Rotundo, R.L. and Taylor, P.) Plenum Publishing Corp. 323-326

Kryger, G., Harel, M., Giles, K., Toker, L., Velan, B., Lazar. A., Kronman, C., Barak, D., Ariel, N., Shafferman, A., Silman, I. and Sussman, J.L. (2000). Structures of recombinant native and E202Q mutant human acetylcholinesterase complexed with the snake-venom toxin fasciculin-II. *Acta Cryst.* **D56**,1385-1394

Kuster, B., Wheeler, S.F., Hunter, A.P., Dwek, R.A. and Harvey, D.J. (1997). Sequencing of N linked oligosaccharides directly from protein gels: in-gel deglycosylation followed by matrix assisted laser desorption/ionization mass spectrometry and normal phase high-performance liquid chromatography. *Anal. Biochem.* **250,** 82-101

Langenberg, J.P., de Jong, L.P.A., Otto, M.F.. And Benschop, H.P. (1988). Spontaneous and oxime-induced reactivation of acetylcholinesterase inhibited by phosphoroamidates. *Arch. Toxicol.* **62,** 305-310

Laub, P.B. and Gallo, J.M. (1996). NCOMP - a Windows-based computer program for noncompartmental analysis of pharmacokinetic data. *J. Pharm. Sci.* **85,** 393-395

Lazar, A., Reuveny, S., Kronman, C., Velan, B. and Shafferman, A. (1993). Evaluation of anchorage-dependent cell propagation system for production of human acetylcholinesterase by recombinant 293 cells. *Cytotechnology* **13,** 115-123

Lazar, M. and Vigvy, M. (1980). Modulation of the distribution of acetylcholinesterase molecular forms in a murine neuroblastoma sympathetic ganglion cell hybrid cell line. *J. Neurochem.* **35**, 1067-1079

Lefort, G.P., Stolk, J.M. and Nisula, B.C. (1984). Evidence that desialylation and uptake by hepatic receptors for galactose-terminated glycoproteins are immaterial to the metabolism of human choriogonadotropin in the rat. *Endocrinology* **115,** 1551-1557

Legay, C. Bon, S. and Massoulie, J. (1993). Expression of a cDNA encoding the glycolipid-anchored form of rat acetylcholinesterase. *FEBS Lett.* **315,** 163-166

Lockridge, O., Eckerson, H.W., and La Du, B.N. (1979). Interchain disulfide bond and subunit organization in human serum cholinesterase. *J. Biol. Chem.* **254,** 8324-8330

Lockridge, O. and LaDu, B.N. (1982). Loss of interchain disulfide peptide and dissociation of the tetramer following limited proteolysis of native human serum cholinesterase. *J. Biol. Chem.* **257,** 12012-12018

Lockridge, O., Blong, R.M., Masson, P., Froment, M-T., Millard, C.B. and Broomfield, C.A. (1997). A single amino acid substitution Gly117His confers phosphotriesterase (organophosphorus acid anhydride hydrolase) activity on human butyrycholinesterase. *Biochemistry* **36,** 786-795

Loewenstein-Lichtenstein, Y., Glick, D., Gluzman, N., Sternfeld, M., Zakut, H. and Soreq, H. (1996). Overlapping drug interaction sites of human butyrylcholinesterase dissected by site-directed mutagenesis. *Mol. Pharmacol.* **50,** 1423-1431

Lundblad, R. L. and Bradshaw, R. A. (1997). Application of site-specific chemical modifications in the manufacture of biopharmaceutical: I. An overview. *Biotechnol. Appl. Biochem.* **26**, 143-151

Maglothin, J.A., Wins, O. and Wilson, I.B. (1975). Reactivation and aging of diphenyl phosphoryl acetylcholinesterase. *Biochim Biophys Acta* **403**, 370-387

Main, A.R. (1976). In: *Biology of Cholinergic Function* (Goldberg, A.M. and Hanin, I. Eds.) pp. 269-353, Raven Press, New York.

Masson, P., Froment, M.T., Bartels, C. and Lockridge, O. (1996a). Asp70 in the peripheral anionic site of human butyrylcholinesterase. *Eur. J. Biochem.* **235**, 36-48

Masson, P., Legrand, P., Bartels., C.F., Froment, M.T., Schopfer, L.M. and Lockridge, O. (1996b). Role of aspartate 70 and tryptophan 82 in binding of succinyldithiocholine to human butyrylcholinesterase. *Biochemistry* 36, 2266-2277.

Masson, P., Fortier, P.L., Albaret, C., Froment, M.T., Bartels, C.F. and Lockridge, O. (1997). Aging of di-isopropyl-phosphorylated human butyrylcholinesterase. *Biochem. J.* **327,** 601-607

Masson. P., Xie, W., Froment, M.T., Levitsky, V., Fortier, P.L., Albert, C. and Lockridge, O. (1999). Interaction between the peripheral site residues of human butyrylcholinesterase D70 and Y332, in binding and hydrolysis of substrates. *Biochim. Biophys. Acta* **1433,** 281-293

Massoulie, J., Pezzementi, L., Bon, S., Krejci, E. and Vallette, F.M. (1993). Molecular and cellular biology of cholinesterases. *Prog. Neurobiol.* **41**, 31-91

Massoulie, J., Anselmet, A., Bon, S., Krecji, E., Legay, C., Morel, N. and Simon, S. (1999). The polymorphism of acetylcholinesterase: post-translational processing, quaternary associations and localization. *Chemico. Biol. Interact.* **119-120,** 29-42

Massoulie, J., Anselmet, A., Bon, S., Krejci, E., Legay, C., Morel, N. and Simon, S. (1998). Acetylcholinesterase: C-terminal domains, molecular forms and functional localization. *J. Physiol.* **92**, 183-190

Matsuura, F., Ohta, M., Ioannou, Y.A. and Desnick, R.J. (1998). Human α-galactosidase A: characterization of the N-linked oligosaccharides and secreted glycoforms overexpressed by Chinese hamster ovary cells. *Glycobiology* **8**, 329-339

Maxwell, D.M., Castro, C.A., De La Hoz, D.M., Gentry, M.K., Gold, M.B., Solana, R.P., Wolfe, A.D. and Doctor, B.P. (1992). Protection of rhesus monkeys against soman and prevention of performance decrement by pretreatment with acetylcholinesterase. *Toxicol. Appl. Pharmacol.* **115,** 44-49

Mechraf, Y. and Novotny, M.V. (1998). Mass spectrometric mapping and sequencing of N-linked oligosaccharides derived from submicrogram amounts of glycoproteins. *Anal. Chem.* **70**, 455-463

Mendelson, I., Kronman, C., Ariel, N., Shafferman, A. and Velan, B. (1998). Bovine acetylcholinesterase: cloning, expression and characterization. *Biochem. J.* **334,** 251-259

Michel, H.O., Hackley Jr, B.E., Berkowitz, L., List, G., Hackley, E.B., Gilliam, W. and Paukan, M., (1967). Aging and dealkylation of soman-inactivated eel cholinesterase. *Arch. Biochem. Biophys.* **121**, 29-34

Milatovic, D. and Johnson, M.K. (1993). Reactivation of phosphorodiamidated acetylcholinesterase and neuropathy target esterase by treatment of inhibited enzyme with potassium fluoride. *Chem.-Biol. Interactions* **87**, 425

Millard, C. and Broomfield, C. (1992). A computer model of glycosylated butyrylcholinesterase. *Biochem. Biophys. Res. Commun.* **189,** 1280-1286

Millard, C.B., Lockridge, O. and Broomfield, C.A. (1995). Design and expression of organophosphorus acid anhydride hydrolase activity in human butyrylcholinesterase. *Biochemistry* **34,** 15925-15933

Millard, C.B., Lockridge, O. and Broomfield, C.A. (1998). Organophosphorus acid anhydride hydrolase activity in human acetylcholinesterase: synergy results in somanase. *J. Biochem.* **37**, 237-247

Millard, C.B., Kryger, G., Ordentlich, A., Harel, M., Raves, M.L., Greenblat, H., Segall, Y., Barak, D., Shafferman, A., Silman, I. and Sussman, J.L. (1999a). Crystal structure of aged phosphonylated acetylcholinesterase: nerve agent reaction products at the atomic level. Biochemistry **38**, 7032-7039

Millard, C.B., Koellner, G., Ordentlich, A., Shafferman, A., Silman, I. and Sussman, J.L. (1999b). Reaction products of acetylcholinesterase and VX reveal a mobile histidine in the catalytic triad. *J. Am. Chem. Soc.* **121**, 9883-9884

Monard, C. and Quinchon, (1961). Preparation and physical properties of isopropyl methylflurophosphonate (I) preparation and physical properties of two samples of a pure standard product. *J. Bull. Soc. Chim. Fr.* 1084-1087

Monfardini, C. and Veronese, F.M. (1998). Stabilization of substances in circulation. *Bioconjug. Chem.* **9**, 418-450

Monica, T.J., Andersen, D.C. and Goochee, C.F. (1997). A mathematical model of sialylation of N-linked oligosaccharides in the trans-Golgi network. *Glycobiology* **7,** 515-521

Morel, N., Leroy, J., Ayon, A., Massoulie, J. and Bon, S. (2001). Acetylcholinesterase H and T dimers are associated through the same contact; mutations at this interface interfere with the C-terminal T peptide, inducing degradation rather than secretion. J. Biol. Chem. **276**, 37379-37389

Mutero, A. and Fournier, D. (1992). Post-translational modifications of *Drosophila* acetylcholinesterase. *In vitro* mutagenesis and expression in Xenopus oocytes. J. Biol. Chem. **267**, 1695-1700

Nachmansson, D. and Wilson, I.B. (1951). The enzymatic hydrolysis and synthesis of acetylcholine. *Adv. Enzymol.* **12,** 259-339

Nachon, F., Ehret-Sabatier, L., Loew, D., Colas, C., van Dorsselaer, A. and Goeldner, M. (1998). Trp82 and Tyr332 are involved in two quaternary ammonium binding domains of human butyrylcholinesterase as revealed by photoaffinity labeling with [3H]DDF. *Biochemistry* **37,** 10507-13

Nair, H.K., Lee, K. and Quinn, D.M. (1993). M-(*N,N,N*-Trimethyl-ammonio)trifluoroacetophenone: A fentomolar inhibitor of acetylchlolinesterase. *J. Am. Chem. Soc.* **115,** 9939-9941

Nair, H.K., Seravalli, J., Arbuckle, T. and Quinn, D.M. (1994). Molecular recognition in acetylcholinesterase catalysis: free-energy correlations for substrate turnover and inhibition by trifluro ketone transition-state analog. *Biochemistry* **33,** 8566-8576

Nakaoka, R., Tabata, Y., Yamaoka, T. and Ikada, Y. (1997). Prolongation of the serum half-life period of superoxide dismutase by poly(ethylene glycol) modification. *J. cont. Release* **46,** 253-261

Narita, M., Bu, G., Olis, G.M., Higuchi, D.A., Hertz, J., Broze, Jr., J.G. and Schwartz, A.L. (1995). Two receptor systems are involved in the plasma clearance of tissue factor pathway inhibitor *in-vivo*. *J. Biol. Chem.* **270**, 24800-24804

Ohno, K., Brengman, J., Tsujino, A. and Engel, A.G. (1998). Human endplate acetylcholinesterase deficiency caused by mutations in the collagen-like tail subunit ColQ) of the asymmetric enzyme. *Proc. Natl. Acad. Sci. USA* **95,** 9654-9659

Okafo, G., Burrow, L., Carr, S.A., Roberts, G.D. Johnson, W. and Camilleri, P. (1996). A coordinated high-performance liquid chromatographic, capillary electrophoretic, and mass spectrometric approach for the analysis of oligosaccharide mixtures derivatized with 2-aminoacridone. *Anal. Chem.* **68,** 4424-4430

Okafo, G., Langridge, A., North, S., Organ, A., West, A., Morris, M. and Camilleri, P. (1997). High-performance liquid chromatographic analysis of complex N-linked glycans derivatized with 2-aminoacridone. *Anal. Chem.* **69,** 4985-4993

Opdenakker, G., Rudd, P.M., Ponting, C.P. and Dwek, R.A. (1993).Concepts and principles of glycobiology. *FASEB J.* **7**, 1330-1337.

Ordentlich, A., Barak, D., Kronman, C., Flashner, Y., Leitner, M., Segall, Y., Ariel N., Cohen, S., Velan, B., and Shafferman, A. (1993a). Dissection of the human acetylcholinesterase active center - determinants of substrate specificity: Identification of residues constituting the anionic site, the hydrophobic site, and the acyl pocket. *J. Biol. Chem.* **268,** 17083-17095

Ordentlich, A., Kronman, C., Barak, D., Stein, D., Ariel, N., Marcus, D., Velan, B., and Shafferman, A. (1993b). Engineering resistance to 'aging' in phosphylated human acetylcholinesterase - role of hydrogen bond network in the active center. *FEBS Lett.* **334**, 215-220

Ordentlich, A., Barak, D., Kronman, C., Ariel, N., Segall, Y., Velan, B., and Shafferman, A. (1995). Contribution of aromatic moieties of tyrosine 133 and of the anionic subsite tryptophan 86 to catalytic efficiency and allosteric modulation of cholinesterase. *J. Biol. Chem.* **270,** 2082-2091

Ordentlich, A., Barak, D., Kronman, C., Ariel, N., Segall, Y., Velan, B. and Shafferman, A. (1996). The architecture of human acetylcholinesterase active center probed by interactions with selected organophosphate inhibitors. *J. Biol. Chem.* **271**, 11953-11962

Ordentlich, A., Barak, D., Ariel, N., Segall, Y., Velan, B. and Shafferman, A. (1998). Exploring the active center of human acetylcholinesterase with stereomers of an organophosphorus inhibitor with two chiral centers. *J. Biol. Chem.* **273**, 19509-19517

Ordentlich, A., Barak, D., Kronman, C., Benschop, H., De Jong, L.P.A., Ariel, N., Barak, R., Segall, Y., Velan, B. and Shafferman, A. (1999). Exploring the active center of human acetylcholinesterase with stereomers of an organophosphorus inhibitor with two chiral centers. *Biochem.* **38**, 3055-3066

Papac, D.I., Wong, A. and Jones, A.J.S. (1996). Analysis of acidic oligosaccharides and glycopeptides by matrix-assisted laser desorption/ionization time-of-flight mass spectrometry. *Anal. Chem.* **68,** 3215-3223

Powell, A.K. and Harvey, D.J. (1996). Stabilization of sialic acids in N-linked oligosaccharides and gangliosides for analysis by positive ion matrix-assisted laser desorption/ionization mass spectrometry. *Rapid Commun. Mass Spectrom.* **10,** 1027-1032

Prody, C.A., Zevin-Sonkin, D., Gnatt, A., Goldberg, O., and Soreq, H. (1987).Isolation and characterization of full length cDNA clones coding for cholinesterase from fetal human tissues. *Proc. Natl. Acad. Sci. U.S.A.* **84**, 3555-3559

Rademacher, T.W., Parekh, R.B. and Dwek, R.A. (1988). Glycobiology. Annu. Rev. Biochem. **57**, 785-838

Radic, Z., Reiner, E. and Taylor, P. (1991). Role of the peripheral anionic site on acetylcholinesterase: inhibition by substrates and coumarin derivatives. *Mol. Pharmacol.* **39,** 98-104

Radic, Z., Gibney, G., Kawamoto, S., MacPhee-Quigley, K., Bongiorno, C., and Taylor, P. (1992). Expression of recombinant acetylcholinesterase in Baculovirus system: kinetic properties of glutamate 199 mutants. *Biochemistry* **31**, 9760-9767

Radic, Z., Pickering, N.A., Vellom, D.C., Camp, C. and Taylor, P. (1993). Three distinct domains in the cholinesterase molecule confer selectivity for acetyl- and butyrylcholinesterase inhibitors. *Biochemistry* **32**, 12074-12084

Radic, Z., Duran, R., Vellom, D.C., Li, Y., Cervenansky, C. and Taylor, P. (1994).Site of fasciculin interaction with acetylcholinesterase. *J Biol. Chem.* **269**, 11233-11239

Radic, Z., Kirchhoff, P.D., Quinn, D.M., McCammon, J.A. and Taylor, P. (1997). Electrostatic influence on the kinetics of ligand binding to acetylcholinesterase. Distinction between active center ligands and fasciculin. *J. Biol. Chem.* **272,** 23265-23277

Ralston, J.S., Rush, R.S., Doctor, B.P. and Wolfe, A.D. (1985). Acetylcholinesterase from fetal bovine serum. Purification and characterization of soluble G4 enzyme. *J. Biol. Chem.* **260,** 4312-4318

Rao Thotakura, N. and Blithe, D.L. (1995).Glycoprotein hormones: glycobiology of gonadotrophins, thyrotrophin and free α subunit. *Glycobiol.* **5**, 3-10

Raveh, L., Ashani, Y., Levi, D., De La Hoz, D., Wolfe, A.D. and Doctor, B.P. (1989). Acetylcholinesterase prophylaxis against organophosphate poisoning: Quantitative correlation between protection and blood-enzyme level in mice. *Biochem. Pharmacol.* **38,** 529-534

Raveh, L., Grunwald, J., Marcus, D., Papier, Y., Cohen, E. and Ashani, Y., (1993). Human butyrylcholinesterase as a general prophylactic antidote for nerve agent toxicity. *In vitro* and *in vivo* quantitative characterization. *Biochem. Pharmacol.* **45,** 2465-2474

Raves, M.L., Harel, M., Pang, Y-P., Silman, I., Kozikowski, A.P. and Sussman J.L. (1997). Structure of acetylcholinesterase complexed with the nootropic alkaloid, (-)- huperzine A. *Nature Struc. Biol.* **4,** 57-63

Renkin, E.M., and Gilmore, J.P. (1973). In: *Renal Physiology* (Orloff, J. and Berliner, R.W, Eds) pp 185-248 American Physiology Society, Bethesda, MD.

Rosenbary, J., Rabl, C.R. and Neumann, E. (1996). Binding of the neurotoxin fasciculin 2 to the acetylcholinesterase peripheral site drastically reduces the association and dissociation rate constants for N-methylacridinium binding to the active site. *Biochemistry* **35**, 7298-7304

Rosenberry, T.L. and Richardson, J.M. (1977).Structure of 18S and 14S acetylcholinesterase. Identification of collagen-like subunits that are linked by disulfide bonds to catalytic subunits. *Biochemistry* **16**, 3550-3558

Rotundo, R.L. and Fambrough, D.M. (1979). Molecular forms of chicken embryo acetylcholinesterase in vitro and in vivo. *J. Biol. Chem.* **254,** 4790-4799

Rotundo, R.L., Rossi, S.G. and Anglister, L. (1997). Transplantation of quail collagen-tailed acetylcholinesterase molecules onto the frog neuromuscular synapse. *J. Cell. Biol.* **136**, 367-374

Rowland, M. and Tozer, T. N. (1989). *Clinical Pharmacokinetics: Concepts and Applications*, Lea & Febiger, Philadelphia, USA

Rudd, P.M., Morgan, B.P., Wormald, M.R., Harvey, D.J., van den Berg, C.W., Davis, S.J., Ferguson, M.A.J. and Dwek, R.A. (1997). The glycosylation of the complement regulatory protein, human erythrocyte CD59. *J. Biol. Chem.* **272**, 7229-7244

Sakane, T. and Pardridge, W.M. (1997). Carboxyl-directed PEG-conjugation of brain-derived neurotropic factor markedly reduces systematic clearance with minimal loss of biological activity. *Pharm. Res.* **14**, 1085-1091

Sareneva, T., Cantell, K., Pyhala, L., Pirhonen, J. and Julkunen, I. (1993). Effect of carbohydrates on the pharmacokinetics of human interferon-gamma. *J. Interferon Res.* **13**, 267-269

Saxena, A., Doctor, B.P., Maxwell, D.M., Lenz, D.E., Radic, Z. and Taylor, P. (1993). The role of glutamate-199 in the aging of cholinesterase. *Biochem. Biophys. Res.Comm.* **197**, 343-349

Saxena, A., Quian, N., Kovach, I.M., Kozikowski, A.P., Pang, Y.P., Vellom, D.C., Radic, Z., Quinn, D., Taylor, P. and Doctor, B.P. (1994). *Protein. Sci.* **3,** 1770-1778

Saxena, A., Maxwell, D. M., Quinn, D. M., Radic, Z., Taylor, P. and Doctor, B. P. (1997a). Mutant acetylcholinesterases as potential detoxification agents for organo-phosphate poisoning. *Biochem. Pharmacol.* **54**, 269-274

Saxena, A., Raveh, L., Ashani, Y. and Doctor, B.P. (1997b). Structure of glycan moieties responsible for the extended circulatory life time of fetal bovine serum acetylcholinesterase and equine serum butyrylcholinesterase . *Biochemistry* **36,** 7481-7489

Saxena, A., Viragh, C., Frazier, D. S., Kovach, I. M., Maxwell, D. M., Lockridge, O. and Doctor, B. P. (1998a). The pH dependence of dealkylation in soman-inhibited cholinesterases and their mutants: further evidence for a push-pull mechanism. Biochemistry **38**, 15086-15096

Saxena, A., Ashani, Y., Raveh, L., Stevenson, D., Pate, T. and Doctor, B.P. (1998b). Role of oligosaccharides in the pharmacokinetics of tissue-derived and genetically engineered cholinesterases. *Mol. Pharmacol.* **53,** 112-122

Schalk, I., Ehret-Sabatier, L., Le Feuvre, Y., Bon, S., Massoulie, J. and Goeldner, M. (1995). 6-Coumarin diazonium salt: a specific affinity label of Torpedo acetylcholinesterase peripheral site. *Mol. Pharmacol.* **48,** 1063-1067

Segall, Y., Waysbort, D., Barak, D., Ariel, N., Doctor, B.P., Grunwald, J. and Ashani, Y. (1993). Direct observation and elucidation of the structures of aged and nonaged phosphorylated cholinesterases by ^{31}P NMR spectroscopy. *Biochemistry* **32**, 13441-13450

Shafferman, A., Kronman, C., Flashner, Y., Leitner, S., Grosfeld, H., Ordentlich, A., Gozes, Y., Cohen, S., Ariel, N., Barak, D., Harel, M., Silman, I., Sussman, J.L. and Velan. B., (1992a). Mutagenesis of human acetylcholinesterase. *J. Biol. Chem.* **267,** 17640-17648

Shafferman, A., Velan, B., Ordentlich, A., Kronman, C., Grosfeld, H., Leitner, M., Flashner, Y., Cohen, S., Barak, D., and Ariel, N. (1992b). Substrate inhibition of acetylcholinesterase: residues involved in signal transduction from the surface to the catalytic center. *EMBO J.* **11**, 3561-3568

Shafferman, A., Ordentlich, A., Barak, D., Kronman, C., Ber, R., Bino, T., Ariel, N., Osman, R. and Velan, B. (1994). Electrostatic attraction by surface charge does not contribute to the catalytic efficiency of acetylcholinesterase. *EMBO J.* **13**, 3448-3455

Shafferman, A., Ordentlich, A., Barak, D., Kronman, C., Ariel, N., Leitner, M., Segall, Y., Bromberg, A., Reuveny, S., Marcus, D., Bino, T., Lazar, A., Cohen , S. and Velan, B. (1995). *Molecular aspects of catalysis and of allosteric regulation of acetylcholinesterases.* In: Enzymes of the Cholinesterase Family (Eds. Balasubarmanian, A.S., Doctor, B.P., Taylor, P., Quinn, D.M.) Plenum Publishing Corp. 189-196

Shafferman, A., Ordentlich, A., Barak, D., Stein, D., Ariel, N. and Velan, B. (1996a). Aging of phosphylated human acetylcholinesterase: catalytic processes mediated by aromatic and polar residues of the active center. *Biochem. J.* **318,** 833-840

Shafferman, A., Barak, D., Ordentlich, A., Kronman, C., Ariel, N., Grosfeld, H., Marcus, D., Lazar, A., Segall, Y. and Velan, B. (1996b). Molecular manipulation of bioscavengers for organophosphorus agents. *Proceedings of Medical Defense Bioscience Review* **1**, 23-32

Shafferman, A., Ordentlich, A., Barak, D., Kronman, C., Grosfeld, H., Stein, D., Ariel, N., Segall, Y. and Velan, B. (1996c). Enzyme engineering towards novel OP-hydrolases based on the human acetylcholinesterase template. *Phosphorus, Sulfur and Silicon* **109-110**, 3930-3960

Shafferman, A., Ordentlich, A., Barak, D., Stein, D., Ariel, N. and Velan, B. (1997). Aging of somanyl-acetylcholinesterase adducts: facts and models. *Biochem. J.* **324**, 996-997

Silman, I., Harel, M., Axelsen, P., Raves, M. and Sussman, J.L. (1994). Three-dimensional structures of acetylcholinesterase and of its complexes with anti cholinesterase agents. *Biochem. Soc. Trans.* **22,** 745-749

Simon, S., Krejci, E. and Massoulie, J. (1998). A four-to-one association between peptide motifs: four C-terminal domains from cholinesterase assemble with one proline-rich attachment domain (PRAD) in the secretory pathway. *EMBO. J.* **17,** 6178-6187

Smedsrod, B. and Einarsson, M. (1990) Clearance of tissue type plasminogen activator by mannose and galactose receptors in the liver. *Thrombosis Haemostasis* **63**, 60-66

Smith, P.L., Kaetzel, D., Nilson, J., and Baenziger, J.U. (1990). The sialylated oligosaccharides of recombinant bovine lutropin modulate hormone bioactivity. *J. Biol. Chem.* **265**, 874-881

Smith, P. L., Skelton, T. P., Fiete, D., Dharmesh, S. M., Beranek, M. C., MacPhail, L., Broze, G. J. and Baenziger, J. U. (1992). The asparagine-linked oligosaccharides on tissue factor pathway inhibitor terminate with SO_4-4GalNAcß1,4GlcNAcß1,2Manα. *J. Biol. Biochem.* **267**, 19140-19146

Smith, P.L., Bousfield, G.R., Kumar, S., Fiete, D. and Baenziger, J.U. (1993). Equine lutropin and choriogonadotropin bear oligosaccharides terminating with S04-GalNAc and Sial 2,3 Gal respectively. *J. Biol. Chem.* **268,** 795-802

Soreq, H. and Zakut, H. (1990). Expression and in vivo amplification of the human acetylcholinesterase and butyrylcholinesterase genes. *Prog. Brain Res.* **84,** 51-61

Soreq, H., Ben-Aziz, R., Prody, C.A., Seidman, S., Gnatt, A., Neville, A., Lieman-Hurwitz, J., Lev-Lehman, E., Ginzberg, D., Lapidot-Lifson, Y. and Zakut, H. (1990). Molecular cloning and construction of the coding region for human acetylcholinesterase reveals a G+C-rich attenuating structure. *Proc. Natl. Acad. Sci. USA* **87**, 9688-9692

Stieger, S., Butikofer, P., Wiesmann, U.N. and Brodbeck, U. (1989). Acetylcholinesterase in mouse neuroblastoma NB2A cells: analysis of production, secretion, and molecular forms. *J. Neurochem.* **52,** 1188-1196

Sussman J.L, Harel, M., Frolow F., Oefner, C. Goldman A. and Silman, I. (1991). Atomic resolution of acetylcholinesterase from Torpedo californica: A prototypic acetylcholine binding protein. *Science* **253,** 872-879

Szkudlinski, M.W., Rao Thotakura, N., Tropea, J.E., Grossman, M. and Weintraub, B.D. (1995). Asparagine-linked oligosaccharide structures determine clearance and organ distribution of pituitary and recombinant thyrotropin. *Endocrinol.* **136**, 3325-3330

Takeuchi, M., Takasaki, S., Shimada, M. and Kobata, A. (1990). Role of sugar chains in the *in vitro* biological activity of human erythropoietin produced in recombinant Chinese hamster ovary cells. *J. Biol. Chem.* **265**, 12127-12130

Tanigawara, S., Hori, R., Okumara, K., Tsuji, J., Shimizu, N., Noma, S., Suzuki, J., Livingston, D., Richards, S.M., Keyes, L.D., Couch, R.C. and Erickson, M.K. (1990). Pharmacokinetics in chimpanzees of recombinant human tissue-type plasminogen activator produced in mouse C127 and Chinese hamster ovary cells. *Chem Pharm. Bull.* **38,** 517-522

Taylor, P.B., Rieger, F., Shelanski, M.L. and Greene, L.A. (1981). Cellular localization of the multiple molecular forms of acetylcholinesterase in cultured neuronal cells. *J. Biol. Chem.* **256,** 3827-3830

Taylor, P. (1990). Anticholinesterase agents. *In* The Pharmacological Basis of Therapeutics, 8th Ed. (Gilman, A.G., Goodman, L.S., Rall, T.W. and Murad, F. Eds.), pp. 131-149, Macmillan Publishing Co., New York.

Taylor, P. and Radic, Z. (1994). The cholinesterases: from genes to proteins. *Pharmac. Toxicol.* **34**, 281-320

Thomas, J.J., Bakhtiar, R. and Siuzdak, G. (2000). Mass spectrometry in viral proteomics. *Acc. Chem. Res.* **33**, 179-187

Thomas, P. and Zamcheck, N. (1983). Role of the liver in clearance and excretion of circulating carcino-embryonic antigen. *Dig. Dis. Sci.* **28,** 216-224

Thompson C. M. and Fukuto, T. R. (1982). Mechanism of cholinesterase inhibition by methamidophos. *J. Agric. Food Chem.* **30,** 282-284.

Thompson, C.M., Ryu, S. and Berkman, C.E. (1992). Consequence of phosphorus stereochemistry upon the postinhibitory reaction kinetics of acetylcholinesterase poisoned by phosphorothiolates. *J. Am. Chem. Soc.* **114**, 10710-10715

van der Kaaden, M.E., Rijken, D.C., Groeneveld, E., van Berkel, T.J.C. and Kuiper, J. (1995). Native and non-glycosylated recombinant single-chain urokinase-type plasminogen activator are recognized by different receptor systems on rat parenchymal liver cells. *Thrombosis Haemostasis* **74**, 722-729

Velan, B., Kronman, C., Grosfeld, H., Leitner, M., Gozes, Y., Flashner, Y. Sery, T., Cohen, S., Benaziz, R., Seidman, S., Shafferman, A. and Soreq, H. (1991a). Recombinant human acetylcholinesterase is secreted from transiently transfected 293 cells as a soluble globular enzyme. *Cell. Mol. Neurob.* **11,** 143-156

Velan, B., Grosfeld, H., Kronman, C., Leitner, M., Gozes, Y., Lazar, A., Flashner Y., Marcus, D., Cohen, S., and Shafferman, A. (1991b). The effect of elimination of intersubunit disulfide bonds on the activity, assembly and secretion of recombinant human acetylcholinesterase. *J. Biol. Chem.* **266**, 23977-23984

Velan, B., Kronman, C., Ordentlich, A., Flashner, Y., Leitner, M., Cohen, S. and Shafferman, A. (1993). N-glycosylation of human acetylcholinesterase: effects on activity, stability and biosynthesis. *Biochem. J.* **296**, 649-656

Vellom, D.C., Radic, Z., Li, Y., Pickering, N.A., Camp, S. and Taylor, P. (1993). Amino acid residues controlling acetylcholinesterase and butyrylcholinesterase specificity. *Biochemistry* **32,** 12-17

Veronese, F.M., Monfardini, C., Caliceti, P., Schiavon, O., Scrawen, M.D. and Beer, D. (1996). Improvement of pharmacokinetic, immunological and stability properties of asparaginase by conjugation to linear and branched monomethoxy poly(ethylene glycol). *J. Cont. Release* **40**, 199-209

Vignay, M., Bon, S., Massoulie, J. and Gisiger, J. (1979). The subunit structure of mammalian acetylcholinesterase; Catalytic subunits, dissociating effect of proteolysis and disulfide reduction of the polymeric forms. *J. Neurochem.* **33,** 559-565

Vignay, M., Martin, G.R. and Grotendorst, G.R. (1983). Interactions of asymmetric forms of acetylcholinesterase with basement membrane compartments. *J. Biol. Chem.* **258**, 8794-8798

Viragh, C., Harris, T. K., Reddy, P. M., Massiah, M. A., Mildvan, A. S. and Kovach, I.M. (2000). NMR evidence for a short, strong hydrogen bond at active site of cholinesterase. *Biochemistry* **39,** 16200-16205.

Vostal, J.G. and McCauley, R.B. (1991). Pro-thrombin plasma clearance is mediated by hepatic asialoglycoprotein receptors. *Thromb. Res.* **63,** 299-309

Warshawsky, I., Bu, G., and Schwartz, A.L. (1993). 39-KD protein inhibits tissue-type plasminogen activator clearance in vivo. *J. Clin. Invest.* **92,** 937-944

Weikert, S. Papac, D., Briggs, J.,, D., Tom, S., Gawlitzek, M., Lofgren, J., Mehta, S., Chisholm, V., Modi, N., Eppler, S., Carroll, K., Chamow, S., Peers, D., Berman, P. and Krummen, L. (1999). Engineering Chinese hamster ovary cells to maximize sialic acid content of recombinant glycoproteins. *Nature Biotechnology* **17,** 1116-1121

Weinstein, J., de Souza-e-Silva, U. and Paulson, J.C., (1982). Purification of a Galβ1--> 4GlcNac α2-->6 sialyltransferase and a Galβ1-->3(4)GlcNacα2-->3 sialyltransferase to homogeneity from rat liver. *J. Biol. Chem.* **257,** 13835-13844

Weiss, P. and Ashwell, G. (1989). The asialoglycoprotein receptor: properties and modulation by ligand. *Prog. Clin. Biol. Res.* **300,** 169-184

Welply, J.K. (1991). Protein glycosylation: function and factors that regulate oligosaccharide structure. *Biotechnology* **17**, 59-72

Wilson, B.W., Hooper, M.J., Hensen, M.E. and Neiberg, P.S. (1992). Reactivation of organophosphorus inhibited ache with oximes. In: organophosphates chemistry, fate and effects (Chambers, J.E. And Levi, P.E. Eds.), pp.107-137, Academic Press, San Diego.

Wittwer, A.J. and Howard, S.C. (1990). Glycosylation at Asn-184 inhibits the conversion of single chain to two-chain tissue-type plasminogen activator by plasmin. *Biochem.* **29**, 4175-4180

Wolfe, A.D., Rush, R.S., Doctor, B.P., Koplovitz I. and Jones, D., (1987). Acetylcholinesterase prophylaxis against organophosphate toxicity. *Fundam Appl Toxicol* **9,** 266-270

Yan, S.B., Chao, Y.B. and van Halbeek, H. (1993). Novel Asn-linked oligosaccharides terminating in GalNAc beta (1,4) alpha (1,3) GlcNAc are present in recombinant human PKC expressed HEK293 cells. *Glycobiology* **3,** 597-608

Yates, C.M., Simpson, J., Moloney, A.F.J., Gordon, A. and Reid, A.H. (1980). Alzheimer like cholinergic deficiency in Down Syndrome. *Lancet*, **2,** 979-980

Younkin, S.G., Rosenstein, C., Collins, P.L. and Rosenberry, T.L. (1982). Cellular localization of the molecular forms of acetylcholinesterase in rat diaphragm. *J. Biol. Chem.* **257,** 1363-1367

Zalipsky, S. and Lee C. (1992). Use of functionalized poly(ethylene glycol)s for modification of polypeptides. In: Poly(Ethylene Glycol) Chemistry, Biotechnical and Biomedical Applications. (J. M. Harris, Ed.), pp 347-370. Plenum Press, New York

Zalipsky, S. (1995). Functionalized poly(ethylene glycol) for preparation of biologically relevant conjugates. *Bioconjug. Chem.* **6**, 150-165

PERSONNEL RECEIVING PAY*

ARIEL NAOMI

BARAK DOV

CHITLARU THEODOR

COHEN OFER

KAPLAN DANA

KRONMAN CHANOCH

LAZAR ARIE

LAZAR SHIRLEY

ORDENTLICH ARIE

SELIGER NEHAMA

SERY TAMAR

SILBERSTEIN LEA

SOD-MORIA GALIT

STEIN DANA

* Partial or Full Salary